PILLARED COFACIAL PORPHYRINS: SYNTHESIS, STRUCTURE, AND APPLICATION

By

Ismail Abdalmuhdi

A DISSERTATION

Submitted to
Michigan State University
in partial fulfillment of the requirements
for the degree of

DOCTOR OF PHILOSOPHY

Department of Chemistry

1985

ABSTRACT

PILLARED COFACIAL PORPHYRINS:

SYNTHESIS, STRUCTURE, AND APPLICATION

By

Ismail Abdalmuhdi

A series of diporphyrin and monoporphyrin compounds has been synthesized and examined for the catalytic activity toward the four-electron reduction of dioxygen on graphite surfaces, a process that is very essential to the cathode reaction in the air-powered batteries (i.e., fuel cells).

Stepwise synthetic methods were developed based on coupling of ethyl 3-ethyl-4-methyl-2-pyrrolecarboxylate with aldehyde compounds to produce methine-substituted 5,5′-bis(ethylcarboxylate)dipyrrylmethanes which upon hydrolysis and decarboxylation gave the corresponding α-free dipyrrylmethanes. Porphyrins were obtained from the α-free dipyrrylmethanes upon coupling, in acidic media, with 5,5′-diformyl-3,3′-diethyl-4,4′-dimethyl-2,2′-dipyrrylmethane. Meso di-substituted porphyrins were obtained in good yields by direct coupling of mono-aldehydes with 5,5′-unsubstituted 3,3′-diethyl-4,4′-dimethyl-2,2′-dipyrrylmethane. All the free bases of the porphyrin compounds were isolated by chromatography and further

purified by recrystallization from CH_3OH/CH_2Cl_2 solution before the metal ions into the porphyrin macrocylic ligands.

The catalytic activities were studied by the technique of rotating ring-disk electrode cyclic voltammetry. It was found that among all the examined compounds, the cofacially arranged, 1,8-anthracene-(DP-A) and 1,8-biphenylene-diporphyrins (DP-B) were the most effective and stable catalysts for the oxygen four-electron reduction process. Most other porphyrins were found to catalyze the two-electron reduction to hydrogen peroxide.

X-ray crystallographic studies on (DP-A) and (DP-B) have shown a plane-to-plane separation of 3.88 Å and 3.45 Å, respectively. Although there is no clear connection between the catalytic activity (toward four-electron reduction) and the interplanar separation of the porphyrin rings, it was observed that the geometry of the macrocycles in these catalysts has a profound impact on their catalytic activities.

TO MY FAMILY

ACKNOWLEDGEMENTS

I would like to express my sincere appreciation to Professor C.K. Chang for his inspiration, guidance, and support during the course of this work and the preparation of this dissertation. I would also like to thank all my colleagues for the fruitful discussions, and for their cooperation and encouragement.

Financial support from the National Science Foundation, Dow Chemical Company in the form of a Summer Fellowship, and SOHIO Company in the form of a one year Industrial Fellowship are also acknowledged.

Above all, I would like to thank my family for their faith and encouragement which made all of this possible.

Special thanks are due to Ms. Margaret Lynch for her contribution by typing this dissertation.

TABLE OF CONTENTS

PAGE

PAGE

LIST OF TABLES

LIST OF FIGURES

LIST OF SCHEMES

LIST OF APPENDIX FIGURES

CHAPTER 1

INTRODUCTION

CHAPTER ONE

INTRODUCTION

A. Significance and Objectives of the Present Work

A major part of the effort in this work was focused on the synthesis and study of binuclear metal complexes of covalently linked cofacial diporphyrins. The two porphyrin rings in these diporphyrins were held in a face-to-face configuration by rigid spacers of different lengths.

These models are considered of great significance. Syntheses of these novel compounds were themselves challenging, since they required the application of various organic and inorganic synthesis techniques. In addition they have the unusual capability of placing two metal ions at selected distances and thus can display interesting properties arising from metal-metal interactions. Furthermore, and from a biochemical point of view, these compounds represent a class of elaborately designed bioinorganic models for many essential biological systems, such as the chlorophyll "special pair" photosynthetic units [1,2]; chlorophyll aggregate models for studying excitation energy and charge transfer proceses [3]; cytochrome c oxidase models that are capable of catalyzing the multielectron reduction of oxygen; and monooxygenases models by which

molecular oxygen can be activated.

In particular, metal complexes of cofacial diporphyrins have recently received considerable attention [4-13]. When adsorbed on graphite, the dicobalt derivatives of these dimers were able to catalyze the four-electron reduction of oxygen to water at ca. +0.68 V *vs* NHE at low pH [13]. Therefore, these electrocatalysts are very promising, since they may constitute a major contribution in fuel cell technlogy by replacing the expensive platinum in the electrodes. It is also hoped that the the availability of these compounds will offer a better understanding of the mechanism of dioxygen reduction.

B. Cytochrome Oxidase

Cytochrome c oxidase, the terminal enzyme in the respiratory metabolism of all aerobic organisms, i.e., animals, plants, yeasts, algae, and some bacteria is responsible for catalyzing the reduction of dioxygen to water. This enzyme is bound to the mitochondrial inner membrane of the living cell (Fig. 1), and it is considered very essential for the oxidation of foodstuff and generation of energy [14-16]. The catalytic activity of cytochrome c oxidase toward the reduction of oxygen is demonstrated by its ability to transfer reducing equivalents from ferro-cytochrome c to molecular oxygen, as shown by

Equation (1). The electrons are provided by reduced cytochrome c:

$$O_2 + 4Cyt\ c^{2+} + 4H^+ \longrightarrow 2H_2O + 4Cyt\ c^{3+} \qquad (1)$$

The free energy generated in the process is usually used to promote oxidative phosphorylation and consequently becomes available as ATP, to satisfy the energy requirements of the living cell. For instance, it is estimated that 90% of the energy for heart muscle contraction is provided through aerobic metabolism via cytochrome

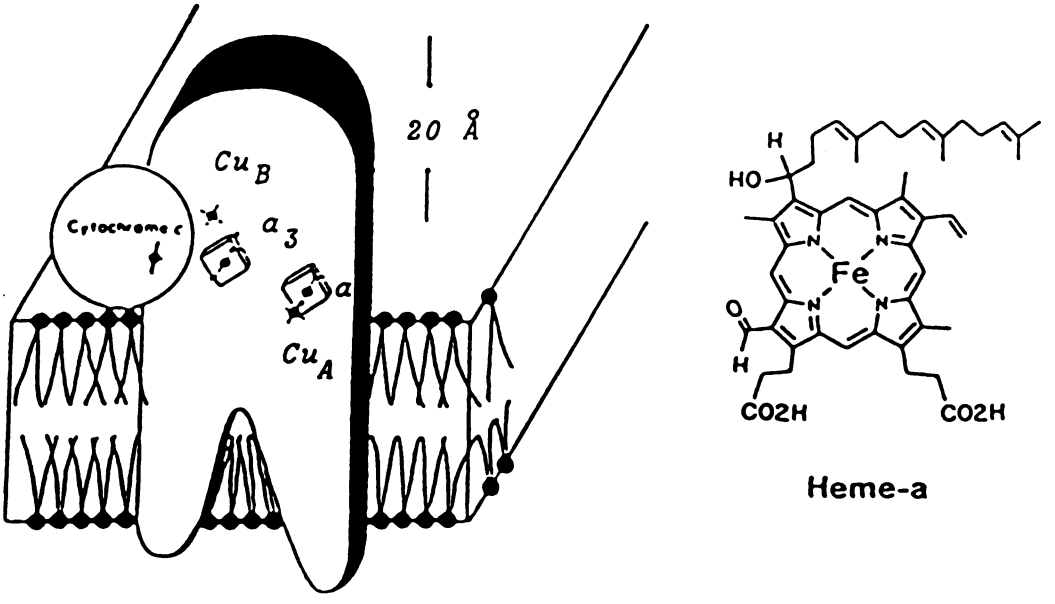

Figure 1 *A schematic representation of the gross structure of the redox centers in a membranous cytochrome oxidase* [*16b*].

oxidase [17,18]. The essential nature of cytochrome oxidase is exemplified by the fact that it is considered responsible for more than 90% of the oxygen consumption by living organisms on earth [19].

Biologically, the general significance of cytochrome c oxidase is believed to exceed that of hemoglobin, since the latter is only an auxiliary in the cell respiration process and its function is solely to carry oxygen to the tissues via the bloodstream. This is essential only in bulky animals, where oxygen diffusion through the surface is usually not sufficient [14a].

It is well established that the active unit of the enzyme contains two heme groups (heme a and a_3), and two protein-bound copper ions (Cu_A and Cu_B). The major difference between heme a and heme a_3 is that the first is usually of low spin and doesn't bind ligands, while heme a_3, on the other hand, is of high spin and has the ability to bind various ligands, such as O_2 and CO in the ferrous state and HCN, H_2S and HN_3 in the ferric state [20].

Although the structural relationship between iron and copper of the enzyme is far from established, the magnitude of the antiferromagnetic coupling observed for the oxidized Fe^{3+}-Cu^{2+} suggests that the iron and copper atoms are separated by no more than a few atoms [21,22].

The functioning enzyme which is provided with electrons from the electron transport chain by cytochrome c, uses

these electrons to reduce dioxygen bound at the active site, then communicates the energy released in this reduction to the site of oxidative phosphorylation, (Fig. 2).

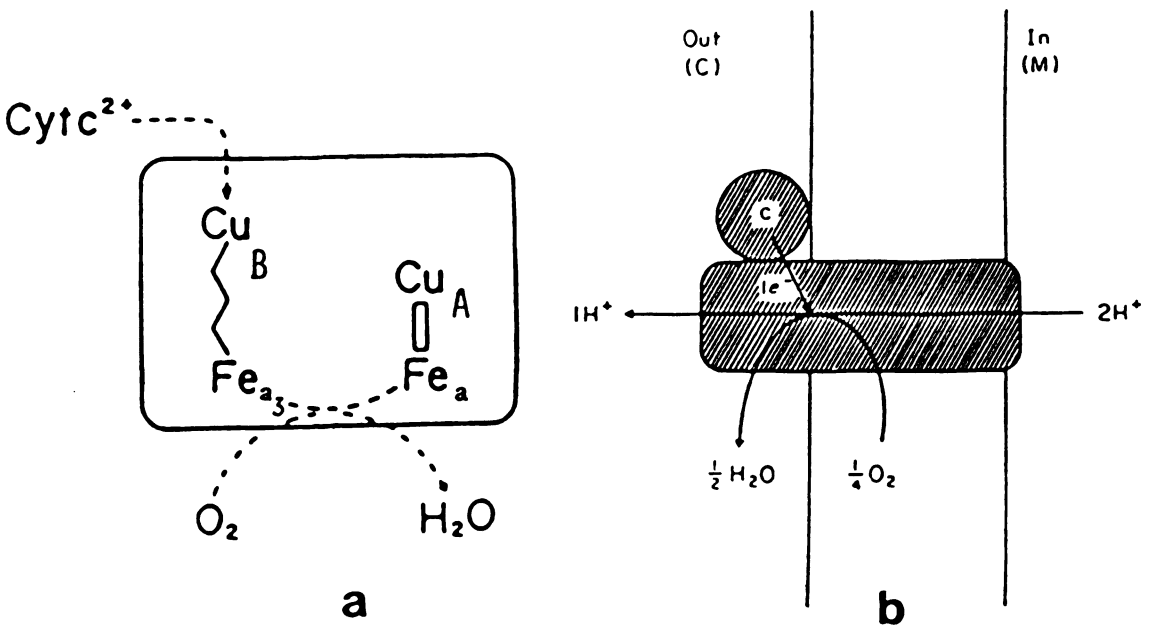

Figure 2 (a) A schematic representation of the asymmetric reduction of cytochrome oxidase by cytochrome c. In this case cytochrome c is shown introducing electrons into only one of the iron-copper couples with the reduction of dioxygen to water induced by electrons that originate on only one of the iron atoms. (b) A schematic view of proton translocation by cytochrome oxidase. The point of O_2 reduction has been drawn near the C side of the membrane, but may also be located closer to the M side. Uptake of H^+ from the M side and release on the C side show the net observed stoichiometry (per transferred electron). If the "substrate" protons required to reduce O_2 to H_2O are taken from side C, the proton pump must translocate $2H^+/e^-$ across the membrane in order to preserve the overall stoichiometry observed [25b].

C. The Chemistry of Dioxygen Reduction

The chemical inertness of dioxygen at first seems surprising because the transformation to water is so strongly thermodynamically favorable (≈80 kcal/mole) [23,24]. However, on the basis of the standard redox potentials, the simplest reduction step, the one-electron step to superoxide, is thermodynamically highly unfavorable [25]. Hence reactions involving dioxygen must either have enormous driving energies to go through the superoxide or have access to a two-electron step to peroxide. It is most likely that oxygen reduction by a low energy pathway proceeds via the two-electron reduction to peroxide as the first recognizable product [26].

The other property of dioxygen that contributes to the slowness of its reactions is its electronic structure. In common with most stable molecules, dioxygen has an even number of electrons. Uncommonly, though, the molecule is paramagnetic with two unpaired electrons in the two highest occupied molecular orbitals. Since both peroxide and oxide are completely spin paired, reactions involving dioxygen must involve spin reversal and are therefore spin forbidden and slow. The forbiddance can be removed if dioxygen can interact with a paramagnetic center to participate in exchange coupling. The transition metal ions frequently have unpaired electrons and turn out to be excellent cata-

lysts for dioxygen reduction [27].

Despite the long history of transition metal ion induced reduction of dioxygen, surprisingly little is known about the mechanism of the reaction [28]. Perhaps the most studied of these metal ion oxygenation reactions is that between the nitrogen ligand complexes of Co(II) and dioxygen. Upon oxygenation, a cobalt(III) complex is formed. It is now known that the first step in this reaction is the formation of an unstable $Co^{II}-O_2$ [29], and upon standing, a second Co(II) ion is added to produce the μ-peroxo bridged complex (reactions 2 and 3). In the presence of a second bridging ligand, such as amido- or hydroxo-, the μ-peroxo complex is stabilized and can be isolated (reaction 4). In the absence of the second bridging ligand, however, further

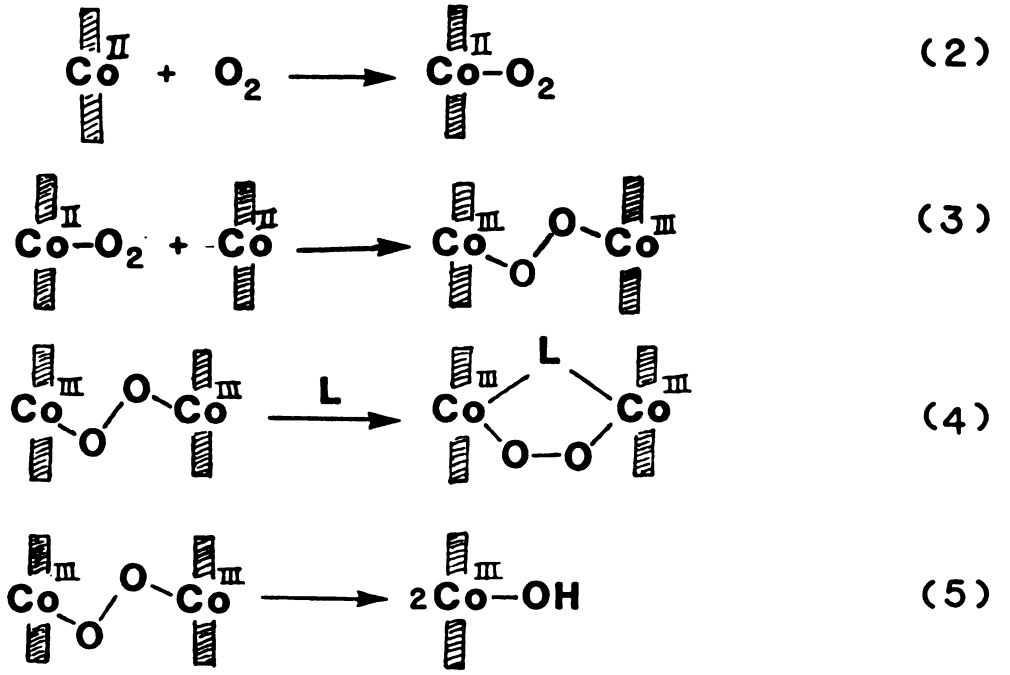

oxidation by a series of, as yet, not completely understood steps and the cobalt(III) product results (reaction 5) [30].

Of special relevance to cytochrome c oxidase, the reactions of hemes [31,32] as well as simple aquo ferrous ions [33] with dioxygen seems to proceed through two-electron reduction of bridged intermediates. Thus, unprotected heme models react cleanly with dioxygen to form μ-oxobishemins irreversibly, as shown by reactions (6) through (9). This indeed represents a major problem in trying to mimic the O_2 or CO binding of hemoglobin or myoglobin by synthetic models.

$$Py\text{–}Fe^{II}\text{–}Py \longrightarrow Py\text{–}Fe^{II} + Py \qquad (6)$$

$$Py\text{–}Fe^{II} + O_2 \longrightarrow Py\text{–}Fe^{II}\text{–}O_2 \qquad (7)$$

$$Py\text{–}Fe^{II}\text{–}O_2 + Py\text{–}Fe^{II} \longrightarrow Py\text{–}Fe^{III}\text{–}O_2\text{–}Fe^{III}\text{–}Py \qquad (8)$$

$$Py\text{–}Fe^{III}\text{–}O_2\text{–}Fe^{III}\text{–}Py \longrightarrow Fe^{III}\text{–}O\text{–}Fe^{III} + 2Py \qquad (9)$$

When the solvent medium is able to provide protons, solvolysis to produce H_2O_2 would likely follow the formatin

of the μ-peroxobishemin complex and the sequence (6)-(8). However, where solvolysis cannot occur, as in

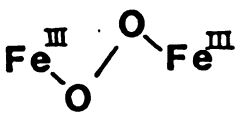

$$\longrightarrow 2\,Fe^{IV}\text{-}O^{\bullet} \qquad (10)$$

$$Fe^{IV}\text{-}O^{\bullet} + Py\text{-}Fe^{III} \longrightarrow Fe^{III}\text{-}O\text{-}Fe^{III} + Py \qquad (11)$$

aprotic solvents, formation of the ferryl [Fe^{IV}-O] intermediate, as shown in reactions (10) and (11), is reasonable [32]. But in no instance does our current knowledge about the mechanism of the reduction reaction extend beyond the bridged dimer. Apparently, the peroxide formed in the initial reaction is a kinetically inert (fully spin-paired) molecule that does not readily accept additional electrons despite the favorable thermodynamics for reduction to water.

The organization of cytochrome c oxidase to carry out the reduction of dioxygen to water must reflect the mechanism by which electrons are supplied, the thermodynamic requirements of the oxidation states accessible to oxygen, and the chemical transformation of oxygen enroute to water. Many mechanistic approaches for this process have been suggested although none of them has been fully documented and thus remains speculative [34]. However, we suggested a reasonable mechanism for the reduction of dioxygen to water by dicobalt cofacial diporphyrin catalysts, cf. Chapter III (Electrochemistry).

D. Fuel Cells

Among the large variety of fuel cells, the oxygen-hydrogen cell is considered the most advanced [35,36]. The basic design of the cell is shown in Fig. 3, which consists of a solid electrolyte ion-exchanger membrane, electrocatalysts, current collectors, coolant tubes, water wicks, and gas-feed tubes. The membrane is nonpermeable to the reactant gases, hydrogen and oxygen, which thus prevent them from coming into contact, but permeable to hydrogen ions, which are the current carriers in the electrolyte. The two electrodes in the fuel cell, which consist of the electrocatalyst (usually finely divided platinum metal) and a plastic material for water-proofing, are in the form of finely metallic wire screens.

Oxygen, either pure or in air, is as important to electrochemical conversion as it is to chemical combustion and to life [37]. Thus, particularly all earth based fuel cells use O_2 as the cathodic reactant. Oxygen is reduced at the cathode, in acid solution, to water through a four-electron process according to Equation (12)

$$O_2 + 4H^+ + 4e^- \longrightarrow 2H_2O \qquad (12)$$

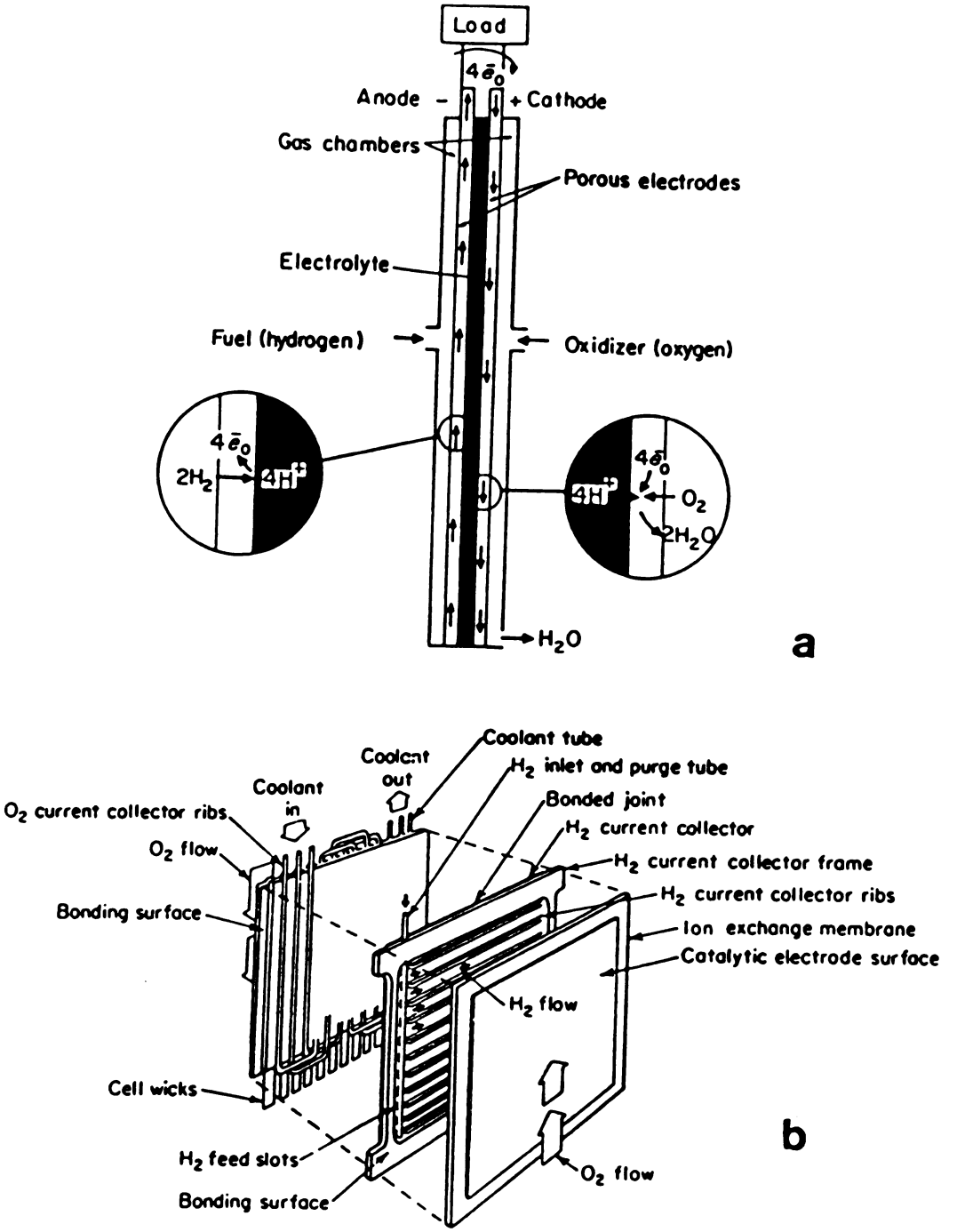

Figure 3 (a) A single cell in the General Electric ion exchange-membrane H_2/O_2 fuel cell. (b) Assembly of a single cell in the General Electric H_2/O_2 fuel cell [38,40].

Although H_2/O_2 fuel cells are being used in large scales in specialized areas, two main problems still should be solved before this type of cells become economically competitive for general applications. In order to perform efficiently, the cell should operate at relatively high temperature. Secondly, the only active electrocatalyst, until now, is the expensive platinum metal which makes the whole process very costly. This has prompted research efforts to develop a cheaper electrocatalyst that can catalyze the reduction of dioxygen to water efficiently.

It has been shown, in the past few years, that a grphite surface coated with a binuclear dicobalt diporphyrin, in which the porphyrin rings are held in a face-to-face configuration, enables the reduction of dioxygen to occur via a four-electron pathway at a potential near that of the platinum electrode [6-12]. The only active catalyst for the four-electron electroreduction of oxygen, that has been previously reported, contains two porphyrin rings that are linked covalently by two four-atom amide linkages (DP-4, cf. Figure 6). Because of the instability of the amide linkages under the electroreduction conditions and in an attempt to improve the catalytic activity of the four-electron catalysts, we have synthesized and examined a series of diporphyrins and monoporphyrin compounds (cf. Figure 7). The new catalysts are found to be much more stable than the amide-linked dimers because they do not contain any potentially active functional groups.

CHAPTER 2

SYNTHESIS

CHAPTER TWO

SYNTHESIS

A. Cofacial Porphyrins

The face-to-face diporphyrins that have been prepared and studied previously by our group [4-7] and others [8-13], in which the two porphyrin rings are constrained in a cofacial configuration by amide linkages, were obtained basically by direct coupling of the corresponding monoporphyrin diacid chloride with monoporphyrin diamine (Scheme 1)

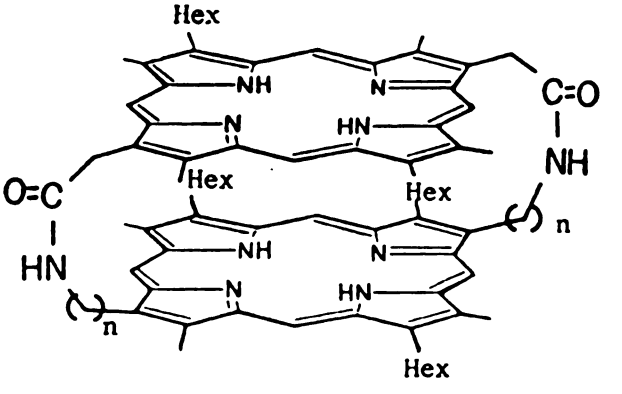

n = 1, 2 and 3.

SCHEME 1

The amide linkage is a reasonably reactive functional group, and although such linkages maintain their integrity under physiological conditions, this is not necessarily the case in the laboratory. Indeed, it has been observed that such covalently linked diporphyrins readily cleave to monomeric species [41] in acid solution where the electroreduction of dioxygen should proceed.

To enhance the stability of the dimers under such conditions, however, we have introduced more stable and more rigid aromatic connecting groups between the two porphyrin rings [42-44]. And we found that the new dimers show extraordinary stability and electrocatalytic activity toward oxygen reduction to water [45-48].

Although a great deal of synthetic work has been done on porphyrins, very few of these syntheses dealt with meso substituted monoaryl porphyrins [49,50]. None of those synthetic methods gave reasonable yields of diporphyrins, therefore we developed a stepwise approach.

To synthesize 1,8-anthracene di-etioporphyrin 6 [42], anthracenedicarboxaldehyde 1 (obtained from 1,8-dichloroanthraquinone according to literature methods [51-53]) was reacted with 4 equivalents of ethyl 3-ethyl-4-methyl-2-pyrrolecarboxylate 2 [54] in dry ethanol and in the presence of catalytic amounts of conc. hydrochloric acid, (Scheme 2). The resultant tetra-ethyl ester 3 was saponified in an alkaline medium (hydrolysis in acidic solution always led to decomposition of the dipyrrylmethane) to give

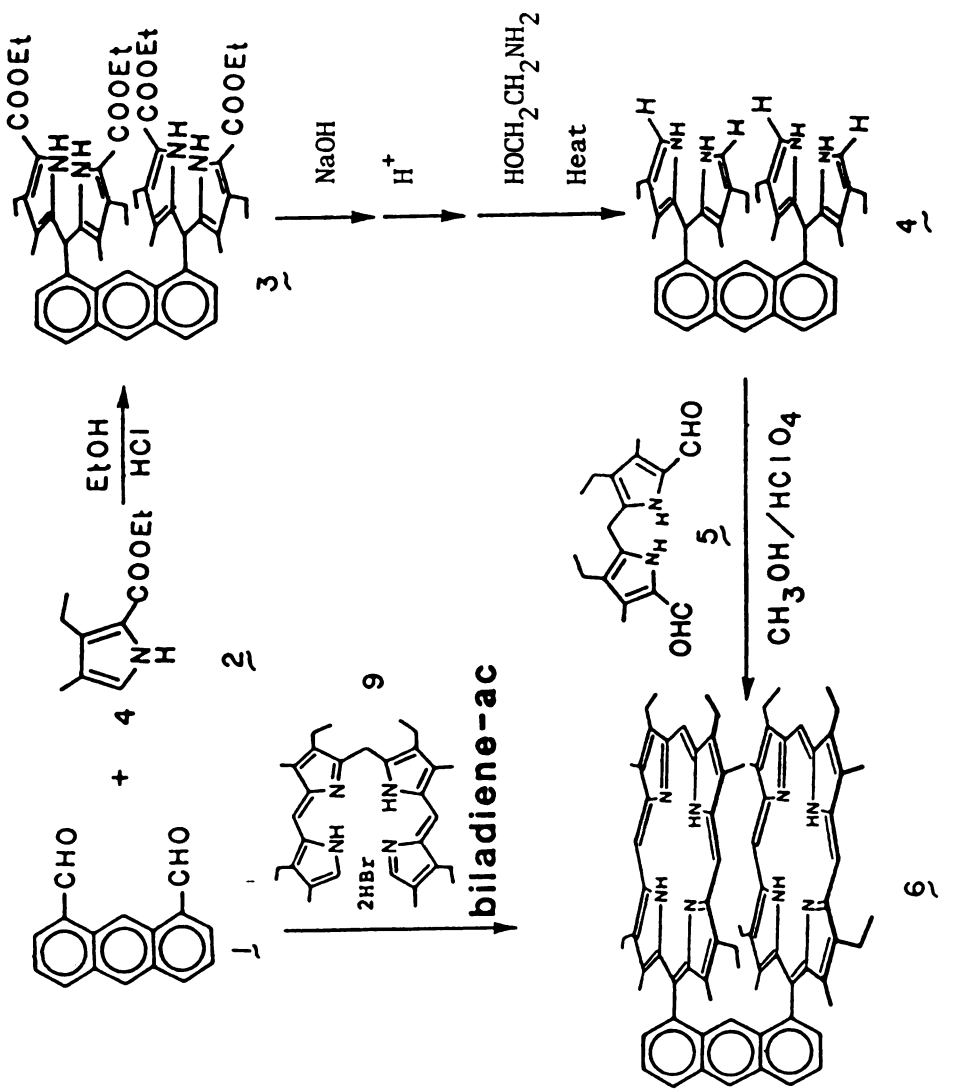
COOEt
NH
3
NaOH
H+
HOCH2CH2NH2
Heat
4
EtOH
HCl
2
+ 4
CHO
CHO
1
9
2HBr
biladiene-ac
OHC
5
CH3OH/HClO4
6

SCHEME 2

the bis(dipyrrylmethane) tetracarboxylic acid quantitatively. For decarboxylation, heating in glycerol (Fischer's method [55]) was first tried but it was very inconvenient. In looking for a suitable solvent capable of absorbing carbon dioxide, 2-aminoethanol was found to be excellent and at its boiling point, 1,8-bis(5,5′-dicarboxyl-4,4′-diethyl-3,3′-dimethyl-2,2′-dipyrrylmethane) anthracene was smoothly decarboxylated to give 4 in quantitative yield, the carbon dioxide forming 2-aminoethanol bicarbonate [56]. Cyclization of 4 with (5,5′-diformyl-3,3′-diethyl-4,4′-dimethyl-2,2′-dipyrryl)methane, 5 [57] was carried out in methanol containing catalytic amounts of 70% perchloric acid. The diporphyrin 5 was obtained in >20% yield. Surprisingly, when the cyclization was carried out by the standard MacDonald procedure [58] (HI-HOAc, at room temperature) no evidence at all for the desired diporpyrin was observed.

The bis(methoxymethyl)dipyrrylmethene, 7, was found to react with the unsubstituted dipyrrylmethane 4 in boiling benzene and subsequent oxidation produced the anthracene-diporphyrin 6 in 7-10% yield (Scheme 3). Bis(methyoxymethyl)dipyrrylmethenes have been employed to construct bilenes [59-61] previously, but the condensation with dipyrrylmethane in such a direct manner to form porphyrin, to our knowledge, has not been reported. This route may be a useful alternative for the general (2+2) porphyrin cyclizations. The reaction is carried out in the absence of

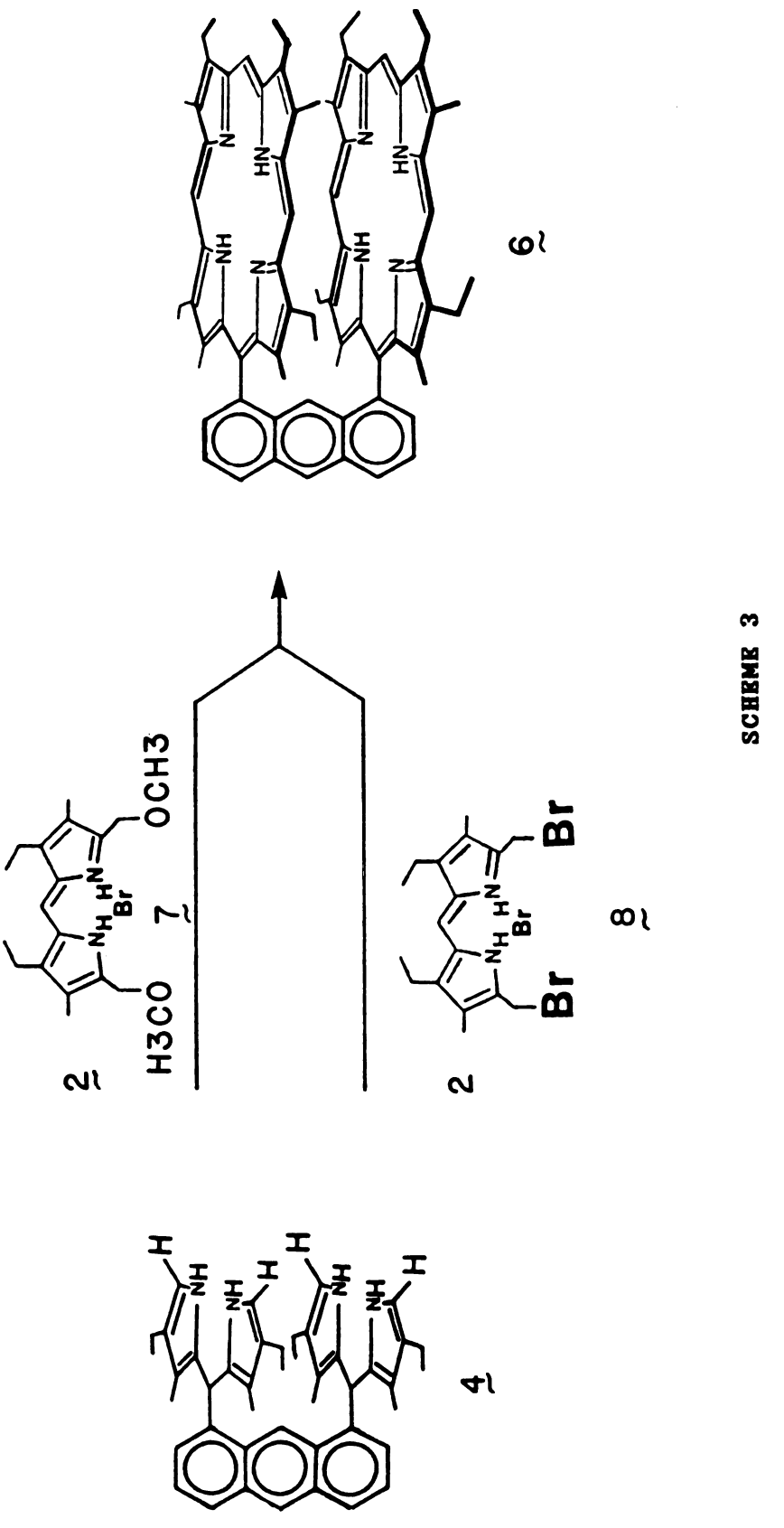

SCHEME 3

excess protons; thus there should be little danger of scrambling of substituents. Indeed, the sharp singlet NMR peaks of the meso protons, as well as that of the methyl groups in the diporphyrin, clearly ruled out any other substitution patterns. We have applied this approach successfully to prepare meso monophenyletio porphyrin and octaethylporphyrin from appropriate precursors [42].

The cyclization was also possible (although with lower yield) when bis(bromomethyl)dipyrrylmethene hydrobromide 8, was used instead of bis(methoxymethyl)dipyrrylmethene hydrobromide, as shown in (Scheme 3).

The dipyrrylmethene hydrobromide, 8, was obtained by treatment of ethyl 4,5-dimethyl-3-ethyl-2-pyrrolecarboxylate [62,63] with 48% hydrogen bromide in formic acid and reacting the resultant orange crystals with Br_2/HOAc. Bis-(methoxymethyl)dipyrrylmethene hydrobromide, 7, was obtained from 8 by refluxing in dry methanol.

In yet another attempt, trace amounts of the diporphyrin, 6, was obtained by direct cyclization of 1,8-anthracene-dicarboxaldehyde with two equivalents of 1,19-dideoxytetraethyltetramethylbiladiene-ac dihydrobromide, 9, [49] in methanol and in the presence of HBr/HOAc, cf. (Scheme 2).

Similarly 1,8-biphenylene diporphyrin 14 was obtained in 9% yield by condensation of 1,8-biphenylenedicarboxaldehyde 12 [64-67] and the α-free pyrrole 2, followed by saponification, decaboxylation, and coupling with 5,5′-di-

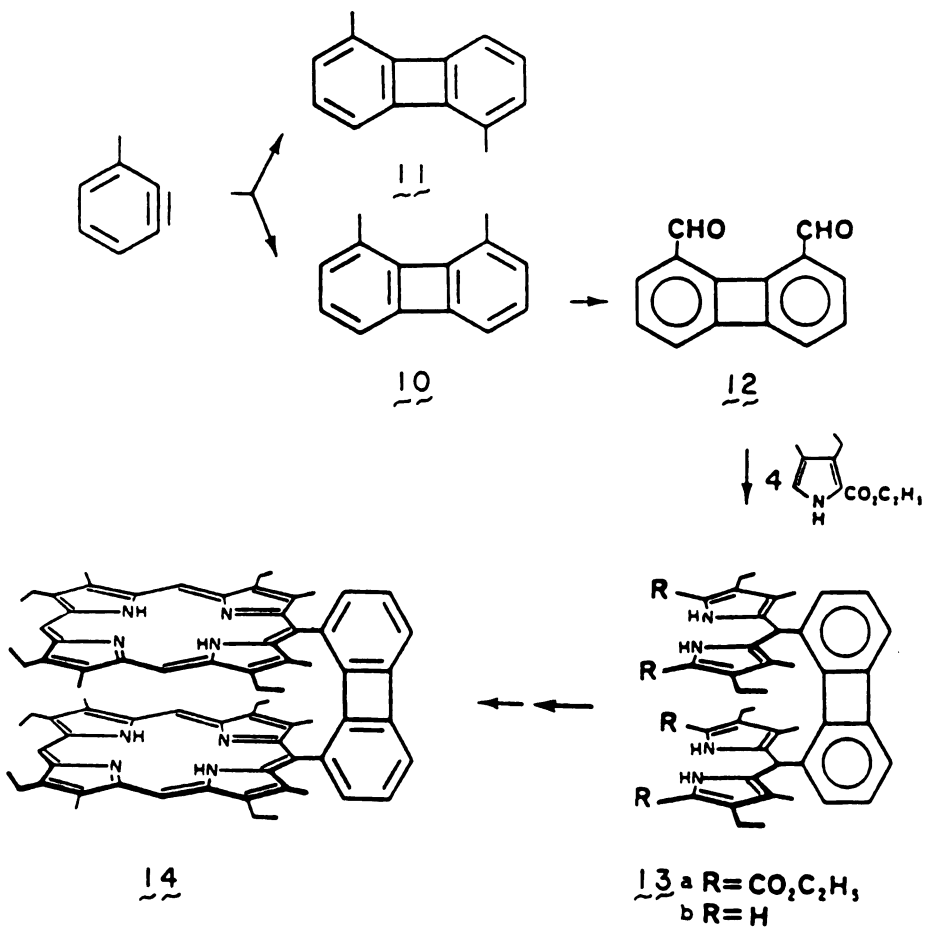

11 10 12

14

13 a R=$CO_2C_2H_5$
b R=H

SCHEME 4

formyldipyrrylmethane 5 in 0.4% $HClO_4$/methanol solution, (Scheme 4). The 1,8-biphenylenedicarboxaldehyde 12 was prepared by DMSO oxidation of the dimethyl precursor 10 [65]. Methylbenzyne was condensed *in situ* [64] to yield a mixture of 1,8-10 and 1,5-dimethylbiphenylene 11. The separation of the two isomers was found to be much easier if the mixture was converted first to the dialdehydes and then the isomers isolated by chromatography. Attempts to condense 12 with a mixture of pyrrole and benzaldehyde invariably produced only tetraphenylporphyrin and an untractable material.

The "triple-deckered triporphyrin" 20 (Scheme 5) [44], was synthesized by using the dipyrrylmethane aldehyde 15, as the key intermediate. 3 Was obtained in 73% yield by reacting 2 equivalents of pyrrole 2 and 1,8-anthracenedicarboxaldehyde 1. The formyl group in 15 had to be converted into a nonreactive form before the dipyrrylmethane could be manipulated further. Thus 15 was reduced to the alcohol 16, which after saponification and decarboxylation, was cyclized into meso-substituted porphyrin 17 by using the modified MacDonald procedure [43] with an overall yield of more than 40%. The aldehyde functional group was then restored by oxidation. The aldehyde porphyrin 18, behaving analogously to a substituted benzaldehyde, was allowed to react with equivalent amounts of α-free dipyrrylmethane 19 to yield the triporphyrin 20. This approach has been used for preparing 5,15-diphenyl-porphy-

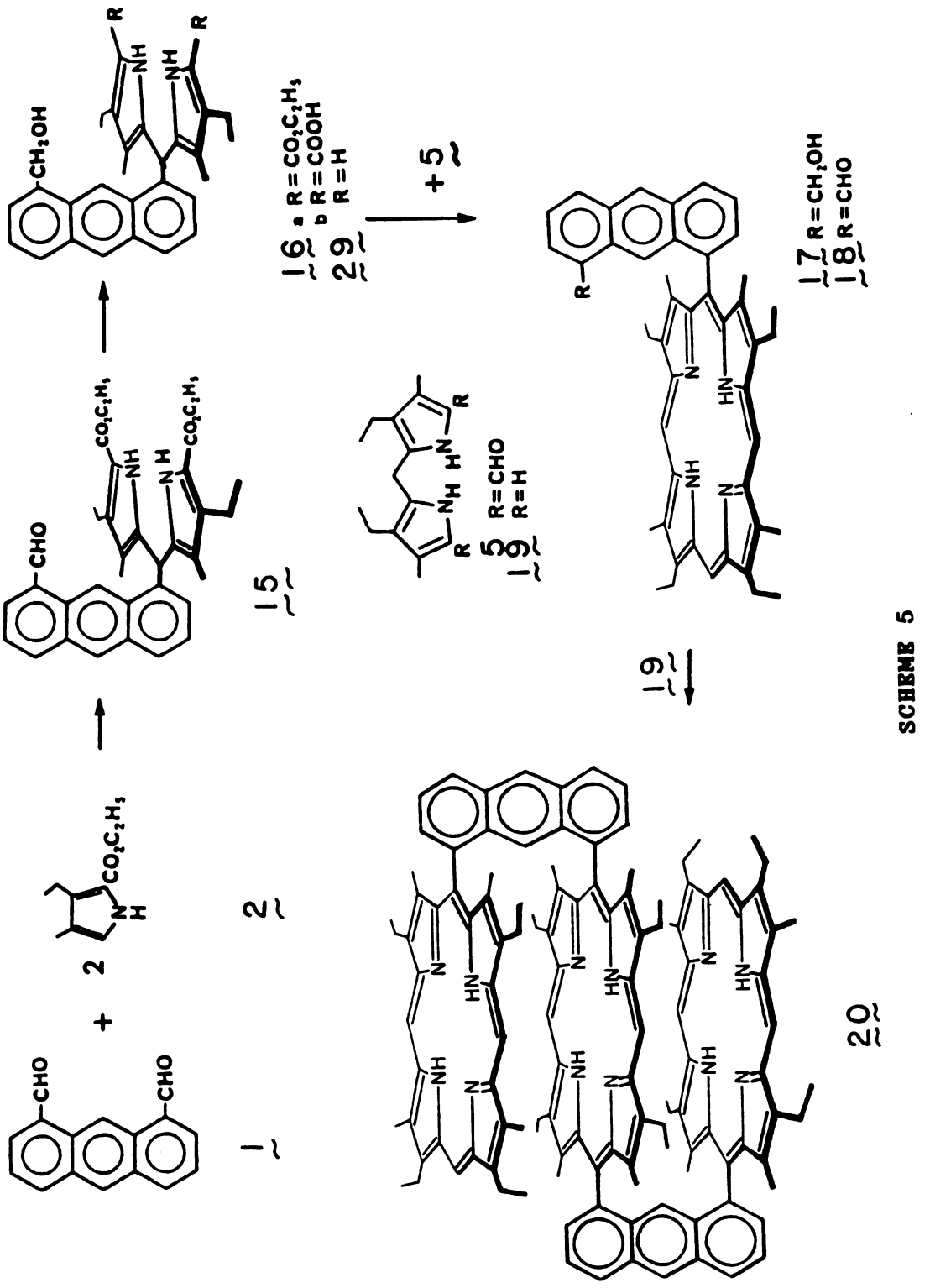
CHO
CHO
1
+ 2
CO2C2H5
N
H
2
CHO
CO2C2H5
NH
NH
CO2C2H5
15
CH2OH
R
NH
NH
R
16 a R=CO2C2H5
b R=COOH
29 R=H
+5
5 R=CHO
19 R=H
R
N
HN
NH
N
17 R=CH2OH
18 R=CHO
19
20

SCHEME 5

rin [68,69]. In principle, atropisomers can result from this reaction, but in this present case, because of the steric bulk, the alternative cis arrangement of the two anthryl groups about the center porphyrin was not possible. Although the conversion yield from 18 to 20 was not high, the unreacted aldehyde 18 could be recovered for recycling.

We found that the most efficient and convenient way to isolate the cofacial porphyrins 6, 14, and 20 from the reaction mixture was to isolate their metal-complexes (usually Zn-complexes) by chromatography, since they have very different R_f-values from the impurities. The free-base diporphyrins were then regenerated from the pure zinc complexes by treatment with a dilute solution of hydrochloric acid.

Various attempts to prepare the rigid dianthryl-diporhyrin 21 have been made (Scheme 6). 1,8-Antracenedicarboxaldehyde 1 was treated variably with 2 equivalents of 3,3′-diethyl-4,4′-dimethyl-2,2′-dipyrrylmethane 19 in methanol and in the presence of p-toluenesulfonic acid (Gunter's method) [72], no diporphyrin was formed and the only porphyrin obtained from this reaction was found to be trace amounts of etioporphyrin II in addition to the dark brown untractable polymeric material.

To increase the possibility of the formation of 21, we believed that coupling of cis dianthrylporphyrin dialdehyde 24 (which was obtained by a stepwise method) with 2 equivalents of the α-free dipyrrylmethane 19 would lead to the

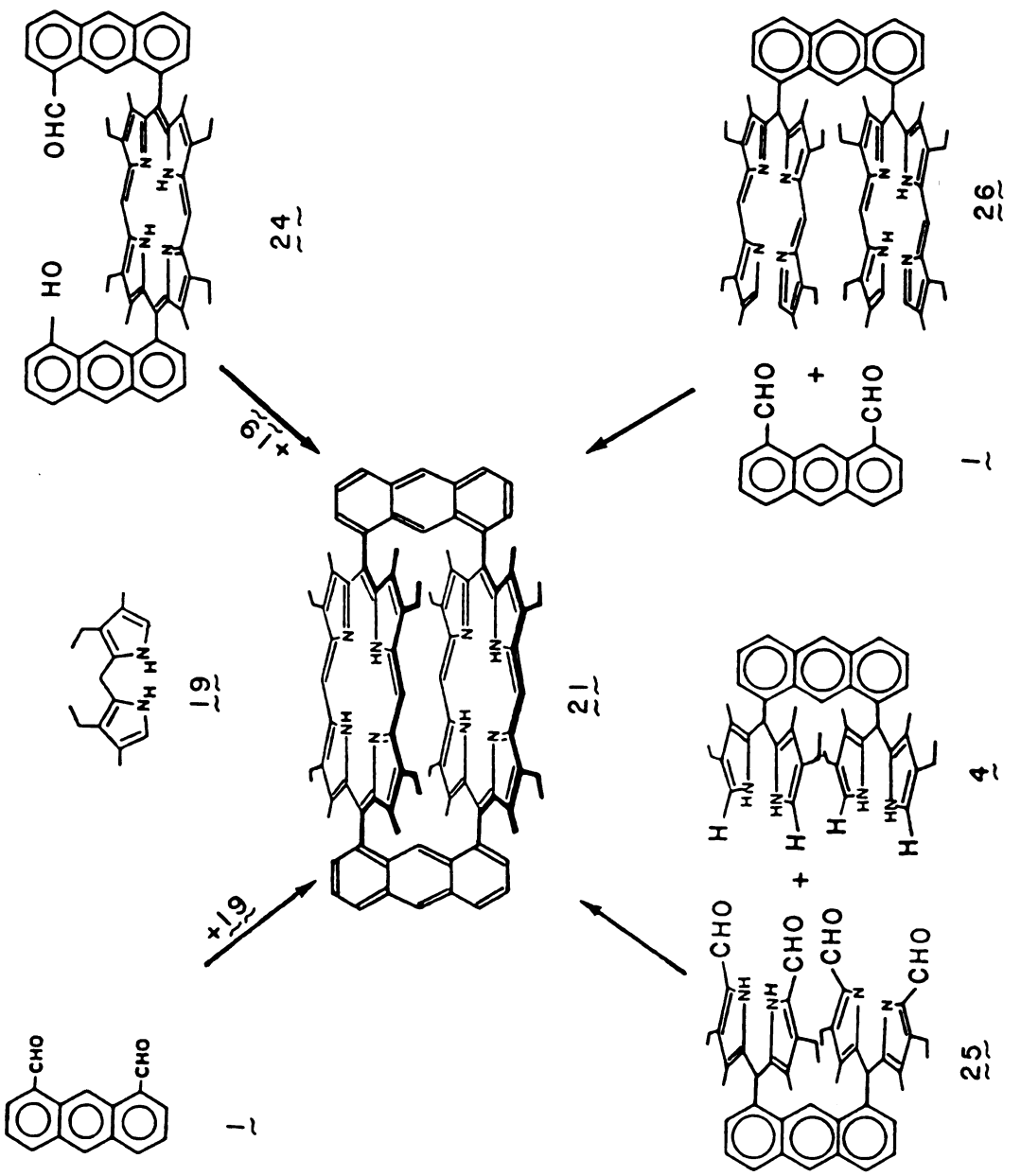

SCHEME 6

formation of 21. After stirring the reactants in methanol/methylene chloride (70:30) solution containing catalytic amounts of p-TsOH, for 20 h, the unreacted dianthrylporphyrin 24 was recovered and no diporphyrin was formed.

In another attempt, the bis(biladiene-ac) 26 was let to react with 1,8-anthracenedicarboxaldehyde 1 in acetic acid. It produced a highly colored polymeric material, with no indication for the formation of 21. Similar results were also obtained by coupling bis(α-free dipyrrylmethyl)anthracene 4 and bis(5,5′-diformyl dipyrrylmethyl)anthracene 25, in acidic methanol.

We suspected that the failure of formation of 21 may be caused by the improper orientation of the pyrrole rings and the high steric hindrance in the dipyrrylmethane intermediates.

In an attempt to vary the distance between the porphyrin rings in the dimers, we considered the possibility of using different aromatic connectors, such as 1,8-fluorenedicarboxaldehyde 27 and 1,8-naphthalene dicarboxaldehyde hydrate, 28 (prepared according to literature) [70,71]. Because of the short distance between the aldehyde groups in these two species, they tend to form hemiacetal and acetal derivatives, especially when the reactions are carried out in acidic alcohol media. However, when the reaction between these dialdehydes and ethyl 3-ethyl-4-methyl-2-pyrrolecarboxylate 2 was carried out in non-alcoholic solvents such as benzene and in the presence of p-toluene-

sulfonic acid, no formation of dipyrrylmethane was achieved.

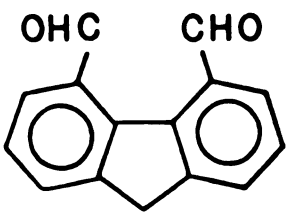

27

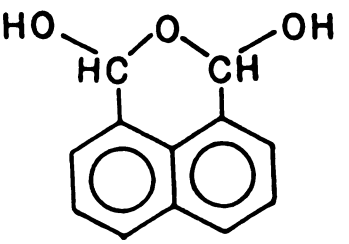

28

The difficulties in preparing the dipyrrylmethane intermediates from 27 and 28 could be mainly due to steric factors.

B. Meso Mono-substituted Porphyrins

Of major interest is the selectively controlled reaction between dialdehyde species (such as 1,8-anthracene and 1,8-diphenylene dicarboxaldehydes) with only two equivalents of the α-free ethyl 3-ethyl-4-methyl-2-pyrrolecarboxylate 2, in which one of the aldehyde groups is reacted while the other is left intact. Our major concern, however, was to apply this process in the synthesis of a series of important mono- and di-meso substituted porphyrins.

When 1,8-anthracenedicarboxaldehyde 1 was reacted in ethanol with 2 equivalents of α-free pyrrole 2, it produced the dipyrrylmethylanthracene aldehyde 15, as a yellow crystalline solid, cf. (Scheme 5). To protect the aldehyde group, it was reduced to the alcohol. The decarboxylated α,α-unsubstituted dipyrrylmethane 29 was coupled with 5,5′-diformyldipyrrylmethane 5 to produce the meso substituted porphyrin 17. In addition, 29 was also used to prepare the meso disubstituted porphyrins, cf. Section C of this chapter.

The anthracene porphyrin-alcohol 17 was converted into methanesulfonate derivative 30 by heating at reflux with excess amounts of methanesulfonyl chloride in dry dichloromethane. The reaction progress was followed by thin layer chromatography (tlc), since the sulfonate ester product has a much higher R_f value than the porphyrin-alcohol starting material. The reaction was complete after ~48 h. It was observed that when amine bases such as pyridine or triethylamine were added to the reaction, in an attempt to reduce the accumulation of the hydrogen chloride that evolved from the reaction, a very dark green solution was usually obtained and the reaction became messy, and lower overall conversion was obtained. However, it seemed that addition of such bases was not necessary since the porphyrin's nitrogens can trap the evolved HCl. The resultant sulfonate ester-porphyrin 30 could be isolated by chromatography, although in many cases, it was not necessary and

not recommended. After total removal of all solvents, the crude residue was used in the next step without any problems.

To introduce the bis(2-pyridyl-β-ethyl)amine ligand, the crude sulfonate ester 30 was treated with relatively excess amounts of the amine 31 [72] in dry dichloromethane, (Scheme 7). The excess amine was removed by washing the reaction solution with dilute hydrochloric acid (~5%) taking advantage of the difference in solubility of the bis(2-pyridyl-β-ethyl)ammonium chloride and the ammonium salt of 32 in water.

Under similar reaction conditions, sulfonate ester-porphyrin 30 was used to prepare porphyrin-crown 34 by coupling with Kryptofix-22, 33.

1,8-Napthalene dialdehyde or its hemiacetal derivative 28 failed to react with α-free pyrrole after several variations in reaction conditions. Hydrolysis of the hemiacetal linkage in acidic solution before the reaction also gave a negative result.

To avoid this obstacle, acenaphthenequinone 35, was reacted smoothly [73] with 2 equivalents of ethyl 3-ethyl-4-methyl-2-pyrrole-carboxylate 2 in ethanol to give the dipyrrylmethane derivative 36 in a very good yield (Scheme 8). Under basic hydrolysis conditions, the carbonyl group cleaved to form the acid dipyrrylmethane 37, after neutralization. Decarboxylation of 37 afforded the α,α-unsubstituted dipyrrylmethane 38 in quantitative yield

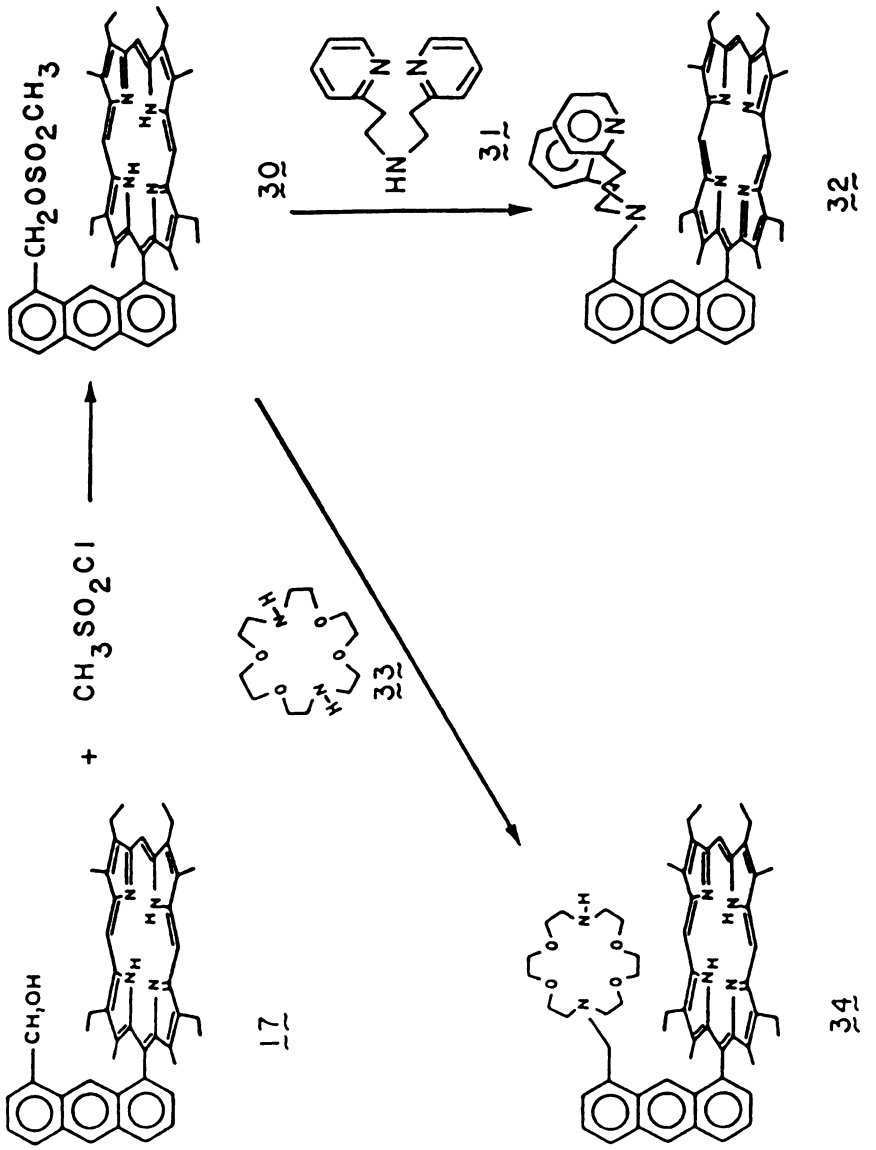

SCHEME 7

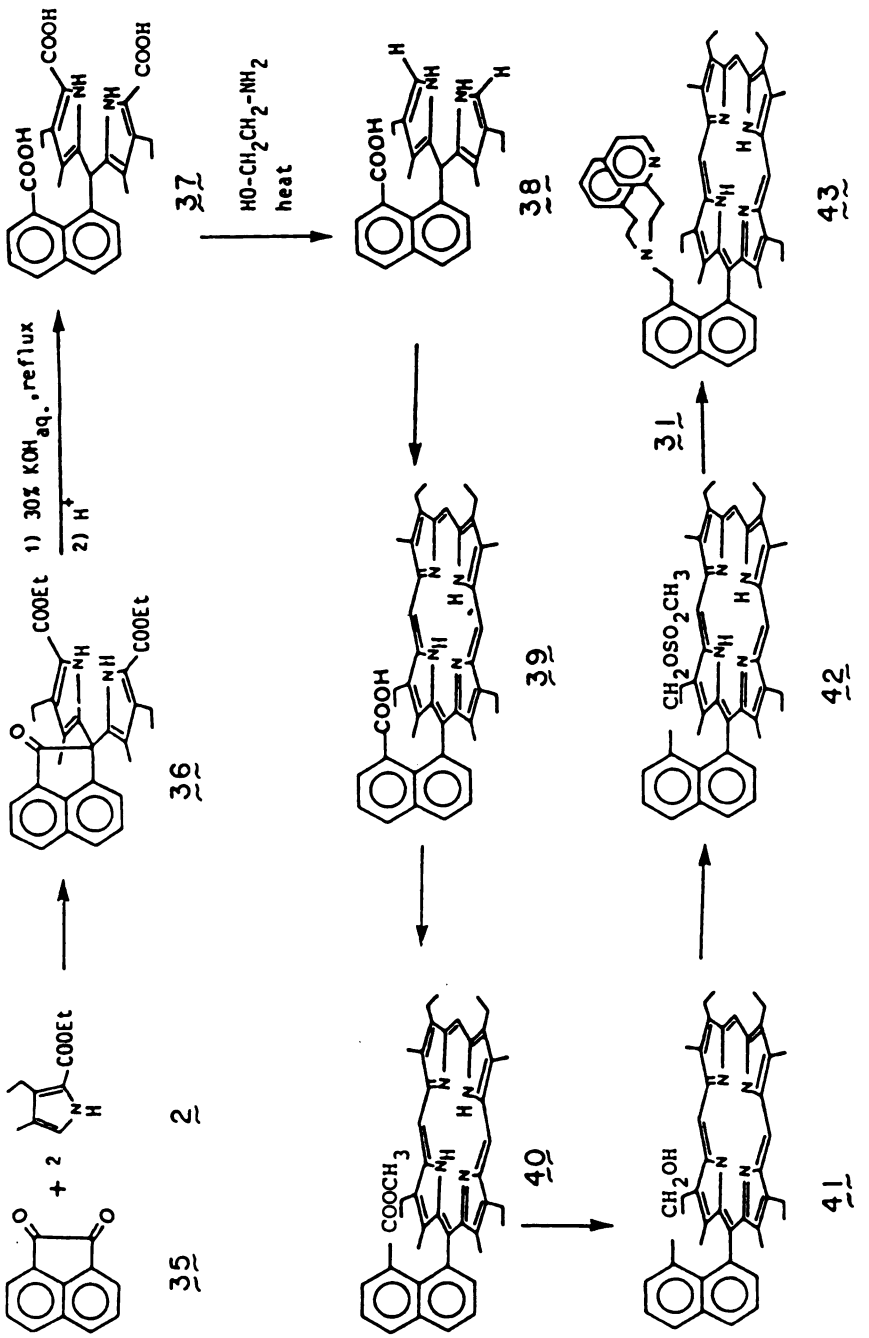

SCHEME 8

which upon coupling with 5,5′-diformyl-3,3′-diethyl-4,4′-dimethyl-2,2′-dipyrrylmethane 5 in methanol gave the naphthalene porphyrin-acid 39. Esterification was possible by refluxing the acid chloride derivative of 39 in methanol. Reduction of the naphthyl porphyrin methyl ester 40 by $LiAlH_4$/THF gave the corresponding alcohol 41 which was used to prepare the bis(2-pyridyl-β-ethyl)amine derivative, 43, through a procedure very similar to that of the anthracene analogue.

Various other meso substituted monoarylporphyrin compounds were synthesized by a straightforward stepwise approach (Scheme 9).

C. Meso Disubstituted Porphyrins

Various disubstituted monoporphyrins were synthesized by direct coupling of the aldehyde compounds with 3,3′-diethyl-4,4′-dimethyl-2,2′-dipyrrylmethane according to Gunters procedure [68]. This was found to be the most convenient method for preparing symmetrically meso disubstituted porphyrins and gave the highest yield. However, when unsymmetrically disubstituted porphyrins are required, we found that the best way is to use the step-by-step approach, using species such as the α,α′-unsubstituted dipyrrylmethane 29 which upon coupling with α,α′-diformyldipyrrylmethanes, with a substituent at the the methine carbon, gives the disubstituted porphyrins (Scheme 10).

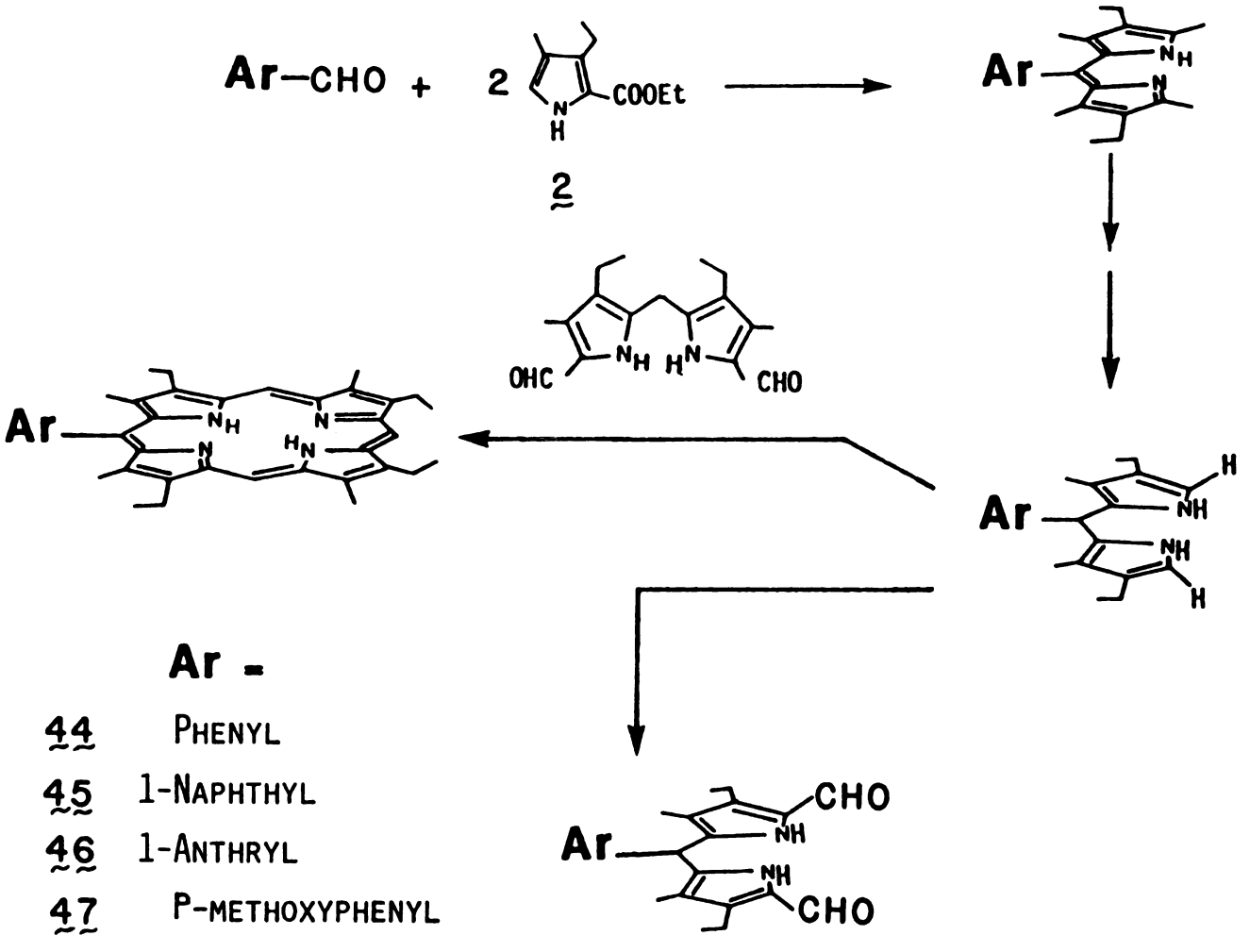

Ar -

44 PHENYL

45 1-NAPHTHYL

46 1-ANTHRYL

47 P-METHOXYPHENYL

SCHEME 9

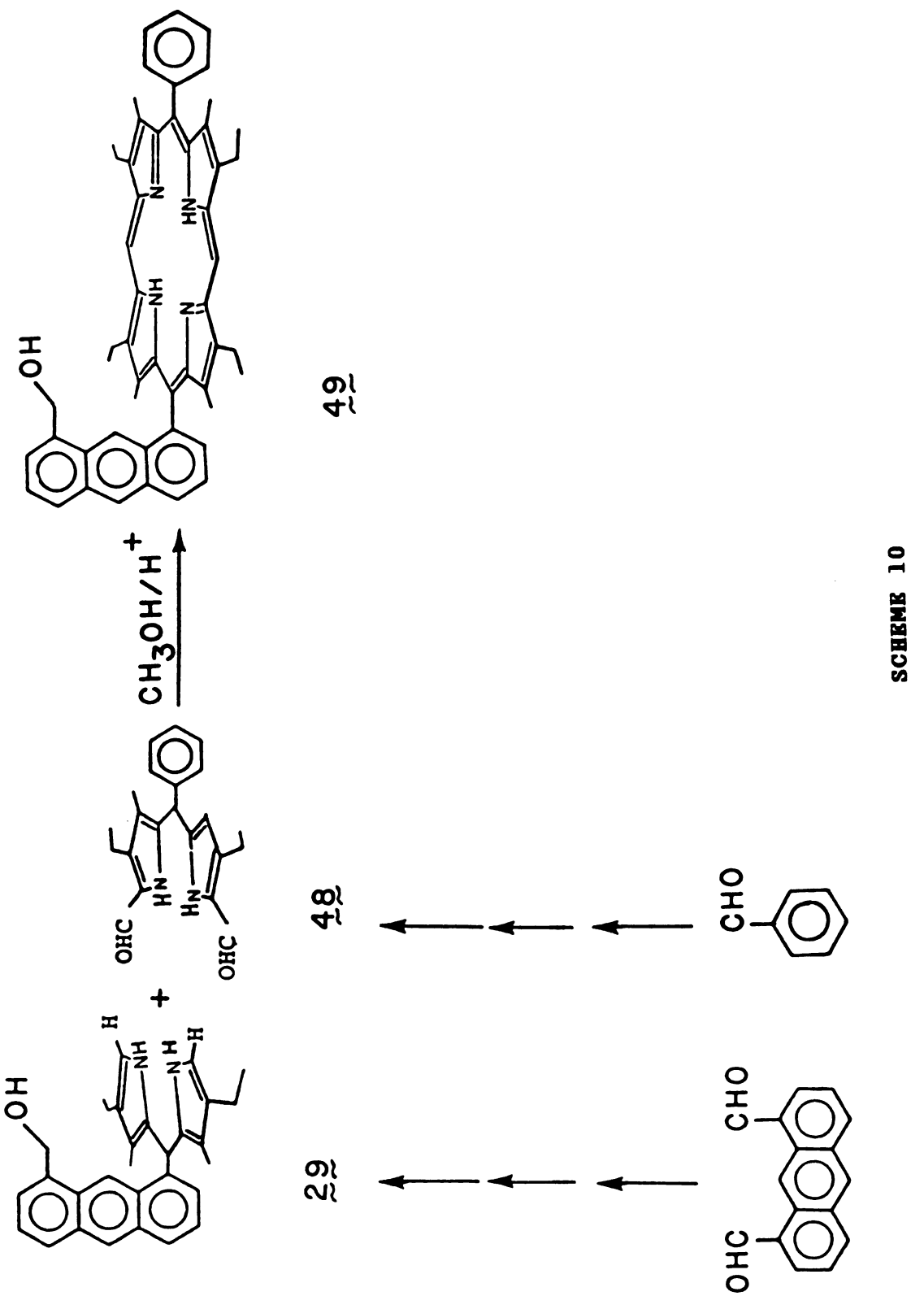

SCHEME 10

To synthesize the disubstituted porphyrin 55, we employed two methods. 8-Methoxycarboxylanthracenecarboxaldehyde 51 was obtained by partial reduction of the corresponding dimethylester 50 with lithium aluminum hydride, followed by oxidation of the crude alcohol. Separation of 51 from the 1,8-anthracene dicarboxaldehyde (the complete reduction product) was achieved by column chromatography. Direct coupling of 51 with the α,α'-unsubstituted dipyrrylmethane 19 in methanol/p-toluenesulfonic acid gave a fairly good yield of the dimethyl-ester dianthrylporphyrins 52 and 53 (~1:1 isomeric mixture). Hydrolysis of the diester 52 in acid medium (hydrochloric acid/formic acid, 1:4 v/v) afforded the corresponding diacid porphyrin, 55 (Scheme 11). Although the overall yield of this method starting with 51 was good and the work-up was convenient, the separation and purification of 51, which was very laborious.

Another approach to synthesize the diacid porphyrin 55 was also employed, starting with the α,α'-free dipyrryl methane anthracene aldehyde 54. Upon cyclization of 54 and α,α'-diformyl-dipyrrylmethane 56 (obtained by Vilsmeier's formylation of 54) and oxidation of the formed porphyrinogen by tetrachloro-o-benzoqinone (o-chloranil) gave an isomeric mixture of trans and cis dialdehyde-porphyrins 57 and 58. Oxidation of the aldehyde groups was affected by treatment with Jone's reagent in acetone at low temperature; if the oxidation is carried out at room temperature

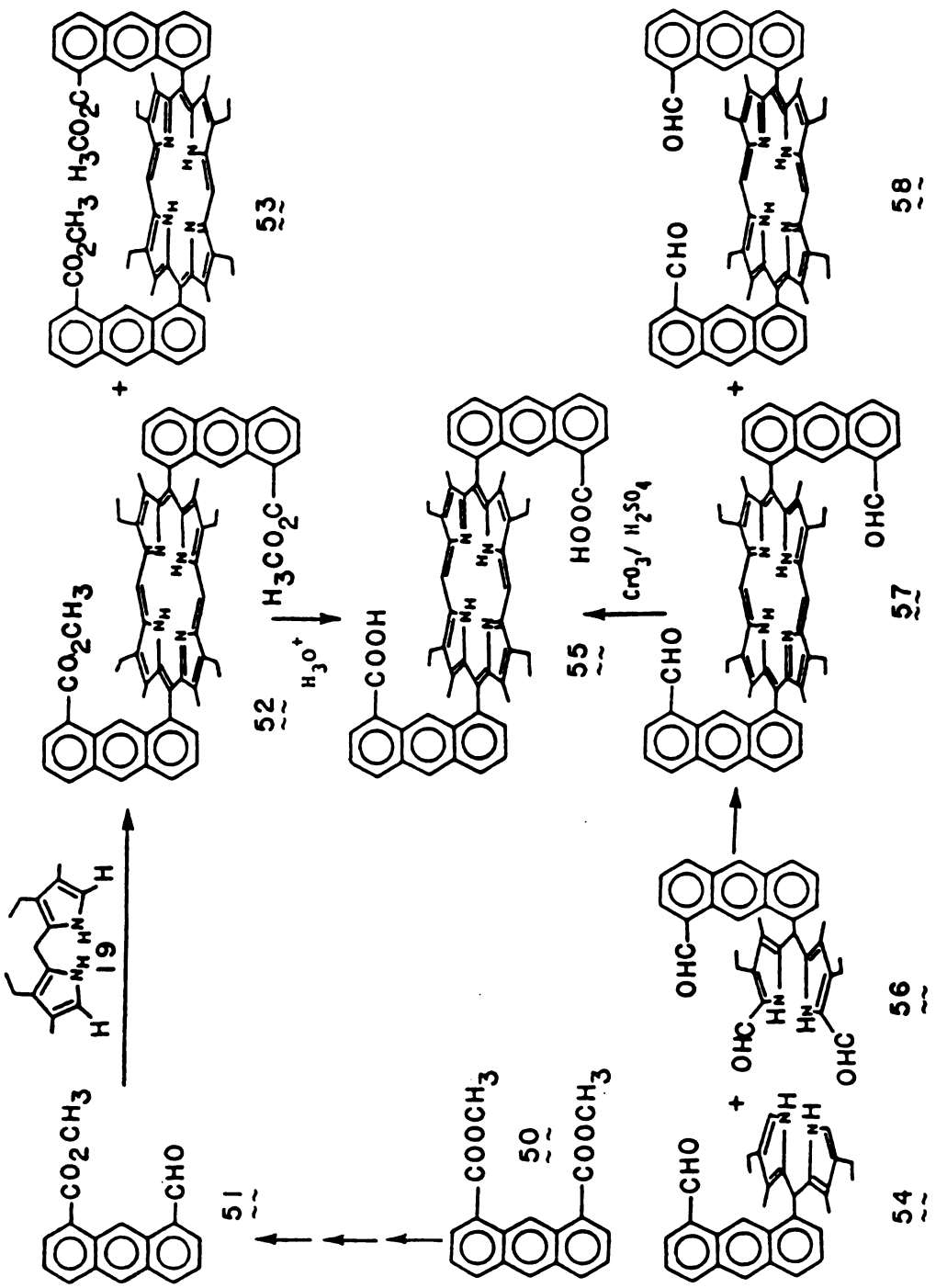

SCHEME 11

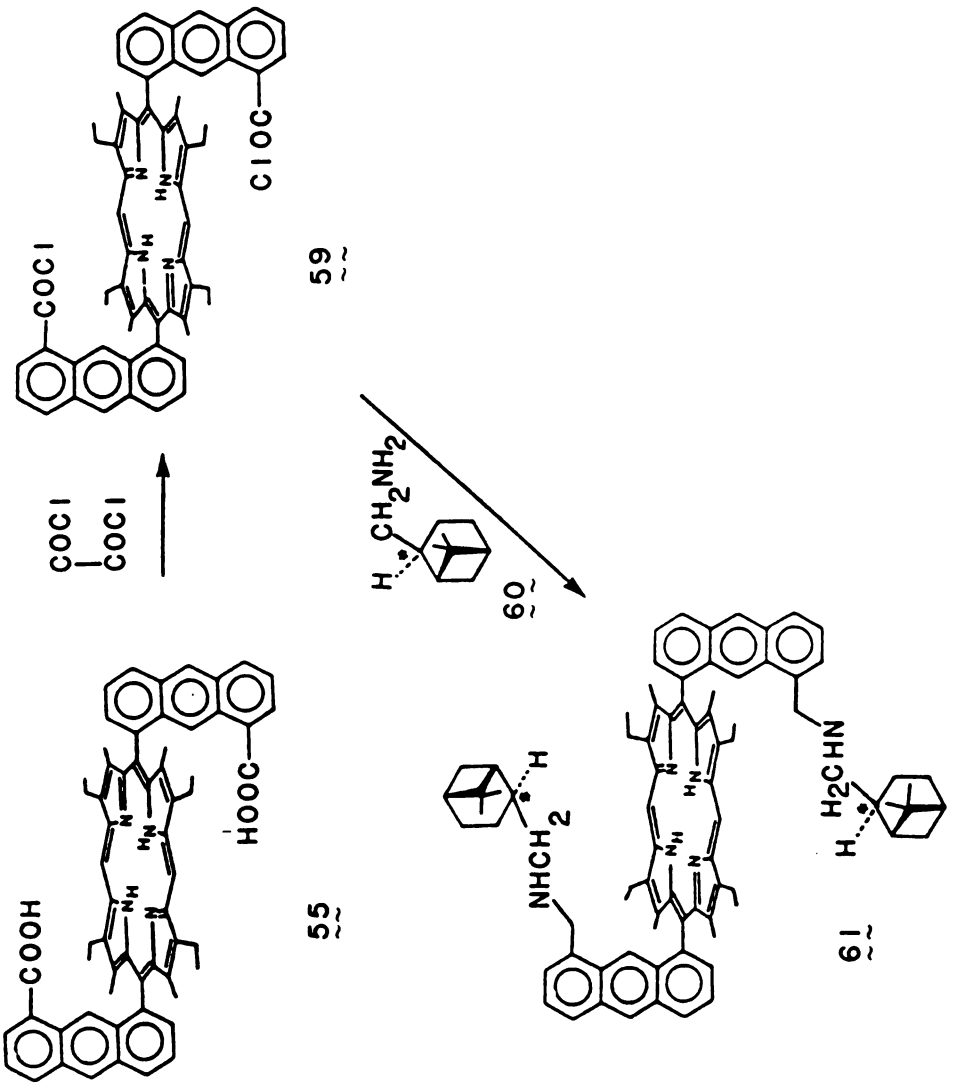

SCHEME 12

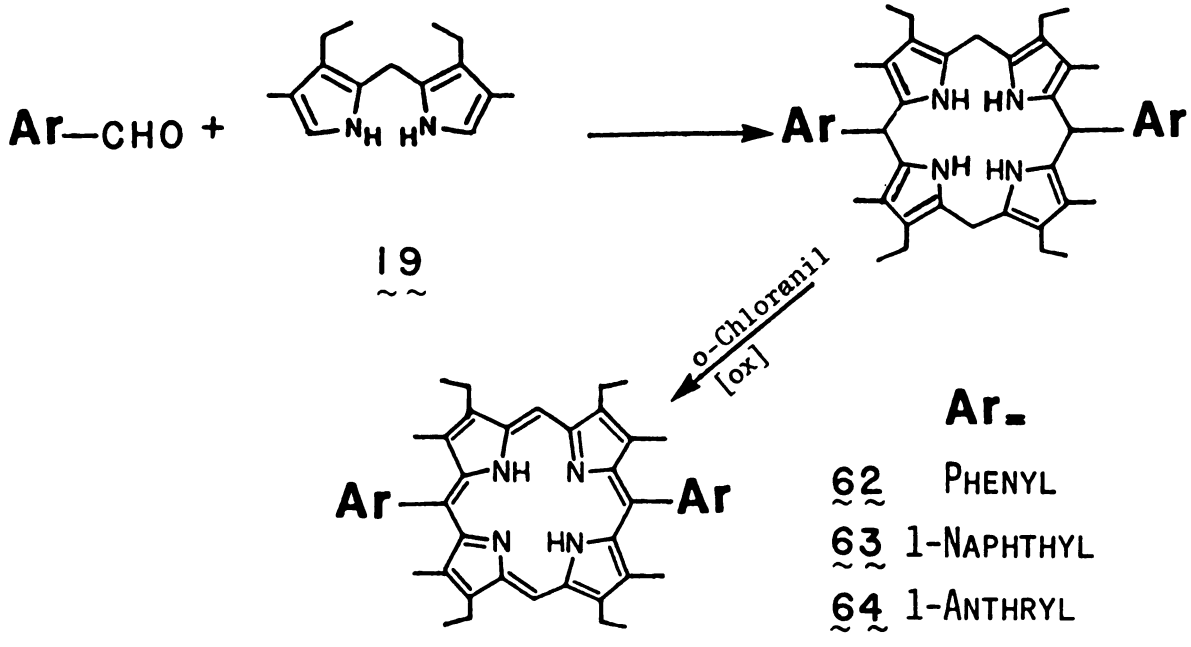

Ar=

62 PHENYL

63 1-NAPHTHYL

64 1-ANTHRYL

65 P-METHOXYPHENYL

66 8-NITRONAPHTHYL

SCHEME 13

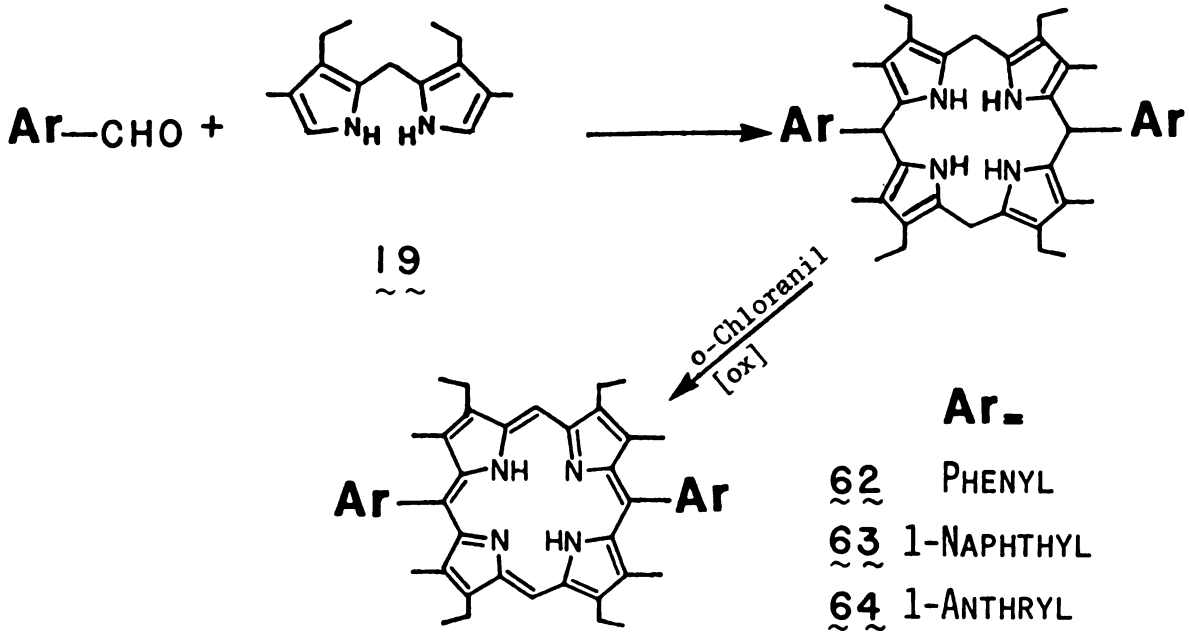

Ar-

62 PHENYL

63 1-NAPHTHYL

64 1-ANTHRYL

65 P-METHOXYPHENYL

66 8-NITRONAPHTHYL

SCHEME 13

or higher, it may lead to the insertion of chromium in the porphyrin.

The diacid porphyrin 55 was used as a precursor to introduce asymmetric substituents and to synthesize the chiral porphyrin, 61, by treatment of the diacid chloride derivative, 59, with a relatively excess amount of (-)-cis myrtanylamine 60 in dry CH_2Cl_2 (Scheme 12).

Various other meso disubstituted porphyrins were synthesized by direct coupling of the aldehyde species with 3,3′-diethyl-4,4′-dimethyl-2,2′-dipyrrylmethane (Scheme 13).

D. Metal Insertion

Metals were inserted into the free-base porphyrins according to general methods depending on the nature of the metal and the solubility of the porphyrin compounds.

In choosing these methods, we were concerned in minimizing the solubility problems, problems associated with the acidity or basisity (donor strength) of the solvent, problems caused by the intrinsic stability of the metal carrier, and problems arising from lability of the metalloporphyrin moiety under the reaction conditions.

Insertion of Copper, Zinc, Nickel and Manganese:

The complexes of these metals were prepared by addition of a saturated methanolic solution of metal(II) acetate to dichloromethane solution of the porphyrin. The product was isolated by filtration of the methanolic solution after

partial evaporation of dichloromethane.

Insertion of Iron:

Iron was inserted by the ferrous sulfate method, by heating a solution of the free-base in pyridine/acetic acid together with a saturated aqueous solution of iron(II) sulfate under argon.

Insertion of Cobalt:

Cobalt complexes were prepared by heating a saturated methanolic solution of cobaltous chloride together with a dichloromethane solution of the free-base porphyrin containing a trace amount of sodium acetate. Co(II) complexes were precipitated by graduate evaporation of dichloromethane.

Insertion of Mono-Metal in Diporphyrins:

Insertion of a single metal ion into one of the two porphyrin rings of the dimers was achieved by titrating a methylene chloride solution of the free-base diporphyrin with 1 equivalent of zinc acetate in methanol. The insertion progress was monitored by tlc. The resultant mono zinc diporphyrin was purified by chromatography.
Single metal ions, other than zinc, were then inserted by metalation of the mono zinc-free base dimer and removal of zinc, by treatment with dilute hydrochloric acid solution.

Insertion of Mixed-Metals in Diporphyrins:

In the case of mixed metal dimers, the second metal ion

complexes. The sequence of metal insertion is shown in Scheme 14.

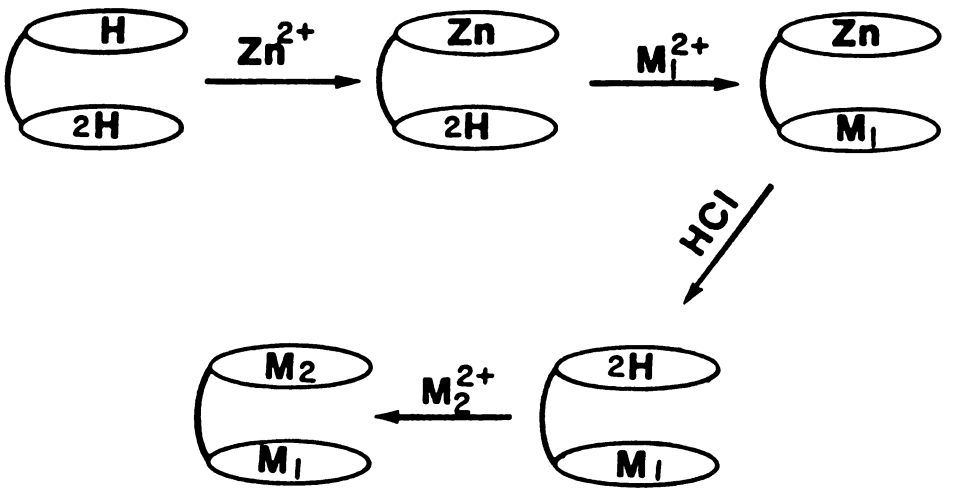

SCHEME 14

CHAPTER 3

ELECTROCHEMISTRY

CHAPTER 3

ELECTROCHEMISTRY

A. Introduction

The idea of developing metal complexe based on electro-catalysts that can efficiently mediate the multi-electron reduction of dioxygen on graphite electrodes has a great significance as such catalysts are very essential to the cathode reaction in the air-batteries (fuel cells).

Stepwise (one- or two-electron) reduction of molecular oxygen is highly unfavorable because of the involvement of relatively unstable intermediates (Figure 4). Reduction of dioxygen, which has a triplet ground state, requires over-coming the conservation of spin and orbital angular momen-tum. This problem can be circumvented by using transition metal complexes with low-lying paramagnetic states.

Upon searching for efficient catalysts for the reduc-tion of oxygen, several monometallic macrocyclic complexes have been tested [74]. The most effective macrocycles were found to contain four nitrogen donor atoms. However, these studies have revealed that none of such complexes was able to catalyze the reduction of O_2 to water, and that these single-metal complexes were capable only of reduction of

Midpoint Reduction Potentials of O_2

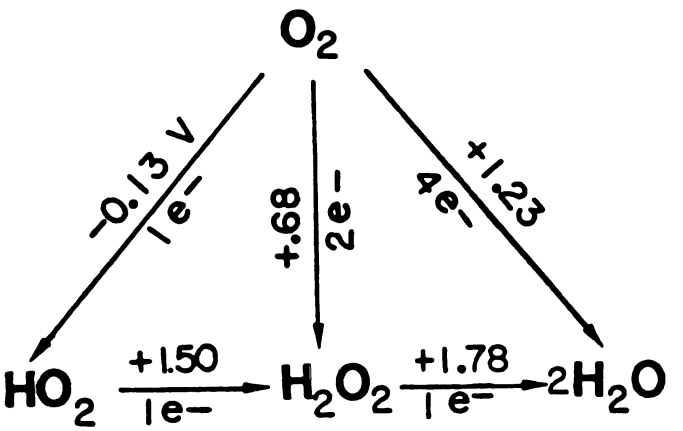

Figure 4 Standard reduction potentials of oxygen, in volts versus SHE.

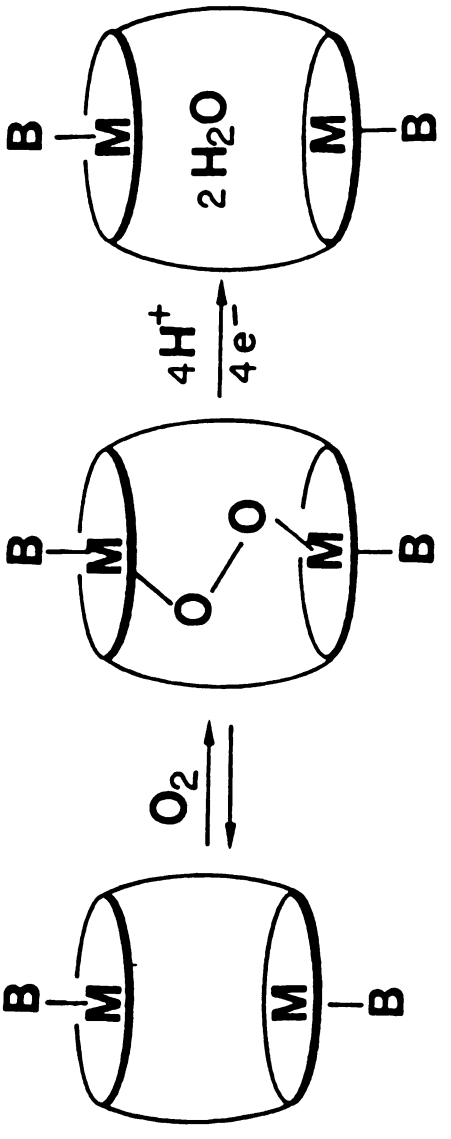

Figure 5 A proposed reaction of O_2 with cofacial binary metalloporphyrins. B is an axial ligand too bulky to fit in the cavity. Ovals represent porphyrin rings.

oxygen to hydrogen peroxide [75,76]. The two-electron reduction is the first step for the stepwise reduction of oxygen molecules to water, Equations (13) and (14)

$$O_2 + 2H^+ + 2e^- \rightleftharpoons H_2O_2 \qquad E^\circ = 0.44 \text{ V } \underline{\text{vs}}. \text{ SCE} \qquad (13)$$

$$H_2O_2 + 2H^+ + 2e^- \rightleftharpoons 2H_2O \qquad E^\circ = 1.54 \text{ V } \underline{\text{vs}}. \text{ SCE} \qquad (14)$$

However, it is the direct four-electron reduction of oxygen molecules to water that has the greatest practical application in fuel cell technology, Equation (15)

$$O_2 + 4H^+ + 4e^- \rightleftharpoons 2H_2O \qquad E^\circ = 0.99 \text{ V } \underline{\text{vs}}. \text{ SCE} \qquad (15)$$

Since the equilibrium concentration of hydrogen peroxide at the desirable operational potential of an O_2/H_2 fuel cell (+0.99 V vs. SCE) is relatively low ($\leq 10^{-18}$ M [13]), an extremely high reaction rate (i.e. driving force) is required to subsequently reduce the hydrogen peroxide to water. Therefore, more attention was focused on binuclear metal complexes in which the two metal centers may act in concert to bind and reduce oxygen by simultaneously transferring two electrons from each metal, Figure 5.

In this work, a number of cobalt monoporphyrins and diporphyrins (Figures 6 and 7) have been examined for electrochemical catalytic activity toward oxygen reduction.

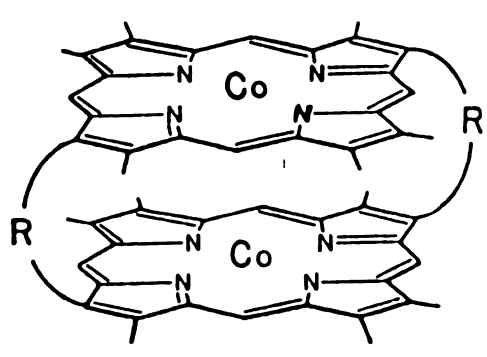

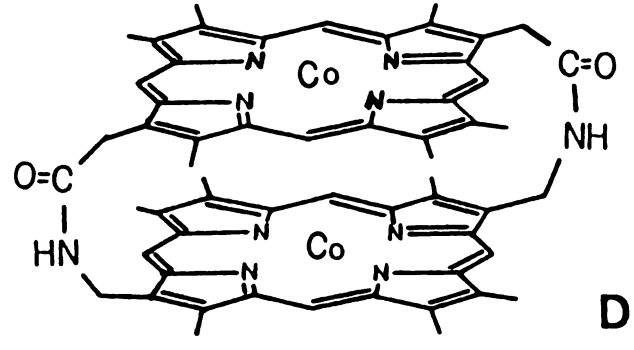

DP-4

DP-5 R= $CH_2CON(n\text{-}Bu)CH_2CH_2$

DP-6 R= $CH_2CH_2CON(n\text{-}Bu)CH_2CH_2$

DP-7 R= $CH_2CH_2CON(n\text{-}Bu)CH_2CH_2CH_2-$

Figure 6 Structures of porphyrins previously examined for electrocatalytic activity.

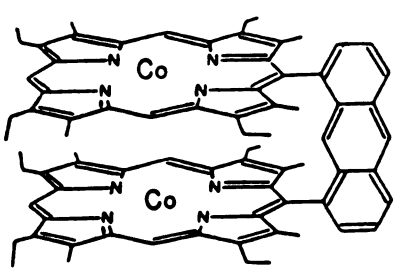

6a

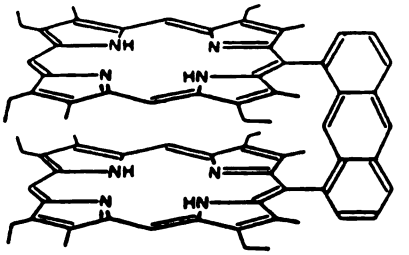

6

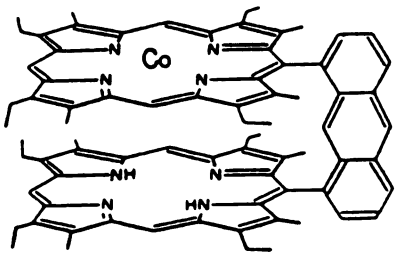

6b

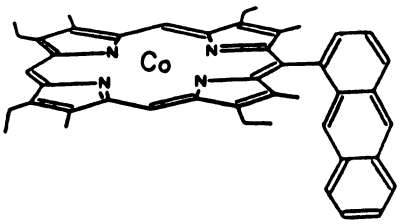

46

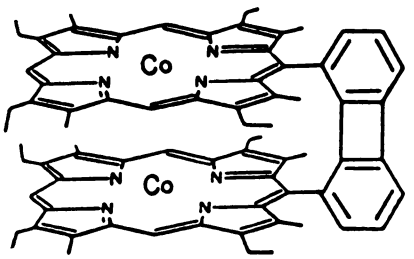

14a

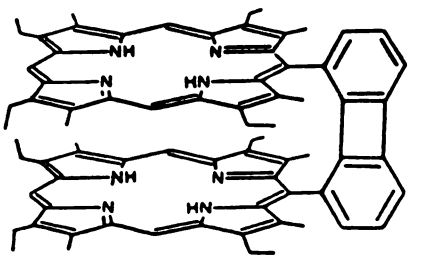

14

Figure 7 Structures of porphyrins examined in this study.

B. Rotating Ring-Disk Voltammetry

In studying the catalytic activity of the metal complexes of the cofacial diporpyrins toward the electroreduction of oxygen, we have made extensive use of the *rotating ring-disk* voltametry technique [77,78], by which it is possible to measure quantitatively the (unwanted) hydrogen peroxide production.

Figure 8 shows a schematic assembly of the ring-disk electrode which consists of a pyrolytic graphite disk with a concentric platinum ring. The porphyrin to be tested is usually applied to the graphite disk by immersing the electrode in a dilute solution of the catalyst in dichloromethane [79,80]. When the electrode is rotated, fresh electrolyte (saturated with oxygen) is drawn vertically toward the disk surface and then ejected radially across the disk to the ring. The disk potential is usually controlled by a potentiostat and the current-potential profile of the disk records the redox reaction. Meanwhile, the ring is held at a constant potential where any hydrogen peroxide reaching it is rapidly oxidized to dioxygen but no other electrode reactions take place. The ring current response thus monitors hydrogen peroxide production, and the ratio of $(-i_R/i_D N)$, where i_R and i_D are diffusion-limited currents at the ring and the disk respectively, and N is the collection efficiency of the electrode [74], can measure the relative contributions of the four-electron and

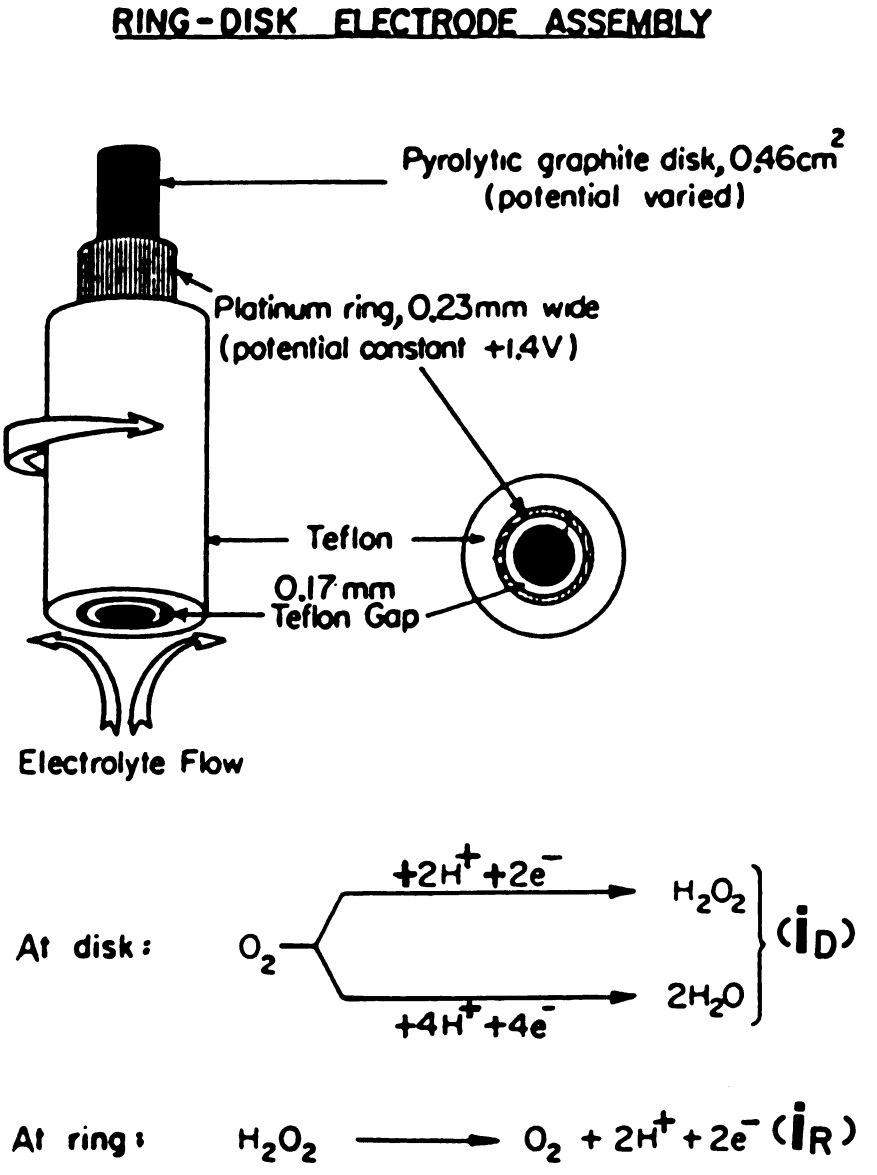

Figure 8 A schematic depiction of a rotating ring-disk electrode.

two-electron reduction process. Moreover, possible contributions to the disk current arising from subsequent reactions of H_2O_2 (reduction to water or disproportionation to dioxygen and water) may be evaluated by examining the dependence of the current ratio on electrode rotation rate. At higher rotation rates, hydrogen peroxide is removed from the disk surface before further reaction can take place, resulting in an increase in the ring current and a decrease in the disk current. Invariance of the current ratio with rotation rate indicates that H_2O_2 is formed only as a parallel product in the dioxygen reduction, and not as an intermediate [81].

The average number of electrons involved in the oxygen reduction at the disk can be obtained from the following relation

$$n_{av} = 4-2\left[\frac{-i_R}{Ni_D}\right] \qquad (16)$$

It is clear that if no ring current is detected, $i_R = 0$, then $n_{av} = 4$. If oxygen reduction at the disk entirely follows two electron pathways (i.e. to H_2O_2), $-i_R = i_DN$, then $n_{av} = 2$. The values of n can also be directly obtained from the limiting current using the Levich relation [77] or the corresponding slope of the Levich plot (i_ℓ <u>vs</u>. $(\omega)^{1/2}$.

C. Data and Results*

i) Voltammetric Responses of the Diporphyrins in the Absence of Oxygen.

The solid line in Figure 9 is a cyclic voltammogram obtained with a graphite electrode coated with dicobalt diporphyrin **6a** in the absence of dioxygen. Compounds **6b** and **14a** gave similar responses. The dashed lines resulted when the electrode was coated with the cobalt-free diporphyrin, **6**, and the dotted curve represents the response of the uncoated graphite electrode. The current peaks obtained with the bare graphite electrode arise from the reduction and oxidation of quinone-like functional groups present on the graphite surface [82] which become sharper and somewhat larger in the presence of the adsorbed diporphyrin. The prominent pair of cathodic and anodic peaks centered at ca. +0.3 V in Figure 9 probably arise from a cobalt(III/II) couple, and the less prominent pair of peaks near +0.7 V may represent the second cobalt in complex **6a**. However, the poorly resolved response at the more positive potential appears only on the first scan with a freshly

---

*This work was done in cooperation with Professor F.C. Anson and Dr. H.-Y. Liu of the California Institute of Technology.

Figure 9 *Cyclic voltammograms for 1.2×10^{-9} mol·cm^{-2} of complex 6a adsorbed on graphite electrodes: dashed line, electrode coated with cobalt free diporphyrin, 6; dotted line, background current at an uncoated electrode. Supporting electrolyte: 1 M CF_3COOH saturated with argon. Scan rate: 100 mV s^{-1}.*

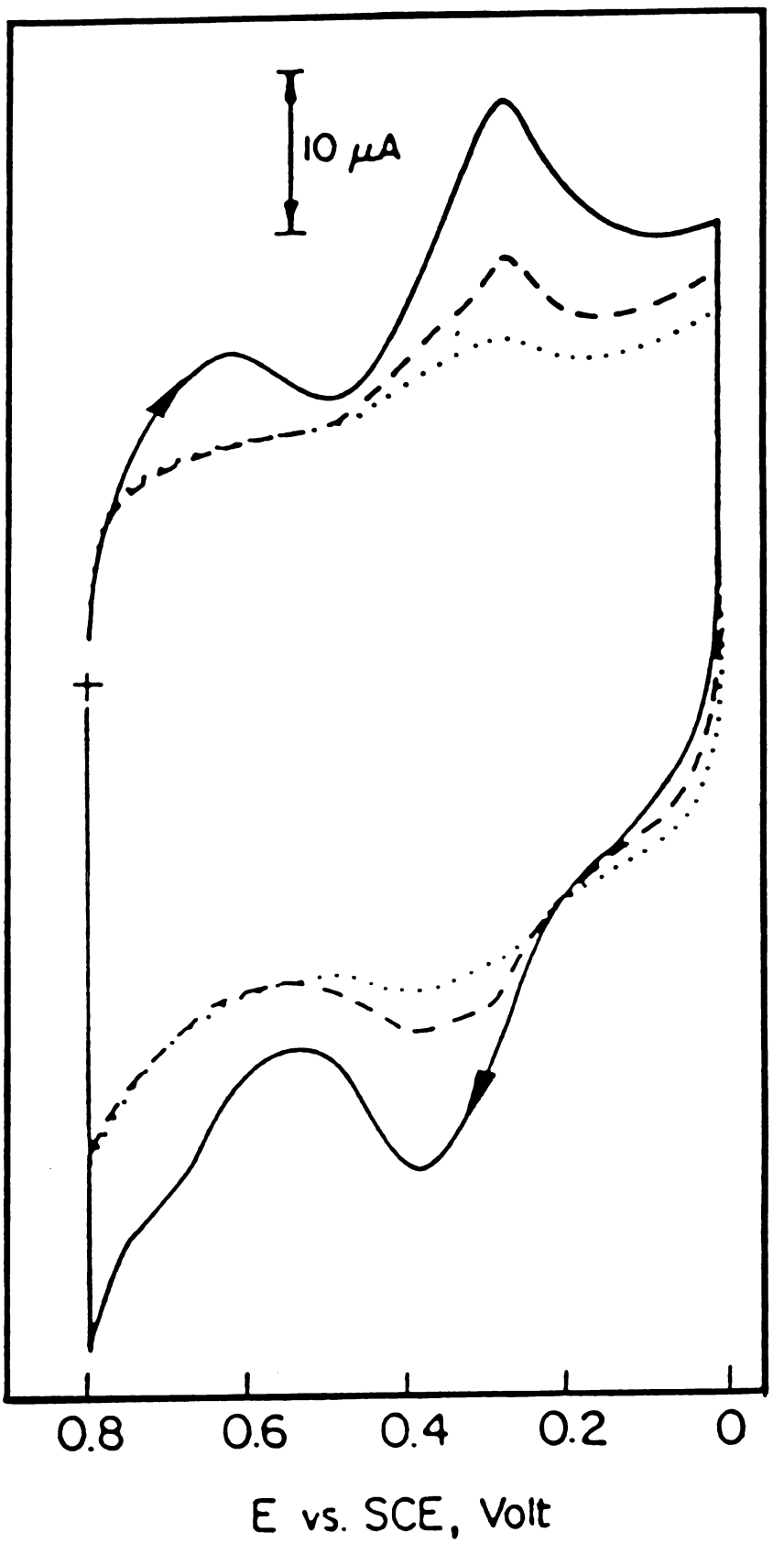
10 μA
0.8
0.6
0.4
0.2
0
E vs. SCE, Volt

polished and coated electrode while the response near +0.3 V is much more persistent. The transitory nature of the response near +0.7 V makes its assignment uncertain.

Cyclic voltammograms for a solution of compound 6a in dichloromethane (Figure 10A) exhibit two peaks in the potential range where the cobalt(III) centers are expected to be reduced. (Additional peaks appear at more positive potentials that presumably arise from ligand oxidation processes were not examined in detail.) The presence of two peaks in Figure 10A is the principle reason for our suggesting that the small peak near +0.7 V in Figure 9 makes the point at which the first cobalt (III) center in adsorbed compound 6a is reduced. The area between the solid and the dashed curves at the prominent peak near +0.3 V in Figure 9 corresponds to approximately 0.8 electron per molecule of porphyrin initially deposited on the electrode. It therefore seems unlikely that this wave corresponds to the reduction of more than one cobalt center in the molecule.

Two better formed and separate peaks are also presented in voltammograms of the analogous amide-linked dicobalt diporphyrin adsorbed on graphite electrodes. The separation in peak potentials for the two identical cobalt centers in this complex has been attributed to electronic interactions that cause the formal potentials of the two metal centers to differ [12].

Figure 10 *Cyclic voltammograms for 1.37 mM* 6a *(A),* 6b *(B), and* 6 *(C) in dichloromethane, using polished glassy carbon electrode (0.34 cm^2). Supporting electrolyte: tetrabutylammonium perchlorate. Scan rate: 100 mV s^{-1}.*

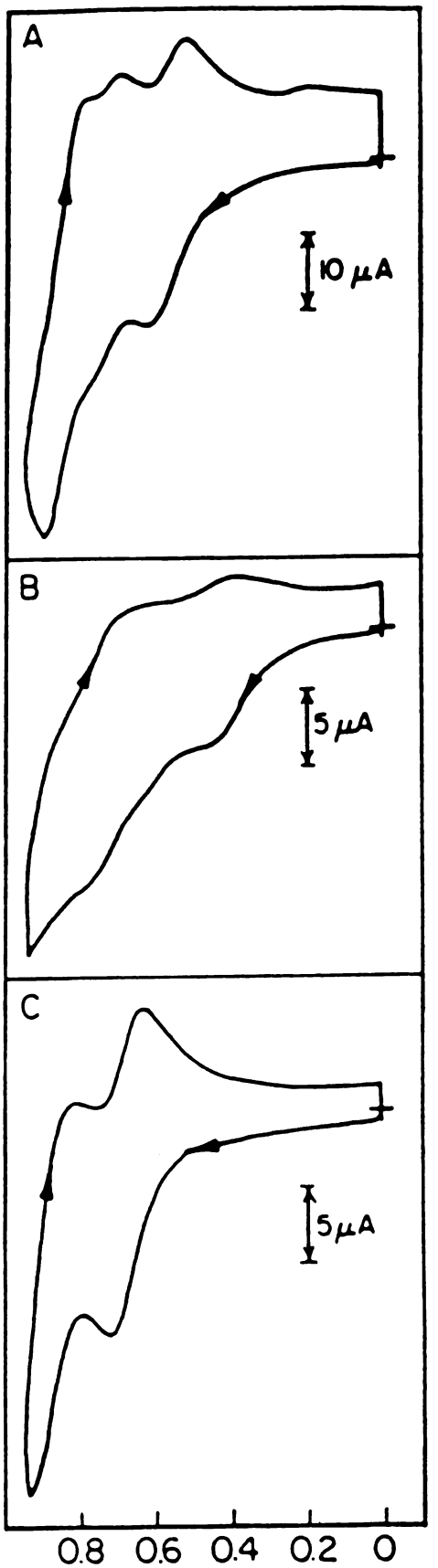
A
10 μA
B
5 μA
C
5 μA
0.8
0.6
0.4
0.2
0
E vs. SCE, Volt

Complex 6b, with only one cobalt center, yields a single prominent pair of voltammetric peaks centered near +0.35 V when adsorbed on the electrode surface. When dissolved in dichloromethane, compound 6b exhibits only poorly formed voltammograms such as that in Figure 10B. Two anodic waves are evident. The more positive wave is believed to correspond to the oxidation of the metal-free base porphyrin ring in 6b because it appears at potentials similar to that of the first oxidation wave for the metal free dimer 6. However the electrochemical responses exhibited by 6 (Figure 10C) and its various cobalt, copper, zinc, and mixed metal derivatives in dichloromethane are difficult to interpret unambiguously because the waves for the porphyrin rings are not clearly separated from those for the metal centers. No clear pattern could be discerned as to the effect of monometalation on the formal potentials for the oxidation of the metalated and unmetalated porphyrin rings. It appears that linking the two porphyrin rings by an anthracene molecule produces rather complex coupling between the two rings and metal ions present in them.

ii) Catalysis of the Reduction of Oxygen:

Current-potential responses for the reduction of O_2 at a rotating graphite disk-platinum ring electrode are shown in Figure 11. The solid curves in Figure 11A were obtained when the graphite disk was coated with 6a and the platinum ring was held at a potential where any H_2O_2 (formed at the disk and reaching the ring) would be reoxidized to O_2. The

Figure 11 *Current-potential curves for the reduction of O_2 at the rotating graphite disk-platinum ring electrode. The polished pyrolytic graphite disk was coated with 1.2×10^{-9} mol·cm^{-2} of (A) complex 6a or (B) complex 6b. Ring potential: 0.9 V. Rotation rate: 100 rpm. Supporting electrolyte 1 M CF_3COOH saturated with O_2. The disk potential was scanned at 10 mV s^{-1}. The dashed curves are the disk and ring currents obtained under the same conditions from coatings of an active amide-linked cofacial porphyrin Co_2DP-4.*

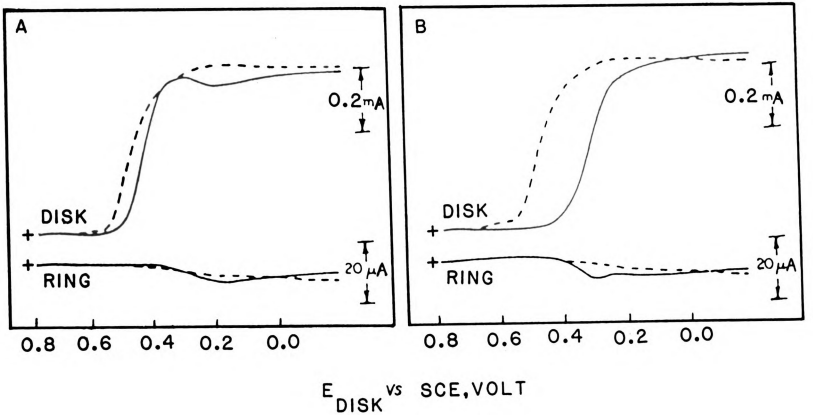
A
B
0.2mA
0.2 mA
DISK
RING
20 μA
20 μA
0.8 0.6 0.4 0.2 0.0
0.8 0.6 0.4 0.2 0.0
E DISK vs SCE, VOLT

small maximum in the disk current response was not examined in detail. Similar behavior was also observed in the case of amide-linked cofacial dicobalt porphyrins (Figure 6) and was found to be strongly dependent on the polishing procedures employed to prepare the graphite surfaces before the porphyrins were adsorbed [91]. The same was true here, the maximum became less pronounced on successive scans with the same electrode coating as the limiting current at potentials more negative than the current maximum diminished. The magnitude of the current maximum was a function of the rate at which the potential was scanned; this is not present under true steady-state conditions. These features suggest that the current maximum may result from a small fraction of the adsorbed porphyrin catalysts that temporarily exhibits a higher activity toward the reduction of O_2. That the polishing procedure used to prepare the graphite surface strongly influences the prominence of the maximum indicates that interactions of the cobalt centers with functional groups present on the graphite surface may alter the activity of the catalyst.

The most noteworthy feature of the disk and ring currents in Figure 11A is their demonstration that the O_2 reduction yields very little H_2O_2 at potentials near +0.45 V, and even at +0.2 V the ratio of ring to disk currents indicates that relatively little of the O_2 is reduced to H_2O_2. Thus the dimeric cobalt porphyrin, 6a, provides a four-electron-reduction pathway for oxygen.

We were surprised to find that compound **6b**, with only one cobalt ion present in the dimeric porphyrin ligand, is also capable of catalyzing the four-electron pathway for the reduction of O_2. The rotating ring-disk current-potential curves for O_2 reduction with this catalyst are shown as the solid curves in Figure 11B. The disk current is as large as that obtained with the dicobalt catalyst, and there is very little ring current. The major differences between the responses obtained with electrodes coated with **6a** or **6b** are the less positive potential at which the O_2 reduction commences for catalyst **6b** and the slightly more gradual approach to the limiting current plateau. For comparison, the dashed curves in Figure 11 show the responses that result when the most active form of the amide-linked cofacial dicobalt catalyst described [83] previously was applied to the same polished graphite disk electrode. The reduction commences at slightly more positive potentials than with **6a** and significantly more positive than with **6b**, but the limiting disk currents are about the same for all three catalysts and exceed substantially the value corresponding to the two-electron reduction of O_2.

Levich [84] and Koutecky-Levich [85] plots of the plateau currents and electrode rotation rates for the reduction of O_2 at electrodes coated with **6a** and **6b** are shown in Figure 12. As the electrode rotation rate increases, catalyst **6b**, with only a single cobalt center, is able to

sustain notably larger plateau currents than catalyst 6a. The nonlinearity of the Levich plots (Figure 12A) with increasing curvature at higher rotation rates signals the likely presence of a chemical step that precedes the electron transfer and limits the current to values below the convection diffusion limit. Previous studies [12] have assigned the current limiting step to the formation of a cobalt(II)-O_2 adduct that is the reducible species. The Koutecky-Levich plots in Figure 12B, while linear, have slopes that differ somewhat from that of the dashed line calculated for the four-electron reduction of oxygen. The difference in slopes is in the direction expected if O_2 were reduced to a mixture of H_2O and H_2O_2 at the catalyst-coated electrodes. This is also consistent with the magnitudes of the anodic ring currents at potentials on the plateaus of the disk current-potential curves in Figure 11.

The presence of a mixed reaction pathway complicates the interpretation of the intercept of the Koutecky-Levich plots in Figure 11B. However, the ring-disk curves in Figure 11A indicate that the major pathway must involve four electrons. On this basis, it is possible to obtain an approximate value of the rate constant, k, governing the current-limiting chemical reaction from Equation 17 [12]

$$k = \frac{i_F}{4F\Gamma_{cat} C_{O_2}} \qquad (17)$$

Figure 12 *Levich (A) and Koutecky-Levich (B) plots of the plateau current for the reduction of oxygen at graphite electrodes coated with* 1.2×10^{-9} *mol·cm*$^{-2}$ *of complex* $\underset{\sim\sim}{6a}$ [■] *or complex* $\underset{\sim\sim}{6b}$ [●]. *Supporting electrolyte: 1 M* CF_3COOH *saturated with air. The dashed lines are the calculated responses for the correction-diffusion limited reduction of* O_2 *by four electrons, taking* $[O_2] = 0.24$ *mM and* $D_{O_2} = 1.8 \times 10^{5}$ *cm*^{2} *s*$^{-1}$.

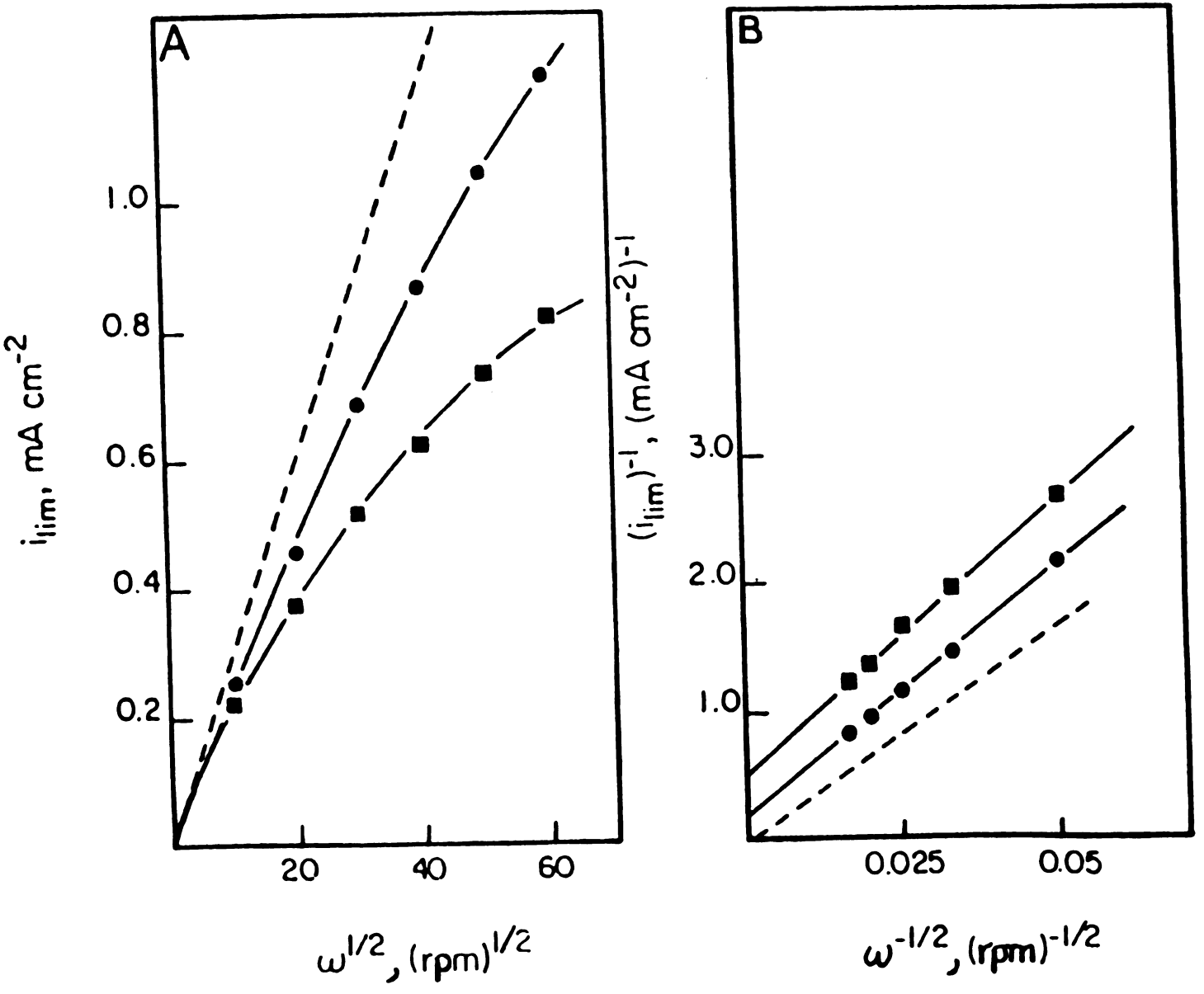
A
B
1.0
0.8
0.6
0.4
0.2
20
40
60
i_{lim}, mA cm^{-2}
$\omega^{1/2}$, (rpm)$^{1/2}$
3.0
2.0
1.0
0.025
0.05
$(i_{lim})^{-1}$, (mA cm^{-2})$^{-1}$
$\omega^{-1/2}$, (rpm)$^{-1/2}$

where i_F is the reciprocal intercept of the Koutecky-Levich plot, F is Faraday's constant, Γ_{cat} is the quantity of a catalyst adsorbed on the electrode, and C_{O_2} is the concentration of O_2 in the solution. The values of k obtained from the intercept of the lines in Figure 12B are 2×10^4 and 5×10^4 M^{-1} s^{-1} for catalysts 6a and 6b, respectively. These values are somewhat smaller than the value of 3×10^5 M^{-1} s^{-1} measured previously for the amide-linked cofacial dicobalt porphyrin [12]. Thus the rate of reaction between O_2 and complex 6a may be somewhat slower than it is with the doubly linked analogue despite the greater cavity accessibility suggested by the more open structure of the former complex. However, the uncertainties in the values of Γ_{cat} and the presence of mixed reaction pathways render this conclusion very tentative.

iii) pH Dependence of O_2 Reduction:

The course of the catalyzed reduction is influenced significantly by changes in the pH of the supporting electrolyte. Disk plateau currents at electrodes coated with 6a or 6b are plotted in Figure 13 as a function of pH. At electrodes coated with 6a the current decreases somewhat between pH 0 and 2 but then remains essentially constant up to pH 12 before decreasing to about one-half of its initial value at pH 14. The currents obtained up to pH 12 are significantly larger than the two-electron diffusion-convection limited value so that 6a continues to provide a four-electron reduction of O_2. As the pH is raised, an

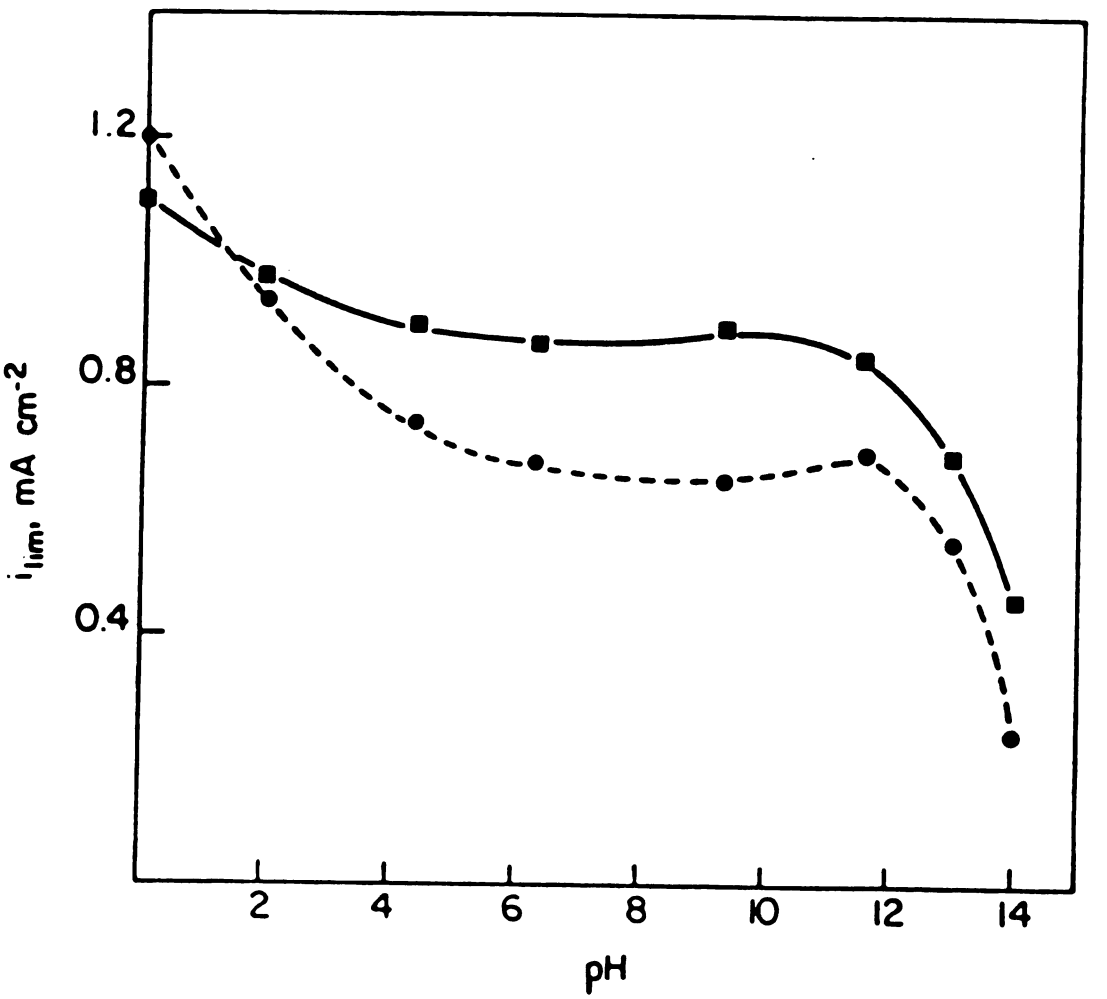

Figure 13 *pH Dependence of plateau currents for the reduction of O_2 at rotating graphite disk electrodes coated with 1.2×10^{-9} mol·cm^{-2} of complex 6a [●] or complex 6b [■]. Electrode rotation rate: 100 rpm. Other conditions as in Figure 12.*

increasing fraction of O_2 is reduced to H_2O_2 instead of H_2O.

iv) Catalysis of the Reduction of H_2O_2:

If the monocobalt diporphyrin, **6b**, were a catalyst for the reduction of H_2O_2 to H_2O at potentials close to those where it catalyzes the reduction of O_2, an explanation for the unexpectedly large limiting current in Figure 11B would be at hand. This possibility would be consistent with the appearance of a small ring current in Figure 11B if **6b** catalyzed the reduction to H_2O_2 at a much lower rate than it catalyzes the reduction of O_2. The slight rise in disk current and corresponding decrease in ring current at potentials less positive than ca. +0.1 V in Figure 11A suggest that **6a** may also function as a catalyst for the electroreduction of hydrogen peroxide to water [45]. Since most previous studies have not reported pronounced catalytic activity of cobalt porphyrins toward H_2O_2 reduction [86,87], we examined this point in some detail.

Shown in Figure 14A are current-potential curves for the reduction of H_2O_2 at a rotated graphite disk electrode before (curve 1) and after it was coated with **6a** (curve 2) or **6b** (curve 3). The potential of the electrode was held at values no more positive than +0.45 V between scans to avoid the formation of O_2 by oxidation of the H_2O_2. It is clear from curves 1, 2 and 3 in Figure 14A that both **6a** and **6b** are catalysts for the reduction of H_2O_2. However, even with the low rotation rates employed, the plateau currents

are much smaller than the calculated diffusion-convection limited Levich current [84] for a two-electron reduction process. This is evident from the Levich and Koutecky-Levich plots shown in Figure 14 B and C, respectively. Thus, a slow chemical step preceding the electron transfer reactions apparently limits the magnitude of the plateau currents for the reduction of H_2O_2 as well as O_2. That the rate of the preceding chemical step is much slower in the case of H_2O_2 is evident from the large intercepts of the lines in Figure 14C. It is conceivable that 6a and 6b catalyze the disproportionation of H_2O_2 so that the electrode reaction proceeding during its reduction involves only the reduction of O_2 as in Figure 11. We regard this possibility as unlikely, however, because the potentials where the catalyzed reduction of H_2O_2 commences in Figure 14A are significantly less positive than those where O_2 is reduced (Figure 11). If the totally irreversible reduction of H_2O_2 occurred by its prior disproportionation to O_2 and H_2O, the reduction would be expected to commence at about the same potential where O_2 is reduced. Only a potential dependence of the disproportionation reaction could alter this conclusion, and there is no reason to invoke such a potential dependence at potentials that are removed from those where the cobalt centers in the adsorbed porphyrins exhibit their redox activity.

The lack of significant catalysis of the disproportionation of H_2O_2 by complex 6a and 6b adsorbed on the

Figure 14 *(A) Current-potential curves for the reduction of 1 mM H_2O_2 at rotated graphite disk electrodes: uncoated electrode (1); electrode coated with 1.2×10^{-9} mol·cm^{-2} of complex 6a (2); complex 6b (3); or complex 46 (4). Supporting electrolyte: 1 M CF_3COOH saturated with argon. (B) Levich plots for H_2O_2 reduction as catalyzed by complex 6a [●] or complex 6b [▲]. (C) The corresponding Koutecky-Levich plots. The dashed lines were calculated for the diffusion-convection limited reduction by two electrons.*

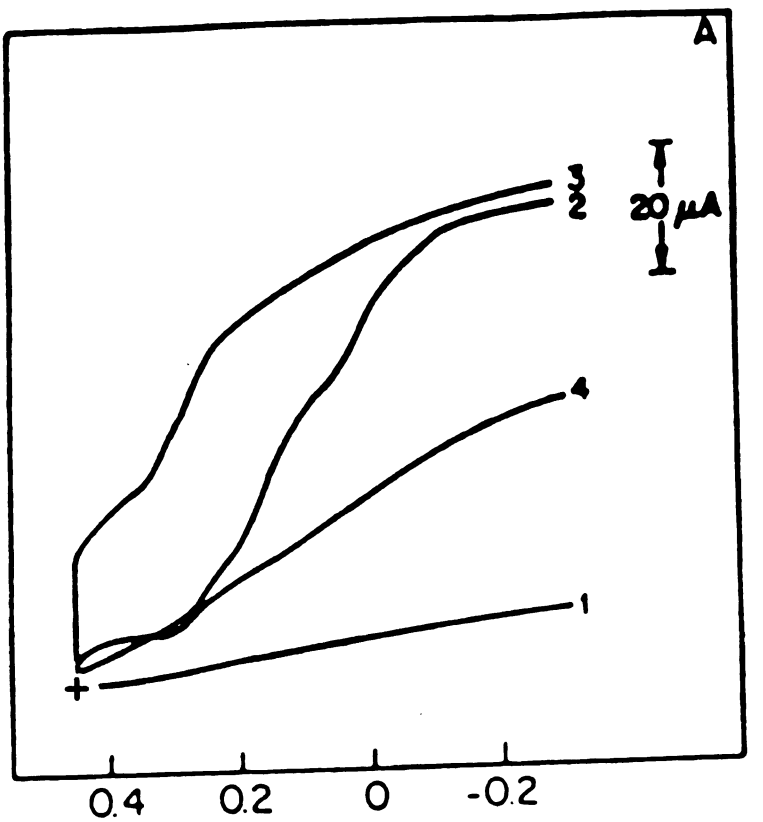
A
3
2
20 μA
4
1
+
0.4
0.2
0
-0.2
E vs. SCE, Volt

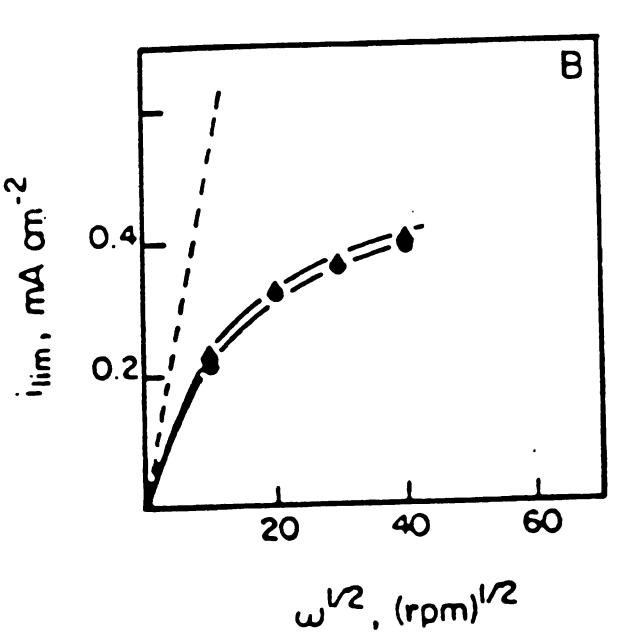
B
i_{lim}, mA cm^{-2}
0.4
0.2
20
40
60
$\omega^{1/2}$, (rpm)$^{1/2}$

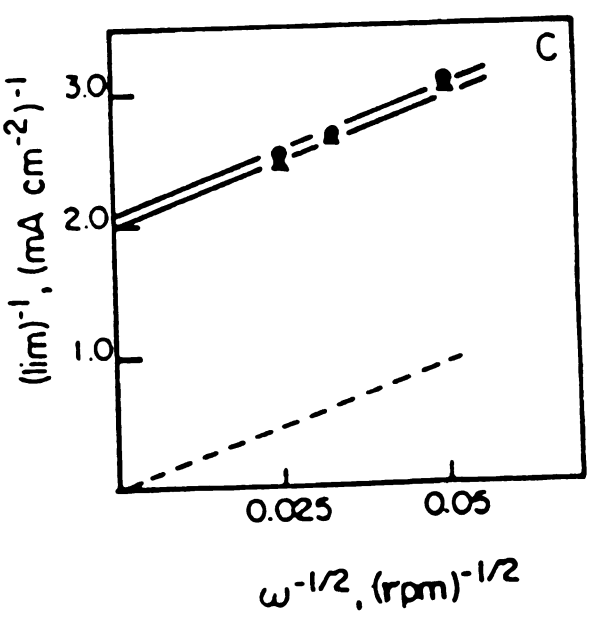
C
$(i_{lim})^{-1}$, (mA cm^{-2})$^{-1}$
3.0
2.0
1.0
0.025
0.05
$\omega^{-1/2}$, (rpm)$^{-1/2}$

graphite disk was also demonstrated by means of the rotating ring-disk electrode in a dioxygen-free solution of H_2O_2. The anode current measured at the platinum ring at +0.9 V was essentially the same when the graphite disk (not connected to the potentiostat) was coated with complex **6a** or **6b** as when it was uncoated. This was true with rotation rates as low as 400 rpm. Disproportionation of the H_2O_2 at the surface of the disk would have produced a decrease in ring current so that the equality of the ring currents in the two experiments indicates that the disproportionation reaction proceeds too slowly to be important in these experiments.

v) pH Dependence of H_2O_2 Reduction:

The catalytic activities of **6a** and **6b** toward the reduction of H_2O_2 show notably different pH dependences. Plateau currents at disk electrodes coated with each catalyst and rotated at low rate are shown in Figure 15. **6a** sustains small disk currents over a wide pH range while with **6b** a decline in current begins as early as pH 2. Both complexes become relatively inert for H_2O_2 reduction above pH 12. The difference in pH dependences of the activities of the two catalysts toward the reduction of H_2O_2 helps to explain the corresponding differences in the overall rates with which they catalyze the reduction of O_2 in the pH range from ca. 2 to 12 (Figure 13). Complex **6b** loses its activity for the reduction of H_2O_2 in the same pH range where it yields diminished plateau currents for the reduc-

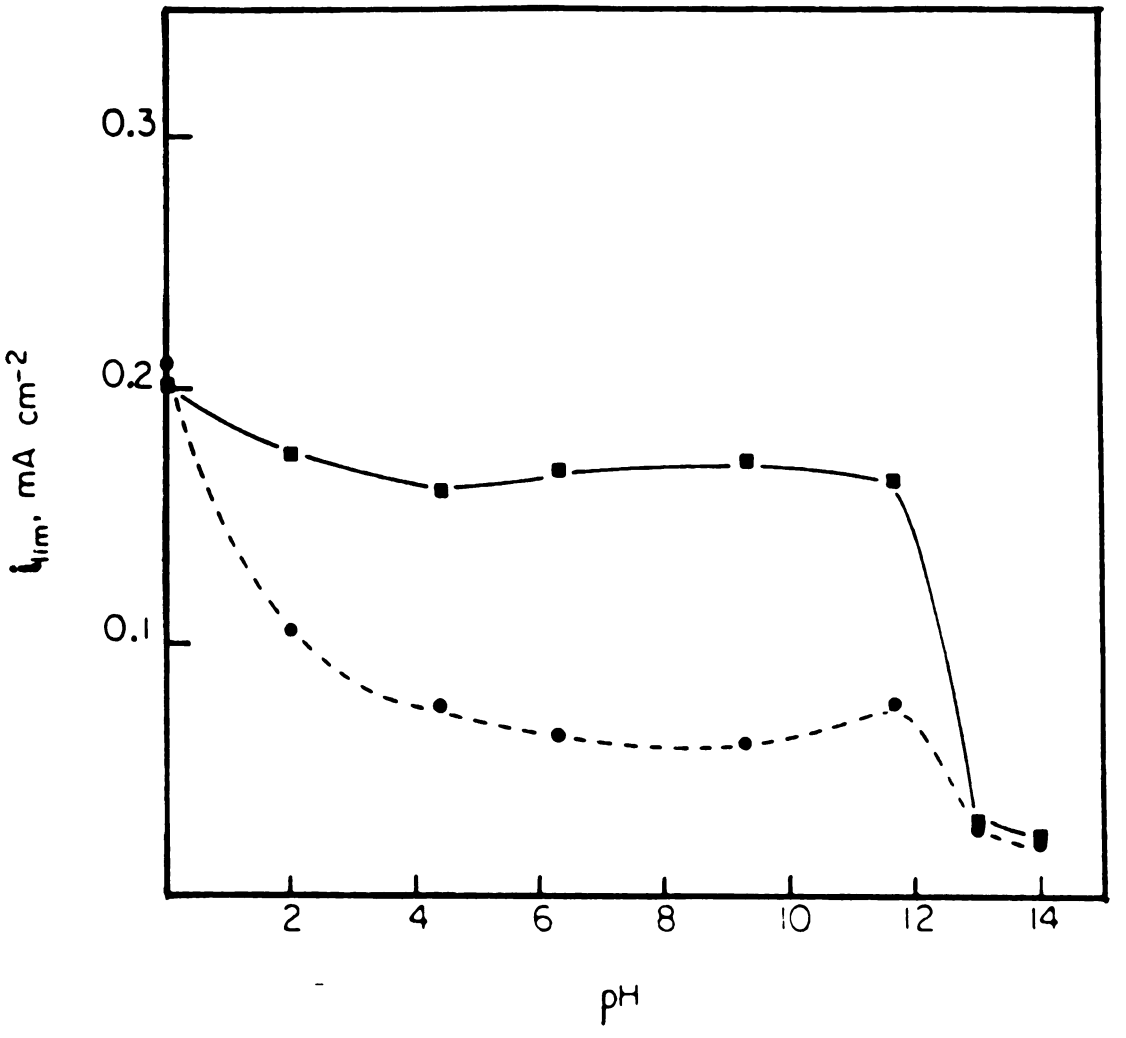

Figure 15 pH Dependence of plateau currents for the reduction of 1 mM H_2O_2 at rotating graphite disk electrodes coated with 1.2×10^{-9} mol·cm^{-2} of complex 6a [■] or complex 6b [●]. Supporting electrolytes at each pH as in Figure 10. Rotating rate: 400 rpm.

tion of O_2 (Figure 13). If the catalyzed reduction of O_2 by complex 6b involved the production of H_2O_2 as an intermediate one would expect less disk current than if the reaction proceeded directly to H_2O_2 (as with compound 6a).

H_2O_2 exhibits a preference to react with transition-metal reductants by inner-sphere pathways [88]. It seems likely, therefore, that coordination of H_2O_2 to the cobalt center in the porphyrin catalysts precedes its catalyzed reduction. The alternative, outer-sphere pathway in which the cobalt(II) porphyrin transfers an electron to an uncoordinated H_2O_2 molecule is incompatible with the potentials where the catalyzed reduction proceeds: In 1 M CF_3COOH 6a catalyzes H_2O_2 reduction at potentials significantly more negative than those where the first cobalt(III) center is reduced to cobalt(II) and 6b also exhibits catalytic activity at potentials less positive than that where the cobalt(II) porphyrin is first generated (compare Figures 9 and 14A). The cobalt(II) center in the porphyrin is essential; the metal-free diporpyrin ligand and its dicopper(II) derivative are both inert toward the reduction of H_2O_2.

D. Discussion

Complexes 6a and 6b catalyze the electroreduction of H_2O_2 at a much lower rate than they catalyze the electroreduction of O_2. This is apparent from a comparison of the normalized intercepts of the Koutecky-Levich plots in

Figures 12B and 14C. Both the magnitude and the disk current for the reduction of O_2 by complex 6a in Figure 11A and the lack of ring current on the rising part of the reduction wave at the disk electrode require that the O_2 be reduced to H_2O, not to H_2O_2. It follows that the mechanism of the four-electron reduction of O_2 by catalyst 6a cannot involve uncoordinated H_2O_2 as an intermediate. Any H_2O_2 that was released into the solution would be subsequently reduced at the disk too slowly to provide the high disk current observed in Figure 11A or to escape detection at the ring electrode. This assertion was supported by experiments where both O_2 and H_2O_2 were reduced simultaneously at electrode coated with catalyst 6a (Figure 16). At the same point, e.g., -0.3 V, where the O_2 present reduced primarily to H_2O at a high rate, H_2O_2 present in the solution was reduced much more slowly and the simultaneous reduction of O_2 had virtually no effect on the rate of the reduction of H_2O_2 (compare A and C in Figure 16). The two oxidants seem clearly to undergo catalytic reduction by independent pathways.

The catalysis of O_2 reduction to H_2O by complex 6a could involve the coordination of both cobalt centers to the O_2 molecule with the formation of μ-peroxo intermediate (Figure 17). Such an intermediate is not likely to be formed if the source of oxygen is H_2O_2 instead of O_2, especially in acidic solutions. Accordingly, the catalyzed reduction of H_2O_2 probably involves its coordination to a

Figure 16 *Plateau currents for the simultaneous reduction of O_2 and H_2O_2 at a rotating graphite disk electrode coated with 1.2×10^{-9} mol·cm^{-2} of* 6a. *(A) reduction of H_2O_2 in the absence of O_2; (B) repeat of (A) after the solutions were saturated with O_2; (C) difference between the plateau currents in (B) and that for an O_2-saturated solution in the absence of H_2O_2. Supporting electrolyte: 1 M CF_3COOH. Electrode rotating rate: 400 rpm. Plateau currents measured at -0.3 V.*

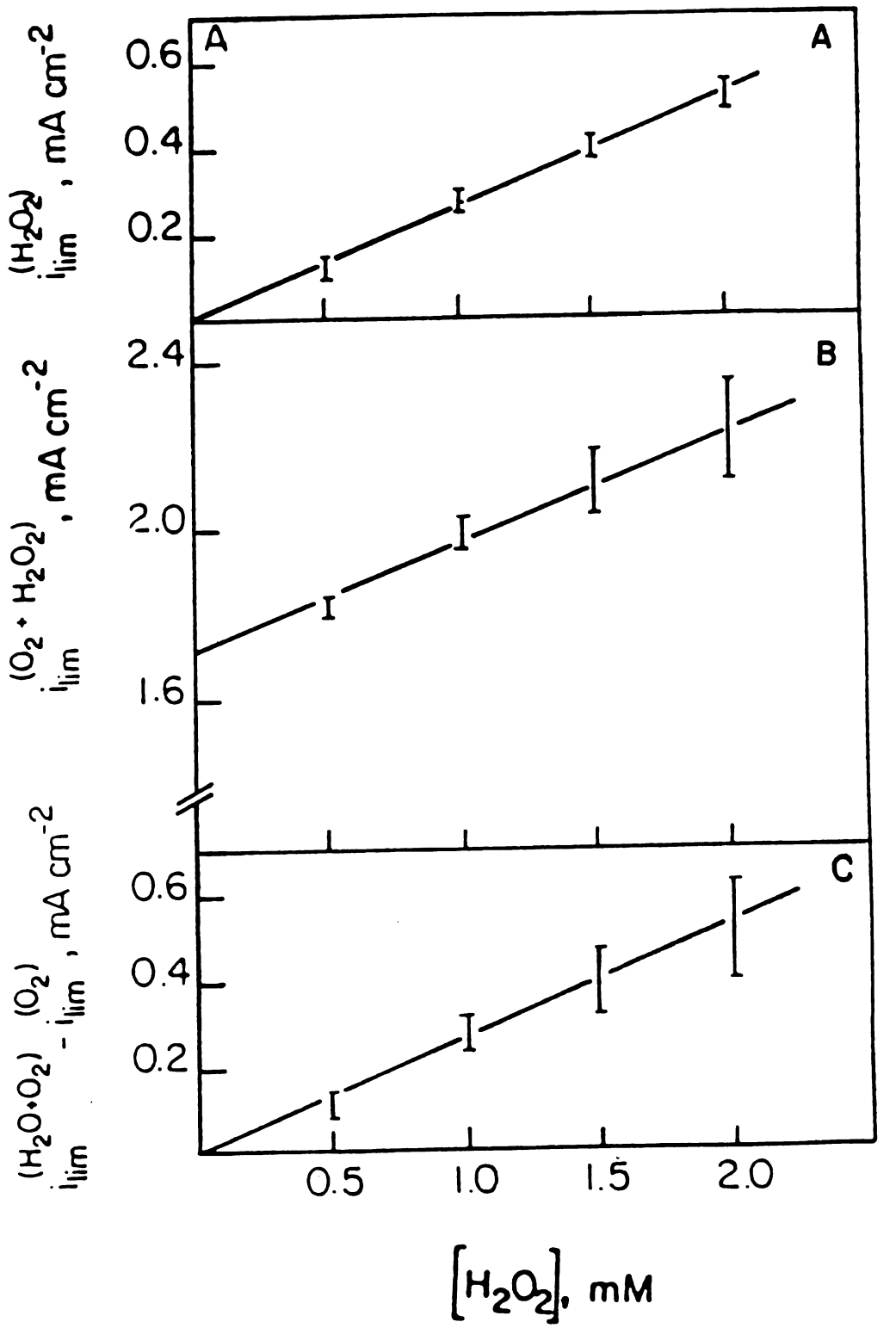
A
B
C
0.6
0.4
0.2
2.4
2.0
1.6
0.5
1.0
1.5
2.0
$i_{lim}^{(H_2O_2)}$, mA cm^{-2}
$i_{lim}^{(O_2+H_2O_2)}$, mA cm^{-2}
$i_{lim}^{(H_2O+O_2)} - i_{lim}^{(O_2)}$, mA cm^{-2}
$[H_2O_2]$, mM

Figure 16 *Plateau currents for the simultaneous reduction of O_2 and H_2O_2 at a rotating graphite disk electrode coated with 1.2×10^{-9} mol·cm^{-2} of* 6a. *(A) reduction of H_2O_2 in the absence of O_2; (B) repeat of (A) after the solutions were saturated with O_2; (C) difference between the plateau currents in (B) and that for an O_2-saturated solution in the absence of H_2O_2. Supporting electrolyte: 1 M CF_3COOH. Electrode rotating rate: 400 rpm. Plateau currents measured at -0.3 V.*

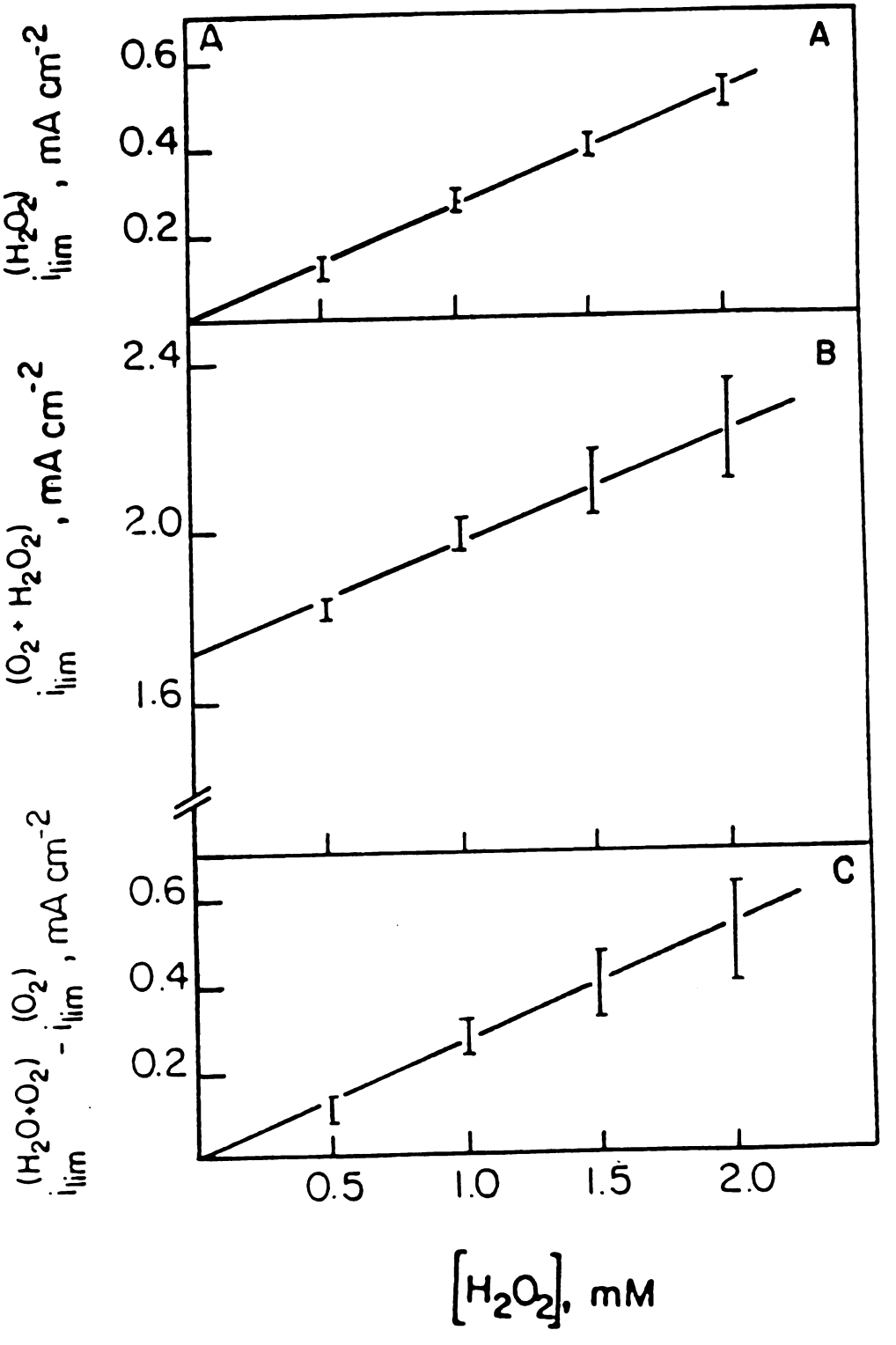
A
B
C
0.6
0.4
0.2
2.4
2.0
1.6
0.5
1.0
1.5
2.0
$i_{lim}^{(H_2O_2)}$, mA cm^{-2}
$i_{lim}^{(O_2+H_2O_2)}$, mA cm^{-2}
$i_{lim}^{(H_2O+O_2)} - i_{lim}^{(O_2)}$, mA cm^{-2}
$[H_2O_2]$, mM

single cobalt center. This would be compatible with the comparable activities toward H_2O_2 exhibited by catalyst 6a and 6b. The smaller limiting currents obtained with 6A and 6b and 4b for the reduction of H_2O_2 compared to that of O_2 would then reflect the lower rate of coordination of H_2O_2 to the cobalt centers in these catalysts.

The extensive four-electron O_2 reduction activity exhibited by 6b was surprising because the analogous doubly amide-bridged cofacial porphyrin containing only a single cobalt center had been reported to serve only as a two-electron reduction catalyst [12]. However, more recent experiments with greater quantities of more thoroughly purified material have shown that the monocobalt cofacial porphyrin does support a four-electron reduction of O_2 [89]. Its four-electron activity declines within a few minutes, and this was one reason why its capacity to catalyze the four-electron reduction was overlooked in the previous studies.

The anthracene bridging group in 6b is not the source of the enhanced activity because the monomeric porphyrin 46a (Fig. 7), shows essentially the same behavior as other monomeric cobalt porphyrins in catalyzing the two-electron reduction of O_2 to H_2O_2 with a further reduction to H_2O proceeding at a much lower rate (Figure 14A, curve 4). The higher activity of 6b toward the four-electron reduction of O_2 might arise from the proximity of the second porphyrin ring that should be protonated in the acidic medium

Figure 17 *A proposed mechanism for the four-electron pathway of the O_2-reduction to water, catalyzed by dicobalt complexes of cofacial diporphyrins in acidic media.*

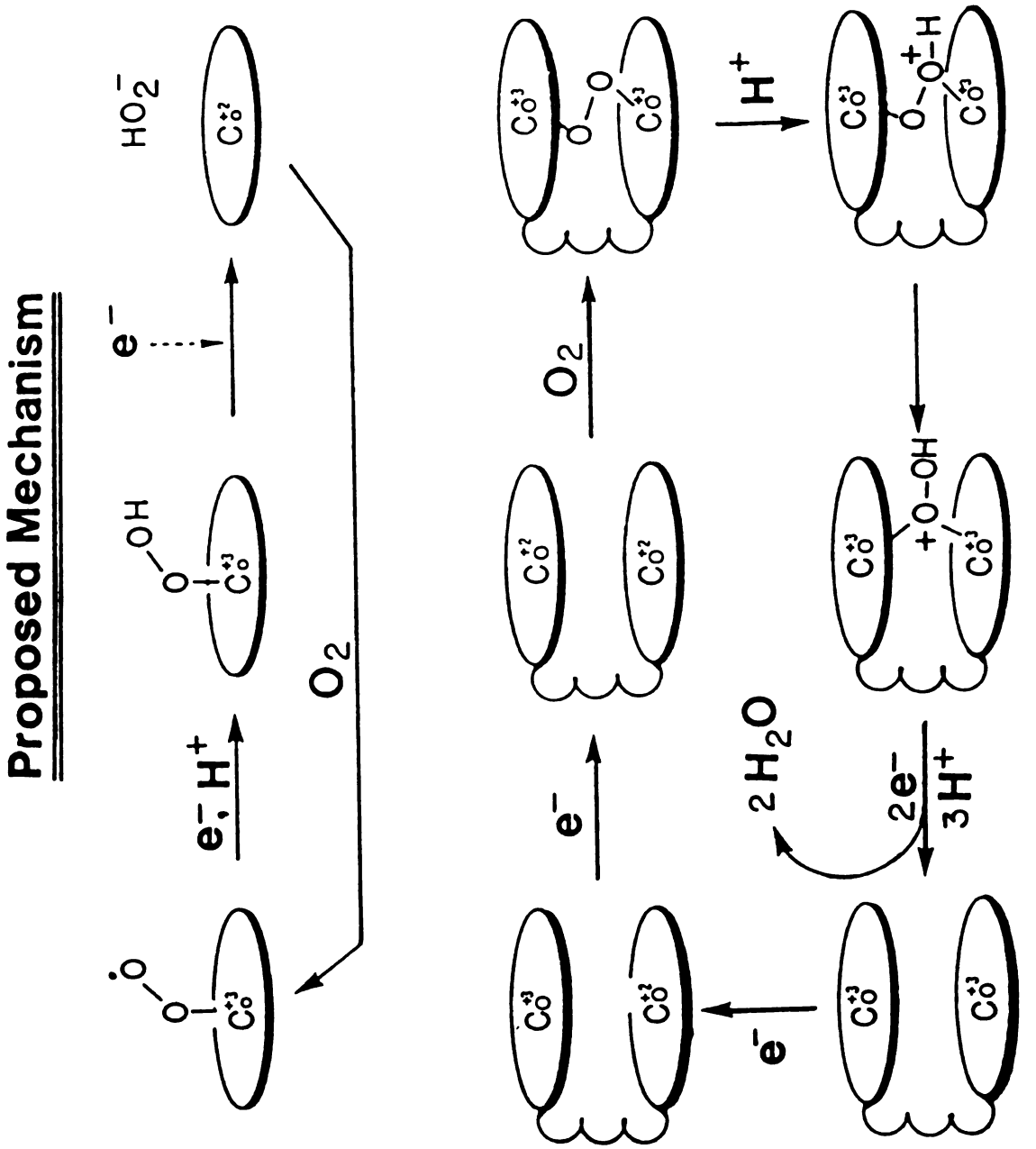
Proposed Mechanism
HO_2^-
e^-
$e^-; H^+$
O_2
O_2
H^+
e^-
e^-
$2H_2O$
$2e^-$
$3H^+$

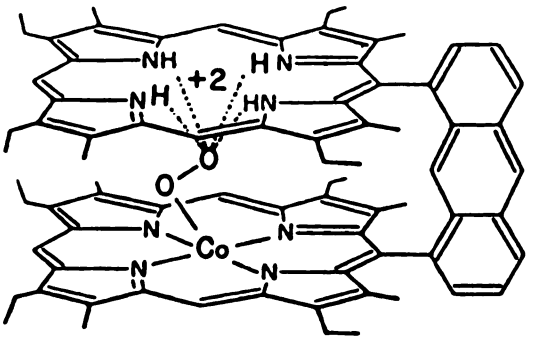

6b

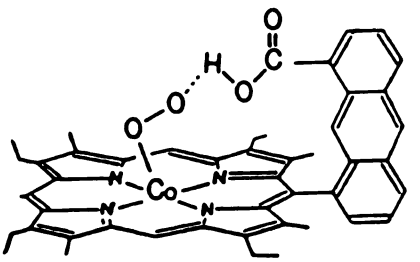

67

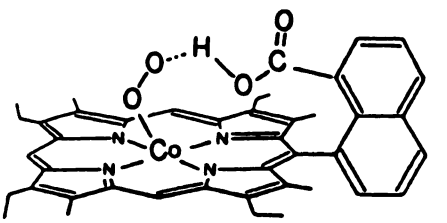

69

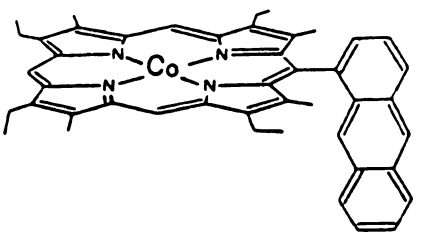

68

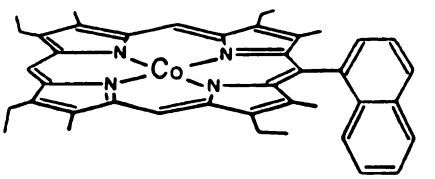

70

Figure 18 Hydrogen bonding in the dioxygen-monocobalt-porphyrin adducts.

employed (Figure 18). It is conceivable that these protons, juxtaposed to the coordinated O_2, could prevent the premature dissociation of, as well as assist in proton transfer to, the partially reduced O_2 coordinated to the cobalt center in the second porphyrin ring. If such *specific proton catalysis* proves to be the case, it would suggest new directions for the design of catalysts for multielectron reduction. Kinetic measurements of oxygen binding to complexes such as 67 and 69 have shown that groups capable of forming a hydrogen bond make a significant contribution to the stability of the oxygen adduct of these complexes, that was reflected by the huge decrease in the off-rate of the ligand binding, compared to that of complexes such as 68 and 70 [90]. However more elaborate studies should be conducted before any definite conclusion can be made in this matter.

E. Conclusion

It is clear that the anthracene and biphenylene-bridged cobalt diporphyrins provide four-electron pathways for the catalysts reduction of O_2 when adsorbed on graphite electrodes. This is true for both the dimetalated and monometalated derivatives. These compounds represent the first effective macrocyclic metal-complex electrocatalysts that do not depend upon the *"four-atom separation"* demonstrated to be essential in the case of the diamide-bridged catalysts.

CHAPTER 4
MOLECULAR STRUCTURE AND PROPERTIES

CHAPTER 4

MOLECULAR STRUCTURE AND PROPERTIES

It is believed that the geometry of the metal complexes of diporphyrin compounds has a strong effect on their behavior toward binding oxygen, and on their catalytic activity toward the multi-electron reduction of dioxygen. It has been observed by Chang [7] and Collman [9] that the activity of such diporphyrin complexes strongly depends on the metal-metal separation. For instance, in the case of diamide-diporphyrins, the only dimer that is catalytically active has four-atom connecting groups separating the porphyrin rings (i.e. DP-4), while dimers with 5-, 6-, or 7-atom bridges (i.e., DP-5, DP-6, and DP-7 respectively, cf. Figure 6) behave, to a large extent, like monomeric porphyrins.

Clearly, a better knowledge of the molecular structure and (chemical and physical) properties of such metalloporphyrins is of great importance toward understanding their catlytic and biological functions.

A. Electronic Spectroscopy

Typical UV-visible spectra of porphyrins consist of an intense absorption band at approximately 400 nm, that arise from π-π^* transition [92], known as the Soret band, and four satellite bands labeled as I, II, III, and IV, located in the region between 700 and 500 nm. The relative positions and intensities of these bands depend upon the nature and location of the substituents on the porphyrin ring. When the macrocycle has six or more alkyl groups in the β-pyrrolic positions, the visible bands have an intensity pattern such that IV > III > II > I, a so-called etio-type spectrum.

In a configuration where two or more porphyrin rings are held in close proximity, interaction between the systems can cause a shift in the peaks positions [93]. The cofacial diporphyrins have distinctly different electronic spectra compared with those for the monoporphyrins. The visible bands of the free-base dimers are generally shifted to a longer wavelength (red shift) and Soret band is shifted to a shorter wavelength (blue shift). The bands also appear to be broadened. The cofacial diporphyrins in acidic solutions also show blue-shifted Soret band and red-shifted visible bands.

These spectral patterns have been diagnostically useful in determining which products are the "cofacial" dimers when new dimer preparations have been tried for the first

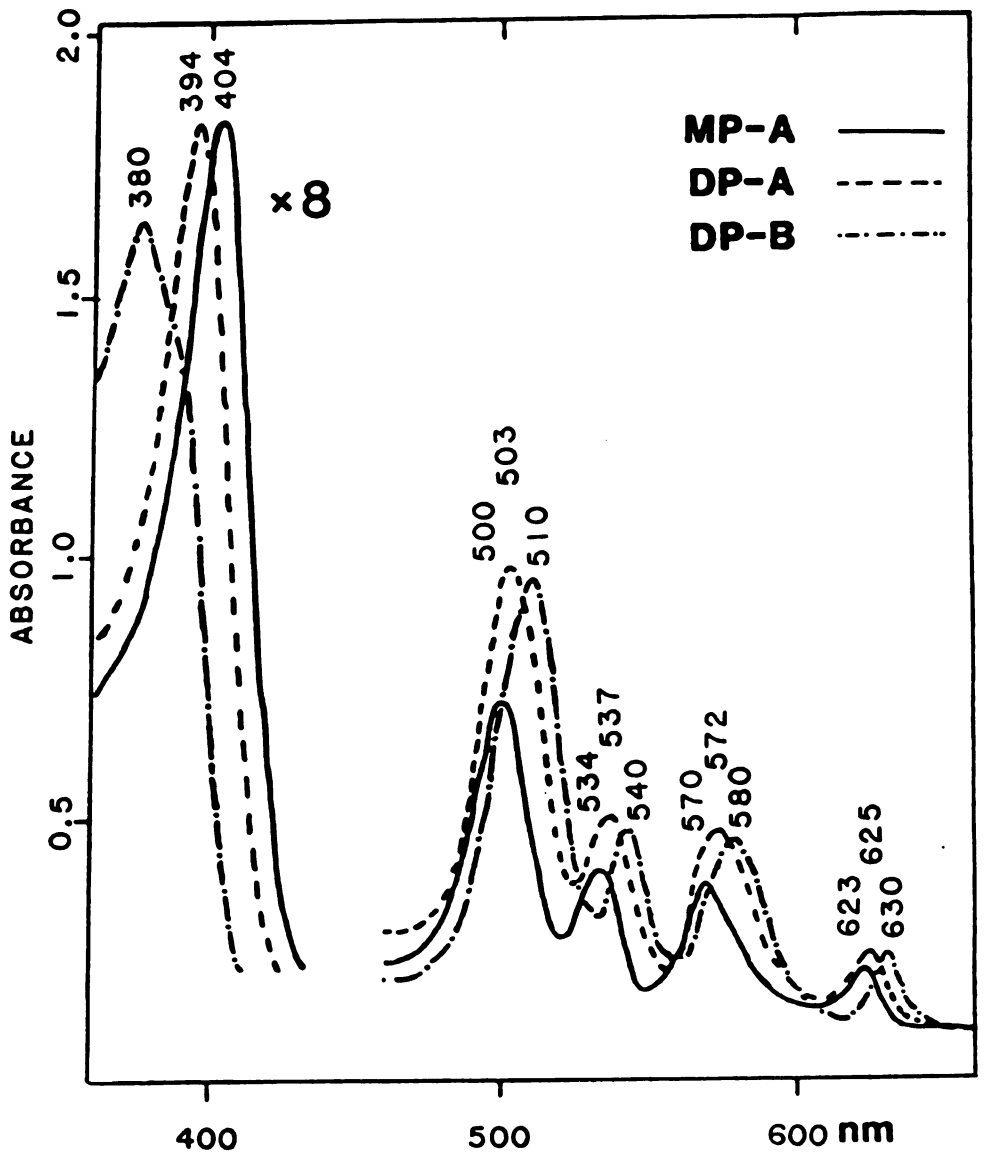

Figure 19 Absorption spectra of anthracene monoporphyrin (MP-A), anthracene diporphyrin (DP-A), and biphenylene diporphyrin (DP-B) in CH_2Cl_2.

time, and provide one piece of evidence of the cofacial nature of those species. Blue-shifted Soret bands and red-shifted visible bands relative to monomeric porphyrin have previously been reported for "face-to-face" porphyrins by Collman et al. [8], and Chang and co-workers [4,5]. Similar spectral shifts were also anticipated for our new dimers, as shown in Figure 19.

While the spectral shifts are quantitatively useful for the identification of dimer compounds, a vigorous explanation for the observed shifts has not been attempted. The problem is confused by the variety of spectral properties reported for other dimer systems. Whereas the singly and doubly linked mesoporphyrin-IX dimers of Ichimura [100], which are not rigidly constrained to a "cofacial" orientation, display blue-shifted Soret band and red-shifted visible band, the β,β'-alkyl-linked porphyrin dimers reported by Pain et al. [94] show no spectral shifts when the porphyrin units are separated by more than two methylene groups. The well-defined "cofacial" dimer of Kagan et al. [95], based on meso-tetraphenylporphyrin, exhibits a broadened but unshifted Soret band and red-shifted visible bands. The doubly linked "cofacial" chlorin system of Wasielewski et al. [96] exhibits no spectral shifts at all. Chang et al. [5,97] have observed strong exciton [98] coupling in their diporphyrin systems. A similar phenomenon was observed in some porphyrin and chlorin aggregates, in particular the μ-oxo-scandium(III) dimers of octaethyl-

porphyrin and meso-tetraphenylporphyrin [99].

B. Nuclear Magnetic Resonance Spectroscopy

NMR spectroscopy is a particularly useful technique for establishing the integrity of cofacial porphyrin dimers. If a porphyrin ring is positioned atop another, the ring current of this second porphyrin can cause additional shifts of the proton resonances [4,5,8], particularly the pyrrolic NH signals. Their resonances are at higher fields than for the monomers. The upfield shift arises from the additional shielding effect of the second porphyrin atop the first. With previous dimers of Chang et al. and Collman and co-workers, an increase in the shielding effect occurs as the interporphyrin distance is shortened. We observed similar upfield shift in our new diporphyrins. Upfield shifts have also been observed for peripheral β-pyrrolic substituents. Wasielewski et al. [96] observed shifts of 0.1 to 0.4 ppm for peripheral substituents of a doubly linked cofacial chlorin dimer. Since all the substituents are moderately shifted upfield, an approximately "face-to-face" or "center-to-center" orientation was inferred. In studies of "special pair" chlorophyll models, dramatic shifts of specific peripheral substituents indicate that "offset" aggregates are present [100,101]. Moderate upfield shifts for all peripheral substituents have been observed for some free-base porphyrins [102] and

Figure 20 *250 MHz NMR of anthracene monoporphyrin (a), anthracene diporphyrin (b), and biphenylene diporphyrin (c) in* $CDCl_3$.

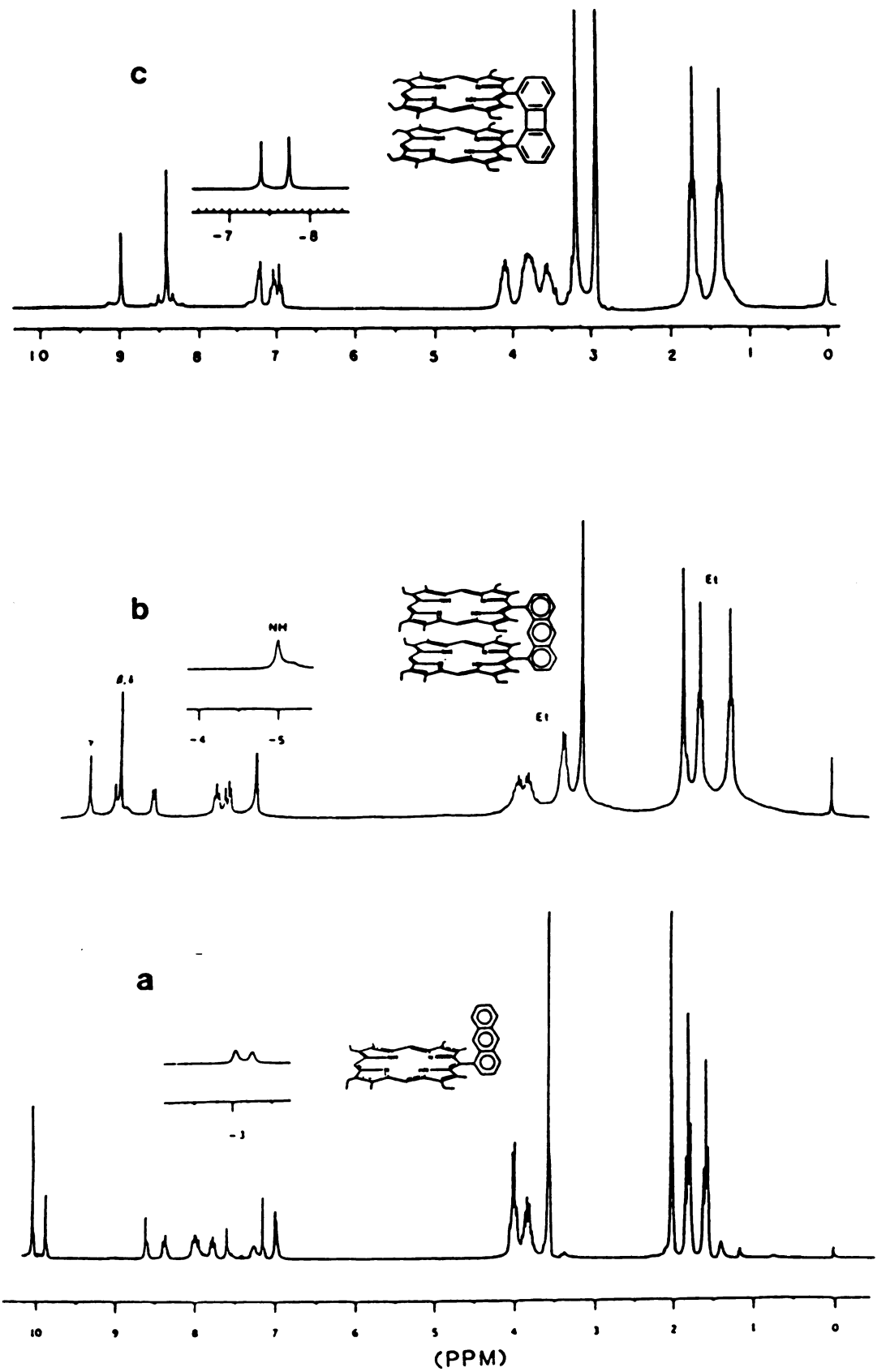
c
-7
-8
10
9
8
7
6
5
4
3
2
1
0
b
NH
-4
-5
E1
E1
a
-3
10
9
8
7
6
5
4
3
2
1
0
(PPM)

metalloporphyrins [103] under conditions in which intermolecular aggregation occurs. A mercury(II) octaethylporphyrin "sandwich" complex has shown similar effects [104]. The spectral data for this complex are consistent with the formation of dimer aggregate with "center-to-center" orientations of the porphyrin monomers.

Figure 20 shows the NMR spectra of the anthracene-, biphenylene-diporphyrins, and anthryl monoporphyrin. In addition to the difference in the extent of the upfield shift of the NH peaks, the peripheral pyrrolic methyl groups closer to the bridging group in the anthracene porphyrins show upfield shifts compared to that of the biphenylene dimer.

C. Electron Spin Resonance Spectroscopies

Simple copper(II) and low spin cobalt(II) porphyrins are S = $^1/_2$ systems with well known ESR characteristics [105]. If two such porphyrins are close enough that the metals interact, the bimetallic systems will have singlet (S = 0) and triplet (S = 1) states separated by the energy J [106]. If the rate of electron exchange between the metals is fast compared to the resonance frequency (10^{10} sec^{-1}), then each electron experiences nuclear spin equal to the total nuclear spin of the two metals (I = 3 for Cu_2^{2+} and I = 7 for Co_2^{2+}) [107,108]. The resulting hyperfine splitting, A, is half that for a related mononuclear S =

$^1/_2$ system. The ESR transitions will be further split by the zero field splitting D. D is composed of two terms, D_{pseudo} (from spin orbital coupling) and D_{dd} (from the electron-electron dipolar interaction). D_{dd} is related to the metal-metal (M-M) separation, r, by the equation

$$r = (0.65\ g_{\parallel}^2/D_{dd})^{1/3}$$

It has been shown that D_{pseudo} can be ignored, and r can be calculated from $D = D_{dd}$ without having a significant effect on the calculated r [109]. A more complete description of the method of determining r is contained in references 107 and 108. Several examples of ESR involving two interacting $S = {}^1/_2$ metals have appeared in the literature [107-115]. Calculated distances have been in agreement with the x-ray crystal structures [109,110].

Interaction of Oxygen with Dimetallic Diporphyrins

Oxygen was found to interact with metal complexes of the diporphyrins to form 1:1 or 2:1 ($M:O_2$), depending on the metal-metal separation [117], (Figure 21).

When a bulky ligand, 1-triphenylmethylimidazole, was mixed with Co(II)-Co(II) diporphyrin (DP-7) and exposed to oxygen, both visible and ESR spectra documented the formation of a (1:1) $Co-O_2$ complex. The oxygenation is reversible, evacuation results in eliminating the superoxo complex and restoring the Co(II) signal. On the other hand, our new Co(II)-Co(II) diporphyrin, with a smaller gap between

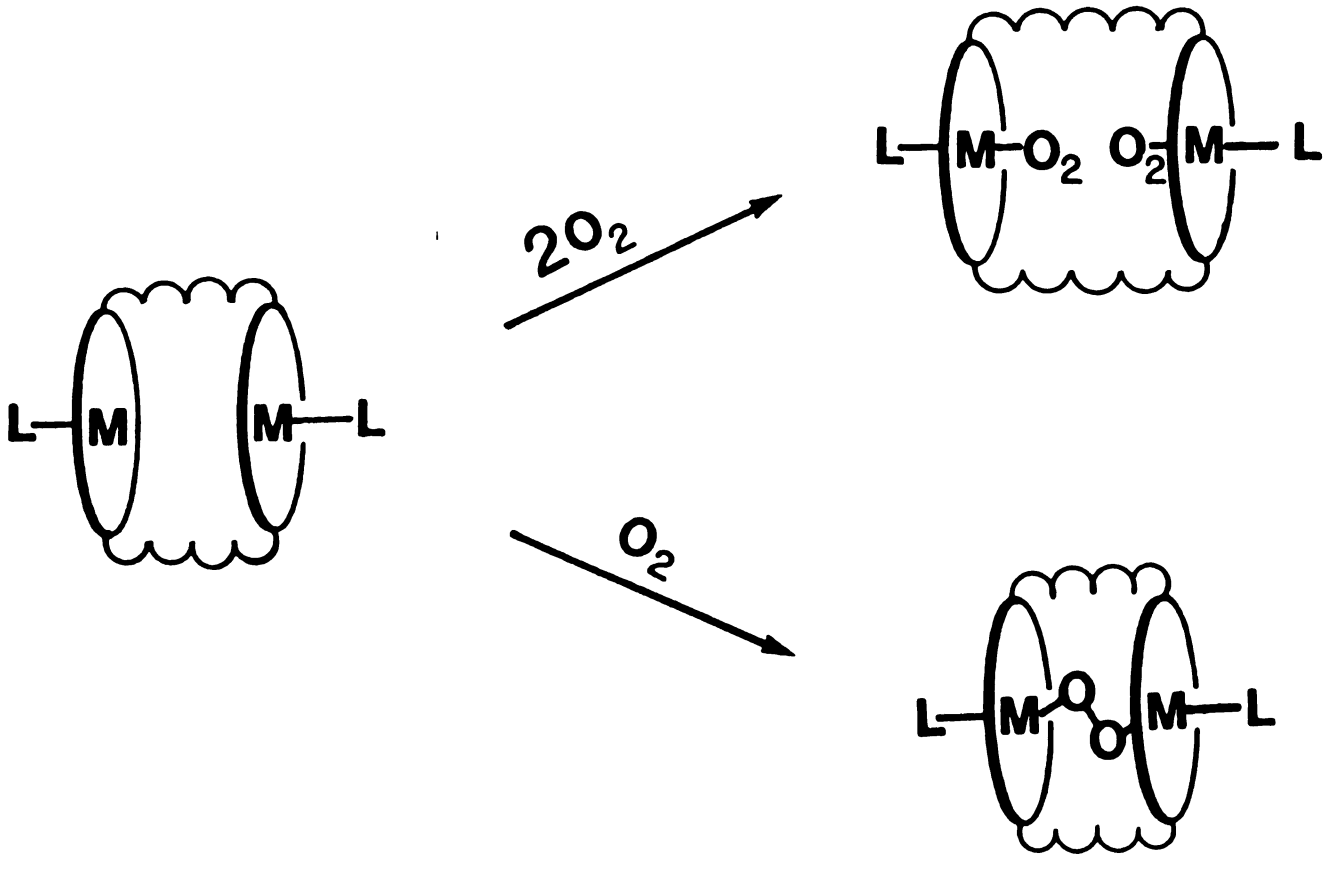

Figure 21 A schematic representation of the interaction between O_2 and dimetallodiporphyrins.

the two cobalt atoms, reacts in a completely different way. Addition of oxygen to the $[\phi_3CIm\text{-}Co(II)]_2$ complex at room temperature instantanously produced a species consistent with the formation of $2Co/_{O2}$ stoichiometry. This complex, written as μ-peroxo [Co-O_2-Co] is diamagnetic and gives no EPR signals; however, when a trace amount of I_2 was added to this solution, a well-defined isotropic spectrum was obtained, consisting of 15 lines, Figure 22. Such spectra could be expected if μ-peroxo dicobalt became oxidized to a μ-superoxo dicobalt complex in which the two equivalent ^{59}Co nuclei would give a total of $(2 \times 2 \times {}^{7}/_{2}) + 1 = 15$ lines [108].

There is little doubt that the ability of such diporphyrins to catalyze the oxygen reduction via a 4-electron process, is related to the structural features and special arrangements of the porphyrin rings in those dimers. We have estimated the interplanar separation from the value of 2D of the EPR spectra of frozen solutions of the copper-copper diporphyrins [43,83,118]. However, this method can only give the interspin distance, r. To determine the interplanar separation, it is necessary to know the angle between the interspin vector and the normal to the porphyrin planes (i.e., the slip angle) as well as r. Furthermore, the determination of r from the value of 2D is not reliable if the dipolar interaction is of the same order of magnitude as the nuclear hyperfine splitting and the interspin vector does not coincide with a principal axis of the

Figure 22 *EPR spectra of μ-superoxo complexes of Co_2DP-A (A) and Co_2DP-B (B). Spectra were obtained by reacting the bis Co^{II} dimers with dioxygen at 23°C in CH_2Cl_2 containing 0.1 M N-tritylimidazole and a trace amount of iodine.*

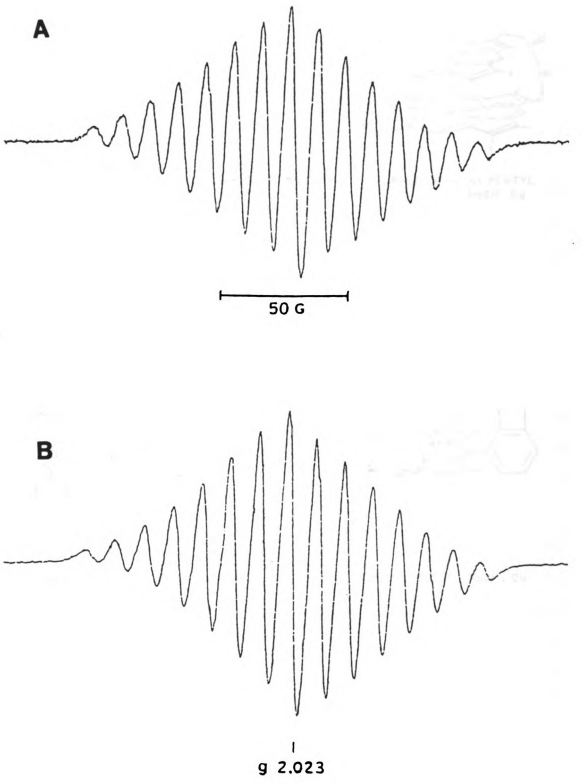
A
50 G
B
g 2.023

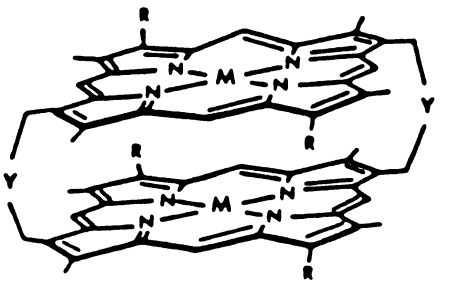

DP-7 R= HEXYL Y=$CH_2CH_2NG_{n-e\omega}CCH_2$ M=2H, Cu

DP-5 R= HEXYL Y=$CH_2NG_{n-e\omega}C$ M=2H, Cu

DP-4 R= PENTYL Y=NHC M=2H, Cu

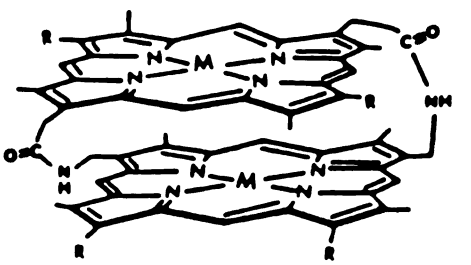

SLIPPED DP-4 R= PENTYL M=2H, Cu

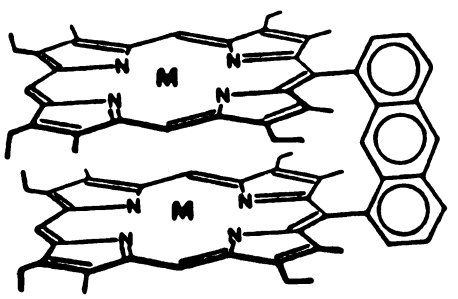

DP-ANTHRACENE M=2H, Cu

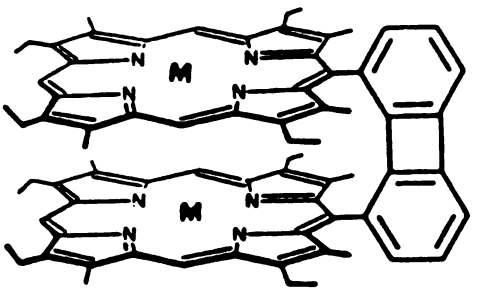

DP-BIPHENYLENE M=2H, Cu

SCHEME 15

nuclear hyperfine tensor [119]. The interspin distance can also be obtained from the intensity of the half-field transitions as well as computer simulation of EPR spectra [119]. The two methods were used here to probe the structural features of the dicopper diporphyrins in frozen solutions [120].

*EPR Spectroscopy of Dicopper Diporphyrins in Frozen Solutions**

The EPR spectra of the allowed transitions for copper-copper diporphyrins in frozen solutions is shown in Figure 23. The dipolar splitting of both the copper parallel and perpendicular lines was well resolved. The simulated spectrum shown in Figure 23A was obtained with r = 4.15 Å, $|J| = 0.5\ cm^{-1}$, and $\phi = 15°$. The value of 2D read from the splitting of the copper parallel lines (800 G) corresponds to r = 4.2 Å. The spectra of the half-field transitions are shown in Figure 24. The nuclear hyperfine splittings by the two copper ions were well-resolved as expected for copper porphyrin dimers [121]. In Figure 23A, the ratio of the intensity of the half-field transitions to the intensity of the allowed transitions for DP-4 was 4.6×10^{-3}, which corresponds to r = 4.04 Å [120]. This value agrees

*This work was done in cooperation with Professor S.S. Eaton of the University of Colorado at Denver.

Figure 23 *X-Band EPR spectra of the allowed transitions for Cu_2DP-4 (A), Cu_2DP-5 (B) and Cu_2DP-B (C) at -180°C in 1:1 toluene/CH_2Cl_2 solution. The spectra were obtained for 1 mM solutions with 1 mW microwave power and 4 G modulation amplitude. The peak marked "A" was attributed to aggregated material. The dotted lines indicate regions in which the calculated curves don't overlay the experimental data.*

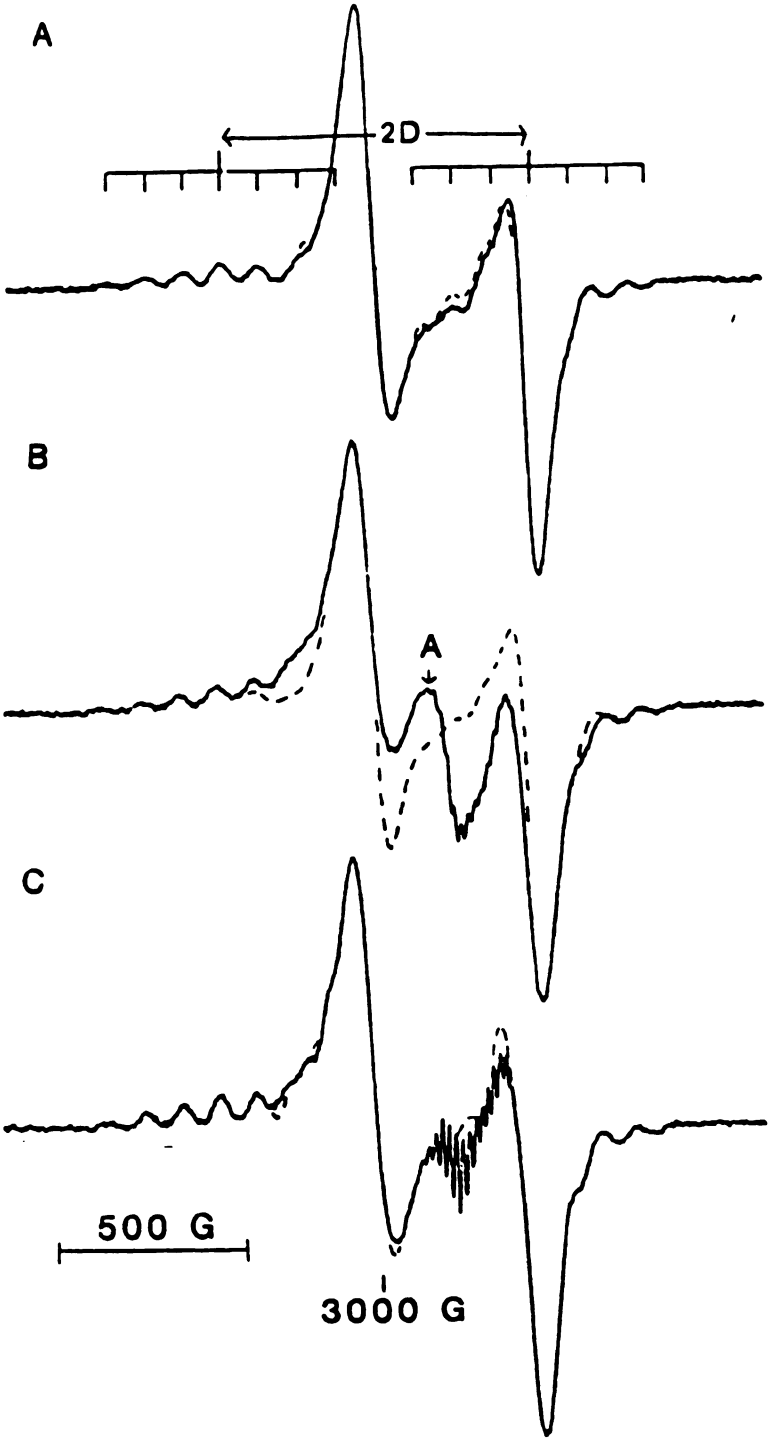
A
2D
B
A
C
500 G
3000 G

Figure 24 *X-Band EPR spectra of the half-field transitions for Cu_2DP-4 (A), Cu_2DP-5 (B), and Cu_2DP-B (C) at -180°C in 1:1 toluene/CH_2Cl_2 solution. The spectra were obtained in 1 mM solutions with 20 mW microwave power at 16 G modulation amplitude. The overall amplification of the spectra in this figure is about 35 times that for Figure 23. The dotted lines indicate regions in which the calculated curves don't overlay the experimental data.*

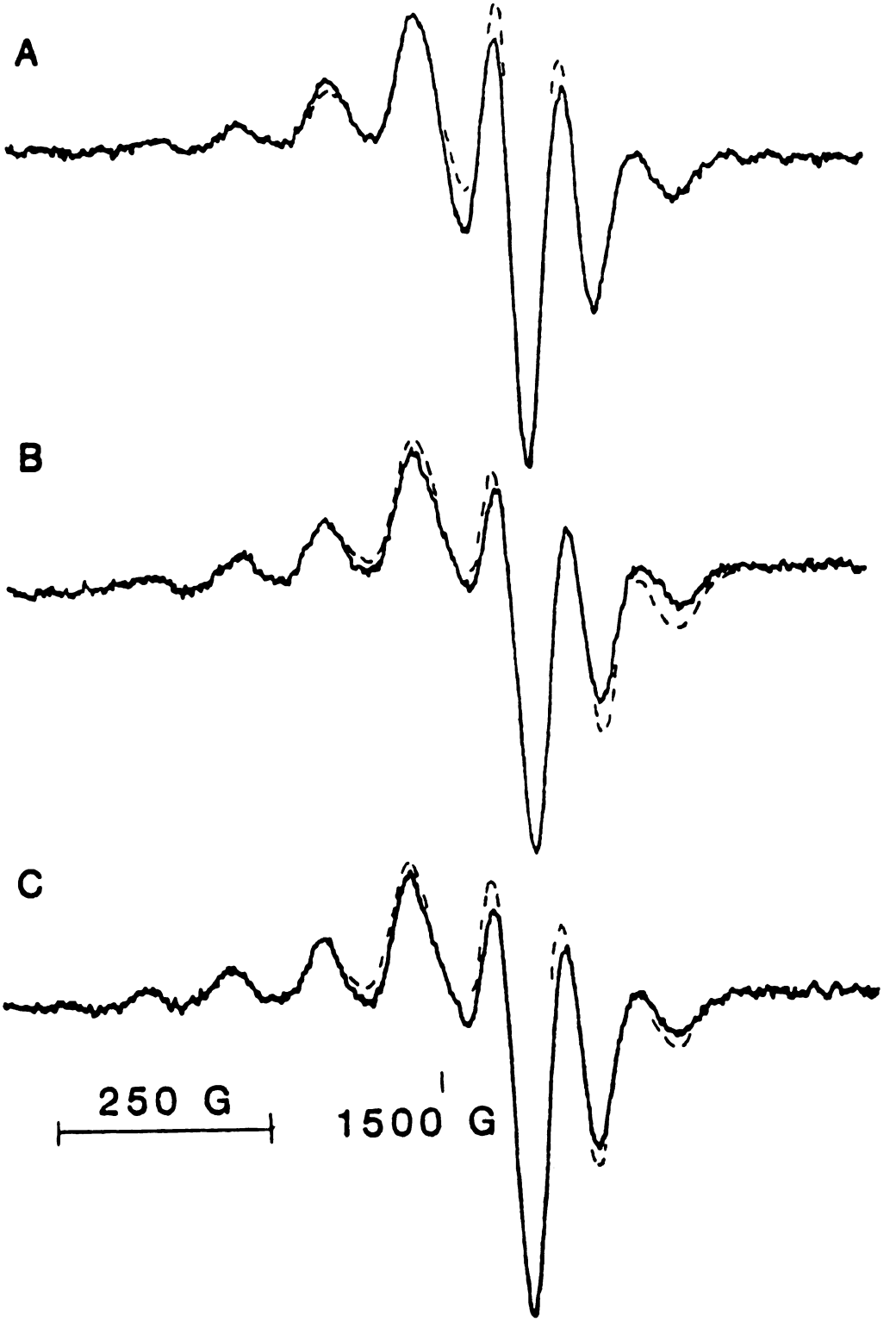
A
B
C
250 G
1500 G

well with the values obtained from 2D and by computer simulation of the allowed transitions. The simulated spectrum was obtained with $\phi = 15°$.

Figures 23C and 24C show the allowed and half-field transitions, respectively, for the copper-copper diporphyrin DP-B. The spectra were similar to that of DP-4 and DP-5. The sharp lines between 3100 and 3200 G in Figure 23C were due to a small amount of monomeric copper porphyrin or to diporphyrin that had copper coordinated to only one of the porphyrins. The simulated spectra were obtained with $r = 4.13$ Å, $|J| = 0.5$ cm^{-1}, and $\phi = 20°$. The value of 2D obtained from copper parallel lines (820 G) corresponds to $r = 4.2$ Å. The relative intensity of the half-field transitions was 4.0×10^{-3}, which corresponds to $r = 4.14$ Å. The X-ray structure of this complex (cf. section D of this chapter), gave a Cu-Cu distance of 3.81 Å [47], which indicates substantial similarity between the structures in solution and the single crystal.

The allowed and half-field transitions for copper-copper diporphyrin DP-7 are shown in Figures 25A and 26A, respectively. The smaller splittings of the allowed transitions for DP-7 than DP-4, DP-5, or DP-B indicated a longer interspin distance. Due to the weaker dipolar interaction, the copper parallel lines on the high-field side of the spectrum were poorly resolved, which precluded an estimate of the value of 2D. The simulated spectrum was obtained with $r = 4.95$ Å, $|J| = 0.5$ cm^{-1}, and $\phi = 40°$.

Figure 25 *X-Band EPR spectra of the allowed transitions for Cu_2DP-7 (A), Cu_2DP-A (B), and slipped Cu_2DP-4 (C) at -180°C in 1:1 toluene/CH_2Cl_2 solution. The spectra were obtained under conditions identical with those described in Figure 23.*

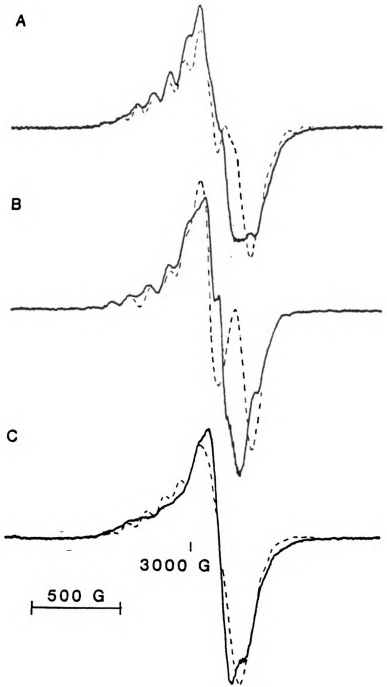
A
B
C
3000 G
500 G

Figure 26 *X-Band EPR spectra of the half-field transitions for Cu_2DP-7 (A), Cu_2-DP-A (B), and slipped Cu_2DP-4 (C) at -180°C in 1:1 toluene/CH_2Cl_2 solution. The spectra were obtained in 1 mM solution with 200 mW microwave power and 16 G modulation amplitude.*

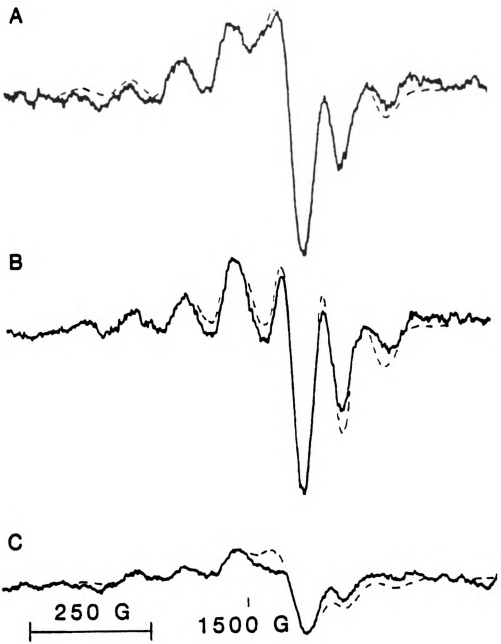
A
B
C
250 G
1500 G

The major discrepancy between the observed and calculated spectrum in Figure 25A was at about 3100 G, which is at the position assigned to aggregated materials. This region of the spectrum was concentration dependent, which suggests that the discrepancy was due to aggregation. The relative intensity of the half-field transitions was 1.3×10^{-3}, which corresponds to r = 5.0 Å. The X-ray crystal structure of DP-7 gave a copper-copper distance of 5.22 Å and a slip angle of 46.6° [122]. Thus the EPR results indicate that the structure in frozen solution is similar to that observed in the single crystal. It should be noted that both the large copper-copper distances and the larger value of ϕ are consistent with the slightly greater slip of one porphyrin plane relative to the other in crystal than in the frozen solution.

The spectra of DP-A (Figures 25C and 26C) were similar to that of DP-7. The simulated spectra were obtained with r = 4.95 Å, $|J| = 0.5$ cm^{-1}, and $\phi = 20°$. The discrepancy between the observed and the calculated spectra at approximately 3100 G was attributed to aggregation of a small amount of the sample. The relative intensity of the half-field transitions (1.4×10^{-3}) gave r = 4.9 Å. The X-ray structure of the nickel-nickel analogue of DP-A gave a metal-metal distance of 4.57 Å and $\phi = 20°$ [47].

The values of the interplanar spacings for these diporphyrins obtained from the values of r and ϕ ($d = r \cos \phi$) are included in Table I. The last column compares the O_2

electroreduction response of the corresponding cobalt derivatives. There appears to be no relationship between r, ϕ, or interplanar spacing and the effectiveness as a 4-electron catalyst. For example, while the three effective 4-electron catalysts DP-4, DP-B and DP-A (M = Co) have a small slip angle, so does DP-5. However, for the "pillar" type complexes and DP-A we have suggested [45] that the rings are flexible enough to achieve whatever structure is advantageous for the formation and cleavage of the cobalt peroxo intermediate, even to overcome the large discrepancy of r between DP-B and DP-A. The answer to this question may be found when mechanisms of the reduction of $Co-O_2-Co$ species are fully understood.

For all of the experimental spectra, it was only possible to simulate the spectra if the absolute value of J was $>0.3\ cm^{-1}$. Thus, although there was no short bond pathway between the two copper ions, there was an exchange interaction that was large on the X-band EPR scale. Such an interaction could occur via interaction between one copper and a nitrogen coordinated to the second copper or via $\pi-\pi$ interaction between the two porphyrins.

Table 1 *Distances and angles obtained for dicopper diporphyrins. (a) Copper-copper distances obtained from the relative intensities of the half-field transitions. (b) Copper-copper distances obtained by simulation of the allowed transitions. (c) Angles between the z-axes of the copper g and A tensors and the interspin vector. (d) Separation between the two parallel porphyrin planes. (e) Percentage of formation of H_2O_2 evaluated from % $H_2O_2 = 2/[1+(ni_D)/(i_R)]$, where i_R and i_D are ring and disk limiting currents, respectively, and N(= 0.182) is the collection coefficient; these data were measured by using dicobalt diporphyrins coated on the graphite of a ring-disk electrode immersed in O_2-saturated 0.5 M aqueous trifluoroacetate acid.*

Table I: Distances & Angles of Cu Diporphyrins

	r Å		d Å[d]	ø deg[c]	%H_2O_2[e]
	half-field[a]	simulation[b]			
DP-7	5.00	4.95	3.80	40	>60
DP-5	4.12	4.15	3.90	20	>40
DP-4	4.04	4.15	4.00	15	5
Slip DP-4	5.70	5.50	3.90	45	>60
DP-B	4.14	4.13	3.90	20	< 7
DP-A	4.90	4.90	4.60	20	< 7

Footnotes are on page 106.

D. X-Ray Crystal Structure of Diporphyrins*

While other methods of characterization (NMR, UV-vis, and EPR) support the identification of the meso-linked cofacial diporphyrins, X-ray crystal structure studies will add to our knowledge an important piece of information about the characteristic features and geometries of these catalysts.

There are only two crystallographic structure studies of diporphyrins in the literature [122,124], but neither is for the active (4-electron reduction process) catalyst and neither is very accurate due to disorder leading to relatively poor diffraction quality.

Figures 27 and 28 show three approximately mutally perpendicular views of Ni_2DP-A and Cu_2DP-B complexes, respectively. It is clear that porphyrin rings are not exactly stacked over one another but rather, have slipped with respect to each other as noted previously in other cofacial porphyrin structures [122-124], and that the porphyrin rings are markedly on-planar. This non-planarity is more significant in the case of Ni_2DP-A complex. The magnitude of the slip is 2.40 Å in Ni_2DP-A with a Ni-Ni distance of

*This work was done in cooperation with Professor A. Tulinsky of this department.

Figure 27 *ORTEP Drawing of Ni_2DP-A excluding the side groups. Views approximately mutually perpendicular: (a) parallel to $C(m_2)$-$C(M_4)$ direction; (b) parallel to $C(m_1)$-$C(m_3)$ direction; (C) nearly perpendicular to porphyrin planes, ring 1 shaded.*

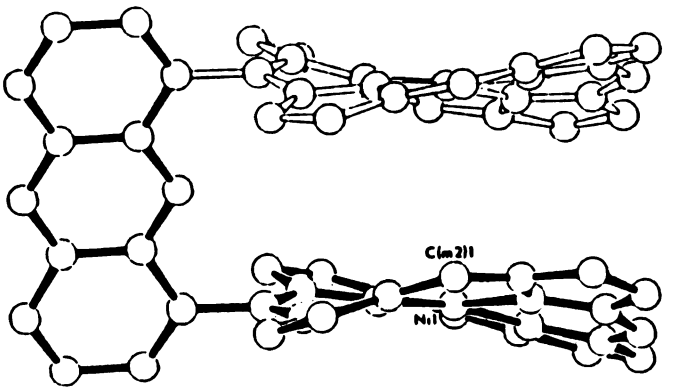

a

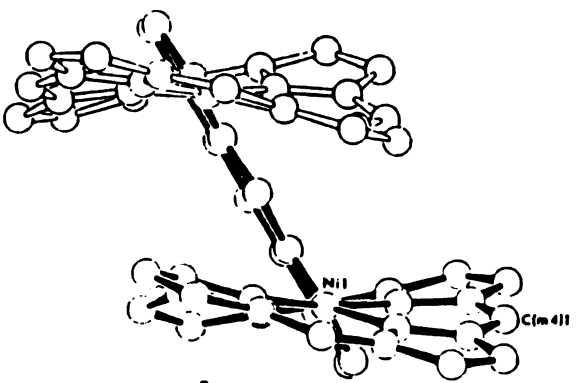

b

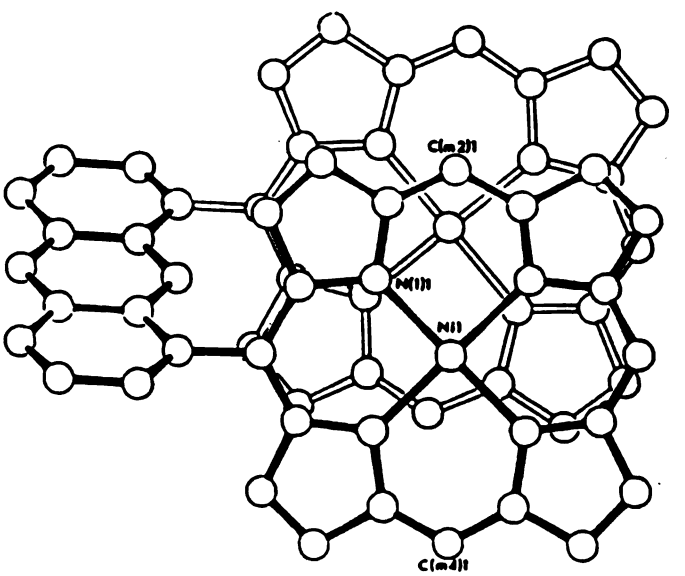

c

Figure 28 ORTEP Drawing of Cu_2DP-B excluding side groups. Otherwise, as in Figure 26.

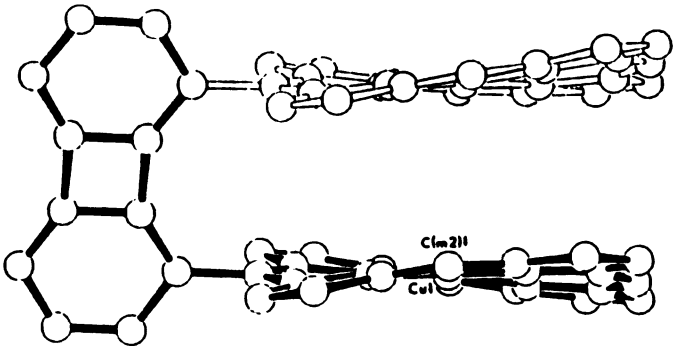

a

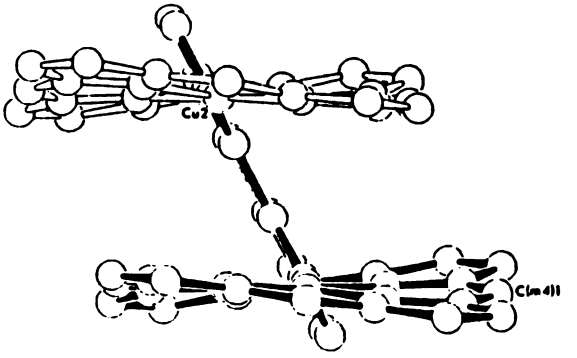

b

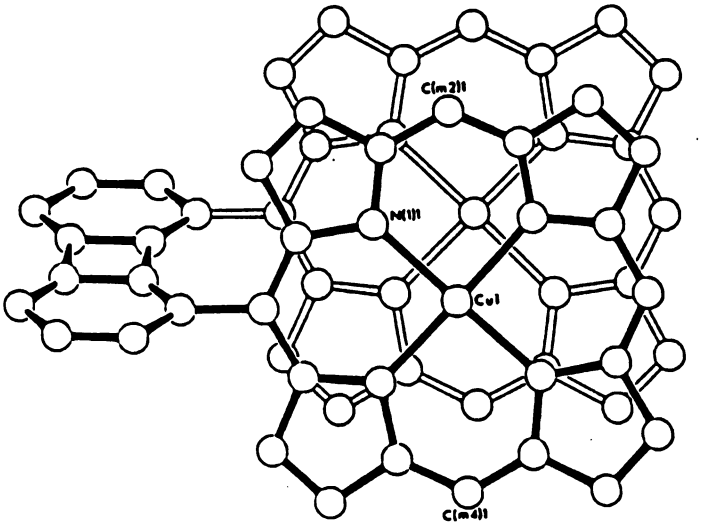

c

4.566 Å. This corresponds to a slip angle of 31.7 degrees [125]. The corresponding values of Cu_2DP-B are: 1.60 Å for slip, 3.807 Å for Cu-Cu distance, and 24.9° for slip angle. The slip exhibited by Ni_2DP-A leads to an average porphyrin plane-to-plane distance of 3.88 Å while that of Cu_2DP-B particularly corresponds to a van der Waals contact at 3.45 Å. However, an examination of a space-filling representation of the structures with the interactive graphics program FRODO [126] shows that the "vacant" interplanar space of both molecules is strikingly similar in both magnitude and extent indicating that the3.88 Å interplanar separation of Ni_2DP-A is only an apparent difference resulting from the greater degree of non-planarity. A perspective stereoview of the molecules is shown in Figure 29.

The fact that Ni_2DP-A doesn't attain as close a ring contact as Cu_2DP-B suggests that either: a) further lateral translation to achieve this is offset by the loss of total number of van der Waals contacts, or (b) further rotation of the porphyrin rings about the connector bond leads to distortive repulsions between the aromatic connector and methyl groups of the porphyrin ring which contribute to the buckling of the porphyrin, since the porphyrin core is much more flexible than the aromatic connector; (c) the degree of non-planarity can also be a factor, by inhibiting further slippage to avoid the development of unfavorable contacts.

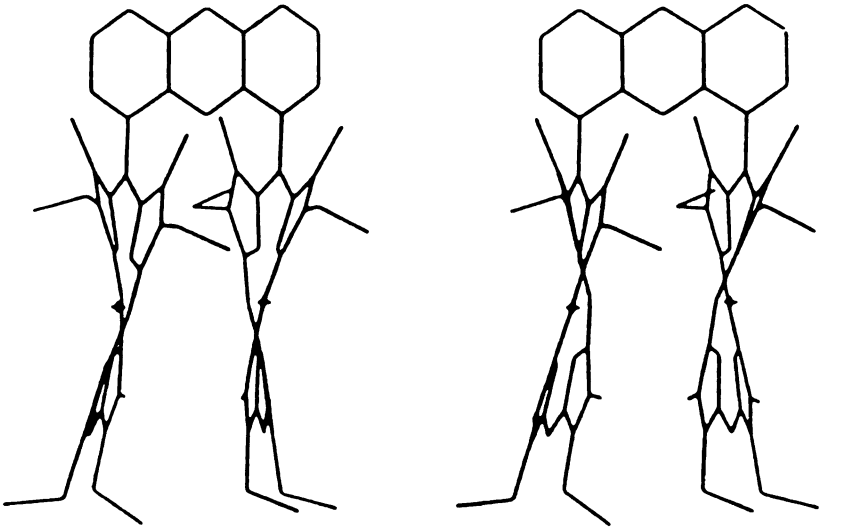

a

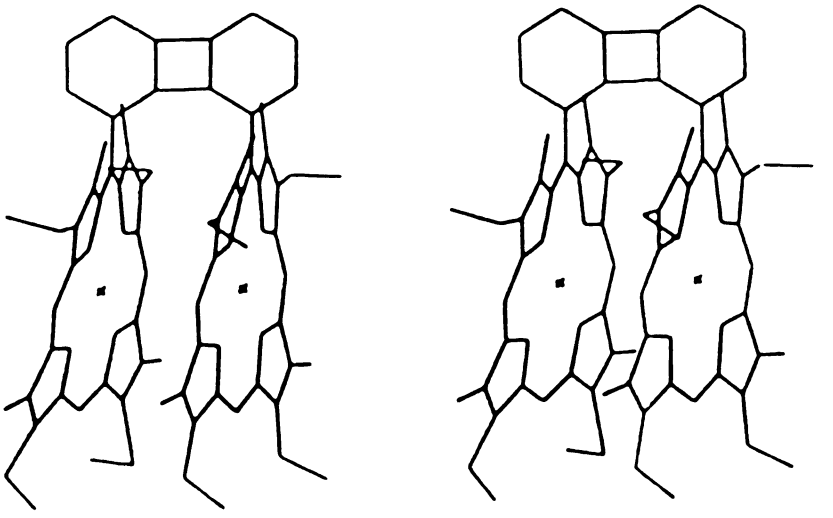

b

Figure 29 Perspective stereoview of Ni_2DP-A (a) and Cu_2DP-B (b).

A summary of the results is shown in Table II, which also includes the EPR results, for comparison. More details of the X-ray crystal structures of these diporphyrins are found in ref. 47.

Table 2 Comparison of distances and angles obtained by X-ray with those obtained by EPR for cofacial porphyrins.

	r, Å		d, Å		φ, deg	
	X-ray[a]	EPR[b]	X-ray	EPR	X-ray	EPR
DP-A	4.56	4.90	3.88	4.60	31.7	20
DP-B	3.80	4.14	3.45	3.90	24.9	20

[a] *Ni-complex of DP-A was used for X-ray, Cu-complexes were used otherwise.*

[b] *r was calculated from the half-field transition.*

The difference in metal-to-metal distances in the diporphyrins is noteworthy. Prior to our study of these compounds it was thought that the metal-metal distance is the most crucial factor that dictates whether or not the cobalt dimer can serve as an effective four electron electrocatalyst for the dioxygen reduction. This is borne out by the fact that among the ten or so amide chain-linked diporphyrins that have been synthesized, only one compound with diametrical $-CH_2-CONH-CH_2$ connecting straps has been shown

to be active [11,91,83]. Increase or decrease in the number of methylene units or transposition of the individual constituents in that series of diporphyrins would lead to near total loss of activity. This is not the case with DP-A and DP-B. As indicated above, the metal separations in the two dimers differ by 0.76 Å yet it doesn't seem to have much of an effect on their electrocatalytic performance. Although the use of such a distance obtained from non-cobalt complexes to discuss the behavior of the cobalt catalysts on a graphite surface is admittedly not direct, on the other hand, there is no evidence to prove that other metalloporphyrins would adopt a grossly different structural configuration in another environment. In fact, both the metal-metal separation and ring-to-ring distance agree well with those obtained by EPR studies in frozen solution (cf. Table II and section C of this chapter). The results of the X-ray studies seems to reiterate the conclusion about the lack of a clear connection between inter-ring separation and a preference for 4-electron versus 2-electron reduction pathways of oxygen. Further structural studies as well as the synthesis of other diporphyrins are obviously needed to more clarify the structure-function relationship of this very important class of catalysts.

EXPERIMENTAL

EXPERIMENTAL

EXPERIMENTAL

EXPERIMENTAL

A. Reagents and Solvents

All reagents and solvents were of reagent grade qualities unless otherwise mentioned, and were purchased. All solvents were distilled before use; methylene chloride, tetrahydrofurane, toluene, benzene, diethylether were distilled from $LiAlH_4$; pyridine, triethyl amine, collidine were distilled from calcium hydride; methanol and ethanol were distilled from sodium. Silica gel for column chromatography (60-200 mesh) was purchased from J.T. Baker (3405); preparative silica gel plates were from Analtech, Inc.; for analytical TCL, Eastman 13181 chromatography sheets were used.

B. Physical and Spectroscopic Methods:

Melting points were obtained on an Electrothermal melting point apparatus and are uncorrected. UV-visible spectra were obtained on a Cary 219 spectrophotometer. The infrared spectra were recorded on a Perkin-Elmer Model 237B spectrophotometer. PMR spectra were obtained on a Varian T-60 or Brucker WM-250 MHz spectrometer, with chemical shifts reported in δ-units measured from tetramethylsilane as the internal standard. Mass spectra were obtained in a Hitachi Perkin-Elmer Instrument RMU-6 mass spectrometer and Finnigan 4000 GC/MS system using the direct inlet mode, at

70 eV ionization energy. High-resolution positive ion mass spectra were obtained on a Kratos MS-50 RF equipped with Ionteck FAB gun, operated at 8 kV. Elemental analyses were performed by Spang Microanalytical Laboratory, Eagle Harbor, Michigan; C, H and N analyses were within ±0.40%.

C. Experimental Procedures

1,8-Bis{[5,5′-bis(ethoxycarbonyl)-4,4′-diethyl-3,3′-dimethyl-2,2′-dipyrryl]methyl} anthracene, 3:

1,8-Anthracene dicarboxaldehyde (7.0 gm, 0.03 mole) and ethyl 3-ethyl-4-methyl-2-pyrrolecarboxylate 2 (21.7 gm, 0.12 mole) were heated in absolute ethanol (200 mL) containing 5 mL of concentrated hydrochloric acid. The solution was refluxed for 1 h and allowed to cool in an ice bath. The yellow crystals (25 gm, 91% yield) were filtered and dried; m.p. 183-185°C. NMR δ 1.10 (12H, t, Et), 1.30 (12H, t, OEt), 1.65 (12H, S, Me), 2.75 (8H, q, Et); 4.30 (8H, q, OEt), 5.88 (2H, s, CH), 6.96 (2H, d, 2 and 7H-anthryl), 7.40 (2H, t, 3 and 6H-anthryl), 8.00 (2H, d, 4 and 5H-anthryl), 8.38 (1H, s, 10H-anthryl), 8.50 (4H, broad, NH), 8.55 (1H, s, 9H-anthryl); MS, m/e 922 (39), 921 (39), 876 (42) 875 (100). Analysis calculated for $C_{56}H_{66}N_4O_8$: C, 72.86; H, 7.21; N, 6.07; found: C, 71.67; H, 7.24, N, 6.08.

1,8-Bis[(4,4′-diethyl-3,3′dimethyl-2,2′-dipyrryl)-methyl]anthracene, 4:

The tetraester 3 (21.0 gm, 22.7 mmol) was dissolved in refluxing ethanol (95%, 250 ml) and hydrolyzed by addition of aqueous sodium hydroxide (5 gm in 30 ml water). The mixture was kept refluxing for 10 h before ethanol was removed as much as possible on a rotary evaporator. The residue was diluted with water (200 mL) and filtered. The filtrate was cooled down by adding ice (~50 gm) and then neutralized by adding glacial acetic acid; the precipitated tetracarboxylic acid was filtered and dried, 19.0 gm (93%), m.p. 170°C (decomposition).

The tetracarboxylic acid was dissolved in ethanolamine (100 mL) and refluxed under nitrogen for 1 hr. The solution, while still hot, was poured into ice-water (~600 mL). Golden crystals of 4 soon separated and were filtered and air dried (11.5 gm, 84% yield, no crystallization was necessary), m.p. 150-151°C. NMR δ 1.15 (12H, t, Et), 1.62 (12H, s, Me), 2.43 (8H, q, Et), 5.98 (2H, s, CH), 6.38 (4H, s, 5H-pyrrole), 7.05 (2H, d, 7H-anthryl), 8.45 (1H, s, 9H-anthryl), 8.70 (1H, s, 10H-anthryl). MS, m/e 635 (65), 634 (45), 525 (100).

α,α-[4,4-Diethyl-5,5′-diformyl-3,3′-dimethyl-2,2′-dipyrryl]toluene, 69:

Benzaldehyde (3.18 gm, 0.03 mole) and ethyl 3-ethyl-4-methyl-2-pyrrolecarboxylate 2 (10.86 gm, 0.06 mole) were

heated in absolute ethanol (300 mL) containing concentrated HCl (5 mL). The solution was refluxed for 1 h and then allowed to stand in ice-water for 2 h. The white crystallized material formed was collected by filtration to give 67, 12.5 gm (94%); m.p. 150-152°C. MS, m/e 450 (95), 270 (100). NMR δ 1.20-1.30 (12H, 2 triplets, Et), 1.70 (6H, s, Me), 2.80 (4H, q, Et), 4.20 (4H, q, OEt), 5.60 (1H, s, CH), 7.3 (5H, m, phenyl), 8.30 (2H, broad, NH).

The above diester was dissolved in hot ethanol (300 ml), to which sodium hydroxide solution (5.0 gm in 20 mL) was added, and the mixture was refluxed continually for 8 h. The solvent was then evaporated and the residue was dissolved in water (750 mL), cooled, and acidified with glacial acetic acid to give a white solid.

After collection by filtration and vacuum drying, the diacid was decarboxylated by heating in ethanolamine (100 ml) for 1 h. The hot mixture was poured into ice-water and the product was extracted twice with dichloromethane (2 × 150 ml). Evaporation of the organic layer afforded the corresponding α,α′-free dipyrrylmethane 68, 7.5 gm (82%), m.p. 95°C (decomposition). NMR δ 1.10 (6H, t, Et), 1.70 (6H, s, Me), 2.85 (4H, q, Et), 5.60 (1H, s, CH), 6.40 (2H, s, 5H-pyrrole), 7.3 (5H, m, phenyl), 8.30 (2H, broad, NH).

Phosphorus oxychloride (3 ml) was added dropwise, while stirring, to a cold solution of the α,α[4,4′-diethyl-3,3′-dimethyl-2,2′-dipyrryl]toluene (5.0 gm) in DMF (50 ml)

at -5°C. The mixture was allowed to stir at low temperature (-5°C to 0°C) under nitrogen for 4 h, then let stand at -15°C for 8 h. Water (200 mL) was added and the aqueous layer was washed several times with methylene chloride until the organic layer was almost colorless. The iminium salt was hydrolyzed by adding 10% NaOH solution dropwise to the aqueous layer until complete precipitation was achieved. The light brown crystalline material was collected by filtration and recrystallized from ethanol (95%) to give white needles 69, 3.5 gm (60%); m.p. 210-212°C. Analysis calculated for $C_{23}H_{26}N_2O_2$: C, 76.21; H, 7.23; found: C, 75.95; H, 7.20. MS, m/e 362 (100), 226 (50. NMR δ 1.10 (6H, t, Et), 1.75 (6H, s, Me), 2.60 (4H, q, Et), 5.45 (1H, s, CH), 7.10 (5H, m, phenyl), 9.25 (2H, s, CHO). 9.55 (2H, broad, NH).

[3,3′-Diethyl-5,5′-bis(methoxymethyl)-4,4′-dimethyl-2,2′-dipyrryl]methene Hydrobromide, 7:

Ethyl 4,5-dimethyl-3-ethyl-2-pyrrolecarboxylate, 70 (15.0 gm, 0.066 mole), suspended in formic acid (88%, 50 mL) was heated in a steam bath. HBr solution (48%, 20 ml) was added and heating was continued for 8 h. The solution was then allowed to stand at room temperature overnight. The orange precipitate was isolated by filtration, washed with acetic acid (20 mL) and ether (50 mL) and dried to give 13.0 gm (59%).

Bromine (6 mL) was added to a stirred suspension of the above dipyrrylmethene in HOAc (120 mL) and the mixture was kept at 80°C for 30 min. The solution was allowed to cool and the precipitate was filtered and washed with ether to give [5,5′-bis(bromomethyl)-4,4′-dimethyl-3,3′-diethyl-2,2′-dipyrryl]methene hydrobromide 8 (10.0 gm, 53% yield). NMR showed the 5,5′-methylene protons at δ 4.95, in contrast to the unbrominated methyl signals at δ 2.67.

The bis(bromomethyl)dipyrrylmethene 8 (5.0 gm) was refluxed in dry methanol (50 mL) for 30 min. The solution was then cooled to room temperature and diluted with ether (50 mL), and the precipitates were filtered to give (3.2 gm, 81% yield), m.p. 285°C dec; NMR δ 1.31 (6H, t, Et), 2.22 (6H, s, Me), 2.77 (4H, q, Et), 3.55 (6H, s, OMe), 5.13 (4H, s, CH_2), 7.38 (1H, s, methine). MS, m/e 316 (98, M^+-HBr), 287 (80), 255 (76), 242 (100).

1,8-Bis[5-(2,8,13,17-tetraethyl-3,7,12,18-tetramethyl)-porphyrinyl]anthracene 6:

A) <u>From 5,5′-bis(methoxymethyl)dipyrrylmethene 7 condensation</u>:

A solution of 1,8-bis[(4,4′-diethyl-3,3′-dimethyl-2,2′-dipyrryl)methyl]anthracene 4 (634 mg, 1 mmol) and [3,3′-diethyl-5,5′-bis(methoxymethyl)-4,4′-dimethyl-2,2′-dipyrryl]methene hydrobromide 7 (794 mg, 2 mmol) in benzene (100 mL) was heated to reflux for 1 h. The solution was cooled to room temperature before tetrachloro-o-benzo-

quinone (1.0 gm) was added and stirred for 1/2 h. TLC (silica gel, $CHCl_3$) revealed the formation of two porphyrins; etioporphyrin II, R_f 0.98 and the anthracene diporphyrin, R_f 0.3. To facilitate the separation of the diporphyrin from impurities with low R_f value, the residue, after removal of benzene, was heated in methylene chloride with methanolic solution of zinc acetate and sodium acetate. The zinc-diporphyrin complex, R_f 0.9 (silica gel, $CHCl_3$) was separated by column chromatography. The free base diporphyrin was obtained by demetalation of the zinc complex upon washing the methylene chloride solution of the complex with 10% hydrochloric acid and purification by chromatography. Yield: 80 mg (7%) of anthracene diporphyrin 6 and 150 mg of etioporphyrin II. NMR of the diporphyrin: δ 1.27 (12H, t, Et), 1.66 (12H, t, Et), 1.87 (12H, s, Me), 3.17 (12H, s, Me), 3.38 (8H, q, Et), 3.90 (8H, 2q, Et), anthryl: 7.58 (2H, t, 2,7-H), 7.71 (2H, t, 3,6-H), 8.50 (2H, d, 4,5-H), 8.90 (1H, s, 10-H), 9.00 (1H, s, 9-H), 8.95 (4H, s, meso-H), 9.34 (2H, s, meso-H), -4.98 (4H, broad, NH). MS, m/e 1131 (89), 1130 (100, 565 (81); high resolution MS, 1130.6670 ($C_{78}H_{82}N_8$); UV-vis λ_{max} nm (ϵ_{mM}), 625 (4.0), 572 (9.0), 537 (10), 503 (22), 394 (232). Analysis calculated for $C_{78}H_{82}N_8$: C, 82.79; H, 7.30; N, 9.90; found: C, 82.81, H, 7.41, N, 9.85.

B) <u>From 5,5′-bis(bromomethyl)dipyrrylmethene 8 condensation</u>:

A solution of α-free bis(dipyrrylmethyl)anthracene 4

(300 mg, 0.47 mmol) and [5,5′-bis(bromomethyl)-3,3′-diethyl-4,4′-dimethyl-2,2′-dipyrryl]methene hydrobromide 8 (470 mg, 0.94 mmol) in glacial acetic acid (50 mL) was refluxed for 2 h, after which time air was passed through the solution for 20 h. The solvent was removed by evaporation, and the residue was dissolved in chloroform (50 ml) and refluxed, together with 20 ml of a saturated methanolic solution of $Zn(OAc)_2$ and NaOAc, for 1/2 h. Work-up, as in part (A), gave 25 mg (4.6% yield) of the diporphyrin 6, in addition to 30 mg of etioporphyrin II. The diporphyrin is identical to the authentic sample prepared by method (A).

C) From Coupling of 1,8-anthracene dicarboxaldehyde with 1,19-dideoxy-2,8,12,18-tetramethylbiladiene-ac dihydrobromide 9:

A suspension of 1,8-anthracene dicarboxaldehyde 1 (117 mg, 0.5 mmol) and 1,19-dideoxytetraethyltetrametylbiladiene-ac dihydrobromide 9 (625 mg, 1 mmol) in dry methanol (10 mL) containing 5 drops of a solution of glacial acetic acid saturated with hydrogen bromide, was refluxed under argon atmosphere for 18 h. The solution was then poured onto water (25 mL) and the products were extracted with $CHCl_3$ (2 × 25 mL). Chromatography (silica gel, CH_2CL_2) gave monoporphyrin anthracene carboxaldehyde 18 (30 mg, 9% yield) and 1,8-anthracene diporphyrin 6 (32 mg, 5.6% yield), together with etioporphyrin II (23 mg, 10% yield). The products were identical in every respect with authentic samples

prepared previously by different methods.

D) From 1,19-dideoxybiladiene-ac 9 condensation with aldehyde:

A suspension of 1,19-dideoxy-2,8,12,18-tetraethyl-3,7,13,17-tetramethyl biladiene-ac dihydrobromide 9 (70 mg, 0.11 mmol) and 5-(8-formyl-1-anthryl)-2,8,13,17-tetraethyl-3,7,12,18-tetramethylporphyrine 18 (76 mg, 0.11 mmol) in MeOH (10 mL) containing 4 drops of acetic acid solution saturated with HBr were heated under reflux for 24 h. The solution was then poured onto a saturated solution of sodium carbonate (50 mL) and the product was extracted with $CHCl_3$ (3 × 25 mL). Column chromatography (silica gel, $CHCl_3$) was used to separate the diporphyrin. For further purification, zinc was inserted in the diporphyrin, chromatographed and then demetalated to give 15 mg (12% yield). The product is identical to the authenic sample.

E) From 5,5′-diformyldipyrrylmethane 5:

To a solution of α-free bis(dipyrrylmethane)anthracene 4 (634 mg, 1 mmol) and 5,5′-diformyl-3,3′-diethyl-4,4′-dimethyl-2,2′-dipyrrylmethane 5 (572 mg, 2 mmol) in methanol (80 mL) was added 70% perchloric acid (0.5 mL). The dark red solution was stirred under argon atmosphere for 12 h at room temperature in the dark, after which time a solution of NaOAc (0.5 gm) in methanol (10 ml) was added, followed by another solution of o-chloranil (200 mg) in methanol (10 mL). After stirring for 1 h, the solvent was removed

and the residue was taken up in CH_2Cl_2 (20 mL) and a solution of zinc acetate (200 mg) in methanol (10 ml) was added. After being stirred for 1 h, the solvents were evaporated and the residue separated by chromatography (silica gel, $CHCl_3$). The isolated Zn(II) diporphyrin was demetalated by washing with 10% HCl in CH_2Cl_2 to give (238 mg, 21%) of the free base diporphyrin, 300 mg of etioporphyrin II was also obtained. The product obtained is similar to the authentic sample.

5-Phenyl-2,8,13,17-tetraethyl-3,7,12,18-tetramethyl porphyrin 44:

A) From the 5,5′-bis(methoxymethyl)dipyrrylmethene hydrobromide 7 condensation:

α-Free phenyldipyrrylmethane 68 (470 mg, 1.5 mmol) and [bis(methoxymethyl)dipyrryl]methene hydrobromide 7 (650 mg, 1.55 mmol) were dissolved in benzene (80 mL) and heated to reflux for 1 h. Tetrachloro-o-benzoquinone (200 mg) was added to the cold solution and stirred at room temperature for 1/2 h. The products were separated by chromatography using silica gel and CH_2Cl_2/hexane (80:20) as eluent to give 160 mg (17.8% yield) of the phenylporphyrin 44. A small amount of etioporphyrin II (30 mg) was obtained. NMR for phenylporphyrin, δ 1.81 (6H, t, Et), 1.90 (6H, t, Et), 2.45 (6H, s, Me) 3.69 (6H, s, Me), 4.05 (8H, 2q, Et), 7.78 (3H, m, 3,4,5-H phenyl), 8.05 (2H, d, 2,6-H phenyl), 9.96 (1h, s, meso), 10.15 (2H, s, meso) -3.30 (2H, broad, NH).

MS, m/e 554 (100), 277 (34); UV-vis, λ_{max} (ϵ_{mM}), 628 (2.5), 559 (6.7, 534 (7.0), 501 (15.5), 402 (188). Analysis calculated for $C_{38}H_{42}N_4$: C, 82.27; H, 7.63, N, 10.10; found: C, 82.14; H, 7.71; N, 10.17.

B) From 5,5′(diformyl)dipyrryl toluene 69 condensation with α,α′-free dipyrryl methane:

α,α[5,5′-Diformyl-4,4′-diethyl-3,3′-dimethyl-2,2′-dipyrryl]toluene 69 (362 mg, 1 mmol) and 4,4′-dimethyl-2,2′-dipyrrylmethane (230 mg, 1 mmol) were stirred in methanol (50 mL) under argon in the presence of perchloric acid (70%, 4 drops), for 18 h. Tetrachloro-o-benzoquinone (100 mg) in methanol (5 ml) was added and stirring was continued for one more hour. Chromatography, as in part (A), gave 182 mg (33% yield) of phenylporphyrin, identical to the authentic sample obtained above. Etioporphyrin II (50 mg) was also obtained.

Octaethylporphyrin from the Condensation of [(methoxymethyl)dipyrryl]methene Hydrobromide 7:

[5,5′-Bis(bromomethyl)-3,3′,4,4′-tetraethyl-2,2′-dipyrryl]methene hydrobromide 8 (12.0 gm) in methanol (200 mL) was heated under reflux for 30 min. The mixture was evaporated to dryness and the residue was triturated with ether/methanol (5:1). The resultant [(methoxymethyl)-dipyrryl]methene hydrobromide 7 (7.5 gm) was used without purification to condense with (3,3′,4,4′-tetraethyl-2,2′-dipyrryl]methene hydrobromide in hot benzene. After oxida-

tion in o-chloranil, octaethylporphyrin was isolated in 28% yield: NMR δ1.09 (24H, t, Et), 2.40 (16H, q, Et), 10.1 (4H, s, meso-H), -3.88 (2H, broad, NH); m.p. 324°C (Lit. m.p. 324-325°C). This porphyrin was identical in every respect with an authentic samples of OEP.

1,8-Bis[(4,4′-diethyl-5,5′-diformyl-3,3′-dimethyl-2,2′-dipyrryl)methyl]anthracene **25**:

To a solution of 1,8-bis[(4,4′-diethyl-3,3′-dimethyl-2,2′-dipyrryl)methyl]anthracene **4** (2.00 gm, 3.1 mmol) in dimethylformamide (15 ml) was added phosphorus oxychloride (5.0 ml) dropwise, while cooling (-5° to 0°C). The solution was then stirred at room temperature under nitrogen atmosphere for 5 h, after which time water (100 ml) was added. The dark brown solution which resulted was washed several times with ether, and the aqueous layer was treated with 10% NaOH solution until complete precipitation was assured. The light brown precipitate was collected by filtration, washed with water (100 ml) and air dried. The tetraaldehyde **25** was purified further by chromatography (silica gel, CH_2Cl_2) to give 1.15 gm (50% yield); m.p. 221-222°C. NMR, δ 1.20 (12H, t, Et), 1.70 (12H, t, Me), 2.65 (8H, q, Et), 5.90 (2H, s, CH), 6.90 (2H, d, 2,7H-anthryl), 7.38 (2H, t, 3,6H-anthryl), 7.90 (2H, d, 4,5H-anthryl), 8.25 (1H, s, 10H-anthryl), 8.40 (1H, s, 9H-anthryl), 8.65 (4H, broad, NH), 9.20 (4H, s, CHO); MS, m/e 747 (20), 719 (15), 634 (28), 178 (100).

1,8-Bis[5-(2,8,12,18-tetraethyl-3,7,13,17-tetramethyl-15-phenyl)porphyrinyl]anthracene 71:

The α-free bis(dipyrrylmethyl) anthracene 4 (500 mg, 0.78 mmol) and α,α-diformyl dipyrryl toluene 69 (572 mg, 1.56 mmol) were stirred in methanol (100 ml) for 15 min, then $HClO_4$ (70%, 1 ml) was added. The reaction mixture was stirred for 24 h in the dark and under argon. Tetrachloro-o-benzoquinone (200 mg) in methanol (20 ml) was added, and stirring was continued for one additional hour. The solvent was then removed by a rotary evaporator. The residue was dissolved in $CHCl_3$ (100 ml) and washed with a saturated solution of sodium carbonate, then with water, and the organic layer was dried over anhydrous sodium sulfate. To the organic layer was added a saturated solution of $Zn(OAc)_2$/NaOAc in methanol (20 ml) and the solution was refluxed for 1 h. The solution was then washed with water. The organic layer was evaporated to dryness and the residue was dissolved in $CHCl_3$ (5 ml) and chromatographed through a silica gel column (CH_2Cl_2); all the red zinc diporphyrin eluate was taken. After concentrating the eluate to 50 ml, it was washed in a separatory funnel with 10% HCl solution (50 ml), a saturated Na_2CO_3 solution (50 ml), then water (2 × 50 ml), successively. Further purification of the free base diporphyrin was carried out by column chromatography (silica gel, 1% CH_3OH/CH_2Cl_2) to give diphenyletioporphyrin II (80 mg, R_f 0.95) and diphenyl

diporphyrin anthracene 71 (100 mg, 9% yield); UV-vis, λ_{max}nm (ϵ_{mM}) 624 (3.8), 570 (10), 535 (13), 502 (26), 393 (218). NMR, δ 1.20 (12H, t, Et), 1.70 (12H, t, Et), 1.85 (12H, s, Me), 3.20 (12H, s, Me), 3.95 (16H, 2q, Et), 7.75 (5H, m, phenyl), anthryl: 7.5 (2H, t, 2,7-H), 8.10 (2H, t, 3, 6-H), 8.45 (2H, d, 4,5-H), 8.75 (1H, s, 10-H), 9.50 (1H, s, 9-H), 10.25 (4H, s, meso-H), -4.95 (4H, broad, NH).

1,8-Bis{5-[2,8-diethyl-3,7,12,18-tetramethyl-13,17-bis(methylpropionate)]-porphyrinyl}anthracene 73:

A procedure similar to that in the anthracene diporphyrin 6 was followed using 1 equivalent of the α-free bis dipyrrylmethane anthracene and 2 equivalents of [5,5′-diformyl-4,4′-dimethyl-3,3′-bis(methylpropionate)-2,2′-dipyrryl]methane 72. Tetra(methylpropionate)porphyrin (10% yield) was obtained in addition to 9% yield of the desired diporphyrin product. NMR of the diporphyrin, 1.20 (12H, t, Et), 1.60 (12H, s, Me), 3.00 (8H, t, methylene), 3.20 (12H, s, Me), 3.30 (8H, t, $-OCH_2-$), 3.50 (12H, s, $-OCH_3$), 4.10 (8H, 2q, Et), anthryl: 7.40 (2H, t, 2,7-H), 7.50 (2H, 5, 3,6-H), 8.50 (2H, d, 4,5-H), 8.80 (1H, s, 10-H), 8.95 (4H, s, meso-H), 9.15 (1H, s, 9-H), 9.30 (2H, s, meso-H), -4.50 (4H, broad, NH). Uv-vis λ_{max}nm (ϵ_{mM}) 623 (4), 570 (9), 534 (11), 502 (25), 391 (220).

1,8-Bis{[5,5′-bis(ethyoxycarbonyl)-4,4′-diethyl-3,3′-dimethyl-2,2′-dipyrryl]methyl biphenylene 13a:

Basically, a similar procedure to the one followed in reacting 1,8-anthracene dicarboxaldehyde with α-free pyrrole was carried out. The α-free pyrrole 2 (4 equivalents) and 1,8-biphenylene dicarboxaldehyde 12 (1 equivalent) were refluxed in ethanol for 1 h, under nitrogen and in the presence of catalytic amounts of concentrated hydrochloric acid. Precipitation of the product was enhanced by adding a few pieces of ice to the cold reaction solution, the white solid obtained by filtration was dried and recrystallized from aqueous ethanol to give 90% yield of the 1,8-bis(dipyrrylmethyl)biphenylene 13, m.p. 123°-125°C. NMR, δ 1.05 (12H, t, Et), 1.25 (12H, t, -OEt), 1.85 (12H, s, Me), 3.75 (8H, q, Et), 4.30 (8H, q, -OEt), 5.50 (2H, s, CH), 7.30-7,80 (6H, m, biphenylene), 8.10 (4H, broad, NH). MS, m/e 896 (15), 850 (22), 804 (30), 715 (100).

1,8-Bis[4,4′-diethyl-3,3′-dimethyl-2,2′-dipyrryl)methyl]-biphenylene 13b:

1,8-Bis{[5,5′-bis(ethoxycarbonyl)-4,4′-diethyl-3,3′dimethyl-2,2′-dipyrryl]methyl}biphenylene 13a (700 mg, 0.78 mmol) was heated at reflux in ethanol (30 mL) containing potassium hydroxide (200 mg) for 6 h under nitrogen atmosphere. Most of the ethanol was then removed under vacuum and the residue was dissolved in water (40 mL), cooled in ice and acidified by glacial acetic acid. The

precipitated acid was separated by filtration and washed with excess water to give 500 mg (90% yield).

The tetra carboxylic acid (500 mg, 0.70 mmol) was dissolved in ethanolamine (10 mL) and heated at 100°C for 1 h under argon. The dark hot solution was added to ice (~25 gm). The white precipitate was filtered and washed with water, 400 mg (93% yield), m.p. 110-113°C. MS, m/e 608 (15), 510 (21), 411 (18), 150 (100); NMR, δ 1.05 (12H, t, Et), 1.85 (12H, s, Me), 3.75 (8H, q, Et), 5.50 (2H, s, CH), 6.50 (4H, broad, singlet, α-H pyrrole), 7.30-7.80 (6H, m, biphenylene), 8.15 (4H, broad, NH).

1,8-Bis[5-(2,8,13,17-tetraethyl-3,7,12,18-tetramethyl)-porphyrinyl]biphenylene 14:

A procedure similar to that of the anthracene diporphyrin analogue was followed. Biphenylene diporphyrin was obtained in 9% yield, starting with α-free bis(dipyrryl)-methylbiphenylene 13b and 2.0 equivalents of (5,5′-diformyl)-3,3′-diethyl-4,4′-dimethyl-2,2′-dipyrryl)methane 5. NMR, δ 1.45 (12H, t, Et), 1.7 (12H, t, Et), 2.90 (12H, s, Me), 3.15 (12H, s, Me), 3.55 (8H, q, Et), 4.00 (8H, 2q, Et), 6.90-7.25 (6H, m, biphenylene), 8.45 (4H, s, meso-H), 9.00 (2H, s, meso-H), -7.40 (2H, s, NH), -7.80 (2H, s, NH); UV-vis, λ_{max}nm (ϵ_{mM}), 630 (2.8), 580 (7.5), 540 (7.8), 510 (13.3), 380 (189.4).

1{[5,5′-Bis(ethoxycarbonyl)-4,4′-diethyl-3,3′-dimethyl-2,2′-dipyrryl)methyl}anthracene 75:

1-Anthracene carboxaldehyde 74 (2.06 gm, 10 mmol) and ethyl 3-ethyl-4-methyl-2-pyrrolecarboxylate 2 (3.62 gm, 20 mmol) were dissolved in ethanol (40 mL) containing 1 mL of concentrated HCl. The solution was refluxed for 1 h under argon and then cooled in an ice bath for 3 h. The yellow crystals which resulted were filtered and dried. Recrystallization from 95% ethanol gave 5.15 gm (94% yield); m.p. 130-132°C. NMR, δ 1.15 (6H, t, Et), 1.40 (6H, t, -OEt), 1.75 (6H, s, Me), 2.80 (4H, q, Et), 4.30 (4H, q, -OEt), 5.80 (1H, s, CH), 7.20-7.60 (9H, m, anthryl), 8.45 (2H, broad, NH); MS, m/e 550 (30), 477 (21), 404 (48), 331 (15), 259 (55), 178 (100).

1-[4,4′-Diethyl-3,3′-dimethyl-2,2′-dipyrryl)methyl]-anthracene 76:

The hydrolysis was carried out by refluxing the diester 75 (5.0 gm) in ethanol (100 mL) to which 2 gm of NaOH (in 10 mL water) was added, for 8 h. Ethanol was evaporated and water (100 mL) was added. Acidification of this aqueous solution by glacial acetic acid gave the diacid after extraction with ether. Decarboxylation was possible by heating the diacid solution in ethanolamine (100 mL) at 150°C for $^1/_2$ h. Pouring the hot solution onto ice (300 gm) and filtration of the yellow solid gave 3.0 gm (81% yield); m.p. 75°-77°C (decomposition). MS, m/e 406

(48), 297 (100), 282 (37), 203 (20); NMR, δ 1.20 (6H, t, Et), 1.65 (6H, s, Me), 2.50 (4H, q, Et), 5.90 (1H, s, CH), 6.40 (2H, s, α-H pyrrole), 7.20-7.60 (10H, m, anthryl and NH).

1-[5-(2,8,13,17-Tetraethyl-3,7,12,18-tetramethyl)-porphyrinyl]anthracene 46:

The procedure is basically the same as that used in the synthesis of the 1,8-anthracene diporphyrin 6. Column chromatography (silica gel CH_2Cl_2/hexane, 50:50) was used to purify the product; 1.30 gm (24% yield). NMR, δ 1.60 (6H, t, Et), 1.85 (6H, t, Et), 2.05 (6H, s, Me), 3.70 (6H, s, Me), 3.90 (4H, 9, Et), 4.05 (4H, q, Et), anthryl: 7.00 (1H, t, 2-H), 7.30 (1H, t, 3-H), 7.60 (1H, s, 10-H), 7.85 (1H, d, 5-H), 8.00 (1H, t, 7-H), 8.10 (1H, d, 4-H), 8.70 (1H, s, 9-H), 9.95 (1H, s, meso-H), 10.20 (2H, s, meso-H), -3.10 (2H, d, NH); UV-vis, λ_{max}nm (ϵ_{mM}) 623 (3.1), 570 (7.7), 534 (9.2), 500 (70.8), 404 (194).

1,5-Bis{[4,4′-diethyl-3,3′-dimethyl-2,2′-dipyrryl]methyl}anthracene 77:

A similar procedure to that of 1,8-analogue was followed: refluxing of 1,5-anthracene dicarboxaldehyde and ethyl 3-ethyl-4-methyl-2-pyrrolecarboxylate in ethanol in the presence of catalytic amounts of concentrated HCl to give 91% yield of 1,5-bis{[5,5′-bis(ethoxycarbonyl)-4,4′-diethyl-3,3′-dimethyl-2,2′-dipyrryl]methyl}anthracene,

after crystallization from aqueous ethanol. M.p. 170°C (decomposition). MS, m/e 923 (15), 876 (100), 875 (75). NMR, δ 1.05 (12H, t, Et), 1.30 (12H, t, -OEt), 1.60 (12H, s, Me), 2.85 (8H, q, ET), 4.25 (8H, q, -OEt), 6.20 (2H, s, methine-H), 8.25 (4H, broad, NH), anthryl: 6.95 (2H, d), 7.50 (2H, t), 8.10 (2H, d), 8.40 (1H, s), 8.50 (1H, s).

The tetra ethyl ester was hydrolyzed by heating in ethanolic alkaline solution, and the resultant acid was decarboxylated by heating in ethanolamine to give the α-free 1,5-bis(dipyrrylmethyl)anthracene in 95% yield. M.p. 120-123°C (decomposition); MS, m/e 634 (25), 525 (15), 416 (90), 94 (100). NMR, δ 1.15 (12H, t, Et), 1.90 (12H, s, Me), 2.45 (8H, q, Et), 6.15 (2H, s, CH), 6.30 (4H, s, 5H-pyrrole), 7.00-8.70 (12H, m, anthryl and NH).

1,5-Bis[5-(2,8,13,17-tetraethyl-3,7,12,18-tetramethy)-porphyrinyl]anthracene 80:

To synthesize 1,5-bis(etioporphyrinyl)anthracene, a similar procedure to that of the 1,8-analogue (method D) was applied. The α-free 1,5-bis(dipyrrylmethyl)anthracene 4 (900 mg, 1.42 mmol) was dissolved in CH_3OH/CH_2Cl_2 (450 mL, 50:50), then 3-ethyl-2-formyl-4-methyl pyrrole 78 (857 mg, 5.67 mmol) in methanol (50 mL) was added in one portion. The solution was stirred for 1½ h while bubbling nitrogen through the solution, after which time 30% HBr/HOAc (3 mL) was added and the stirring was continued for 15 min longer. Diethyl ether (400 mL) was added to the

solution after CH_2Cl_2 was removed on a rotavap, and the precipitated 1,5-bis(biladiene-ac)hydrobromide-anthracene 79 was collected by filtration and used without further purification; 1.00 gm (49% yield) of dark green prisms.

The biladiene-ac derivative (1.00 gm) was dissolved in dry DMF (40 mL) containing anhydrous copper(II) chloride (2.5 gm), the solution was then stirred at 145°C under argon atmosphere for 10 min and poured onto 200 mL water. The diporphyrin copper complex was extracted from the aqueous layer with chloroform (3 × 50 mL), and passed through a silica gel column (using CH_2Cl_2 as an eluent). The dark red eluate was concentrated up to 50 mL and washed with concentrated sulfuric acid, saturated Na_2CO_3 solution and with water, successively. The free base diporphyrin thus obtained was further purified by TLC (silica gel, $CHCl_3$ as an eluent) to give 70 mg (9% yield). UV-vis, λ_{max}^{nm} (ϵ_{mM}), 624 (3.5), 568 (7.8), 536 (8.7), 500 (18.0), 406 (163.6); NMR, δ 1.45 (12H, t, Et), 1.75 (12H, t, Et), 2.05 (12H, s, Me), 3.55 (12H, s, Me), 3.75 (8H, q, Et), 4.05 (8H, 2q, Et), anthryl: 7.75 (2H, t, 2,6-H), 2.90 (2H, t, 3,7-H), 8.20 (2H, d, 4,8-H), 8.50 (2H, s, 9,10-H), 10.3 (2H, s, meso-H), 10.50 (4H, s, meso-H), -3.15 (4H, broad singlet, NH).

8-Formyl-1{[5,5′-bis(ethoxycarbonyl)-4,4′-diethyl-3,3′-dimethyl-2,2′-dipyrryl]methyl}anthracene 15:

To 1,8-anthracene dicarboxaldehyde 1 (500 mg, 2.1 mmol) suspended in dry ethanol (30 mL) was added concentrated hydrochloric acid (0.5 mL). the mixture was stirred at room temperature until all the dialdehyde dissolved. to this solution was added ethyl-3-ethyl-4-methyl-2-pyrrolecarboxylate 2 (774 mg, 4.2 mmol) in ethanol (10 mL) in three portions over a period of 15 min. After the additions, the solution was allowed to reflux for 30 min under nitrogen. A yellow precipitate started to form soon after the completion of addition. The reaction mixture was cooled and the solid was filtered, washed with water and dried (750 mg). The filtrate was concentrated to one-half of the volume and cooled to give a second batch (250 mg) of the dipyrrylmethane. The solids were combined and recrystallized once from benzene to give yellow plates (900 mg, 73%; m.p. 217-218°C; MS, m/e 578 (M^+, 45), 505 (10), 459 (8), 398 (30), 352 (25), 324 (40), 178 (100), NMR, δ 1.10 (6H, t, Et), 1.30 (6H, t, -OEt), 2.00 (6H, s, Me), 2.80 (4H, q, Et), 4.10 (4H, q, -OEt), 6.50 (1H, s, methine CH), 7.00-7.70 (7H, m, anthryl), 8.20 (1H, s, 9-H) anthryl), 8.40 (2H, broad, NH), 10.10 (1H, s, CHO). Analysis calculated for $C_{36}H_{38}N_2O_5$: C, 74.71; H, 6.62; N, 4.84; found: C, 74.58; H, 6.75; N, 4.46.

8-Hydroxymethyl-1-{[5,5′-bis(ethoxycarbonyl)-4,4′-diethyl-3,3′-dimethyl-2,2′-dipyrryl]methyl}anthracene 16a:

To the 8-formyl-1-dipyrrylmethyl anthracene 15 (578 mg, 1.0 mmol) in ethanol (2.0 mL) was added sodium borohydride (30 mg in 0.1 mL of water), and the mixture was stirred at room temperature for 15 min. A solution of NaOH (6N, 0.4 mL) was added. The mixture was heated on a steam bath for 5 min and then poured onto ice. The product was extracted with CH_2Cl_2 (3 × 20 mL) to give a white solid, 550 mg (95% yield); m.p. 128-130°C; MS, m/e 580 (M^+, 10), 553 (12), 399 (12), 308 (25), 176 (100). NMR, δ 1.10 (6H, t, Et), 1.30 (6H, t, -OEt), 2.00 (6H, s, Me), 2.80 (4H, q, Et), 4.10 (4H, q, -OEt), 5.00 (2H, s, CH_2O-), 5.30 (1H, s, OH), 6.50 (1H, s, methine CH), 7.00-7.77 (7H, m, anthryl), 8.2 (1H, s, 9-H anthryl), 8.40 (2H, broad, NH). This solid was used in the next step without further purification.

8-(Hydroxymethyl)-1-{[4,4′-diethyl-3,3′-dimethyl-2,2′-dipyrryl]methyl}anthracene 16b:

The diester dipyrrylmethyl anthracene 16a (500 mg, 0.86 mmol) was saponified by refluxing for 8 h in ethanol (10 mL) containing sodium hydroxide (300 mg) and water (1 mL). After the hydrolysate was concentrated to remove ethanol, water (20 mL) was added and the solution was extracted with dichloromethane (20 mL). The aqueous layer was kept in an ice bath and neutralized with glacial acetic acid, the precipitated white solid was extracted into ether

(3 × 20 mL). After removal of solvent, the crude diacid was dissolved in ethanolamine (5 mL) and heated to a gentle reflux under nitrogen for 1 h. The dark hot solution was poured into ice water (50 mL); the resultant light yellow solid was collected by filtration. This material was chromatographed on silica gel (CH_2Cl_2) to give pure α-free dipyrrylmethane (360 mg, 95% yield); m.p. 98-100°C; MS, m/e 436 (M^+, 7), 327 (20), 298 (8), 229 (10), 176 (100). NMR, δ 1.10 (6H, t, Et), 2.00 (6H, s, Me), 2.30 (4H, q, Et), 5.00 (2H, s, O-CH_2), 5.20 (1H, s, OH), 6.20 (1H, s, methine CH), 6.30 (2H, s, α-H pyrrole), 7.00-7.77 (7H, m, anthryl), 8.20 (1H, s, 9H-anthryl), 8.40 (1H, broad, NH).

5-[8-(Hydroxymethyl)-1-anthryl]-2,8,13,17-tetraethyl-3,7,12,18-tetramethylporphine 17:

To a solution of the decarboxylated 8-(hydroxymethyl)-1-[(4,4′-diethyl-3,3′-dimethyl-2,2′-dipyrryl)methyl]-anthracene **16b** (347 mg, 1.20 mmol) and the 5,5′-diformyl-3,3′-diethyl-4,4′-dimethyl-2,2′-dipyrrylmethane **5** (347 mg, 1.20 mmol) in dry methanol (70 mL) was added 70% perchloric acid (0.5 mL). The dark red solution was stirred for 12 h at room temperature in the dark, after which a solution of sodium acetate (0.5 gm) in methanol (10 mL) was added, followed by another solution of o-chloranil (200 mg) in methanol (10 mL). After 1 h, the mixture was evaporated; the residue was taken up by CH_2Cl_2 (2 × 20 mL) and a zinc acetate (200 mg) in methanol (10 mL) was added. After

being stirred for 1 h, the mixture was evaporated and the residue was separated by chromatography (silica gel, CH_2Cl_2). The isolated Zn(II) porphyrin complex was demetalated by washing with 10% hydrochloric acid in dichloromethane: yield, 400 mg (48%). NMR, δ -3.00 (2H, d, NH), 1.70 (6H, t, Et), 1.90 (6H, t, Et), 2.10 (6H, s, Me), 3.70 (6H, s, Me), 3.80 (2H, s, CH_2O-), 3.90 (4H, q, Et), 4.10 (4H, q, Et), 10.00 (1H, s, meso-H), 10.30 (2H, s, meso-H), anthryl: 7.10 (1H, d), 7.40 (1H, t), 7.80 (2H, m), 8.00 (1H, d), 8.10 (1H, d), 8.40 (1H, d), 8.70 (1H, s); UV-vis, λ_{max}^{nm} (ϵ_{mM}) 624 (2.4), 569 (6.0), 535 (6.5), 502 (13.0), 405 (129.0). Analysis calculated for $C_{47}H_{48}N_4O$: C, 82.42; H, 7.06; N, 8.18; found: C, 82.33; H, 7.15; N, 8.09.

5-(8-Formyl-1-anthryl)-2,8,13,17-tetraethyl-3,7,12,18-tetramethylporphine 18:

Oxidation of the anthracene alcohol porphyrin 17 (280 mg, 0.4 mmol) was effected by addition of its solution in pyridine (30 mL) to a cold solution of chromic trioxide (350 mg) in pyridine (20 mL) at 0-5°C. After stirring for 15 min, the ice bath was removed and the solution was stirred at room temperature for 4 h and then poured into water (100 mL). The product was extracted into dichloromethane (3 × 50 mL) and purified by chromatography (silica gel, CH_2Cl_2) to give the corresponding aldehyde 18 in quantitative yield; NMR, δ -3.10 (2H, d, NH), 1.67 (6H, t, Et), 1.85 (6H, t, Et), 2.03 (6H, s, Me), 3.68 (6H, s, Me), 3.85

(4H, q, Et), 4.03 (4H, q, Et), 9.38 (1H, s, CHO), 9.91 (1H, s, meso-H), 10.15 (1H, s, meso-H), anthryl: 7.40 (1H, t), 7.67 (1H, d), 7.85 (1H, t), 8.10 (1H, d), 8.28 (1H, d), 8.46 (1H, d), 8.75 (1H, s), 9.00 (1H, s). UV-vis λ_{max}nm (ϵ_{mM}) 624 (2.4), 569 (6.1), 535 (6.6), 502 (13.5), 404 (140.0); MS, m/e 682 (M^+, 5), 655 (8), 654 (12), 178 (100).

trans-5,15-Bis{8-[5-(2,8,13,17-tetraethyl-3,7,12,18-tetramethylporphyrinyl]-1-anthryl}-2,8,12,18-tetraethyl-3,7,13,17-tetramethylporphine 20:

To the porphyrin aldehyde 18 (50 mg, 0.073 mmol) suspended in methanol (10 mL) was added first the α-free (3,3′-diethyl-4,4′-dimethyl-2,2′-dipyrryl)methane 19 (17.3 mg, 0.073 mmol) and the solution was deaerated by bubbling argon for 15 min before p-toluenesulfonic acid (3.4 mg, 0.018 mmol) was added. The mixture was stirred at room temperature (under argon, in the dark) for 10 h before the solvent was pumped dry. The residue was dissolved in THF (10 mL), treated with a solution of o-chloranil (10 mg) in THF (5 mL), and stirred for 1 h, and the solvent was removed again by evaporation. This mixture contained a large amount of unreacted porphyrin aldehyde which can be recovered during the isolation of the trimer. The chromatography was carried out with a silica gel column, using CH_2Cl_2 to elute the porphyrin aldehyde 18 and 5% MeOH-CH_2Cl_2 for the triporphyrin 20. The trimer thus obtained was purified further by conversion and chromato-

graphy of the Zn complex, which moves much faster than the free base, to remove impurities of low R_f values. Pure free base triporphyrin was then derived by demetalation of zinc complex using 10% HCl solution: yield, 7.0 mg; UV-vis, λ_{max}^{nm} (ϵ_{mM}) 625 (3.9), 573 (9.3), 538 (8.3), 506 (18.0), 395 (169.0). NMR, δ -4.5 (6H, three singlets clustered together, NH), 0.95 (12H, t, Et), 1.10 (12H, t, Et), 1.45 (12H, t, Et), 1.60 (12H, s, Me), 1.80 (12H, s, Me), 3.02 (12H, s, Me), 3.20 (8H, q, Et), 3.41 (8H, q, Et), 3.55 (8H, q, Et), anthryl: 6.81 (2H, d), 7.35 (2H, d), 7.50 (2H, t), 7.59 (2H, d), 7.60 (2H, s), 8.05 (2H, s), 8.45 (2H, t), 8.72 (2H, s), meso: 8.95 (2H, s), 9.25 (4H, s), 9.30 (2H, s). Analysis calculated for $C_{124}H_{126}N_{12}$: C, 83.46; H, 7.12; N, 9.42; found: C, 83.75; H, 7.30; N, 9.32. High resolution positive ion mass spectra of the triporphyrin have been obtained on Kratos MS-50RF equipped with ion-teck FAB gun, operated at 8 kV. The sample was prepared in 1-thioglycerol matrix containing trifluoroacetic acid. Calculated for monoprotonated trimer: 1784.0306; found, 1784.0140.

5-{8-[(Methanesulfonate)methyl]-1-anthryl}-2,8,13,17-tetraethyl-3,7,12,18-tetramethylporphine 30:

5[8-(Hydroxymethyl)-1-anthryl]-2,8,13,17-tetraethyl-3,7,12,18-tetramethylporphine **17** (345 mg, 0.5 mmol) and excess amounts of methanesulfonyl chloride (2 mL) were dissolved in dry dichloromethane (20 mL). The solution was

heated at reflux until all the porphyrin alcohol reacted (~48 h). The reaction was monitored by TLC. When the reaction was completed, the solvent was pumped dry, and the residue was dissolved in CH_2Cl_2 (3 mL) and purified by column chromatography, using silica gel and CH_2Cl_2 as an eluent. The methyl sulfonate product has a higher R_f value than the corresponding alcohol, 300 mg (80% yield); UV-vis, λ_{max}^{nm} (ϵ_{mM}) 625 (2.4), 570 (6.6), 535 (7.1), 500 (14.3), 405 (125.0). NMR, δ 1.55 (6H, t, Et), 1.75 (6H, t, Et), 1.90 (3H, s, $-SO_2Me$), 2.00 (6H, s, Me), 3.55 (6H, s, Me), 3.75 (2H, s, CH_2SO_3-), 3.85 (4H, q, Et), 4.00 (4H, q, Et), 9.90 (1H, s, meso-H), 10.15 (2H, meso-H), -3.05 (2H, d, NH), anthryl: 7.10 (1H, d), 7.40 (1H, t), 7.85 (1H, t), 8.05 (1H, d), 8.10 (1H, d), 8.15 (1H, s), 8.45 (1H, d), 8.75 (1H, s).

5-{8-[{Bis(2-pyridyl-β-ethyl)amine}methyl]-1-anthryl}-2,8,13,17-tetraethyl-3,7,12,18-tetramethylporphine 32:

A solution of porphyrin methylsulfonate **30** (300 mg, 0.4 mmol) and excess amounts of di(2-pyridyl-β-ethyl)amine **31** (227 mg, 1 mmol) in dry dichloromethane (20 mL) was refluxed under nitrogen; the reaction was complete after 48 h as detected by TLC. After that period, more dichloromethane (30 mL) was added and the solution was washed with 5% hydrochloric acid solution (100 mL) to remove the excess dipyridine ligand, and it was next washed with a saturated solution of Na_2CO_3, and finally washed twice with water

(2 × 100 mL). The organic layer was dried over anhydrous sodium sulfate. The solvent was evaporated on a rotary evaporator and the residue was pumped dry overnight. The product was purified by column chromatography (silica gel, 1% $MeOH/CH_2Cl_2$) and recrystallized from methanol/methylene chloride to give 170 mg (48% yield). UV-vis, λ_{max}nm (ϵ_{mM}) 623 (2.5), 570 (6.5), 534 (7.5), 502 (13.3), 404 (132.0). NMR, δ 0.65 (4H, t, CH_2), 1.50 (4H, t, CH_2), 1.60 (6H, t, Et), 1.85 (6H, t, Et), 2.05 (6H, s, Me), 3.15 (2H, s, CH_2-N), 3.60 (6H, s, Me), 3.85 (4H, q, Et), 4.10 (4H, q, Et), pyridyl: 5.70 (2H, t), 6.20 (2H, t), 7.60 (2H, d), 8.45 (2H, d), anthryl: 7.05 (1H, d), 7.30 (1H, t), 7.80 (1H, t), 7.90 (1H, d), 8.05 (4H, d), 8.90 1H, s), meso-H: 9.95 (1H, s), 10.10 (2H, s), -3.30 (2H, broad doublet, NH).

5-{8-[(1,7,10,16-Tetraoxa-4,13-diazacyclooctadecane)-methyl]-1-anthryl}-2,8,13,17-tetraethyl-3,7,12,18-tetramethylporphine 34:

The methyl sulfonate porphyrin 30 (100 mg, 0.13 mmol) and excess amounts of Kryptofix-22, 33 (1,7,10,16-tetraoxa-4,13,diazacyclooctadecane, 68 mg, 0.26 mmol) were refluxed in dry dichloromethane (20 mL) under nitrogen for 10 h. After the reaction was over, more CH_2Cl_2 (30 mL) was added and the solution was washed with 5% hydrochloric acid solution (50 mL), followed by a saturated solution of sodium carbonate (50 mL) and finally with brine (100 mL). The organic layer was dried over anhydrous sodium sulfate and

the solvent was removed on a rotavap. The residue was dissolved in 1 mL of dichloromethane and purified by chromatography on a silica gel column (1 × 5 inch), CH_2Cl_2 was used first to elute the unreacted methyl sulfonate porphyrin which has a higher R_f-value than the product; chloroform was used next to separate the small amount of porphyrin alcohol which was generated during the reaction possibly by the hydrolysis of the methyl sulfonate, 2% CH_3OH/CH_2Cl_2 was used to elute the porphyrin-crown product. Yield was 35 mg (28%); MS, m/e M^+ 929; UV-vis, λ_{max}nm (ϵ_{mM}), 624 (3.0), 572 (6.0), 535 (8.0), 504 (15), 405 (148.0). NMR, δ 0.60 (4H, t, crown), 1.00 (4H, t, crown), 1.35 (4H, t, crown), 1.50 (4H, t, crown), 1.60 (6H, t, Et), 1.85 (6H, t, Et), 2.05 (6H, s, Me), 2.10 (4H, t, crown), 2.50 (4H, t, crown), 3.10 (2H, s, CH_2-N), 3.80 (4H, q, Et), 4.00 (4H, q, Et), anthryl: 7.00 (1H, d), 7.25 (1H, t), 7.85 (1H, d), 8.00 (1H, d), 8.40 (1H, d), 8.50 (2H, m), 8.80 (1H, s), 8.95 (1H, s), meso: 9.95 (1H, s), 10.10 (1H, s), -3.30 (2H, broad doublet, NH).

2-[5,5′-Bis(ethoxycarbonyl)-4,4′-diethyl-3,3′-dimethyl-2,2′-dipyrryl]acenaphthen-1-one 36:

To a solution of acenaphthenequinone 35 (18.20 gm, 0.10 mol) and ethyl 3-ethyl-4-methyl-2-pyrrolecarboxylate 2 (36.20 gm, 0.20 mol) in absolute ethanol (300 mL) was added a concentrated solution of hydrochloric acid (10 mL). The dark red solution was refluxed under argon atmosphere

for 1 h, after which time the solution was chilled in an ice-bath for 2 h. The light brown crystalline product was then taken by filtration and washed with 100 mL of cold 95% ethanol and dried. Recrystallization from aqueous ethanol gave 45 gm (85% yield) of light brown prisms; m.p. 105-106°C. NMR, δ 1.10 (6H, t, Et), 1.30 (6H, t, -OEt), 1.65 (6H, s, Me), 2.65 (4H, q, Et), 4.30 (4H, q, -OEt), 7.4-8.2 (6H, m, naphthyl), 8.45 (2H, broad, NH). MS, m/e 526 (M^+, 100), 480 (53), 437 (50), 391 (39), 346 (51), 240 (44), 217 (58).

8-[(5,5′-Dicarboxyl-4,4′-diethyl-3,3′-dimethyl-2,2′-dipyrryl)methyl]naphthalene-1-carboxylic acid 37:

A suspension of the diester dipyrrylmethylacenaphthenone 36 (1.40 gm, 2.66 mmol) in 30% aqueous solution of potassium hydroxide (30 mL) was refluxed for 6 h under argon. The dark red-brown solution was diluted by adding water (70 mL), washed twice with chloroform (2 × 50 mL) and the aqueous layer was cooled in ice before being neutralized with glacial acetic acid. The resultant solid was collected by filtration and washed with water (2 × 50 mL); the solid was dissolved in chloroform (100 mL) and dried over anhydrous Na_2SO_4. Evaporation of the organic layer on a rotavap produced the tricarboxylic acid, 1.03 gm (80% yield). No further purification has been done; m.p. 250°C with decomposition; MS, m/e 444 (M^+-CO_2, 20), 400 (18), 355 (27), 126 (100). NMR, δ 1.05 (6H, t, Et), 1.60 (6H, s,

Me), 2.70 (4H, q, Et), 7.30-8.30 (6H, m, naphthyl), 8.50 (2H, broad singlet, NH).

8[(4,4′-Diethyl-3,3′-dimethyl-2,2′-dipyrryl)methyl]-naphthalene-1-carboxylic acid 38:

The decarboxylation of the 5,5′-dicarboxylic groups in 37 was achieved by heating a solution of (1.0 gm, 2.04 mmol) of 37 in ethanolamine (20 mL) at reflux under argon for 1/2 h. The hot dark solution was poured onto ice (50 gm), and the yellow precipitation was collected by filtration and washed with water. Yield was 700 mg (85%); m.p. 100-110°C (decomposition); MS, m/e 400 (7), 355 (20), 291 (10), 126 (100). NMR, δ 1.05 (6H, t, Et), 1.60 (4H, s, Me), 2.70 (4H, q, Et), 6.50 (2H, broad, α-H pyrrole), 7.20-8.30 (6H, m, naphthyl), 8.60 (2H, broad, NH).

Methyl 8-5-(2,8,13,17-tetraethyl-3,7,12,18-tetramethyl)-porphyrinyl]naphthalene-1-carboxylate 40:

(A) <u>From α-free dipyrrylmethane condensation with 5,5′-diformyl dipyrryl methane 5</u>:

The 5,5′-unsubstituted dipyrrylmethyl naphthalene 38 (600 mg, 1.50 mmol) and 5,5′-diformyl-3,3′-diethyl-4,4′-dimethyl-2,2′-dipyrrylmethane 5 (429 mg, 1.5 mmol) were dissolved in dry methanol (20 mL). Argon was bubbled through the solution for 15 min before perchloric acid (70%, 0.4 mL) was added. The solution was stirred at room temperature (under argon in the dark) for 15 h, after which

time a solution of tetrachloro-o-benzoquinone (200 mg) in methanol (10 mL) was added and stirring was continued for one additional hour. Dichloromethane (50 mL) was added and the solution was washed several times with water (50 mL portions) and dried over anhydrous Na_2SO_4. The solvents were removed under vacuum and the residue was dissolved in chloroform (2 mL) and purified by column chromatography (silica gel, 5% methanol/CH_2Cl_2).

The porphyrin acid 39 was dissolved in dry CH_2Cl_2 (10 mL) and oxalyl chloride (0.5 mL) was added. The solution was refluxed for 2 h under argon. The solvents were then pumped dry, and the residue was heated at reflux in methanol (20 mL) for 8 h. The solvent was again removed on a rotavap under vacuum. The residue was purified on a silica gel column (1 × 10 inch) using CH_2Cl_2 to elute the porphyrin naphthalene ester, 200 mg (20% yield) was obtained as dark purple plate after crystallization from methanol/CH_2Cl_2. MS, m/e 662 (55), 590 (10), 331 (10), 126 (15), 85 (100); UV-vis, λ_{max}nm (ϵ_{mM}) 625 (3), 573 (16), 536 (7), 504 (14), 404 (180), NMR δ

(B) From α,α-dicarboxyldipyrrylmethane 37 condensation:

The 5,5′-dicarboxydipyrrylmethyl naphthalene carboxylic acid 37 (1.0 gm, 2.05 mmol) was dissolved in dry CH_2Cl_2 (30 mL) together with 5,5′-diformyl-4,4′-diethyl-3,3′-dimethyl-2,2′-dipyrrylmethane 5 (586 mg, 2.05 mmol). To the solution was added p-toluene sulfonic

acid (800 mg, 4.1 mmol) and stirred at room temperature for 6 h, a saturated methanolic solution of zinc acetate (10 mL) was then added and stirring continued for 12 more hours. After that a solution of o-chloranil (500 mg) in CH_2Cl_2 (5 mL) was added and stirred for an additional hour. Methylene chloride (50 mL) was added and the solution was washed twice with water (2 × 50 mL), evaporation of the organic layer and column chromatography of the residue (silica gel, 1% methanol/CH_2Cl_2) gave the zinc complex of the porphyrin acid after eluting impurities with high R_f volume by pure CH_2Cl_2. The Zn(II) porphyrin acid solution in $CHCl_3$ (50 mL) was shaken with 10% hydrochloric acid (50 mL) in a separatory funnel for ~2 min and the organic layer was washed with water (2 × 50 mL). After evaporation of the solvents, the residue was dissolved in dry CH_2Cl_2 (25 mL) together with oxalylchloride (1 mL) and refluxed under argon for 2 h before the solvents were pumped dry. The porphyrin methyl ester was obtained from the acid chloride by refluxing in methanol and purifying the product by chromatography as in part (A). 240 mg (17.7% yield) was obtained after recrystallization from methanol/CH_2Cl_2. The product was identical in every respect to the authentic sample prepared by method (A).

5-[8-(Hydroxymethyl)-1-naphthyl]-2,8,13,17-tetraethyl-3,7,12,18-tetramethylporphyrin 41:

The porphyrin methyl ester 40 (200 mg, 0.30 mmol) was dissolved in dry THF (25 mL). Warming might be necessary in order to assure complete solubility. Lithium aluminium hydride (38 mg, 1 mmol) was added to the solution at room temperature. After stirring for 2 h, the solvent was removed and the corresponding alcohol was separated from the residue by column chromatography (silica gel, 1% methanol, CH_2Cl_2). 155 mg (80.6% yield) was obtained after recrystallization from methanol/CH_2Cl_2; MS, m/e 634 (M^+, 8), 616 (13), 603 (10), 126 (100). NMR, δ 1.60 (6H, t, Et), 1.85 (6H, t, Et), 2.00 (6H, s, Me), 3.50 (6H, s, Me), 3.60 (2H, s, CH_2O), 3.85 (4H, q, Et), 4.00 (4H, q, Et), 9.90 (1H, s, meso-H), 10.20 (2H, s, meso-H), naphthyl: 7.3-8.00 (6H, m), -3.10 (2H, d, NH). UV-vis λ_{max}nm (ϵ_{mM}) 624 (4), 572 (14), 535 (10), 503 (12), 402 (177).

5 (8-Formyl-1-naphthyl)-2,8,13,17-tetramethyl-3,7,12,18-tetramethyl porphine 81:

A solution of (8-hydroxymethyl)-1-naphthyl porphyrin 41 (170 mg, 0.26 mmol) in pyridine (10 mL) was added at room temperature to chromic trioxide (200 mg) solution in pyridine (20 mL). The resultant solution was stirred under argon in the absence of light for 2 h and then poured into cold water (50 mL) and the corresponding porphyrin aldehyde was extracted with chloroform (3 × 25 mL). The combined

extracts were washed several times with 30 mL portions of water, and the organic layer was evaporated to dryness. The product was separated from the residue by column chromatography using silica gel and CH_2Cl_2 as an eluent, the porphyrin aldehyde has an R_f value of 0.9 compared to 0.6 for the corresponding alcohol. The product was recrystallized once from methanol/CH_2Cl_2 to give 150 mg (88% yield); MS, m/e 632 (M^+, 7), 604 (26), 603 (30), 475 (15), 126 (100). NMR, δ 1.60 (6H, t, Et), 1.80 (6H, t, Et), 2.00 (6H, s, Me), 3.50 (6H, s, Me), 3.80 (4H, q, Et), 3.95 (4H, q, Et), naphthyl: 7.55 (1H, t), 7.70 (1H, d), 7.80 (1H, t), 8.05 (1H, d), 8.30 (2H, d), 7.90 (1H, s, CHO) 9.90 (1H, s, meso-H), 10.10 (2H, s, meso-H), -3.25 (2H, d, NH); UV-vis, λ_{max}^{nm} (ϵ_{mM}) 624 (3), 572 (12), 535 (11), 502 (10) 402 (179).

5{8[(Methanesulfonate)methyl]-1-naphthyl}-2,8,13,17-tetraethyl-3,7,12,18-tetramethylporphine 42:

To a solution of the naphthyl porphyrin alcohol 41 (400 mg, 0.63 mmol) in dry methylene chloride (10 mL) was added methane sulfonyl chloride in excess (1 mL) and pyridine (0.1 mL). The solution was stirred under argon atmosphere until no more alcohol could be detected by TLC (R_f value of alcohol is 0.6, silica gel/CH_2Cl_2), about 8 h. The solvents were then removed on a rotavap and pumped dry under vacuum (~8 h), and the product was purified by chromatography (silica gel plates, CH_2Cl_2). Yield was

229 mg (51%); UV-vis, λ_{max}nm (ϵ_{mM}) 625 (4), 574 (16), 535 (12), 504 (10), 402 (175); MS, m/e, 712 (M^+, 5), 649 (14), 617 (23), 603 (18), 478 (55), 126 (100). NMR, δ -3.05 (2H, d, NH), 0.05 (3H, s, $-SO_2-Me$), 1.55 (6H, t, Et), 1.75 (6H, t, Et), 2.00 (6H, s, Me), 3.45 (6H, s, Me), 3.55 (2H, s, CH_2-O), 3.75 (4H, q, Et), 4.00 (4H, q, Et), 9.85 (1H, s, meso-H), 10.05 (2H, s, meso-H), naphthyl: 7.2-7.95 (6H, m).

5 {8-[{Bis(2-pyridyl-β-ethyl)amine}methyl]-1-naphthyl}-2,8,13,17-tetraethyl-3,7,12,18-tetramethylporphine 43:

A solution of methanesulfonatenaphthyl porphyrin 42 (450 mg, 0.63 mmol) and excess amounts of bis(2-pyridyl-β-ethyl)amine (300 mg, 1.32 mmol) in dry CH_2Cl_2 (20 mg) was heated at reflux under nitrogen for ~20 h. The completion of the reaction was tested by TLC. Methylene chloride (20 mL) was added and the solution was washed with dilute hydrochloric acid (2%, 50 mL), then several times with water (3 × 50 mL). The organic layer was dried over anhydrous sodium sulfate and evaporated. The product was isolated from the residue by chromatography (silica gel plate, $CHCl_3$) to give 200 mg (37.5% yield), dark purple cubic crystals from methanol/CH_2Cl_2. MS, m/e 843 (4), 765 (7), 685 (20), 603 (38), 477 (51), 126 (100); UV-vis, λ_{max}nm (ϵ_{mM}) 624 (3), 574 (13), 534 (12), 503 (11), 403 (150); NMR, δ 0.30 (4H, t, $-CH_2$), 0.80 (4H, t, $N-CH_2$), 1.65 (6H, t, Et), 1.85 (6H, t, Et), 2.05 (6H, s, Me), 2.75 (2H, s,

benzilic-H), 3.50 (6H, s, Me), 3.90 (4H, q, Et), 4.00 (4H, q, Et), 5.40 (2H, d, pyridyl), 6.35 (2H, t, pyridyl), 6.60 (2H, t, pyridyl), 6.70 (2H, d, pyridyl), 7.70-8.40 (6H, m, naphthyl), 9.90 (1H, s, meso-H), 10.00 (2H, s, meso H), -3.15 (2H, d, NH).

5-(8-Carboxyl-1-anthryl)-2,8,13,17-tetraethyl-3,7,12,18-tetramethylporphine 82:

(A) By oxidation of the corresponding alcohol 17:

To a cold solution of the 5-(8-hydroxylmethyl-1-anthryl)porphyrin 17 (684 mg, 1 mmol) in acetone (30 mL), (kept at -5 to 0°C), was added 0.3 mL of Jone's reagent (prepared by dissolving 6.70 gm of CrO_3 in 6 mL of concentrated sulfuric acid and diluting the solution with 50 mL of water). After complete addition of the oxidizing agent, the solution was left to stir at ambient temperature for 10 min, after which time water (25 mL) was added and the porphyrin carboxylic acid was extracted from the aqueous solution with chloroform (3 × 25 mL) and the solvent was removed. The product was purified by column chromatography (silica gel, 5% methanol/CH_2Cl_2, R_f 0.4); 623 mg (89% yield) was obtained. MS, m/e 656 (M^+-CO_2, 40), 478 (16), 178 (55), 44 (100); UV-vis, λ_{max}nm (ϵ_{mM}) 625 (3.0), 570 (5.5), 532 (6.8), 504 (14.7), 404 (122.0). NMR, δ -3.10 (2H, d, NH), 1.70 (6H, t, Et), 1.85 (6H, t, Et), 2.00 (6H, s, Me), 3.75 (6H, s, Me), 3.90 (4H, q, Et), 4.05 (4H, q, Et), 9.95 (1H, s, meso-H), 10.30 (2H, s, meso-H), anthryl:

7.15 (1H, d), 7.40 (1H, t), 7.85 (2H, m), 8.00 (1H, d), 8.10 (1H, d), 8.40 (1H, d), 8.75 (1H, s).

(B) By hydrolysis of porphyrin methyl ester **84**:

To a solution of 5-(8-methoxycarbonyl-1-anthryl)-2,8,13,17-tetraethyl-3,7,12,18-tetramethylporphine **83** (684 mg, 1 mmol) in formic acid (98%, 20 mL) was added concentrated HCl (5 mL). The solution was heated at reflux under argon for 6 h. The solution was then added to 50 mL of ice-water in a separatory funnel and the porphyrin was extracted with $CHCl_3$ (3 × 30 mL). The organic layer was washed with water several times (4 × 50 mL) and dried over anhydrous Na_2SO_4 and the solvents were evaporated on a rotavap until dry. Purification of the product was possible by column chromatography (silica gel, 5% methanol/CH_2Cl_2, R_f, 0.4) to give 91 mg (13% yield). The product was identical in every respect with an authentic sample prepared by method (A).

*8 Methoxycarbonyl-1-anthracenecarboxaldehyde **51**:*

To a suspension of dimethyl 1,8-anthracenedicarboxylate **50** (6.00 gm, 20 mmol) in dry diethyl ether (200 mL) was added lithium aluminum hydride (0.76 gm, 0.02 mmol). The mixture was heated at reflux for 3 h, and then cooled in ice before ethyl acetate (4 mL) was added. The mixture was stirred for 5 more minutes and the solvents were removed by evaporation. To the ice-cooled residue, 6N hydrochloric acid (100 mL) was added portion-wise (10 mL

each portion); the yellow precipitates which resulted were separated by filtration, washed with dilute HCl and with excess water afterward, and then dried in air to give 5.50 gm. No further purification of the products was done at this stage.

The dry solid (5.50 gm) was dissolved in dry pyridine (75 mL) and the solution was added to an ice-cooled chromic trioxide, CrO_3 (22.0 gm) solution in pyridine (100 mL). The mixture was stirred at 0°C for 15 min. After that the ice bath was removed and the dark brown solution was stirred at room temperature for 4 additional hours. The solution was poured onto water (1000 mL) and the brown precipitate which resulted was obtained by filtration, washed with excess water and dried in air. The products were obtained from the brown solid by extracting with benzene (150 mL) in a Soxhlet extractor. Yellow solid obtained by evaporation of benzene was found to contain three components that were separable by column chromatography, on silica gel. The unreduced dimethyl 1,8-anthracenedicarboxylate (0.9 gm) was eluted with 1:5 hexane/CH_2Cl_2 (R_f 0.9); the desired product (monomethyl-ester anthracene carboxaldehyde; 2.0 gm, 37% yield) was eluted with CH_2Cl_2 (R_f 0.7). The third component was 1,8-anthracene dicarboxaldehyde (2.1 gm, 45% yield) obtained by elution with $CHCl_3$ (R_f 0.5). Data for 51: m.p., 150-152°C; MS, m/e 264 (M^+, 12), 236 (16), 221 (28), 206 (60), 192 (65), 178 (94), 83 (100). NMR, δ 4.05 (3H, s, Me), 7.30-

8.20 (6H, m anthryl), 8.45 (1H, s, 10-H anthryl), 10.50 (1H, s, 9-H, anthryl), 10.90 (1H, s, CHO).

8-{[5,5′-Bis(ethoxycarbonyl)-4,4′-diethyl-3,3′-dimethyl-2,2′-dipyrryl]methyl-1-methoxycarbonylanthracene 85:

8-Methoxycarbonyl-1-anthracenecarboxaldehyde 51 (2.64 gm, 10 mmol) and ethyl 3-ethyl-4-methyl-2-pyrrolecarboxylate 2 (3.62 gm, 20 mmol) were dissolved in methanol (50 mL) containing 1 mL of concentrated hydrochloric acid. The solution was refluxed under argon for 1 h. Water (50 mL) was added and the product was extracted with chloroform (2 × 40 mL). The resultant dipyrrylmethane diethyl ester was purified by column chromatography (silica gel), using first hexane as an eluent to remove the impurities of high R_f value and then CH_2Cl_2 to elute the desired product. Yield was 4.86 gm, 80% of light brown solid; m.p. 85°C (decomposition). MS, m/e 608 (M^+, 5), 550 (25), 340 (33), 324 (24), 296 (30), 278 (40), 119 (75), 43 (100); NMR, δ 1.10 (6H, t, Et), 1.20 (6H, t, $-CO_2Et$), 1.95 (6H, s, Me), 3.70 (4H, q, Et), 4.00 (3H, s, $-CO_2Me$), 4.15 (4H, q, $-CO_2Et$), 6.35 (1H, s, methine-H), 7.10-8.20 (7H, m, anthryl), 8.55 (1H, s, 9-H, anthryl), 8.70 (2H, broad, NH).

8-(4,4′-Diethyl-3,3′-dimethyl-2,2′-dipyrryl)methyl]-1-carboxyl anthracene 86:

Methyl 8-dipyrrylmethyl-1-anthracenecarboxylate 85 (3.04 gm, 5.0 mmol) was dissolved in methanol (80 mL) to

which a solution of sodium hydroxide (0.40 gm) in water (5.0 mL) was added. The solution was refluxed for 4 h under nitrogen and the solvent was removed by evaporation. The residue was dissolved in water (100 mL). The aqueous solution was cooled in ice and acidified carefully with glacial acetic acid. The light pink precipitate was filtered, washed with water and dried under vacuum to give the crude tricarboxylic acid. No further purification or identification has been done at this stage.

The crude dry triacid (2.0 gm) was heated at 100°C in ethanolamine (20 mL) for $^1/_2$ h and poured into ice-water (100 mL). The yellow solid was collected by filtration washed with water and dried in air to give 86, 1.0 gm (60% yield), m.p. 100°C (decomposition). NMR, δ 1.20 (6H, t, Et), 1.90 (6H, S, Me), 2.40 (4H, q, Et), 6.30 (1H, s, methine-H), 6.40 (2H, s, α-H pyrrole), 7.10-8.10 (8H, m, anthryl), 8.50 (2H, broad, NH); MS, m/e 450 (M^+, 21), 406 (37), 342 (20), 178 (55), 109 (100).

Trans and cis-5,15-bis[8-hydroxymethyl-1-anthryl]-2,8,12,18-tetraethyl-3,7,13,17-tetramethylporphine 88, 89:

(A) From 8-hydroxymethyl-5,5′-dicarboxyldipyrrylmethane 87 :

8-Hydroxymethyl-1-{[5,5-dicarboxyl-4,4′-diethyl-3,3′-dimethyl-2,2′-dipyrryl]methyl}anthracene 87 (180 mg, 0.34 mmol) was dissolved in dry dichloromethane (100 mL) and trimethyl orthoformate (0.75 mL, 6.87 mmol) was added

followed by a solution of trichloroacetic acid (3.35 gm, 20.0 mmol) in dry CH_2Cl_2 (50 mL). The solution was stirred in the dark under argon for 6 h before a solution of zinc(II) acetate dihydrate (180 mg) in methanol (5 mL) was added, and stirring continued for 48 h. The solution was washed with a saturated solution of Na_2CO_3 (2 × 100 mL), dried over anhydrous Na_2SO_4 and evaporated to dryness *in vacuo*. The residue was dissolved in CH_2Cl_2 (100 mL) and heated to reflux while a solution of $Zn(OAc)_2$ (0.30 gm) in methanol (5 mL) was added and reflux continued for 20 min. The solvents were removed under vacuum to dryness and chromatographed on a silica gel column using CH_2Cl_2 to elute the zinc complex of the cis and trans porphyrins. The separation of isomers by chromatography was not possible at this stage. However, the cis and trans isomers were separable when in the free base form; demetalation was carried out by treatment of the Zn-porphyrin solution in CH_2Cl_2 with 10% HCl solution. Chromatography of the free base mixture was carried out on a silica gel column (1 × 10 inch) using 5% hexane/CH_2Cl_2 to elute the trans isomer (25 mg) and pure CH_2Cl_2 for the cis (20 mg). NMR of the cis isomer, δ -2.20 (2H, broad, NH), 1.75 (12H, t, Et), 2.10 (12H, s, Me), 3.90 (8H, q, Et), 4.00 (4H, s, CH_2-O), 7.20-8.40 (14H, m, anthryl), 8.75 (2H, s, 9-H anthryl), 10.20 (2H, s, meso-H); UV-vis, λ_{max}nm (ϵ_{mM}), 624 (13), 573 (6.0), 543 (5.0), 508 (16), 415 (177). Data for the trans isomer: NMR, δ -2.10 (2H, broad singlet, NH), 1.80 (12H,

t, Et), 2.05 (12H, s, Me), 3.90 (8H, q, Et), 3.95 (4H, s, CH_2O-), 7.20-8.40 (14H, m, anthryl), 8.80 (2H, s, 9-H anthryl), 10.15 (2H, s, meso-H); UV-vis, λ_{max}nm (ϵ_{mM}), 624 (2.3), 573 (7.8), 543 (6.0), 508 (18.0), 415 (178).

(B) From reduction of trans and cis 5,15-bis[8-methoxycarbonyl-1-anthryl-2,8,12,18-tetraethyl-3,7,13,17-tetramethylporphine 52, 53:

Lithium aluminium hydride (100 mg) was added to a solution of a trans/cis mixture of bis[8-methoxycarbonyl-1-anthryl]porphyrin, 52 and 53 (475 mg, 0.5 mmol) in dry THF (50 mL) and the solution was stirred at ambient temperature under argon for 4 h. Ethylacetate (1 mL) was then added and stirring continued for 5 additional minutes. The solvents were pumped out under vacuum and the residue was dissolved in 50 mL of chloroform and the solution was then washed with 10% HCl solution (50 mL), and with water (3 × 50 mL), dried over anhydrous Na_2SO_4 and evaporated to dryness. The cis and trans dialcohol isomers were separated from the residue by column chromatography (silica gel) using 5% hexane/CH_2Cl_2 to elute the trans isomer first and then pure CH_2Cl_2 to elute the cis isomer. The products were identical with authentic samples obtained from method (A). Yields: 250 mg of trans isomer and 151 mg of cis isomer (90% total yield).

5-[8-Methoxycarbonyl-1-anthryl]-2,8,13,17-tetraethyl-3,7,12,18-tetramethylporphine 91:

To a suspension of 8-(4,4′-diethyl-3,3′-dimethyl-2,2′-dipyrrylmethyl)-1-anthracenecarboxylic acid **90** (450 mg, 1 mmol) and 5,5′-diformyl-4,4′-diethyl-3,3′-dimethyl-2,2′-dipyrrylmethane **5** (286 mg, 1 mmol) in dry methanol (100 mL) was added 70% $HClO_4$ solution (0.4 mL). The mixture was stirred at room temperature in the dark for 12 h after which time tetrachloro-o-benzoquinone (200 mg) in methanol (20 mL) was added and stirring continued for 2 additional hours. After evaporation of the solvents, the residue was dissolved in chloroform (50 mL) and the solution was washed with water several times (3 × 50 mL). The residue, after evaporation of the organic layer, was purified by column chromatography (silica gel, 5% methanol/CH_2Cl_2) to produce the 5-[8-carboxyl-1-anthryl]porphyrin, 98 mg (14% yield).

The acid porphyrin, (90 mg, 0.12 mmol) was dissolved, together with oxalyl chloride (0.5 mL), in dry CH_2Cl_2 (20 mL) and the solution was refluxed under argon for 2 h before all the solvents were pumped out *in vacuo*. The residue was heated at reflux in dry methanol (25 mL) for 4 h and the solvent was removed by evaporation under reduced pressure. The methyl ester porphyrin was separated from the residue by chromatography (silica gel column, 1 × 6 inches) using CH_2Cl_2 as an eluent, 73 mg (85% yield) was obtained after recrystallization from methanol/CH_2Cl_2. NMR, δ -3.20 (2H, d, NH), 1.40 (3H, s, -COOMe), 1.60 (6H,

t, Et), 1.85 (6H, t, Et), 2.00 (6H, s, Me), 3.65 (6H, s, Me), 3.85 (4H, q, Et), 4.05 (4H, q, Et), 7.10-8.40 (7H, m, anthryl) 8.60 (1H, s, 9-H anthryl), 9.90 (1H, s, meso-H), 10.10 (2H, s, meso-H). UV-vis, λ_{max}nm (ϵ_{mM}), 624 (2), 568 (6), 532 (7), 498 (14), 402 (165).

5,15-Bis[8-methoxycarbonyl-1-anthryl]-2,8,12,18-tetraethyl-3,7,13,17-tetramethylporphine 52, 53:

8 Methoxycarbonyl-1-anthracenecarboxaldehyde 51 (528 mg, 2 mmol) and 4,4′-diethyl-3,3′-dimethyl-2,2′-dipyrrylmethane 19 (460 mg, 2 mmol) were suspended in dry methanol. After the solution was deaerated by bubbling with argon for 15 min, p-toluenesulfonic acid (96 mg, 0.5 mmol) was added. The mixture was stirred for 15 min and then allowed to stand in the dark at room temperature. After 6 h at room temperature, the solution was cooled and kept at 4°C overnight. The solid was collected by filtration and washed with cold methanol and dried under vacuum to give 510 mg of the porphyrinogen.

To a solution of the crude porphyrinogen, (500 mg) in THF (50 mL), was added a solution of o-chloranil (700 mg) in THF (10 mL) and the solution was stirred at room temperature for 1 h. The solvent was then evaporated and the residue was dissolved in 50 mL chloroform and washed with a saturated aqueous solution of Na_2CO_3 (50 mL) and with water (2 × 50 mL). Evaporation of the organic layer and chromatographing the residue on silica gel column gave a mix-

ture of cis and trans isomers (450 mg, 47% yield) that was not possible to separate by chromatography. NMR of the mixture: δ -2.10 (2H, s, NH), 1.40 (6H, s, -COOMe), 1.75 (12H, t, Et), 2.10 (12H, s, Me), 3.95 (8H, q, Et), 7.10-8.40 (14H, m, anthryl), 8.80 (2H, s, 9-H anthryl), 10.20 (2H, s, meso-H). UV-vis, λ_{max}nm (ϵ_{mM}) 628 (1.3), 572 (5.2), 537 (4.0), 506 (14.3), 416 (165).

trans-5,15-Bis[8-carboxyl-1-anthryl]-2,8,12,18-tetramethyl-3,7,13,17-tetramethylporphine 5:

A. By hydrolysis of the methyl ester 52:

Dimethyl ester porphyrin 52 (250 mg) was dissolved in 98% formic acid (20 mL), concentrated HCl (5 mL) was added, and the solution was heated at reflux for 5 h. Water (50 mL) was added, and the product was extracted from the aqueous layer with $CHCl_3$ (3 × 25 mL); the organic layer was washed several times with water and dried over anhydrous Na_2SO_4 and the solvents were removed *in vacuo*. Column chromatography (silica gel, 2% methanol/CH_2Cl_2) was used to separate the diacarboxylic acid porphyrin from the residue; 35 mg (15% yield) was obtained; MS, m/e 918 (17), 874 (9), 830 (25), 477 (10), 178 (100). NMR, δ -1.15 (2H, s, NH), 1.70 (12H, t, Et), 2.15 (12H, s, Me), 3.90 (8H, q, Et), 7.00-8.45 (14H, m, anthryl), 8.90 (2H, s, 9-H anthryl), 10.30 (2H, s, meso-H). UV-vis, λ_{max}nm (ϵ_{mM}) 627 (3), 574 (5.5), 534 (4), 505 (16.5), 410 (176.4).

B. By oxidation of the corresponding dialdehyde 57:

trans-5,15-Bis(8-formyl-1-anthryl)porphyrin, 57 (250 mg) was dissolved in acetone (20 mL) and stirred at 0°C while adding Jones' reagent, 0.2 mL (prepared by dissolving 6.7 gm of CrO_3 in 6 mL concentrated H_2SO_4 and diluting the solution to 50 mL with water). The oxidation reaction was almost spontaneous, after stirring at 0°C for 10 min, methanol (0.5 mL) was added and the solution was stirred for 5 additional minutes before water (50 mL) was added. The product was extracted from the aqueous layer and worked up as above to give 209 mg (81% yield) which was identical with that of the authentic sample prepared above.

8-Formyl-1-[(4,4′-diethyl-3,3′-dimethyl-2,2′-dipyrryl)-methyl]anthracene 54:

Hydrolysis and decarboxylation of the corresponding diethylester dipyrrylmethane 92, in alkaline medium, produces the α-free species in 70% overall yield. m.p. 180-185°C (decomposition); MS, m/e 435 (3), 327 (10), 298 (6), 94 (100). NMR, δ 1.10 (6H, t, Et), 1.95 (6H, s, Me), 2.85 (4H, q, Et), 6.45 (3H, broad, methine-H + α-H pyrrole), 6.95-8.40 (7H, m, anthryl), 9.90 (1H, s, 9-H anthryl), 10.20 (1H, s, -CHO).

8-Formyl-1-{[5,5′-diformyl-4,4′-diethyl-3,3′-dimethyl-2,2′-dipyrryl]methyl} anthracene 56:

Vilsmeier's formylation was carried out by using phosphorous oxychloride/DMF. The trialdehyde 56 was obtained in 30% yield as a dark brown solid; m.p. 220-223°C (decomposition). MS, m/e 390 (5), 361 (12), 335 (18), 227 (100). NMR, δ 1.10 (6H, t, Et), 1.95 (6H, s, Me), 2.85 (4H, q, Et), 6.35 (1H, s, methine-H), 7.00-8.40 (7H, m, anthryl), 9.90 (1H, s, 9-H anthryl), 10.20 (1H, s, -CHO), 10.40 (2H, s, -CHO).

5,15-Bis[8-formyl-1-anthryl]-2,18,12,18-tetraethyl-3,7,13,17-tetramethylporphine 57, 58:

A. From the coupling of 8-formyl anthracene α-free dipyrrylmethane 54 and 8-formyl-1-(5,5′-diformyldipyrryl-methane)anthracene 57:

The coupling was achieved by stirring in methanol containing catalytic amounts of 70% perchloric acid for 20 h, and the resultant porphyrinogen was oxidized by o-chloranil and purified by chromatography (silica gel, CH_2Cl_2). The yield was 5% of nonseparable cis and trans isomers; NMR, δ -2.20 (2H, s, NH), 1.80 (12H, t, Et), 2.10 (12H, s, Me), 3.90 (8H, q, Et), 7.00-8.5 (7H, m, anthryl), 8.60 (1H, s, 9-H anthryl), 9.50 (2H, s, -CHO). UV-vis, λ_{max}^{nm} (ϵ_{mM}) 625 (2.4), 570 (4.5), 535 (5.7), 504 (13), 410 (174).

B. From oxidation of the corresponding dialcohol porphyrin 88, 89:

Oxidation of a mixture of cis and trans bis(hydroxymethylanthryl)porphyrin (88, 89) by CrO_3/pyridine gave 80% yield of the dialdehyde as a cis and trans mixture. The product was identical in every respect with the sample obtained by procedure (A).

C. From direct coupling of 1,8-anthracene dicarboxaldehyde with 3,3′-diethyl-4,4′-dimethyl-2,2′-dipyrrylmethane, 19:

Trace amounts of the cis and trans isomers were obtained by Gunter's procedure from coupling of equivalent quantities of 1,8-anthracene dicarboxaldehyde and 5,5′-free dipyrrylmethane 19 in methanol and in the presence of p-toluene sulfonic acid. The products were identical in all aspects with the samples obtained by the previous methods.

D. From coupling of partially protected 1,8-anthracene dicarboxaldehyde 93 with 3,3′-diethyl-4,4′-dimethyl-2,2′-dipyrrylmethane, 19:

1,8-Anthracene dicarboxaldehyde 1 (4.68 gm, 20 mmol) and 1,3-propanediol (1.52 gm, 20 mmol) were heated at reflux in dry THF (100 mL) containing molecular sieves (2 gm) and in the presence of catalytic amounts of p-toluenesulfonic acid (0.80 gm). Reflux was continued until complete disappearance of the dialdehyde was assured, as detected by tlc (3-4 h). The solution was filtered and solvents were removed *in vacuo*. The monoacetal-aldehyde

was purified by chromatography (silica gel column, CH_2Cl_2), 0.54 gm (93% yield).

The monoacetal-anthracene aldehyde, **94** (500 mg, 1.7 mmol) was coupled with 3,3′-diethyl-4,4′-dimethyl-2,2′-dipyrrylmethane (394 mg, 1.7 mmol) according to Gunter's method, in methanol and in the presence of p-toluenesulfonic acid. After crystallization from methanol/CH_2Cl_2, 210 mg (24% yield) of bis(acetalanthracene)porphyrin **95**, as a cis/trans isomeric mixture. NMR, δ -2.10 (2H, s, NH), 1.70 (12H, t, Et), 1.95 (8H, t, $-OCH_2$), 2.10 (12H, s, Me), 2.60 (4H, m, CH_2), 3.95 (8H, q, Et), 4.70 (2H, s, CH), 7.3-8.5 (14H, m, anthryl), 8.70 (2H, s, 9-H anthryl), 10.20 (2H, s, meso-H).

Hydrolysis to the dialdehyde derivative was achieved by heating the solution of the diacetal porphyrin **95** (200 mg) in formic acid (20 mL) containing 5 mL of concentrated HCl. After heating on a steam bath for 1 h, water/ice (50 mL) was added and the porphyrin dialdehyde was taken into $CHCl_3$ (2 × 40 mL), washed with a saturated Na_2CO_3 solution (50 mL) and water (2 × 50 mL). Purification of the product was carried out as mentioned in procedure (A) to give 160 mg (90% yield). The products were identical with the samples obtained from the prevous method.

p-Methoxy-α,α-[5,5′-bis(ethoxycarbonyl)-4,4′-diethyl-3,3′-dimethyl-2,2′-dipyrryl]toluene 97:

A solution of p-anisaldehyde 96 (1.0 gm, 7.4 mmol) and ethyl 3-ethyl-4-methyl-2-pyrrolecarboxylate, 2 (2.7 gm, 14.8 mmol) in methanol (50 mL) was refluxed under argon and in the presence of concentrated HCl (2 mL) for 1 h. No precipitation was observed upon cooling in an ice-bath, so water (100 mL) was added to the methanolic solution and the dipyrrylmethane was extracted with dichloromethane (3 × 50 mL) and the organic layer was washed first with a saturated solution of Na_2CO_3 (100 mL) and then twice with water (100 mL each time). The residue obtained by evaporation of the organic solvents was purified by chromatography on a silica gel column using CH_2Cl_2 as an eluent to give 3.2 gm (94% yield) of the product, m.p. 115-120°C (decomposition). MS, m/e 480 (35), 407 (12), 334 (9), 301 (100), 107 (25); NMR, δ 1.10 (6H, t, Et), 1.20 (6H, t, -OEt), 1.90 (6H, s, Me), 2.85 (4H, q, Et), 3.80 (3H, s, -OMe), 4.20 (4H, q, -OEt), 5.60 (1H, s, methine), 6.90 (4H, m, phenyl), 8.40 (2H, broad, NH).

p-Methoxy-α,α-[(4,4′-diethyl-3,3′-dimethyl-2,2′-dipyrryl)]-toluene 98:

Hydrolysis of the corresponding diethylester dipyrrylmethane 97 (3.0 gm), was achieved by refluxing in methanol (100 mL) containing NaOH (2.0 gm in 5 mL H_2O) for 8 h. Acidification of the cold alkaline solution by glacial

acetic acid and extraction with chloroform afforded the diacid.

The crude diacid was heated at reflux in ethanolamine (25 mL) for 1 h and the hot solution was poured onto ice (50 gm). The α-free dipyrrylmethane was taken into chloroform and purified by chromatography (silica gel, CH_2Cl_2) to produce 2.3 gm (90% yield) of a yellow solid; m.p. 95-98°C (decomposition). MS, m/e 336 (24), 229 (100), 107 (38); NMR, δ 1.15 (6H, t, Et), 1.90 (6H, s, Me), 2.80 (4H, q, Et), 3.80 (3H, s, -OMe), 5.60 (2H, s, methine-H), 6.30 (2H, s, α-H pyrrole), 6.90 (4H, m, phenyl), 8.30 (2H, broad, NH).

p-Methoxy-α,α-(5,5′-diformyl-4,4′-diethyl-3,3′-dimethyl-2,2′-dipyrryl)toluene 99:

To a solution of the α-free dipyrrylmethane 98 (3.92 gm, 10 mmol) in dry DMF (12 mL) was added phosphorous oxychloride (0.7 mL) dropwise keeping the temperature of the solution at -5 to 0°C. After the addition was complete, the solution was stirred at low temperature for 3 h before water (100 mL) was added and the resulting solution was washed with CH_2Cl_2 several times (3 × 50 mL). To the aqueous layer was added 10% NaOH solution until a complete precipitation of the dialdehyde was achieved. The precipitates were collected by filtration and recrystalliztion from methanol to give 1.90 gm (48% yield); m.p. 195-198°C. MS, m/e 392 (48), 363 (15), 256 (95), 226 (100)1; NMR, δ

1.15 (6H, t, Et), 1.90 (6H, s, Me), 3.70 (4H, q, Et), 3.75 (3H, s, -OMe), 5.60 1H, s, methine-H), 6.90 (4H, m, phenyl), 9.30 (2H, s, -CHO).

1,8-Bis{5-[2,8,12,18-tetraethyl-3,7,13,17-tetramethyl-15-(p-methoxyphenyl)pophyrinyl}anthracene 100:

The coupling reaction between p-methoxy-α,α(5,5′-diformyl-4,4′-diethyl-3,3′-dimethyl-2,2′-dipyrryl)toluene **99** and α-free 1,8-bis(dipyrryl)methylanthracene **4** was carried out by the standard procedure similar to that followed in the synthesis of 1,8-anthracene diporphyrin. The product was recrystallized from methanol/CH_2Cl_2, the yield was 6%. NMR, δ -3.70 (4H, d, NH), 1.30 (12H, t, Et), 1.40 (12H, t, Et), 2.00 (12H, s, Me), 2.30 (12H, s, Me), 3.70 (16H, 2q, Et), 4.05 (6H, s, -OMe), 7.00-8.50 (15H, m, phenyl + anthryl), 9.00 (1H, s, 9-H anthryl), 9.30 (4H, s, meso-H). UV-vis, λ_{max}nm (ϵ_{mM}) 624 (3.5), 574 (14.0), 541 (10.5), 508 (30), 400 (304).

5-(4-Methoxyphenyl)-2,8,13,17-tetraethyl-3,7,12,18-tetramethylporphine 47:

p-Methoxy-α,α-(5,5′-diformyl-4,4′-diethyl-3,3′-dimethyl-2,2′-dipyrryl)toluene **99** (336 mg, 1 mmol) was coupled with 5,5′-diformyl-4,4′-diethyl-3,3′-dimethyl-2,2′-dipyrrylmethane **5** (286 mg, 1 mmol) by stirring for 20 h in methanol (50 mL) and in the presence of 70% perchloric acid (0.5 mL), under nitrogen. The resultant porphyrinogen was

oxidized *in situ* by adding o-chloranil (200 mg) solution in methanol (10 mL) and stirring for one additional hour. Most of the solvent was removed and the residue was dissolved in chloroform (50 mL) and washed with a saturated solution of sodium bicarbonate (50 mL) and twice with brine (2 × 50 mL). The organic layer was dried over anhydrous Na_2SO_4 and the solvent was taken out on a rotary evaporator. Column chromatography (silica gel, CH_2Cl_2) was used to purify the product (R_f 0.6), 213 mg (36.5% yield) was obtained after crystallization from methanol/CH_2Cl_2. NMR, δ UV-vis, λ_{max}nm (ϵ_{mM}) 624 (4), 570 (6), 534 (8), 504 (12), 404 (132).

5,15-Bis(4-methoxyphenyl)-2,8,12,18-tetraethyl-3,7,13,17-tetramethylporphine 65:

A. <u>From α-free p-methoxyphenyldipyrrylmethane condensation</u>:

p-Methoxy(4,4′-diethyl-3,3′-dimethyl-2,2′-dipyrryl)-toluene, 98 (672 mg, 2 mmol) was condensed with an equivalent amount of p-methoxy-α,α-(4,4′-diethyl-5,5′-diformyl-4,4′-diethyl-3,3′-dimethyl-2,2′-dipyrryl)toluene 99 (784 mg, 2 mmol) in methanol (100 mL) in the presence of catalytic amounts of perchloric acid (70%, 0.8 mL). The solution was stirred under nitrogen, in the dark, for 24 h and then o-chloranil (500 mg) in methanol (20 mL) was added and the solution was stirred for one more hour before the solvent was removed. The product was purified by chromato-

graphing the crude mixture on silica gel (using CH_2Cl_2 as an eluent) to give 322 mg (23.4% yield) of the desired bis(p-methoxyphenyl)porphyrin. NMR, δ -2.45 (2H, s, NH), 1.45 (12H, t, Et), 2.20 (12H, s, Me), 3.80 (8H, q, Et), 4.15 (6H, s, $-OCH_3$), 7.50-8.30 (8H, m, phenyl), 10.15 (2H, s, meso-H). UV-vis, λ_{max}nm (ε_{mM}) 622 (3), 570 (6), 532 (10), 503 (14), 405 (129).

B. By coupling p-anisaldehyde with α-free dipyrrylmethane 19:

p-Anisaldehyde (1.36 gm, 10 mmol) and 4,4′-diethyl-3,3′-dimethyl-2,2′-dipyrrylmethane 19 (2.30 gm, 10 mmol) were dissolved in dry methanol (150 mL), and the solution was deaerated by bubbling argon for 15 min before p-toluenesulfonic acid was added. The solution was stirred under argon and in the dark for 6 h, then cooled and stored at -4°C for 12 h. The precipitate was filtered and dissolved in dry THF (80 mL) and oxidized by stirring with a solution of o-chloranil (1.00 gm) in THF (20 mL) for 1 h. Work-up was carried out by evaporation of the solvent, dissolving the residue in $CHCl_3$ (50 mL) and washing with a saturated solution of Na_2CO_3 and water. Purification of the product was carried out as in procedure (A) to give 1.75 gm (51% yield). The product was identical in every respect with the authentic sample obtained by procedure (A).

5,15-Bis[8-nitro-1-naphthyl]-2,8,12,18-tetraethyl-3,7,13,17-tetramethylporphine 66:

Gunter's procedure was used for coupling of 8-nitro-1-napthaldehyde and 3,3′-diethyl-4,4′-dimethyl-2,2′-dipyrrylmethane 19. The trans-, 66 and cis-, 66a isomers were separated by chromatography, to give 7.5% overall yield. Purification of the products was done by column chromatography (silica gel, CH_2Cl_2) and crystallization from methanol/CH_2Cl_2. NMR, δ -2.2 (2H, s, NH), 1.46 (12H, t, Et), 2.30 (12H, s, Me), 3.90 (8H, q, Et), 7.10-8.20 (12H, m, naphthyl), 10.20 (2H, s, meso-H). UV-vis, λ_{max}nm (ϵ_{mM}) 624 (4), 572 (8), 534 (12), 504 (15), 402 (136).

5,15-Diphenyl-2,8,12,18-tetraethyl-3,7,13,17-tetramethylporphine, 62:

A similar procedure to that described above was followed for coupling of benzaldehyde and an equivalent amount of α-free dipyrrylmethane 19. The desired product was obtained in 54% yield after crystallization from methanol/CH_2Cl_2. NMR, δ -2.10 (2H, s, NH), 1.80 (12H, t, Et), 2.10 (12H, s, Me), 4.00 (8H, q, Et), 7.10-8.40 (10H, m, phenyl), 10.20 (2H, s, meso-H); UV-vis, λ_{max}nm (ϵ_{mM}) 628 (3), 565 (6), 535 (9), 502 (17), 403 (178).

5,15-Bis(1-naphthyl)-2,8,12,18-tetraethyl-3,7,13,17-tetramethylporphine 63:

Gunter's procedure was applied for coupling 1-naphthaldehyde and 3,3′-diethyl-4,4′-dimethyl-2,2′-dipyrrylmethane 19. An inseparable mixture of cis/trans isomers was produced in an overall yield of 46%, after crystallization from methanol/CH_2Cl_2. UV-vis, λ_{max}nm (ϵ_{mM}) 625 (3.5), 559 (5), 534 (8), 503 (13), 404 (172). NMR, δ -2.50 (2H, s, NH), 1.70 (12H, t, Et), 2.45 (12H, s, Me), 4.00 (8H, q, Et), 7.60-8.10 (14H, m, naphthyl), 10.15 (2H, s, meso-H).

5,15-Bis(1-anthryl)-2,8,12,18-tetraethyl-3,7,13,17-tetramethylporphine 64:

A similar procedure to that described above (Gunter's method) was used to couple 1-anthracene carboxaldehyde with 3,3′-diethyl-4,4′-dimethyl-2,2′-dipyrrylmethane 19. A 41% yield of an inseparable cis/trans mixture was obtained. UV-vis, λ_{max}nm (ϵ_{mM}) 629 (4.5), 564 (7), 538 (10), 505 (12), 403 (183). NMR, δ -2.15 (2H, s, NH), 1.85 (12H, t, Et), 2.20 (12H, s, Me), 3.95 (8H, q, Et), 7.10-8.80 (18H, m, anthryl), 10.25 (2H, s, meso-H).

trans-5,15-Bis{8[(-)-cis-myrtanylamide]-1-anthryl}-2,8,12,18-tetraethyl-3,7,13,17-tetraethylporphine 61:

trans-5,15-Bis[8-carboxyl-1-anthryl]etioporphyrin, 55 (918 mg, 1 mmol) was converted into the diacid chloride derivative, 59, by treating the solution of the diacid por-

phyrin in dry dichloromethane (40 mL), with excess amounts of oxalylchloride (0.50 mL, 2 mmol=0.17 mL) in the presence of 5 drops of pyridine. The solution was refluxed for 6 h to achieve complete conversion, the solvents were then pumped out to dryness and the crude diacid chloride was used in the next step without purification.

The crude residue was redissolved in dry dichloromethane (25 mL), to which excess amounts of (-)-cis-myrtanylamine 60 (Aldrich, 98% purity, 500 mg, 2 mmol=306 mg) and the solution was refluxed for 18 h. The solution was then washed with 10% hydrochloric acid solution (50 mL) and then with water (2 × 50 mL). After evaporation of the solvent, the product was separated from the residue by chromatography (silica gel column; chloroform, R_f 0.6) to produce 367 mg (30% yield). UV-vis, λ_{max}^{nm} (ϵ_{mM}) 628 (3.5), 575 (6), 532 (5.5), 504 (14.5), 408 (173). NMR, δ 2.05 (2H, s, NH), 0.95 (2H, m, CH, myrt.), 1.05 (4H, s, CH_2, myrt.), 1.35 (8H, m, CH_2, myrt), 1.50 (9H, m, CH_2+CH, myrt.), 1.75 (12H, t, Et), 1.95 (4H, d, CH_2, myrt.), 2.20 (12H, s, Me), 2.25 (6H, s, CH_3, myrt.), 4.00 (8H, q, Et), 7.50-8.80 (14H, m, anthryl), 9.15 (2H, s, 10-H anthryl), 9.45 (2H, s, 9H-anthryl), 10.20 (2H, s, meso-H).

General Procedure for Metals Insersion:

Insersion of copper, zinc, nickel and manganese.

To a solution of the free-base porphyrin (50 mg) in dichloromethane (50 mL) containing little sodium acetate (10 mg) was added a saturated solution (2 mL) of the metal(II) acetate in methanol. The solution was warmed on a steam bath for 10 min and then stirred at room temperature for $^1/_2$ h. The excess inorganic salts were removed by washing the solution with water, and the metalloporphyrin was isolated by evaporation of the organic layer and purified by chromatography (silica gel, CH_2Cl_2) and recrystallized from dichloromethane/methanol. The yield was almost quantitative.

Insersion of iron

A saturated aqueous solution of ferrous sulfate (3 ml) was added to a solution of the free-base porphyrin (75 mg) in pyridine/acetic acid (1:1 v/v, 50 ml). The solution was heated at reflux for 90 min before water (100 ml) was added. The iron(II) porphyrin was obtained from the aqueous layer by extraction with chloroform. The combined extracts (200 ml) were washed with brine, and the solvents were removed *in vacuo*. The iron porphyrin was recrystallized from a mixture CH_2Cl_2/methanol.

of cobalt(II) chloride (1 ml). The solution was refluxed for 10 min and the solvent was then allowed to evaporate off slowly while methanol (15 ml) was added to replace dichloromethane. The solution was then cooled down in an ice-bath and the precipitated crystals were collected by filtration and washed with little cold methanol to give almost a quantitative yield.

APPENDIX

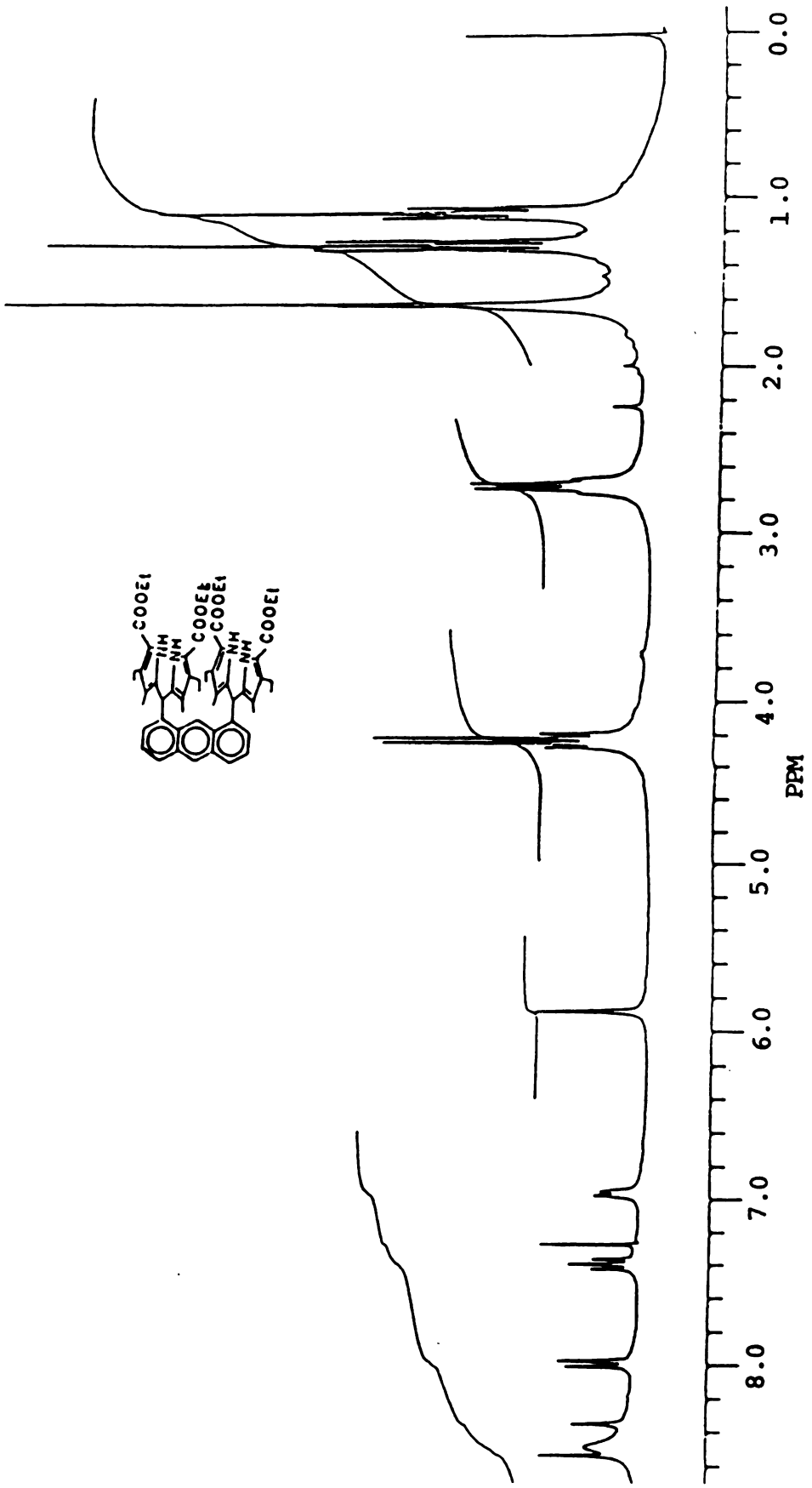

Figure A1 250 MHz ^{1}H NMR spectrum of 1,8-bis{5,5'-bis(ethoxycarbonyl)-4,4'-diethyl-3,3'-dimethyl-2,2'-dipyrrylmethyl}anthracene (3).

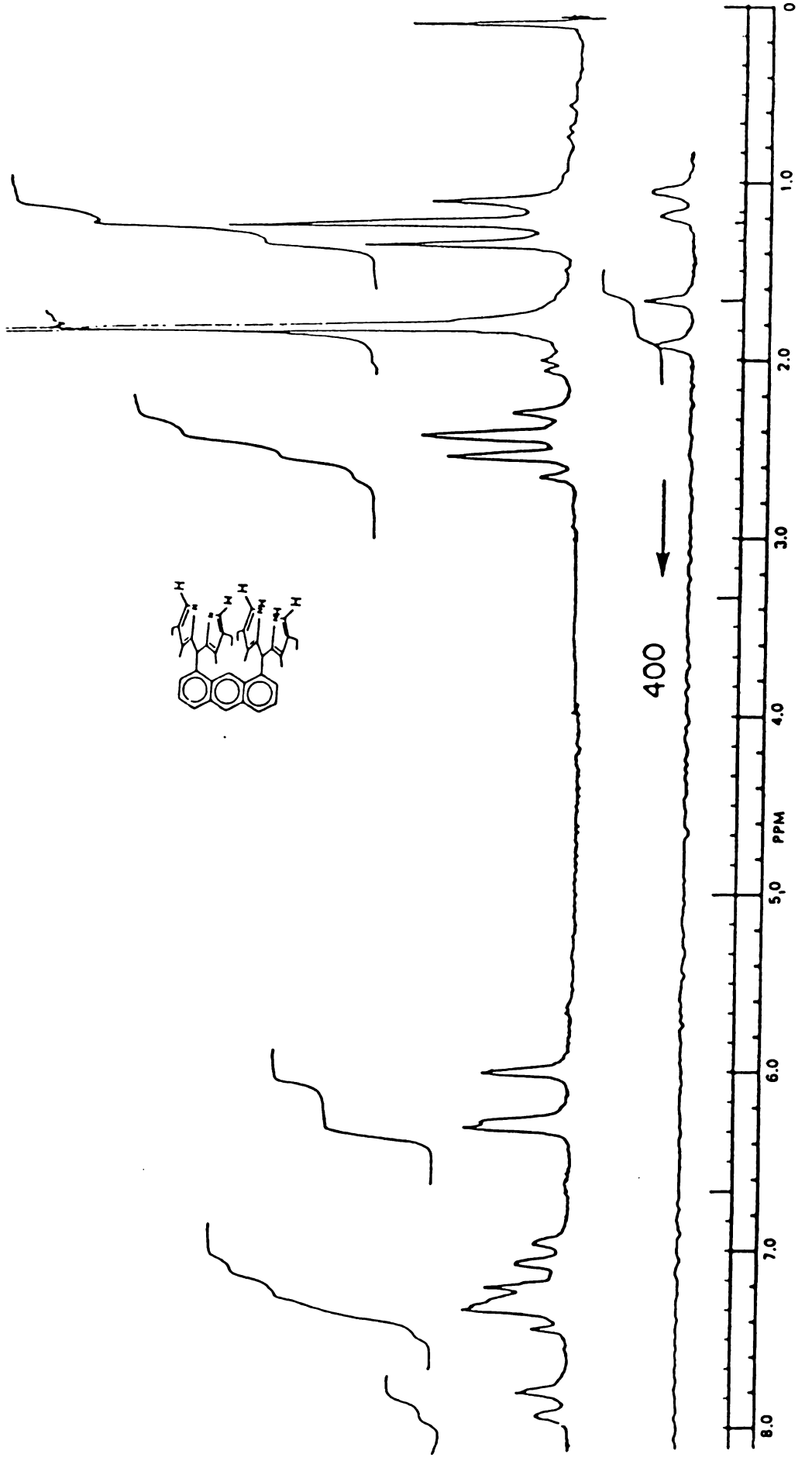

Figure A2 60 MHz ^{1}H NMR spectrum of 1,8-bis[(4,4'-diethyl-3,3'-dimethyl-2,2'-dipyrryl)methyl]anthracene (4).

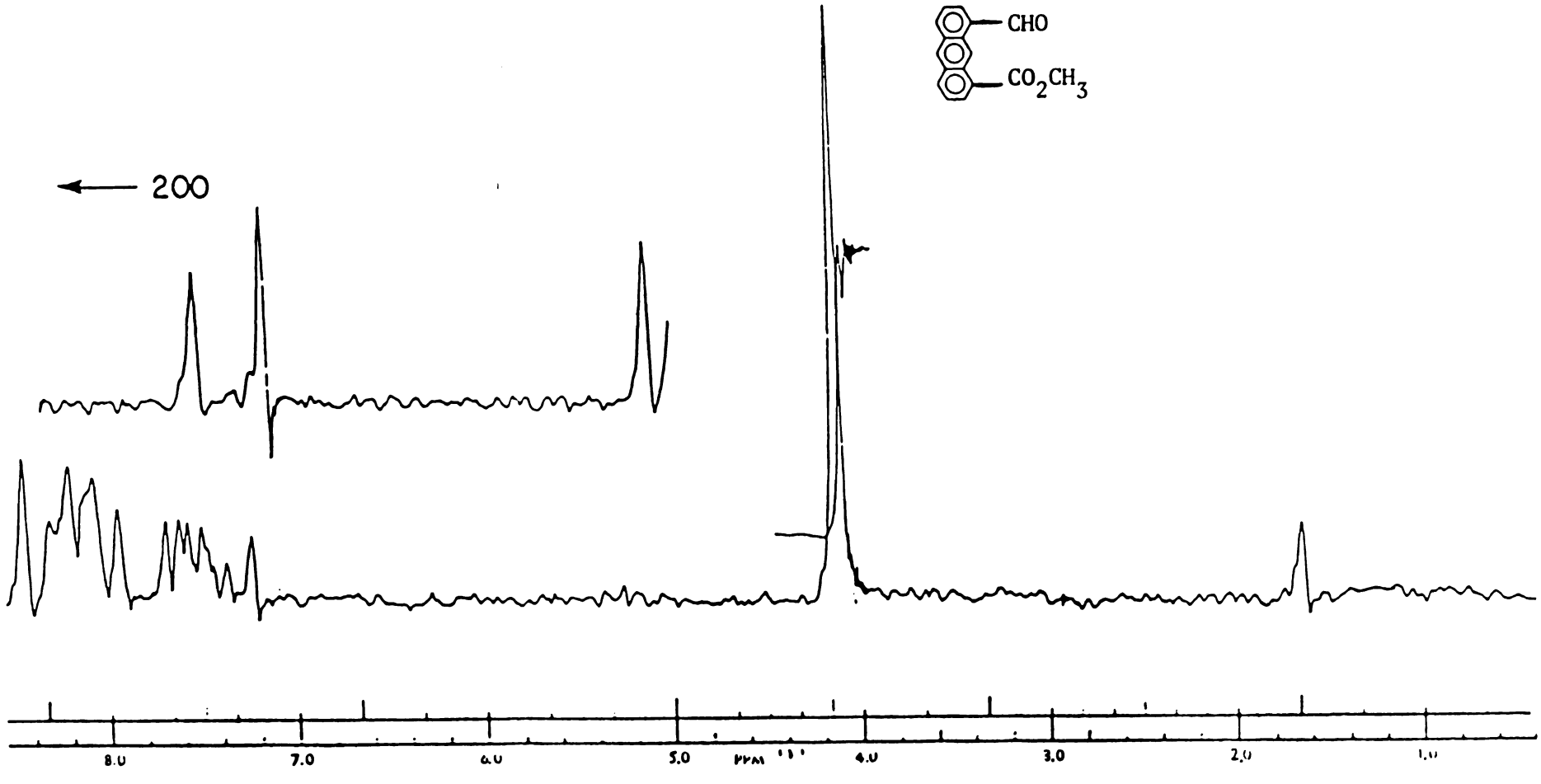

Figure A3 60 MHz ^1H NMR spectrum of 8-methoxycarbonyl-1-anthracene carboxaldehyde (51).

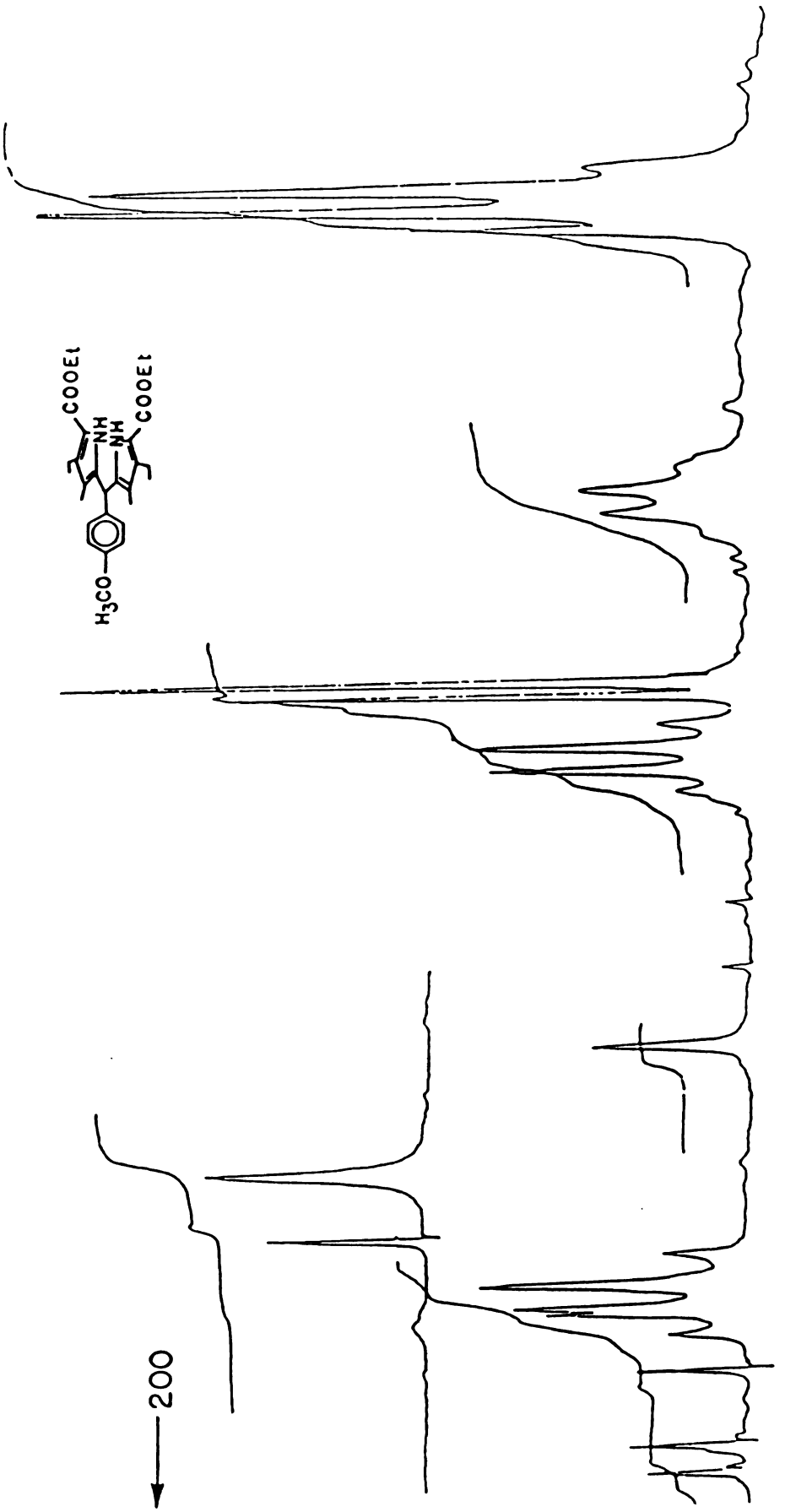

Figure A4 *60 MHz ^1H NMR spectrum of p-methoxy-α,α[5,5'-bis(ethoxycarbony)-4,4'-diethyl-3,3'-dimethyl-2,2'-dipyrryl]toluene (97).*

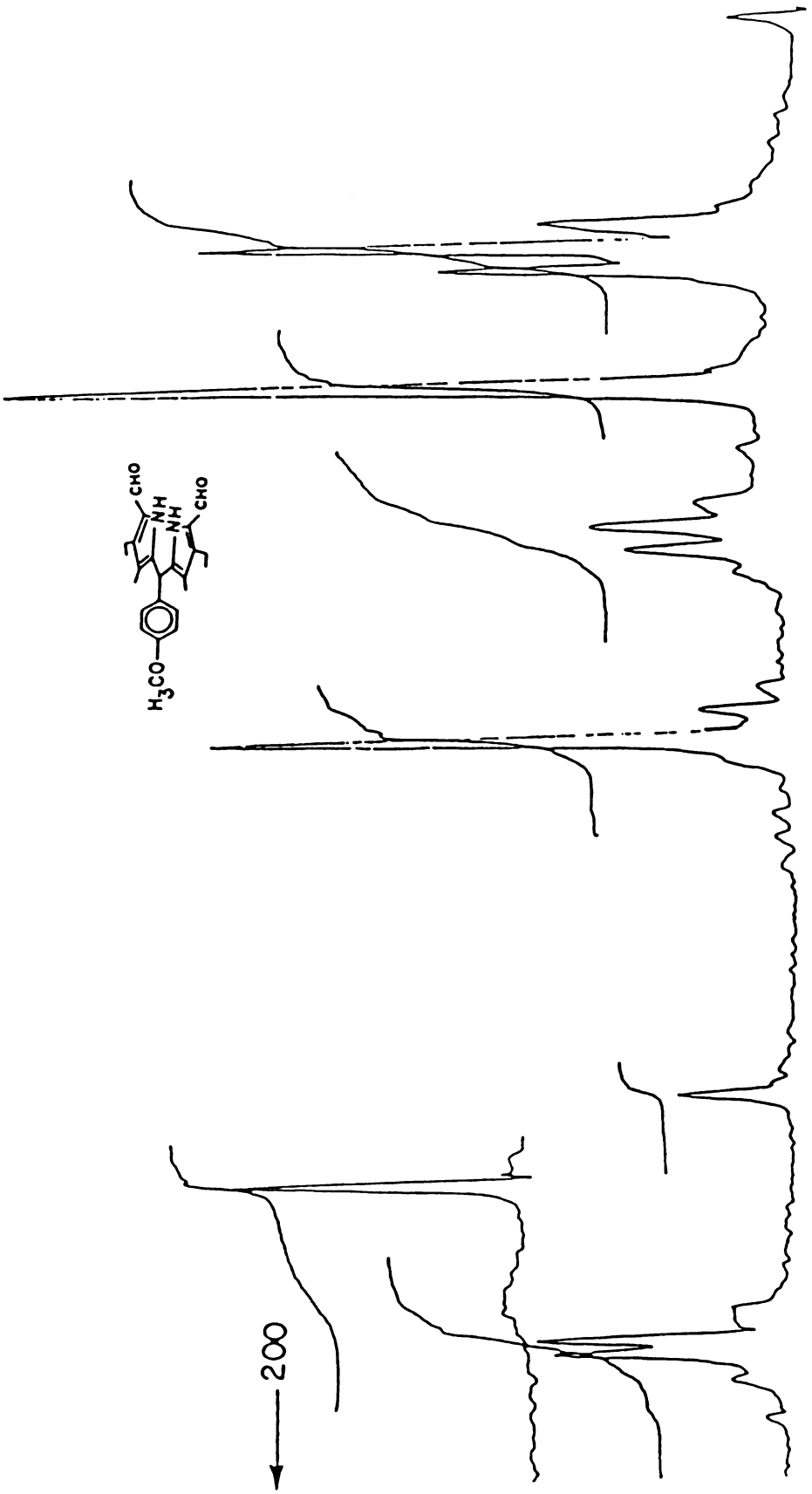

Figure A5 60 MHz ^1H NMR spectrum of p-methoxy-α,α(5,5'-diformyl-4,4'-diethyl-3,3'-dimethyl-2,2'-dipyrryl)toluene (99).

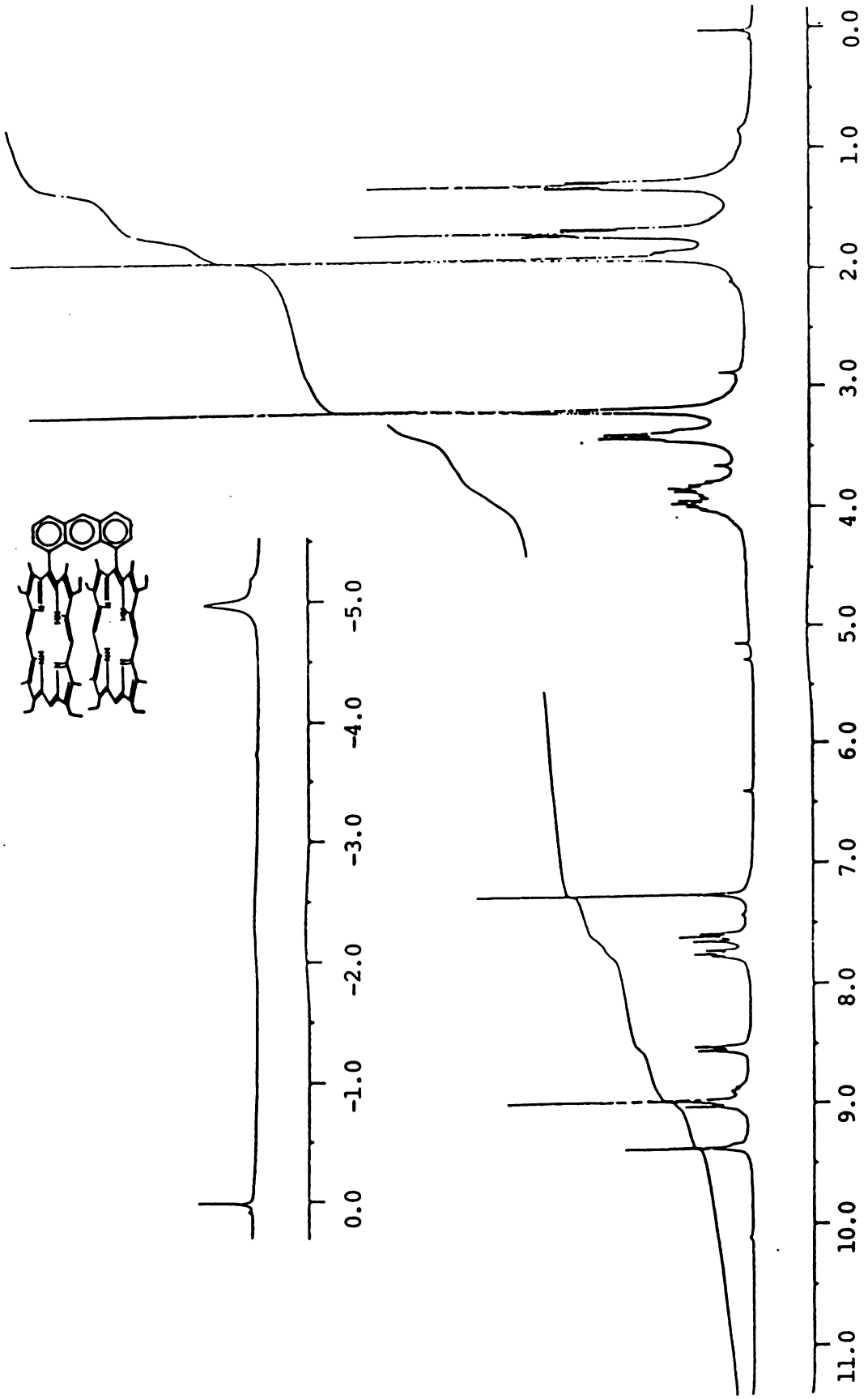

Figure A6 250 MHz ^1H NMR spectrum of 1,8-bis[5-(2,8,13,17-tetraethyl-3,7,12,18-tetramethyl)porphyrinyl] anthracene (6).

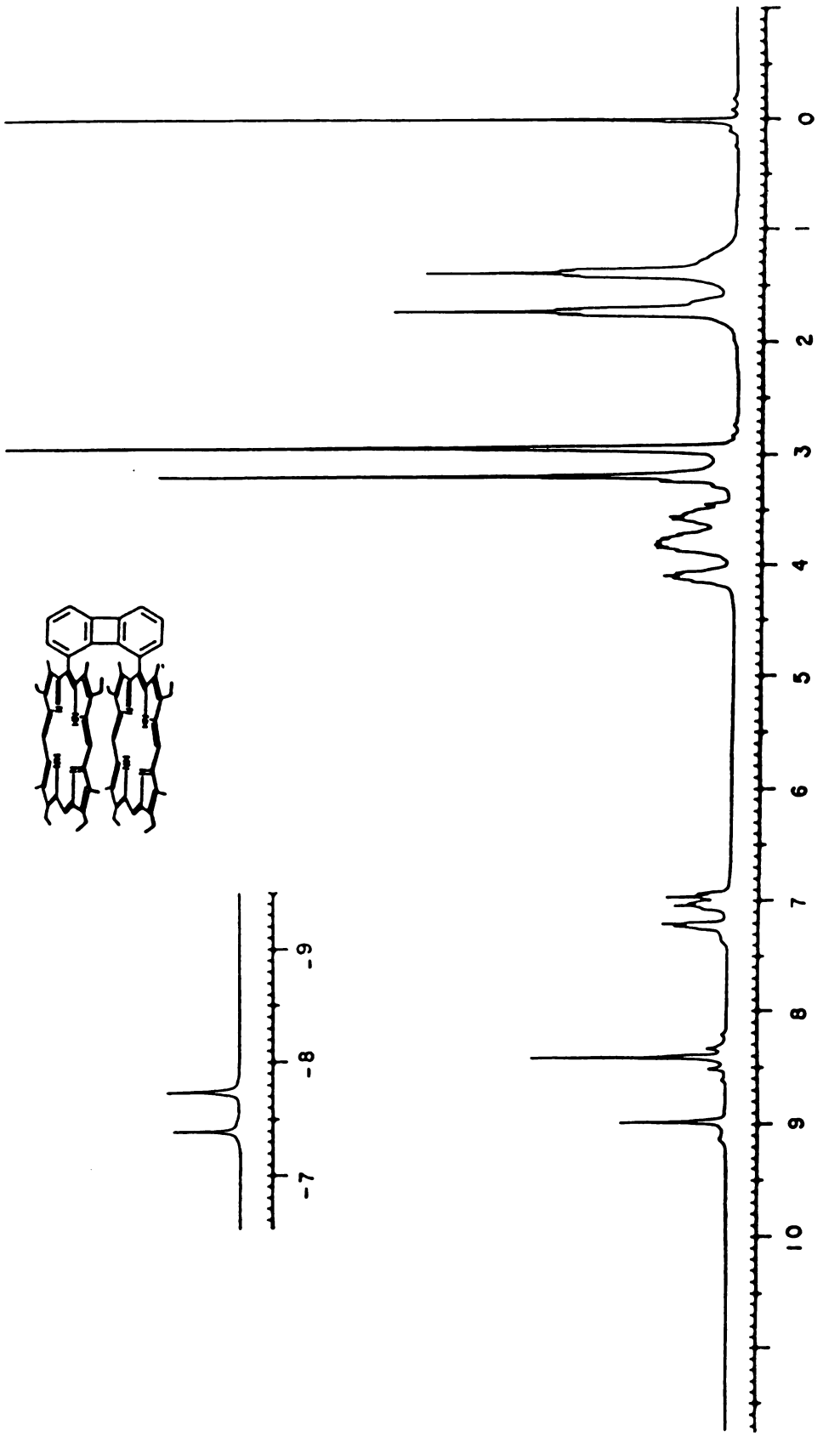

Figure A7 250 MHz ^{1}H NMR spectrum of 1,8-bis[5-(2,8,13,17-tetraethyl-3,7,12,18-tetramethyl)porphyrinyl] biphenylene (14).

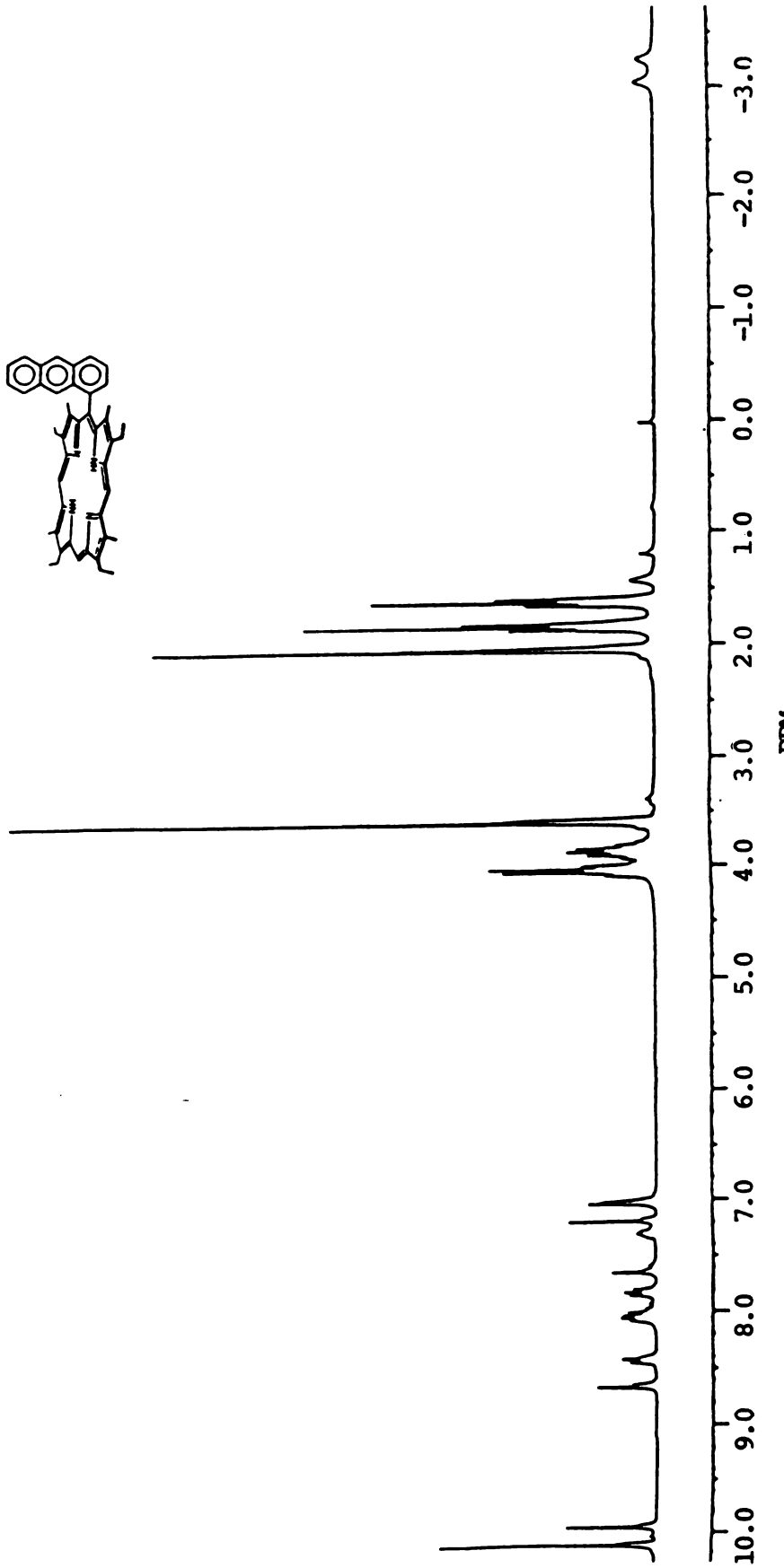

Figure A8 250 MHz ^{1}H NMR spectrum of 1-[5-(2,8,13,17-tetraethyl-3,7,12,18-tetramethyl)porphyrinyl] anthracene (46).

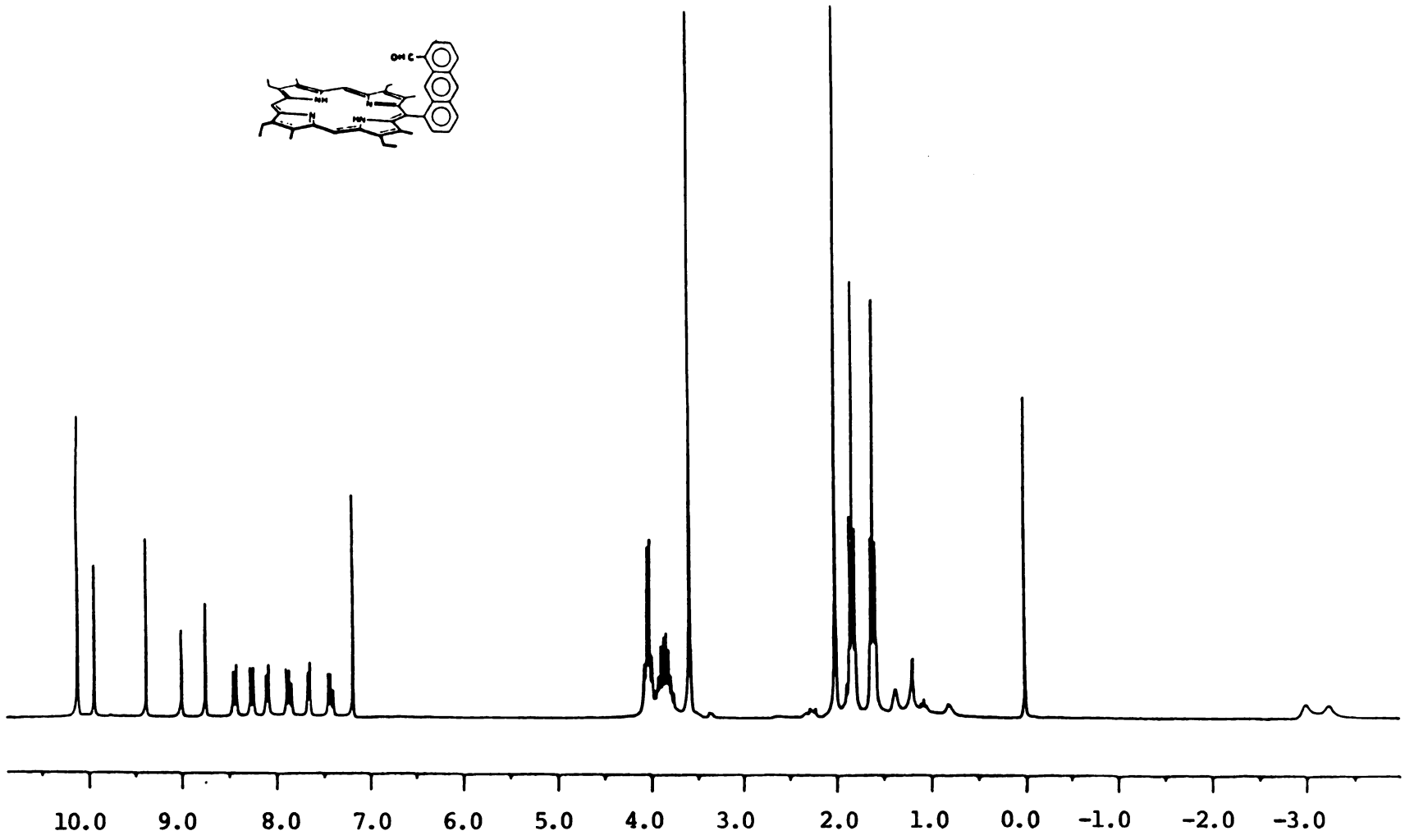

Figure A9 *250 MHz ^{1}H NMR spectrum of 5-(8-formyl-1-anthryl)-2,8,13,17-tetraethyl-3,7,12,18-tetramethyl-porphine (18).*

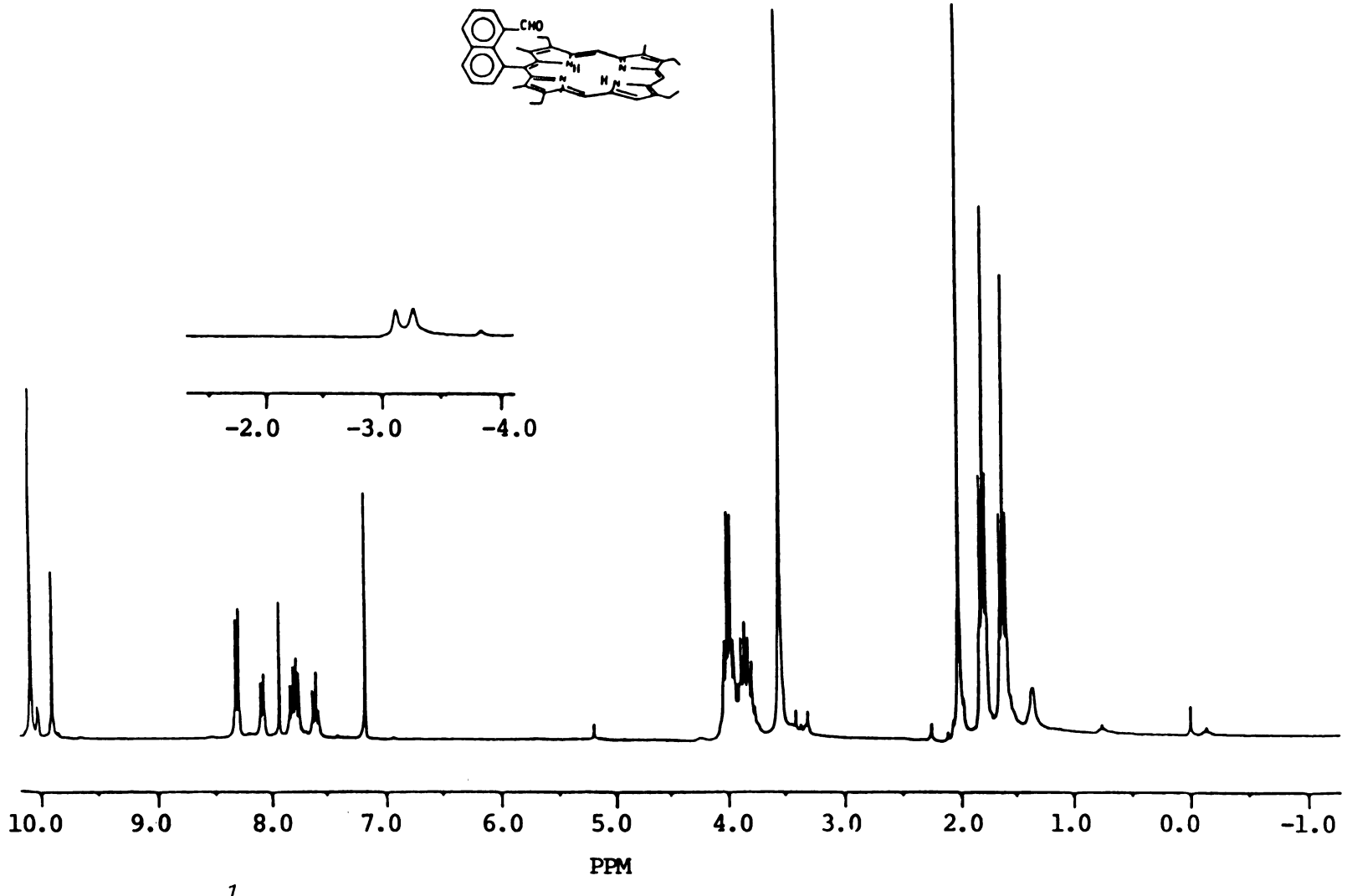

Figure A10 *250 MHz ^{1}H NMR spectrum of 5-(8-formyl-1-naphthyl)-2,8,13,17-tetraethyl-3,7,12,18-tetramethylporphine (81).*

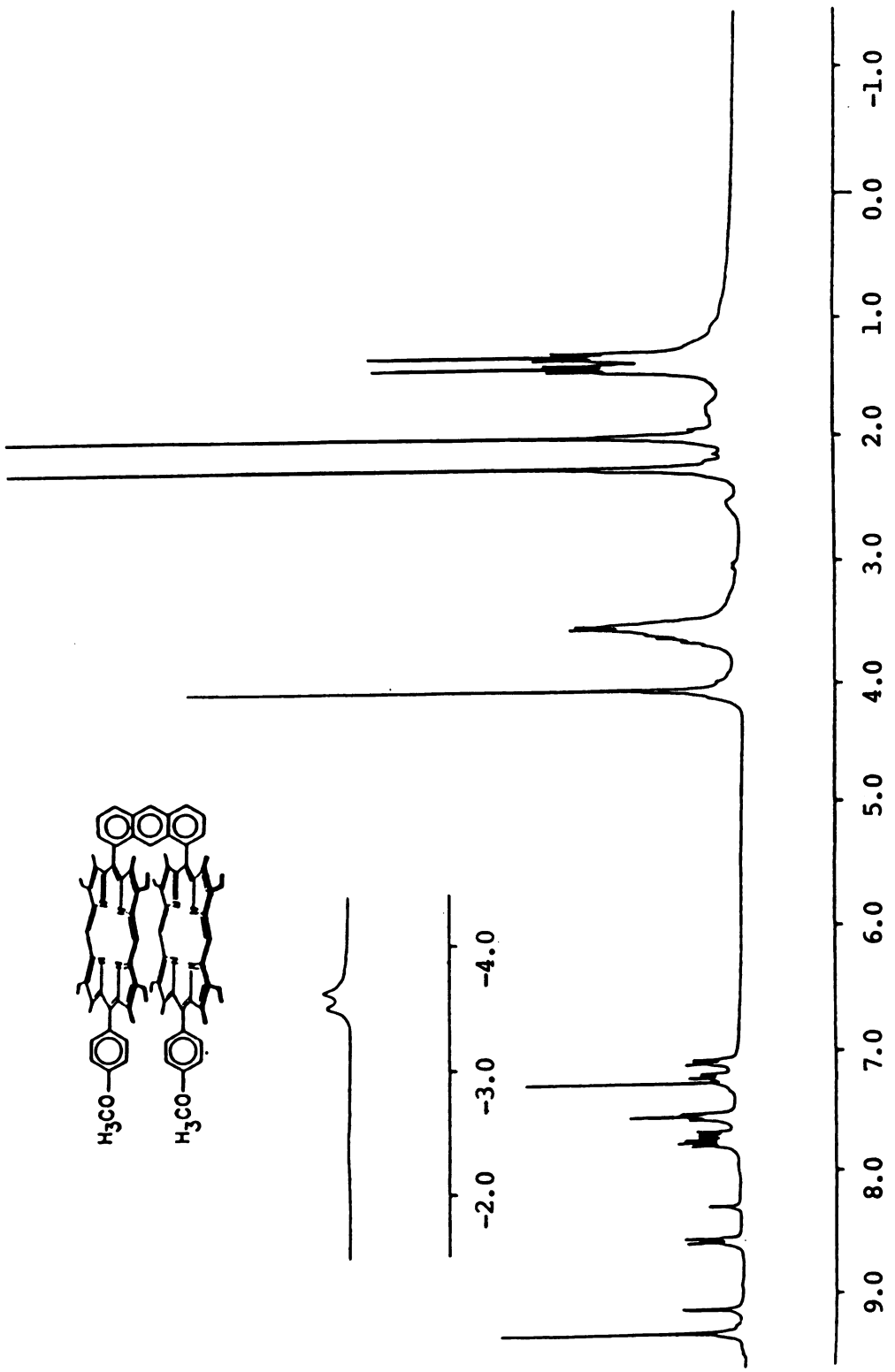

Figure A11 *250 MHz ^1H NMR spectrum of 1,8-bis{5-[2,8,12,18-tetraethyl-3,7,13,17-tetramethyl-15-(p-methoxyphenyl)porphyrinyl]}anthracene (100).*

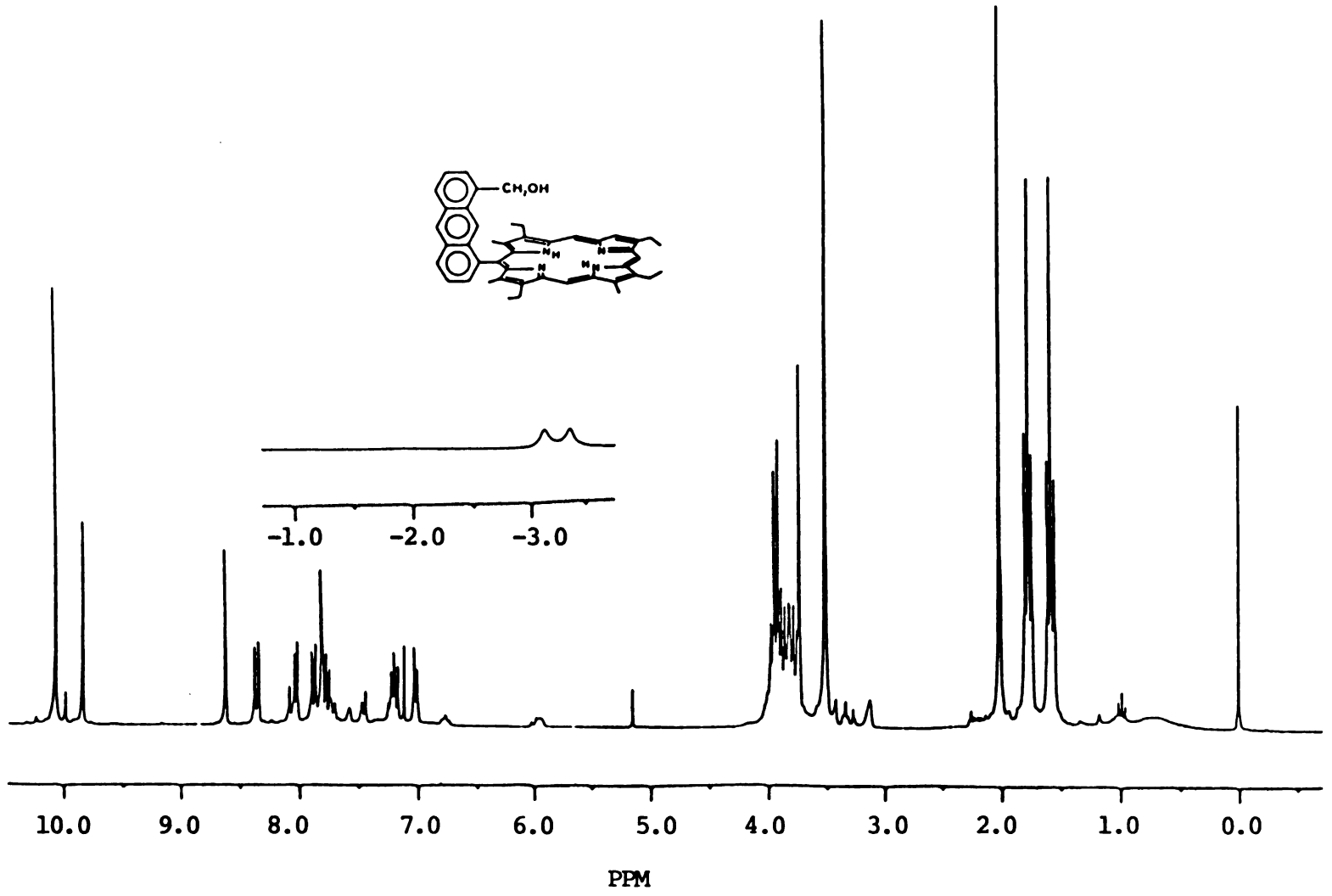

Figure A12 *250 MHz ^{1}H NMR spectrum of 5-[8-(hydroxymethyl)-1-anthryl]-2,8,13,17-tetraethyl-3,7,12,18-tetramethylporphine (17).*

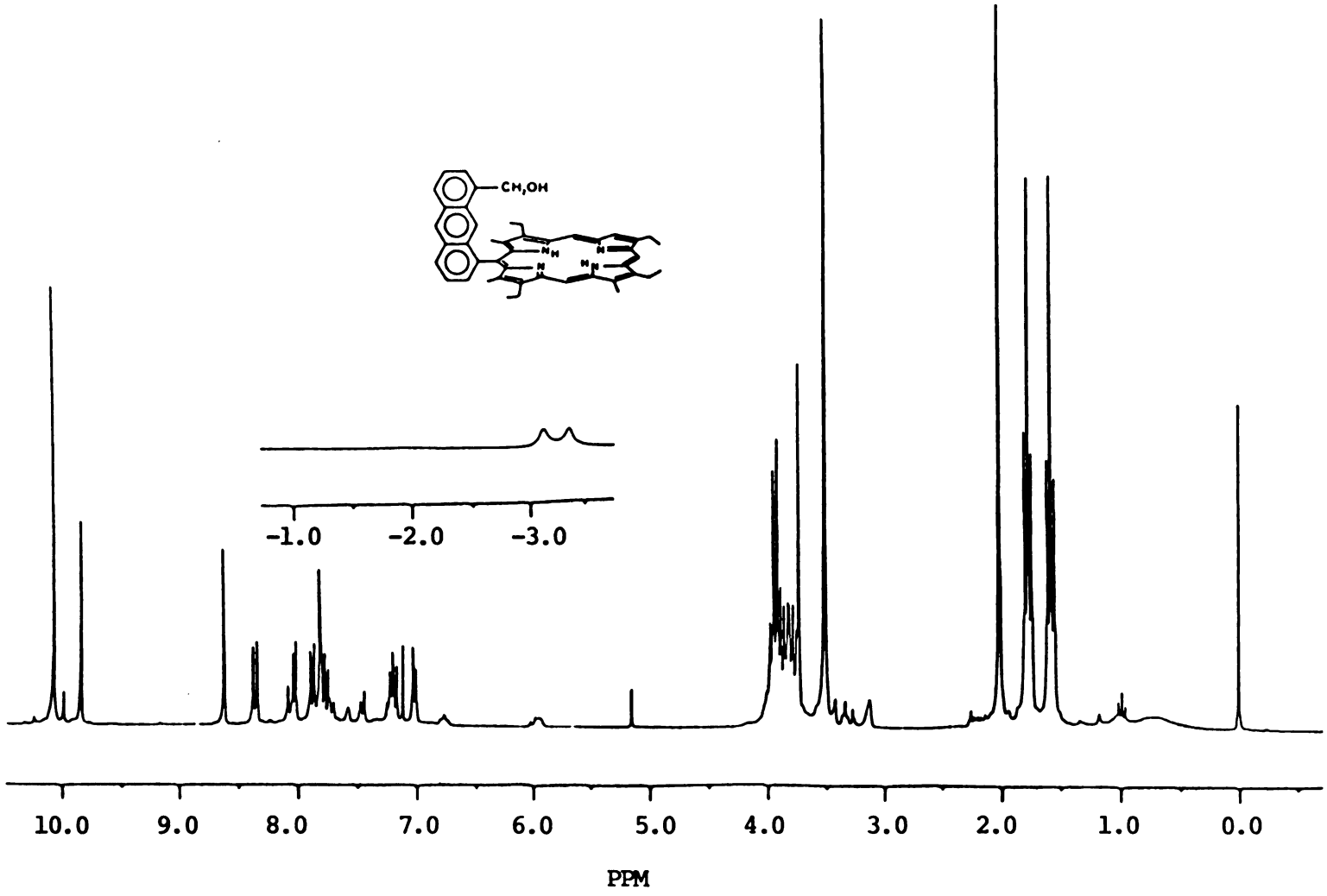

Figure A12 *250 MHz ^{1}H NMR spectrum of 5-[8-(hydroxymethyl)-1-anthryl]-2,8,13,17-tetraethyl-3,7,12,18-tetramethylporphine (17).*

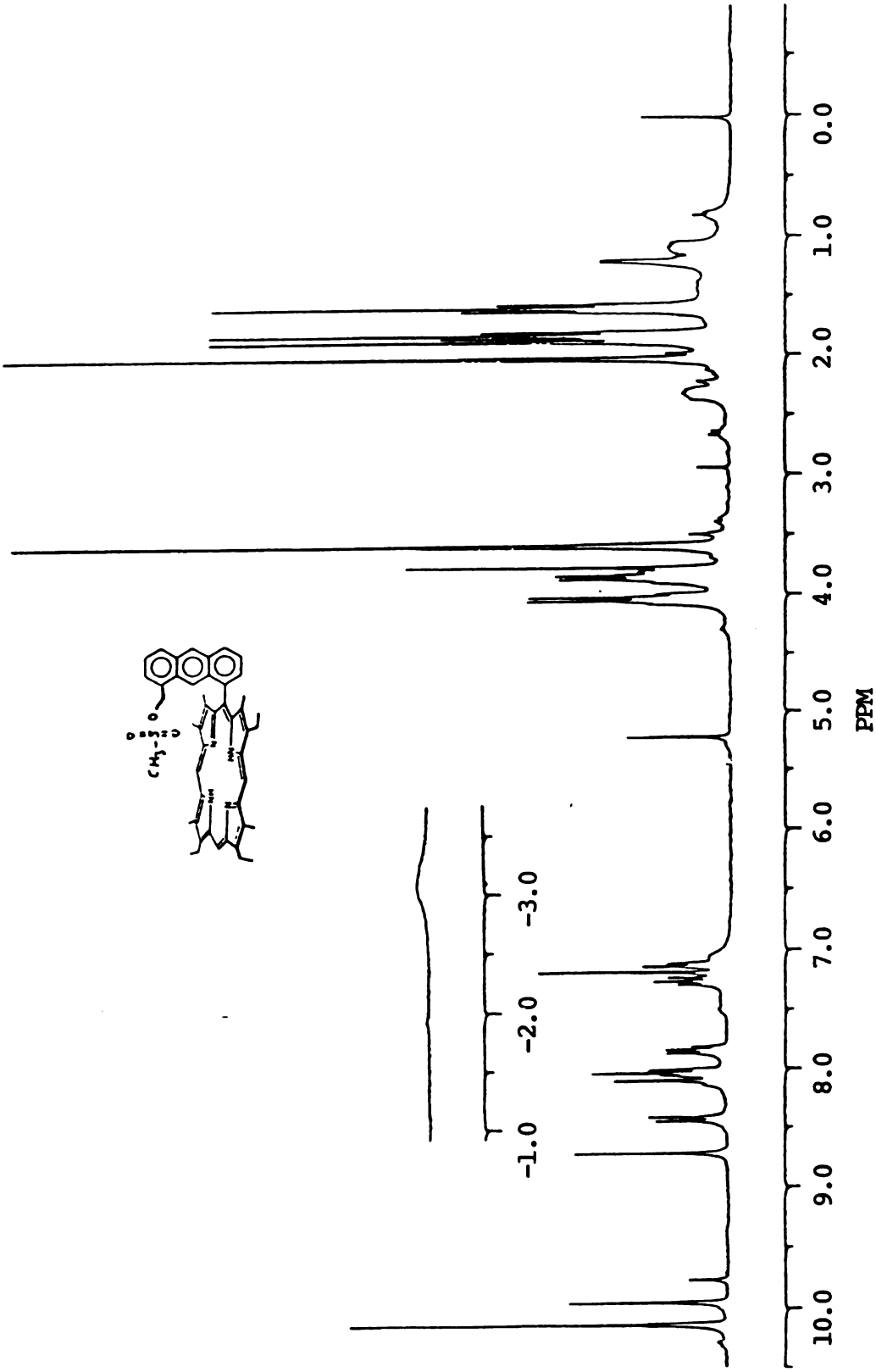

Figure A13 *250 MHz ^{1}H NMR spectrum of 5-{8-[(methane-sulfonate)methyl]-1-anthryl}-2,8,13,17-tetraethyl-3,17,12,18-tetramethylporphine (30).*

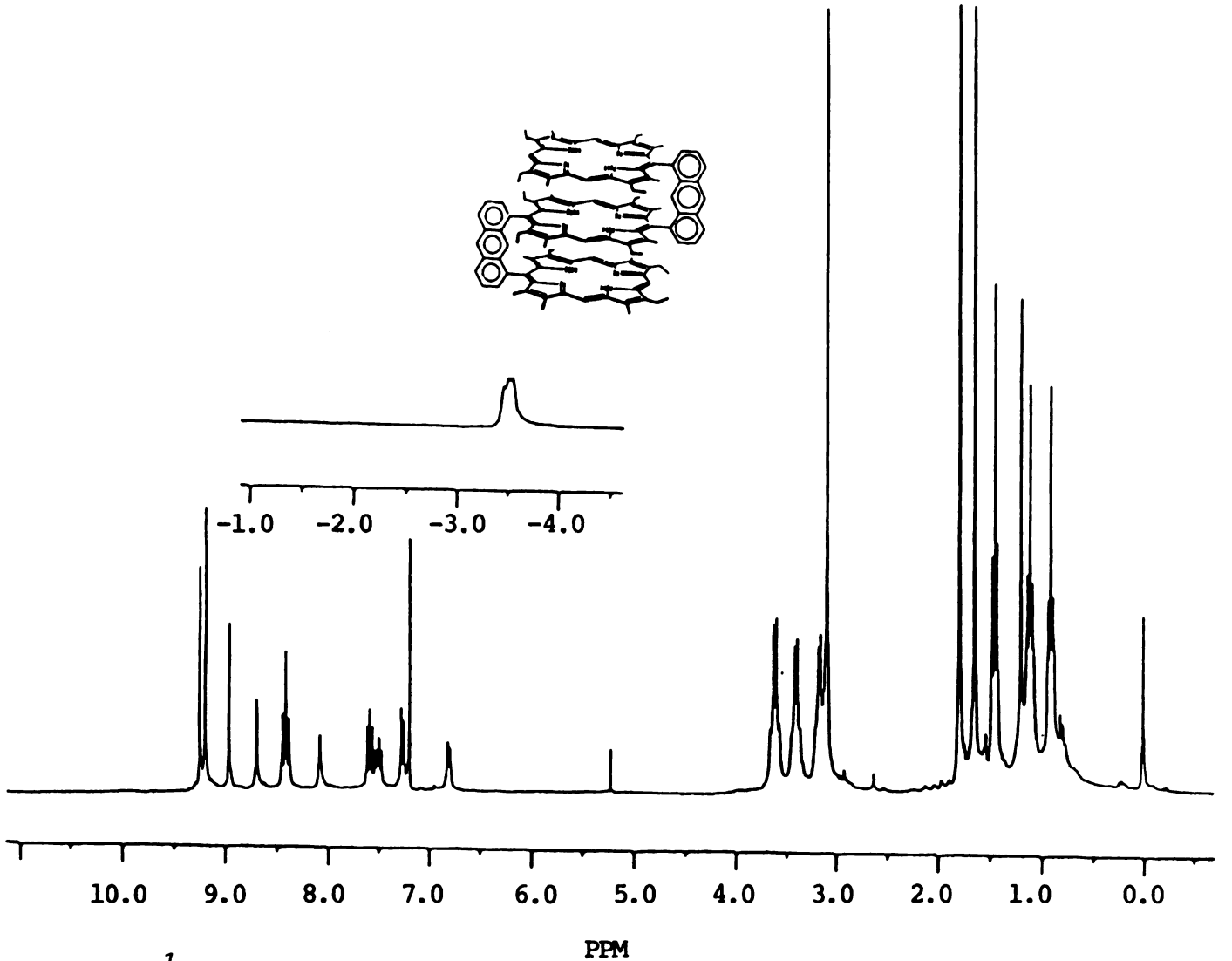

Figure A14 *250 MHz ^{1}H NMR spectrum of trans-5,15-bis{8-[5-(2,8,13,17-tetraethyl-3,7,12,18-tetramethylporphyrinyl]-1-anthryl}-2,8,12,18-tetraethyl-3,7,13,17-tetramethylporphine (20).*

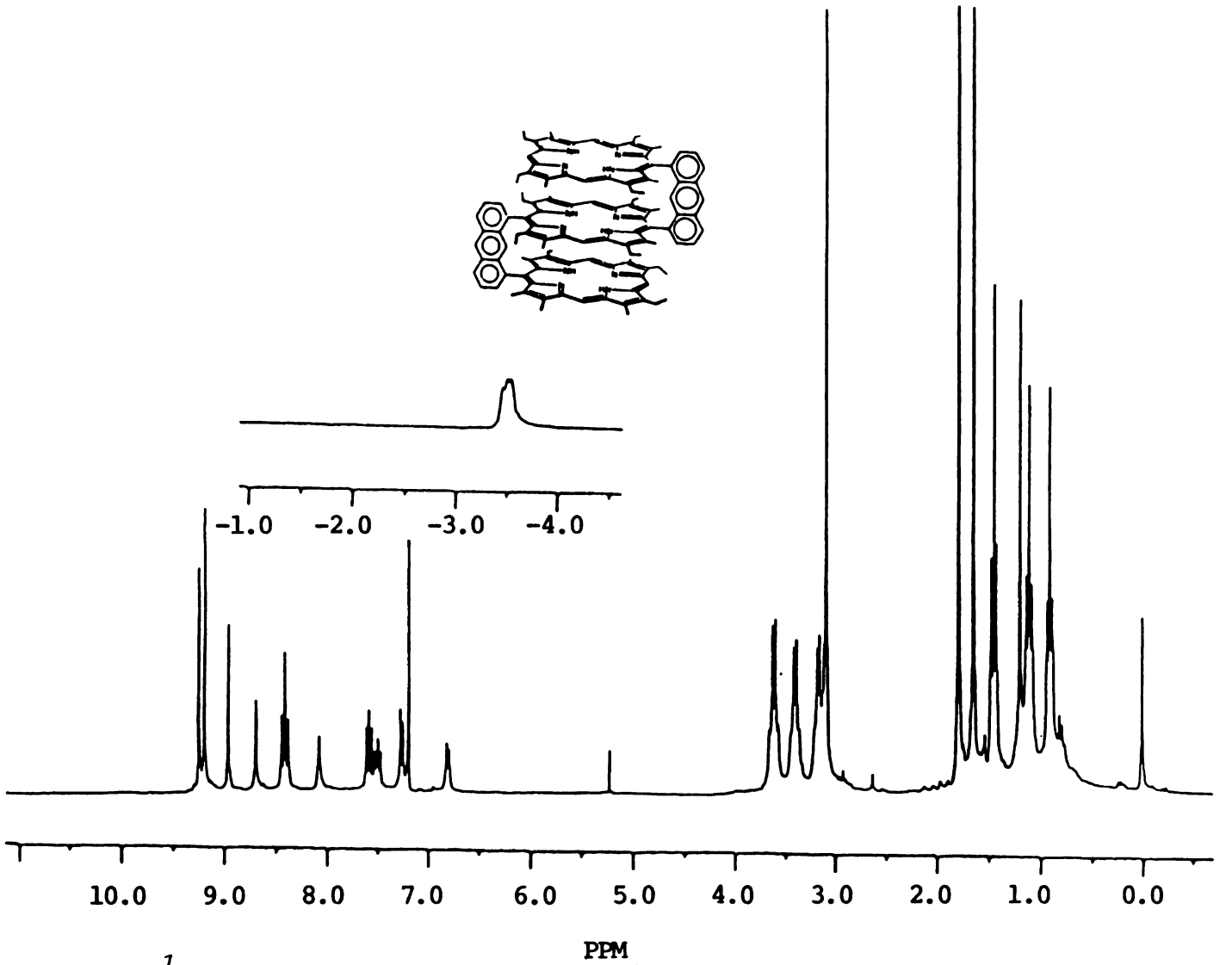

Figure A14 *250 MHz ^{1}H NMR spectrum of trans-5,15-bis{8-[5-(2,8,13,17-tetraethyl-3,7,12,18-tetramethylporphyrinyl]-1-anthryl}-2,8,12,18-tetraethyl-3,7,13,17-tetramethylporphine (20).*

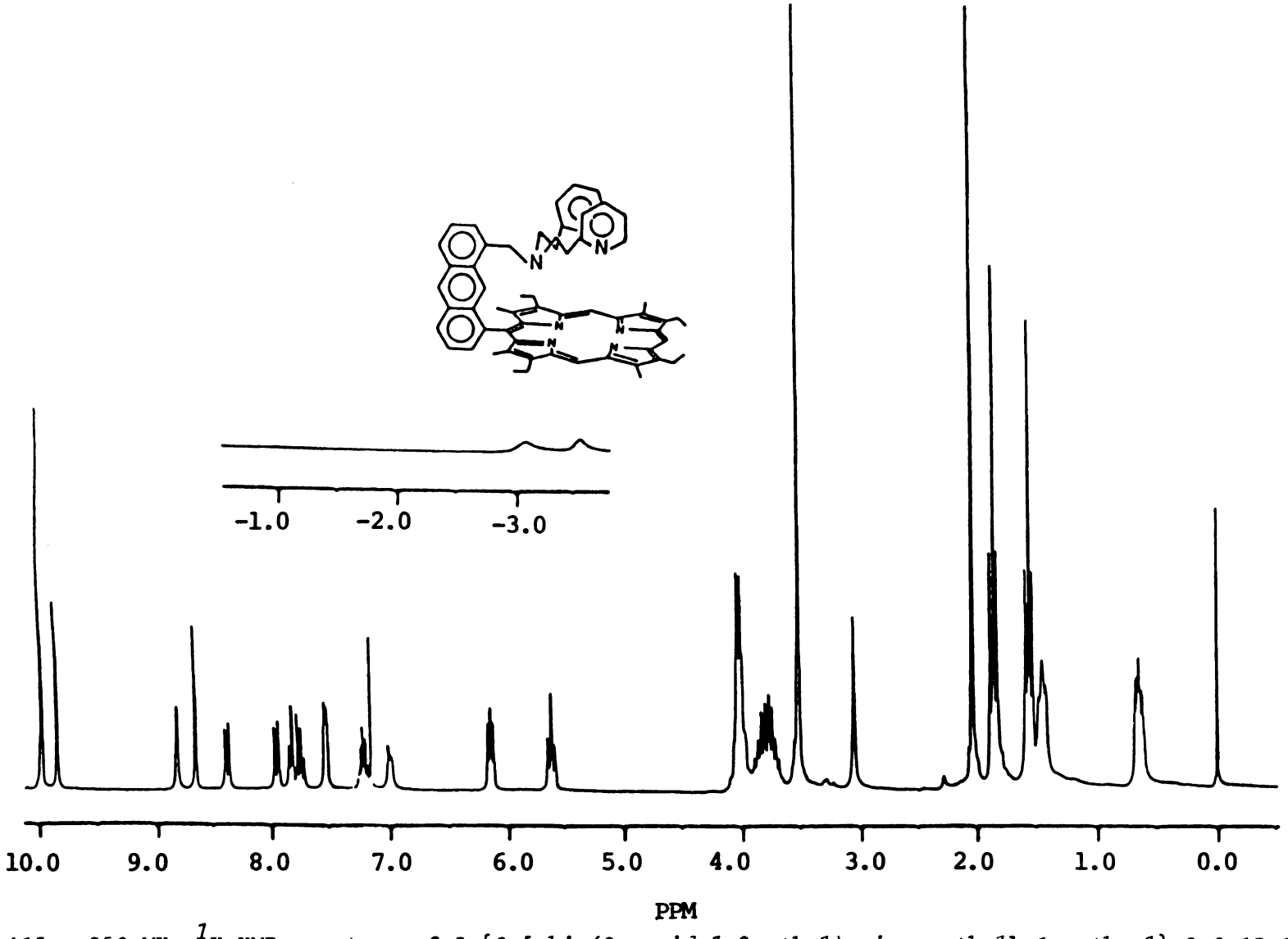

Figure A15 *250 MHz ^{1}H NMR spectrum of 5-{8-[bis(2-pyridyl-β-ethyl)amine methyl]-1-anthryl}-2,8,13,17-tetraethyl-3,7,12,18-tetramethylporphine (32).*

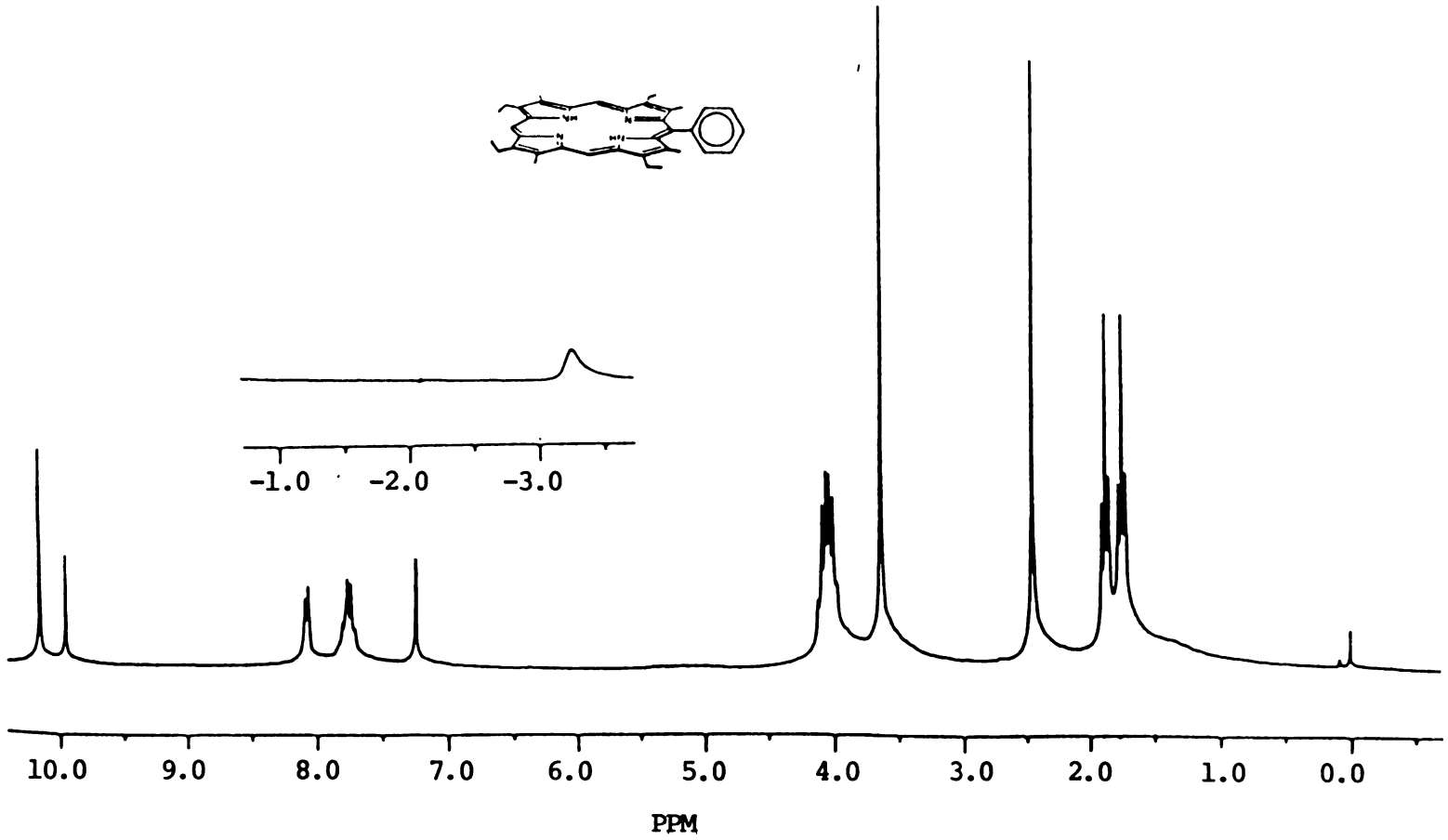

Figure A16 *250 MHz ^{1}H NMR spectrum of 5-phenyl-2,8,13,17-tetraethyl-3,7,12,18-tetramethylporphine (44).*

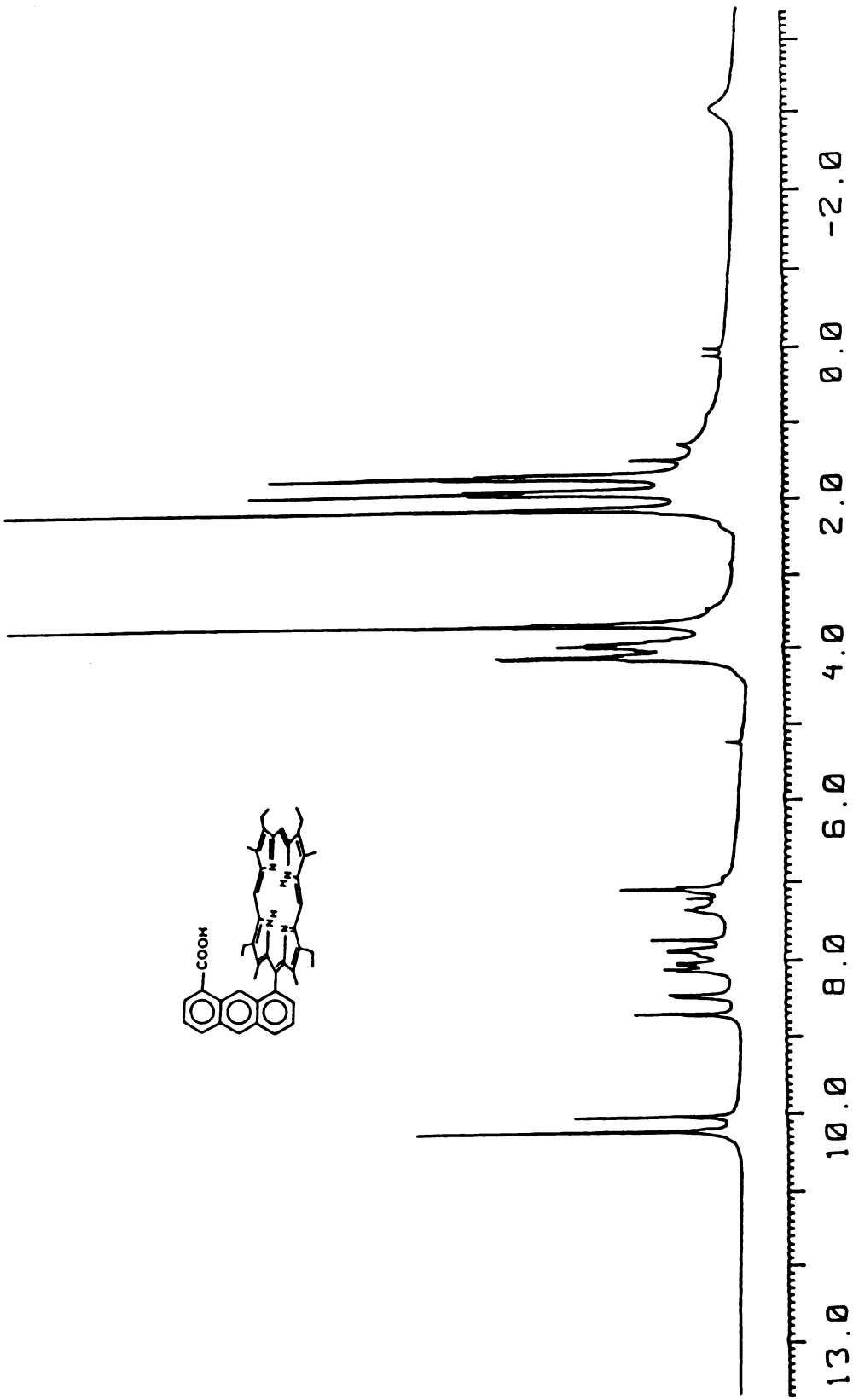

Figure A17 250 MHz ^{1}H NMR spectrum of 5-(8-carboxyl-1-anthryl)-2,8,13,17-tetraethyl-3,7,12,18-tetramethyl-porphine (82).

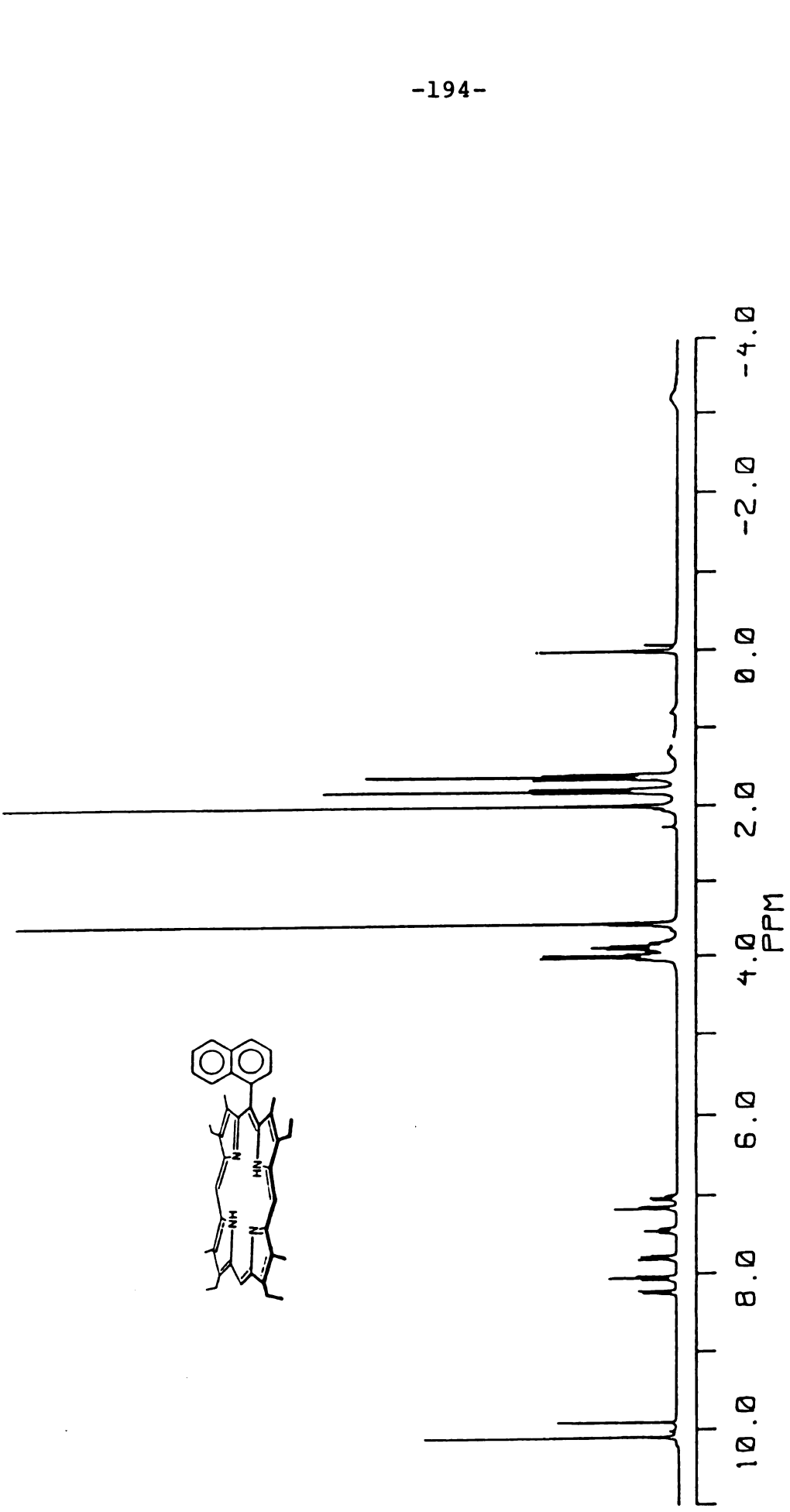

Figure A18 250 MHz ^{1}H NMR spectrum of 1-[5-(2,8,13,17-tetraethyl-3,7,12,18-tetramethyl)porphyrinyl] naphthalene (45).

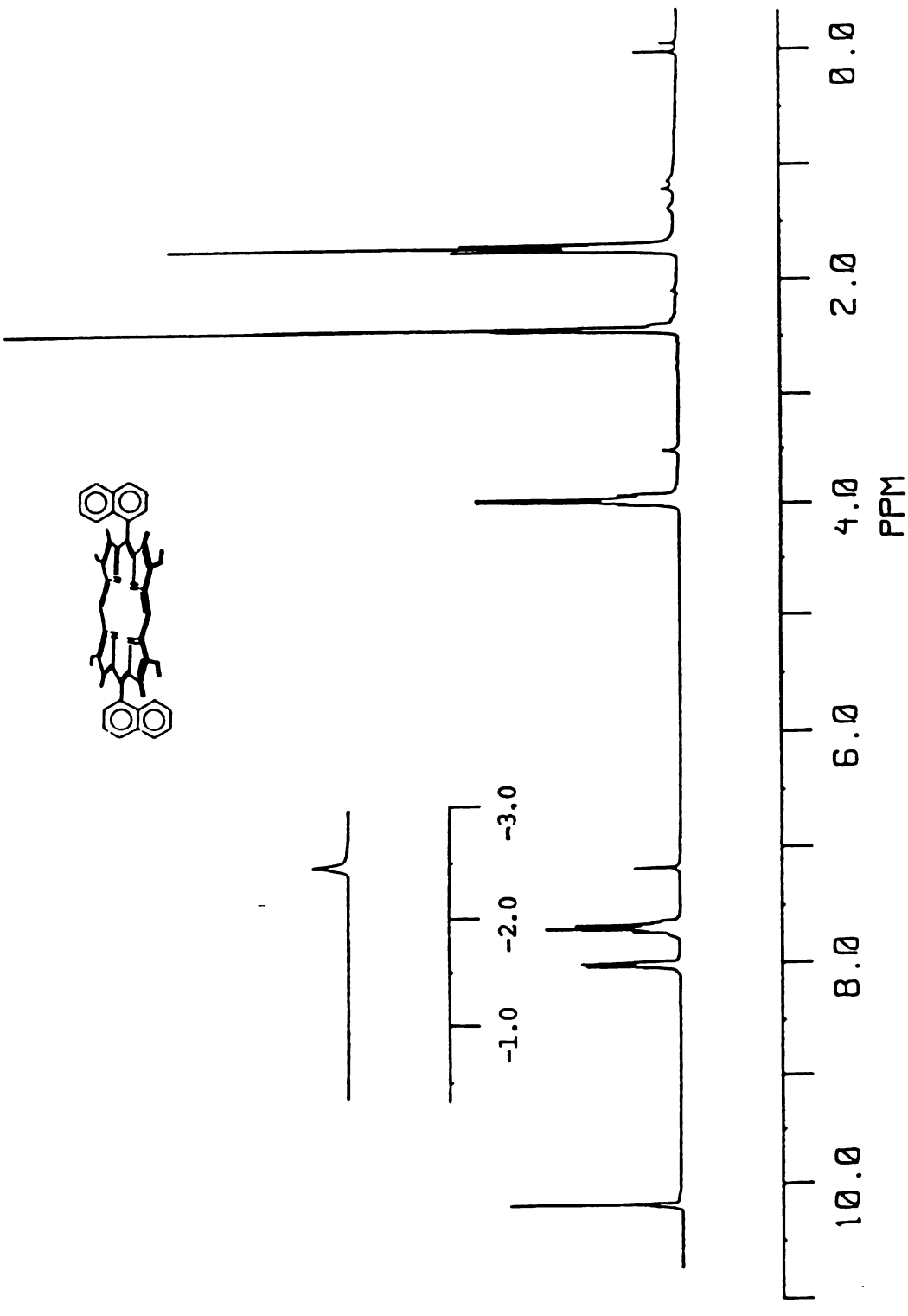

Figure A19 250 MHz ^{1}H NMR spectrum of *trans*-5,15-bis(1-naphthyl)-2,8,12,18-tetraethyl-3,7,13,17-tetramethylporphine (63).

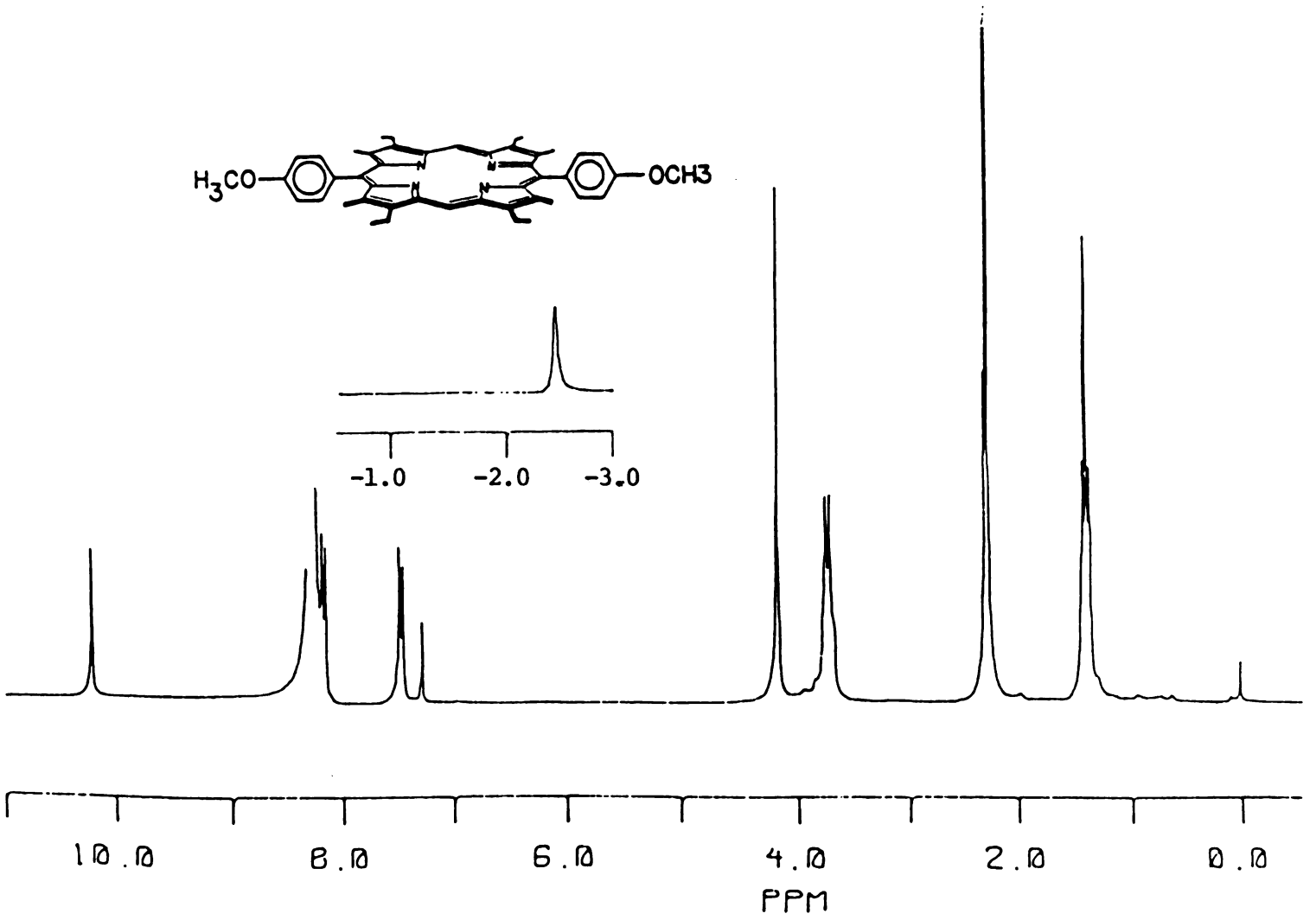

Figure A20 *250 MHz ^1H NMR spectrum of 5,15-bis(4-methoxyphenyl)-2,8,12,18-tetraethyl-3,7,13,17-tetramethylporphine (65).*

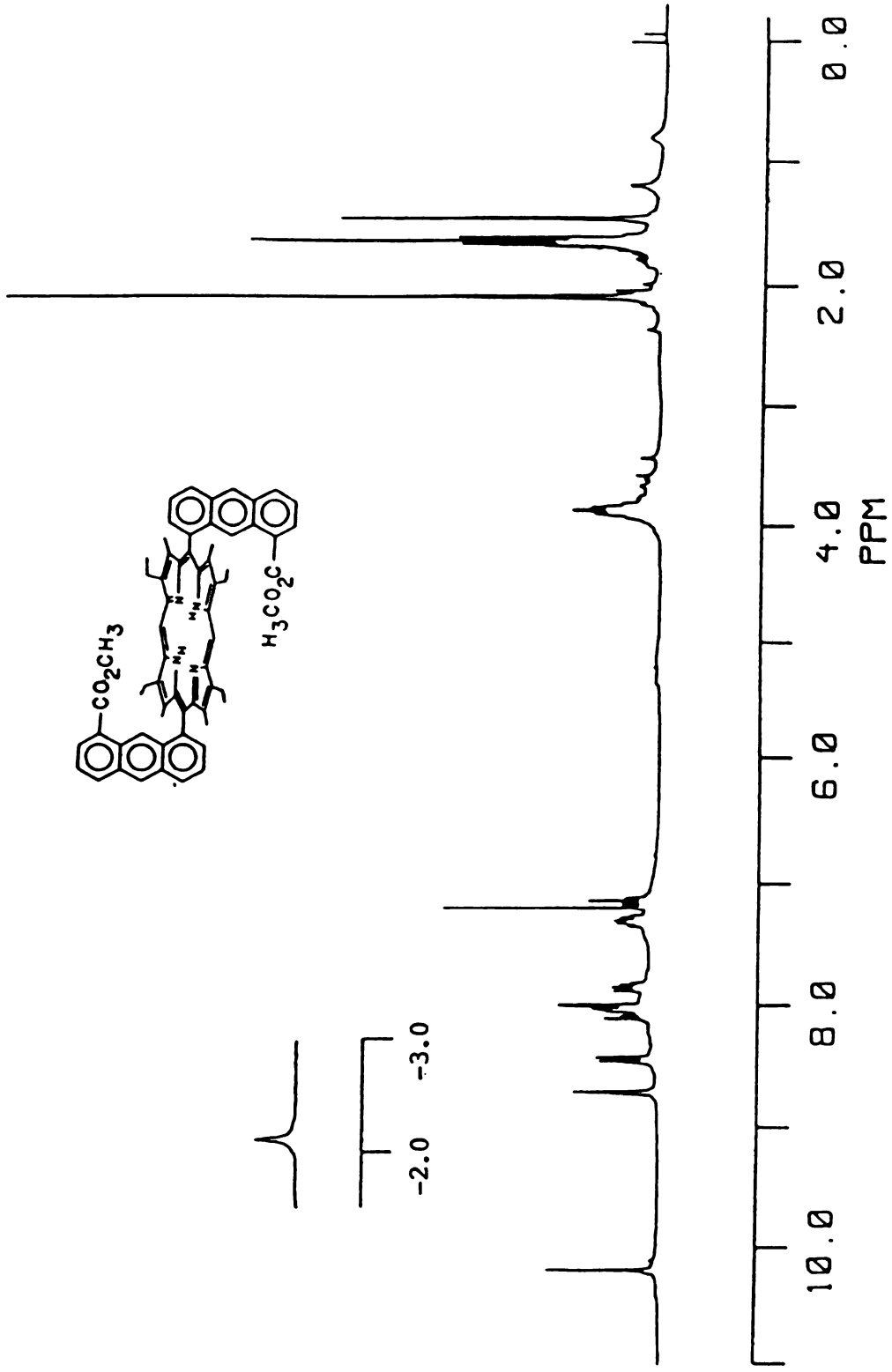

Figure A21 *250 MHz ^1H NMR spectrum of trans-5,15-bis[8-methoxycarbonyl-1-anthryl]-2,8,12,18-tetraethyl-3,7,13,17-tetramethylporphine (52).*

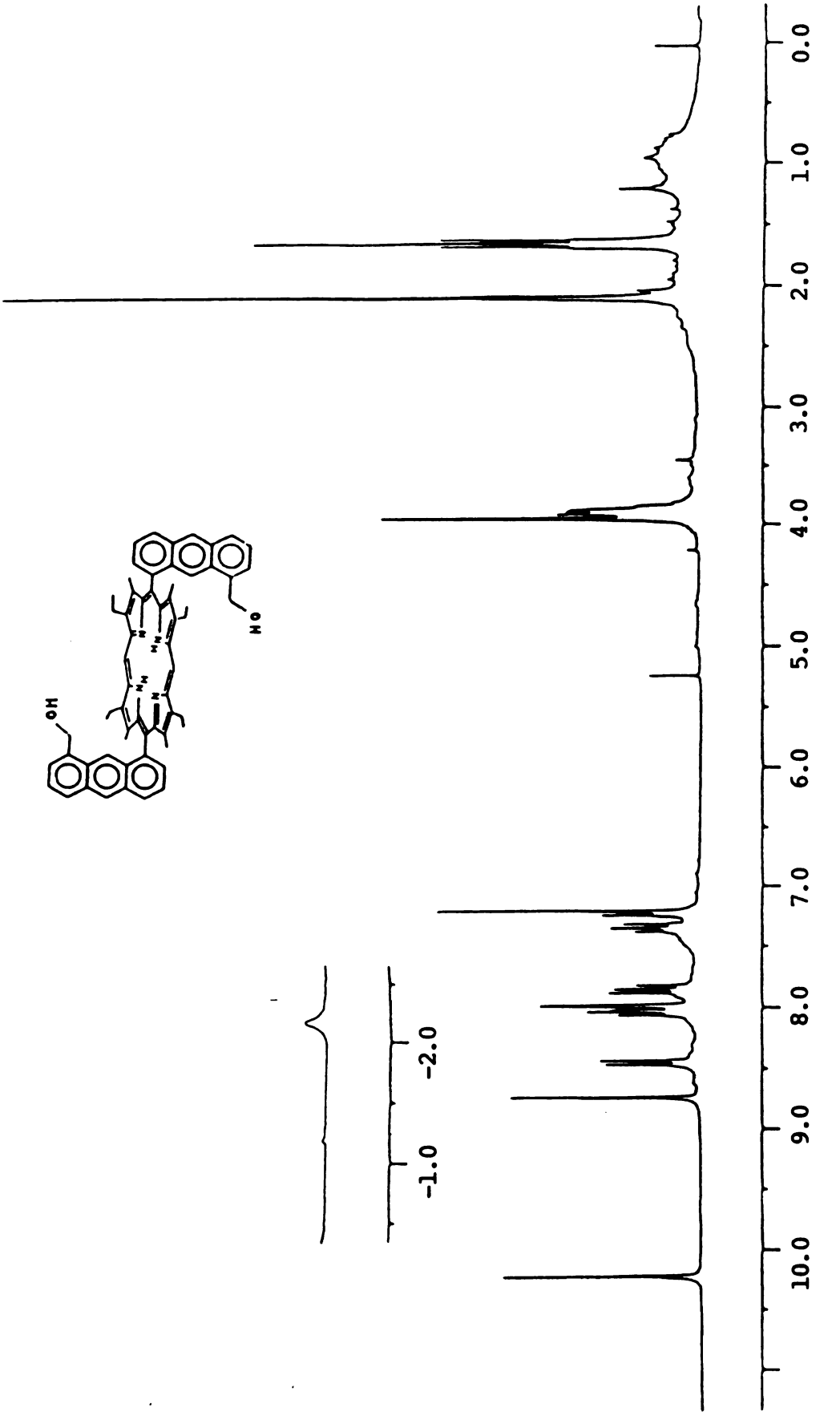

Figure A22 250 MHz ^{1}H NMR spectrum of *trans*-5,15-bis[8-hydroxymethyl-1-anthryl]-2,8,12,18-tetraethyl-3,7,13,17-tetramethylporphine (88).

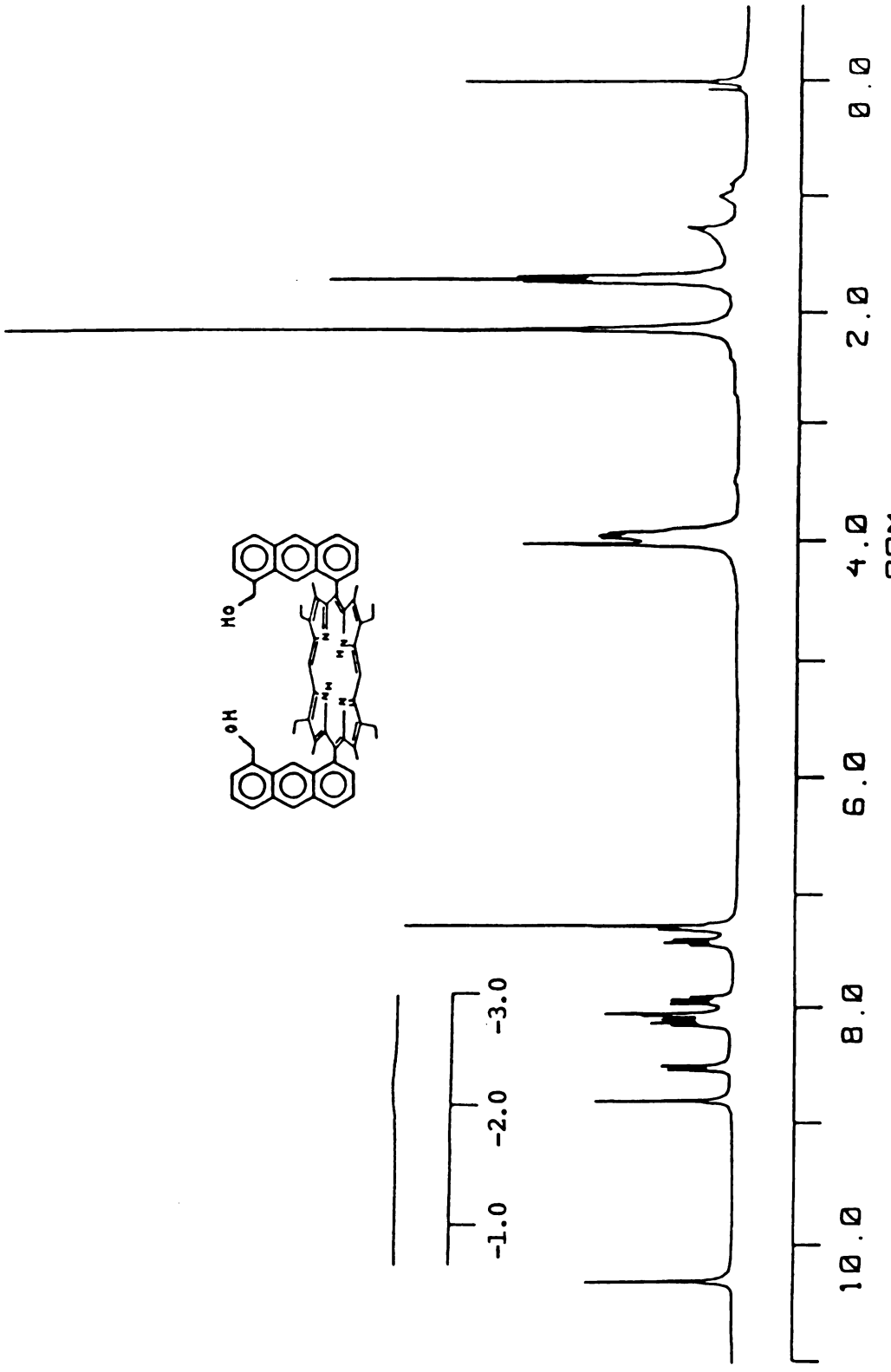

Figure A23 250 MHz ^{1}H NMR spectrum of *cis*-5,15-bis[8-hydroxymethyl-1-anthryl]2,8,12,18-tetraethyl-3,7,13,17-tetramethylporphine (89).

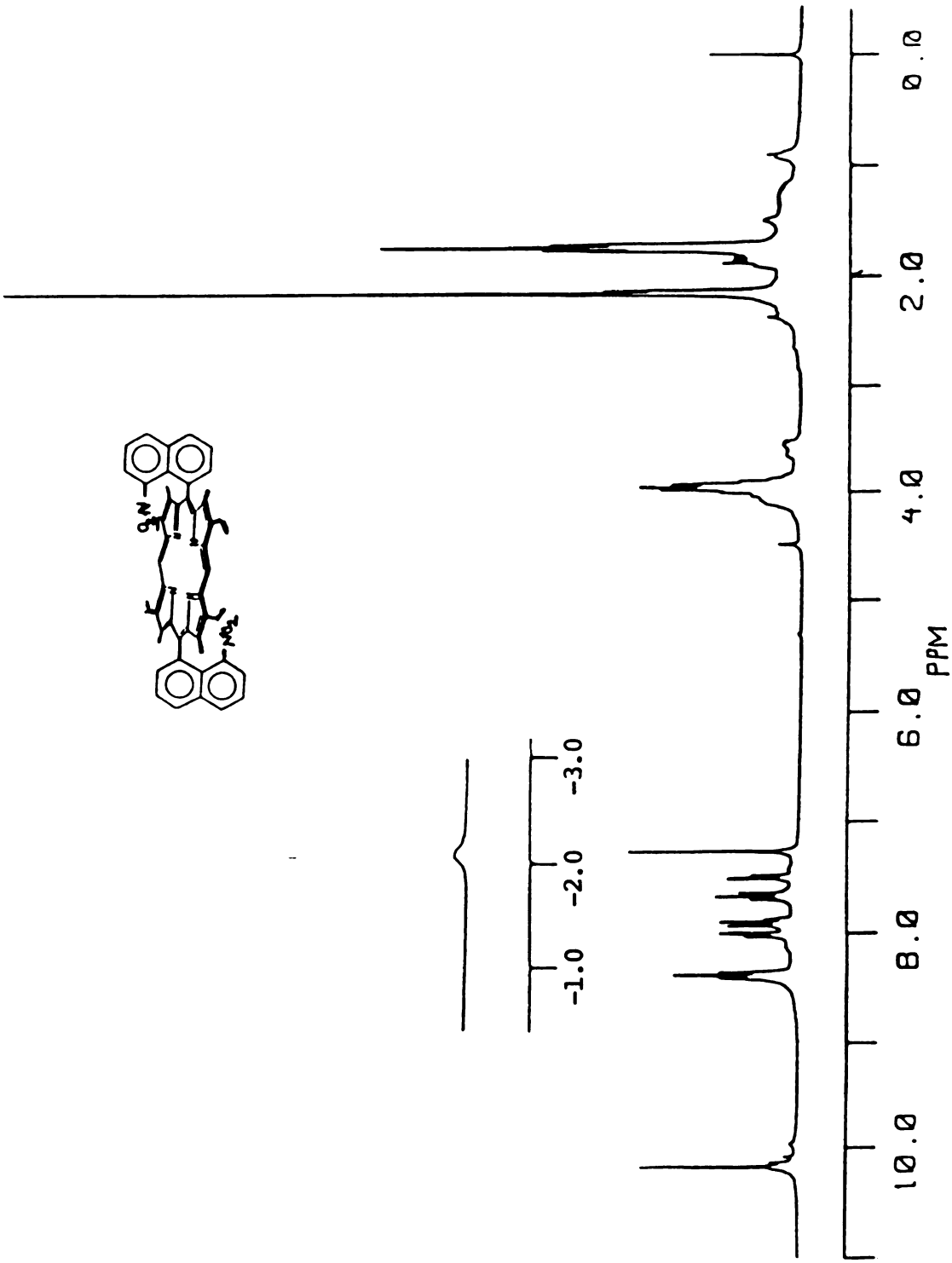

Figure A24 250 MHz ^{1}H NMR spectrum of *trans*-5,15-bis[8-nitro-1-naphthyl]-2,8,12,18-tetraethyl-3,7,13,17-tetramethylporphine (66).

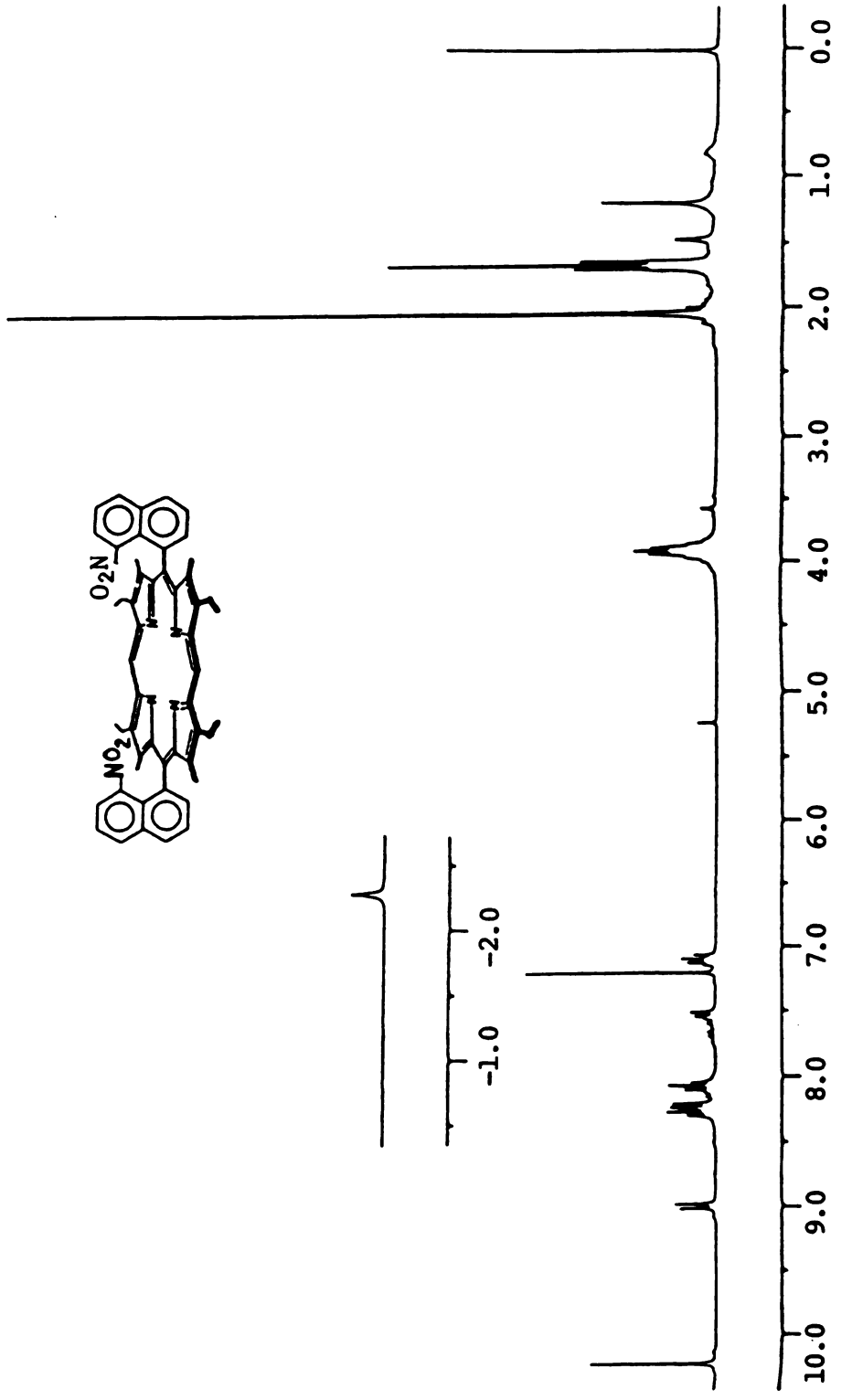

Figure A25 *250 MHz ^1H NMR spectrum of cis-5,15-bis[8-nitro-1-naphthyl]-2,8,12,18-tetraethyl-3,7,13,17-tetramethylporphine (66a).*

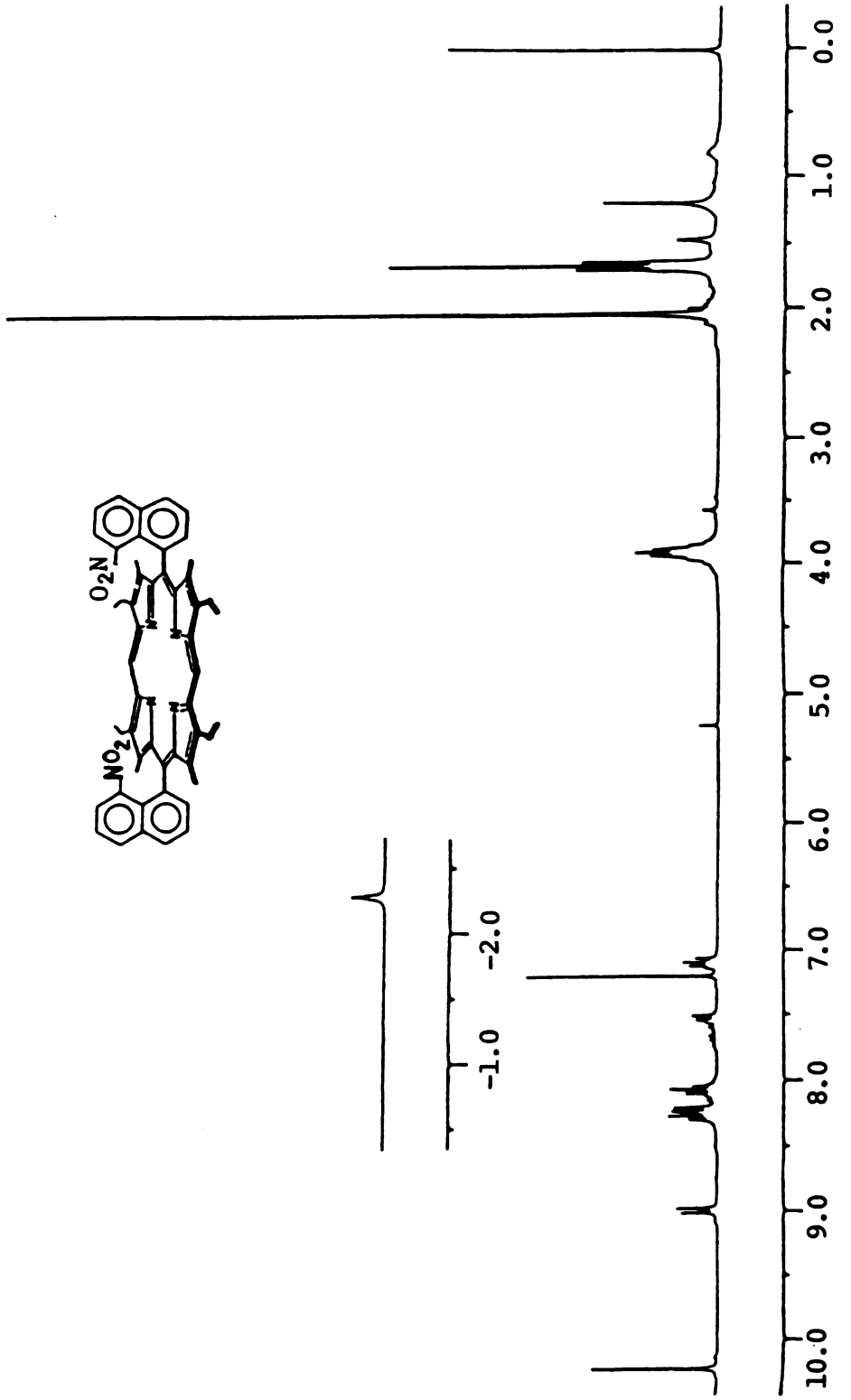

Figure A25 *250 MHz ^1H NMR spectrum of cis-5,15-bis[8-nitro-1-naphthyl]-2,8,12,18-tetraethyl-3,7,13,17-tetramethylporphine (66a).*

REFERENCES

LIST OF REFERENCES

1. Wasielewski, M.R.; Svec, W.A.; Cope, B.T. J. Am. Chem. Soc. 100, 1961 (1978).

2. Netzel, T.L.; Kroger, P.; Chang, C.K.; Fujita, I.; Fajer J. Chem. Phys. Lett. 67, 223 (1979).

3. Netzel, T.L.; Bergkamp, M.A.; Chang, C.K. Proc. Nat. Acad. Sci. USA 79, 413 (1982).

4. Chang, C.K.; Kuo, M.-S.; Wang, C.-B. J. Heterocycl. Chem. 14, 943 (1977).

5. Chang, C.K. J. Heterocycl. Chem. 14, 1285 (1977).

6. Chang, C.K. J. Chem. Soc., Chem. Commun., 800 (1977).

7. Chang, C.K. ACS Adv. Chem. Ser. 173, 162 (1979).

8. Collman, J.P.; Elliott, C.M.; Halbert, T.R.; Tourog, B.S. Proc. Nat. Acad. Sci. USA 74, 18 (1977).

9. Collman, J.P.; Anson, F.C.; Barnes, C.E., Bencosme, C.S.; Geiger, T.; Evitt, E.R.; Kreh, R.P.; Meier, K.; Pettman, R.B. J. Am. Chem. Soc. 105, 2694 (1983).

10. Collman, J.P.; Bencosme, C.S.; Durand, Jr., R.R.; Kreh, R.P.; Anson, F.C. J. Am. Chem. Soc. 105, 2699 (1983).

11. Collman, J.P.; Bencosme, C.S.; Barnes, C.E.; Miller, B.D. J. Am. Chem. Soc. 105, 2704 (1983).

12. Durand, R.R.; Bencosme, C.S.; Collman, J.P.; Anson, F.C. J. Am. Chem. Soc. 105, 2710 (1983).

13. Collman, J.P.; Denisevich, P.; Koval, C.; Anson, F.C. J. Electroanal. Chem. Interfacial Electrochem. 101, 117 (1979).

14. a) Lemberg, M.R. Physiol. Rev. 49, 48 (1969); b) Nicholls, P.; Chance, B. in "Molecular Mechanisms of Oxygen Activation," (O. Hayaishi, ed.), pp. 479-536, Academic Press:New York (1974).

15. Florkin, M. in "Comprehensive Biochemistry," Vol. 31, (M. Florkin and E.H. Stolz, eds.), Elsevier:Amsterdam, pp. 187-235 (1962).

16. a) Caughey, W.S.; Wallace, W.T.; Volpe, T.A.; Yoshikawa, S. in "The Enzymes," (P.D. Boyer, ed.), Vol. 13, Academic Press:New York, pp. 299-337 (1976); b) Wikström, M.; Krab, K.; Saraste, M. in "Cytochrome Oxidase," Academic Press:New York, p. 86 (1981).

17. Challoner, D.R. Nature (London) 217, 78 (1968).

18. Tucker, A. Science 154, 150 (1966).

19. Malmström, B.G. Quart. Rev. Biophys. 6, 389 (1973).

20. Keilin, D.; Hartree, E.F. Proc. Roy. Soc. London B127, 167 (1939).

21. Babcock, G.T.; Vickery, L.E.; Palmer, G. J. Biol. Chem. 251, 7907 (1976).

22. Palmer, G.; Antolis, T.; Babcock, G.T.; Gracia-Iniguez, L.; Tweedle, M.; Wilson, L.J.; Vickery, L.E. in "Mechanisms of Oxidizing Enzymes," (T.P. Singer and R.N. Ondarza, eds.), Elsevier:New York, p. 221 (1978).

23. Tsao, M.S.; Wilmarth, W.K. Adv. Chem. Ser. 36, 113 (1962).

24. Sehested, K.; Rasmussen, O.L.; Fricke, H. J. Phys. Chem. 72, 626 (1968).

25. a) George, P. in "Oxidazes and Related Redox Systems," (T.E. King, H.S. Mason and M. Morrison, eds.), Wiley:New York, p. 3 (1965); b) Wikström, M.; Krab, K.; Saraste, M. in "Cytochrome Oxidase," Academic Press:New York, p. 12 (1981).

26. Wilkins, R.G. Adv. Chem. Ser. 100, 111 (1971).

27. Taube, H. J. Gen. Physiol. 49, 29 (1965).

28. Methews, C.T.; Robins, R.G. Australas. Inst. Mining Met., Proc. [3] 242, 47 (1972).

29. Simplicio, J.; Wilkins, R.G. J. Am. Chem. Soc. 89, 6092 (1967).

30. Stadtherr, L.G.; Prados, R.; Martin, R.B. Inorg. Chem. 12, 1814 (1973).

31. Cohen, I.A.; Caughey, W.S. in "Hemes and Hemoproteins," (B. Chance, R.W. Estabrook and T. Yonetani, eds.), Academic Press:New York, p. 577 (1966).

32. Caughey, W.S.; Davies, T.L.; Fuchsman, W.H.; McCoy, S. in "Structure and Function of Cytochromes," (K. Okunuki, M.D. Kamen and Sekuzu, eds.), University of Tokyo Press:Tokyo, p. 20 (1968).

33. George, P. J. Chem. Soc., 4349 (1954).

34. Caughey, W.S. Ann. N.Y. Acad. Sci. 174, 148 (1970).

35. Bockris, J.O'M.; Srinivasan, S. in "Fuel Cells: Their Electrochemistry," McGraw-Hill:New York (1969).

36. Vielstich, W. in "Fuel Cells," Wiley-Interscience:New York (1970).

37. Gould, R.F. in "Fuel Cell Systems, II," in ACS Adv. Chem. Ser., Vol. 90 (1969).

38. Cohen, R. Proc. Ann. Power Sources Conf. 20, 21 (1966).

39. Maget, H.J.R. in "Handbook of Fuel Cell Technology," (C. Berger, ed.), Chapter 4, Prentice Hall:Englewood Cliffs, NJ (1968).

40. Schanz, J.L.; Bullock, E.: Paper presented in American Rocket Society, September 25-28, Santa Monica, CA (1962)

41. Dolpin, D.; Hiom, J.; Pain III, J.B. Heterocycles 16, 417 (1981).

42. Abdalmuhdi, I.; Chang, C.K. J. Org. Chem. 48, 5388 (1983).

43. a) Abdalmuhdi, I.; Chang, C.K. Angew. Chem. 96, 154 (1984); b) Abdalmuhdi, I.; Chang, C.K. Angew. Chem. Int. Ed. Engl. 23, 164 (1984).

44. Abdalmuhdi, I.; Chang, C. J. Org. Chem. 50, 411 (1985).

45. Abdalmuhdi, I.; Chang, C.K.; Liu, H.Y. J. Am. Chem. Soc. 106, 2725 (1984).

46. Abdalmuhdi, I.; Chang, C.K.; Anson, F.C.; Liu, H.Y. J. Phys. Chem. 89, 665 (1985).

47. Abdalmuhdi, I.; Fillers, J.P.; Ravichandran, K.G.; Chang, C.K.; Tulinsky, A. J. Am. Chem. Soc., in press.

48. Abdalmuhdi, I.; Chang, C.K.; Kondylis, M. J. Am. Chem. Soc., in press.

49. Johnson, A.W.; Kay, I.T. J. Chem. Soc., 1620 (1965).

50. Ogoshi, H.; Sugimoto, H.; Nishiguchi, T.; Watanabe, T.; Matsuda, Y.; Yoshida, Z. Chem. Lett., 29 (1978).

51. Akiyama, S.; Misumi, S.; Nakagawa, M. Bull. Chem. Soc. Jpn. 35, 1829 (1962).

52. Akiyama, S.; Misumi, S.; Nakagawa, M. Bull. Chem. Soc. Jpn. 33, 1293 (1960).

53. Stock, L.M.; Golden, R. J. Am. Chem. Soc. 94, 3080 (1972).

54. Abchibald, J.L.; Walker, D.M.; Shaw, K.B.; Markovac, A.; McDonald, S.F. Can. J. Chem. 44, 345 (1966).

55. Fischer, H.; Berg, M. and Schormüller, S. Ann. 480, 109 (1930).

56. Shneerson, L. and Leibush, M. J. Applied Chem. USSR 19, 869 (1946).

57. Chong, R.; Clezy, P.S.; Liepa, A.J.; Nichol, A.W. Aust. J. Chem. 22, 229 (1969).

58. Arsenault, G.P.; Bullock, E.; MacDonald, S.F. J. Am. Chem. Soc. 82, 4384 (1960).

59. Fischer, H.; Kurzinger, A.Z. Physiol. Chem. 196, 213 (1931).

60. Thonson, A.W.; Kay, I.T. J. Chem. Soc., 2418 (1961).

61. Badger, G.M.; Harris, R.L.N.; Jones, R.A. Aust. J. Chem. 17, 1013 (1961).

62. Fischer, H.; Stangler, G. Justus Leibigs Ann. Chem. 459, 84 (1927).

63. Wang, C.-B.; Chang, C.K. Synthesis, 548 (1979).

64. Wilcox, Jr., C.F.; Uetrecht, J.P.; Grohmann, L. J. Am. Chem. Soc. 94, 2532 (1972).

65. Campbell, C.D.; Rees, C.W. J. Chem. Soc. C, 742 (1969).

66. Logullo, F.M.; Seitz, A.H.; Friedmann, L. Org. Synth. 48, 12 (1968).

67. Wilcox, Jr., C.F.; Granthan, G.D. Tetrahedron 31, 2889 (1975).

68. Gunter, M.J.; Mander, L.N. J. Org. Chem. 46, 4792 (1981).

69. Young, R.; Chang, C.K. J. Am. Chem. Soc. 107, 898 (1985).

70. Yoshida, M.; Kadokura, A.; Minabe, M.; Suzuki, K. Tetrahedron 35, 2237 (1979).

71. Stille, J.K.; Foster, R.T. J. Org. Chem. 28, 2703 (1963).

72. Nelson, S.M.; Rodgers, J. Inorg. Chem. 6, 1390 (1967).

73. Kondylis, M.; Chang, C.K. J. Am. Chem. Soc., in press.

74. Jahnke, H.; Schonborn, M.; Zimmerman, G. Top. Curr. Chem. 61, 133 (1976).

75. Zagal, J.H.; Sen, R.K.; Yeager, E.J. Electroanal. Chem. 83, 207 (1977).

76. Behret, H.; Clauberg, W.; Sandstede, G. Ber. Bunsenges. Phys. Chem. 81, 54 (1977).

77. Albery, W.J.; Hitchman, M.L. in "Ring-Disk Electrodes," Clarenden Press:Oxford (1971).

78. Thirsk, H.R.; Harrison, J.A. "A Guide to the Study of Electrode Kinetics," Academic Press:New York (1972).

79. Brown, A.; Koval, C.; Anson, F.C. J. Electroanal. Chem. 72, 379 (1976).

80. Brown, A.P.; Anson, F.C. J. Electroanal. Chem. 73, 203 (1977).

81. Damjanovic, A.; Genshaw, M.A.; Bockris, J.O'M. J. Chem. Phys. 45, 4057 (1966).

82. Evans, J.F.; Kuwana, T. Anal. Chem. 49, 1632 (1977) and references cited therein.

83. Liu, H.Y.; Weaver, M.J.; Wang, C.B.; Chang, C.K. J. Electroanal. Chem. Interfacial Electrochem. 145, 439 (1983).

84. Levich, V.G. "Physicochemical Hydrodynamics" Prentice-Hall:Englewood Cliffs, NJ (1962).

85. Koutecky, J.; Levich, V.G. Zh. Fiz. Khim. 32, 1565 (1956) and reference 84, pp. 345-357.

86. Durand, Jr., R.R.; Anson, F.C. J. Electroanal. Chem. Interfacial Electrochem. 134, 273 (1982).

87. a) Fujihara, M.; Sunakawa, K.; Osu, T.; Kuana, T. J. Electroanal. Chem. Interfacial Electrochem. 88, 299 (1978).; b) Bettelheim, A.; Kuwana, T. Anal. Chem. 51, 2257 (1979); c) Forshey, P.; Kuwana, T. Inorg. Chem. 20, 693 (1981) 22, 699 (1983); d) Zagal, J.; Bindra, P.; Yeager, E. J. Electroanal. Chem. Interfacial Electrochem. 127, 1506 (1980).

88. Davies, G.; Sutin, N.; Watkins, K.O. J. Am. Chem. Soc. 92, 1892 (1970).

89. Ni, C.-L.; Anson, F.C., private communication.

90. Abdalmuhdi, I.; Chang, C.K.; Kondylis, M. J. Am. Chem. Soc., in press.

91. Collman, J.P.; Denisevich, P.; Konai, Y.; Morrocco, M.; Koval, C.; Anson, F.C. J. Am. Chem. Soc. 102, 607 (1980).

92. Gouterman, M. J. Mol. Spectrosc. 6, 138 (1961).

93. Ichimura, K. Chem. Lett., 641 (1977).

94. Pain III, J.B.; Dolphin, D.; Gouterman, M. Can. J. Chem. 56, 1712 (1978).

95. Kagan, N.E.; Manzerall, D.; Merrifield, R.B. J. Am. Chem. Soc. 99, 5484 (1977).

96. Wasielewski, M.R.; Svec, W.A.; Cope, B.T. J. Am. Chem. Soc. 100, 1961 (1977).

97. Chang, C.K. in "ACS Advances in Chemistry Series," (R. Bruce King, ed.), no. 173 (1979).

98. El-Bayoumi, M.A.; Rawls, H.R.; Kasha, M. Pure Appl. Chem. 11, 371 (1965).

99. Gouterman, M.; Holten, D.; Lieberman, E. Chem. Phys. 25, 139 (1977).

100. Boxer, S.G.; Gloss, G.L. J. Am. Chem. Soc. 98, 5406 (1976).

101. Wasielewski, M.R.; Smith, U.H.; Cope, B.T. J. Am. Chem. Soc. 99, 4172 (1977).

102. Abraham, R.J.; Burbidge, P.A.; Jackson, A.H.; MacDonald, D.B. J. Chem. Soc. B, 620 (1966).

103. a) Abraham, R.J.; Eivazi, F.; Pearson, H.; Smith, K.M. J. Chem. Soc., Chem. Commun., 698, 699 (1976); b) Abraham, R.J.; Barnet, G.H.; Bretschneider, E.S.; Smith, K.M. Tetrahedron 29, 553 (1973); c) Abraham, R.J.; Eirazi, F.; Pearson, H.; Smith, K.M. Tetrahedron 33, 2277 (1977).

104. Hudson, M.F.; Smith, K.M. Tetrahedron 31, 3077 (1975).

105. Subramanian, J. in "Porphyrins and Metalloporphyrins", (K.M. Smith, ed.), Elsevier:New York, pp. 560-571 (1975).

106. Kokoszka, G.; Duerst, R.W. Coord. Chem. Rev. 5, 209 (1970).

107. Sykes, A.G. Prog. Inorg. Chem. 13, 1 (1970).

108. Weil, J.A.; Kinnraid, J.K. J. Phys. Chem. 71, 3341 (1967).

109. Chasteen, N.D.; Belford, R.L. Inorg. Chem. 9, 169 (1970).

110. Belford, R.L.; Chasteen, N.D.; So, H.; Tapscott, R.E. J. Am. Chem. Soc. 91, 4675 (1969).

111. Boas, J.F.; Pilbrow, J.R.; Smith, T.D. J. Chem. Soc. A, 723 (1969).

112. Kokoszka, J.F.; Linzer, M.; Gordon, G. Inorg. Chem. 7, 1730 (1968).

113. Wasson, J.R.; Shyr, C.-I.; Trapp, C. Inorg. Chem. 7, 469 (1968).

114. Blumberg, W.E.; Peisach, J. J. Biol. Chem. 240, 870 (1965).

115. Boas, J.F.; Pilbrow, J.R.; Smith, T.D. J. Chem. Soc. A, 721 (1969).

116. Boyed, P.D.; Smith, T.D.; Price, J.H.; Pilbrow, J.R. J. Chem. Phys. 56, 1253 (1972).

117. Chang, C.K.; Ward, B.; Wang, C.B. J. Am. Chem. Soc. 103, 5236 (1981).

118. Chang, C.K. in "Biochemical and Chemical Aspects of Oxygen," (W.S. Caughey, ed.), Academic Press:New York, pp. 437-454 (1979).

119. Eaton, S.S.; More, K.M.; Sawant, B.M.; Eaton, G.R. J. Am. Chem. Soc. 105, 6560 (1983).

120. Chang, C.K.; Eaton, S.S.; Eaton, G.R. J. Am. Chem. Soc. 107, 3177 (1985).

121. Smith, T.D.; Pilbrow, J.R. Coord. Chem. Rev. 13, 173 (1974).

122. Hatada, M.H.; Tulinsky, A.; Chang, C.K. J. Am. Chem. Soc. 103, 5623 (1981).

123. Collman, J.P.; Chong, A.D.; Jameson, G.B.; Oakley, R.T.; Rose, E.; Schmittou, E.R.; Ibers, J.A. J. Am. Chem. Soc. 516 (1981).

124. Chang, C.K.; Tulinsky, A.; Hatada, M.H. J. Am. Chem. Soc. 102, 7115 (1980).

125. Slip angle = $\sin^{-1}$ [(magnitude of slip)/(metal-metal distance)].

126. Jones, T.A. in "Computational Crystallography," (D. Sayer, ed.), Clarendon Press:Oxford, pp. 303-317 (1982).